

ALBA II

White paper



© ALBA Synchrotron. All rights reserved.

ALBA Synchrotron
Carrer de la Llum 2-26 08290
Cerdanyola del Vallès (Barcelona)
Spain Tel. +34 93 592 4300
Graphic design: Lucas Wainer

Caterina Biscari, on behalf of the ALBA team
May 2023



Generalitat de Catalunya
**Departament de Recerca
i Universitats**



Table of Contents

1. EXECUTIVE SUMMARY	6		
1.2. Resumen ejecutivo	9		
1.3. Resum ejecutivo	11		
2. FROM ALBA TO ALBA II	13		
2.1. ALBA present	14		
2.2. Evolution of synchrotron light sources	17		
2.3. ALBA future	18		
2.4. Bridging to the Spanish and European Research Area	20		
3. SCIENCE AT ALBA II	21		
3.1. Health	23		
3.1.1. Drug Delivery (correlative microscopy)	24		
3.1.2. Integrative biology and time-resolved enzymology	25		
3.2. Energy and environment	27		
3.2.1. Catalysis	27		
3.2.2. Battery research and the correlated ecosystem	33		
3.3. Information and communication technologies	37		
3.3.1. Age of CMOS technology	37		
3.3.2. New ways to overcome the energy consumption challenge: Spintronics	39		
3.3.3. Neuromorphic and Quantum computing	41		
3.4. ALBA II: Essential enabler technology to empower the Spanish user community to address the grand challenges	44		
4. ACCELERATOR AND PHOTON SOURCES	45		
4.1. Accelerators: storage ring upgrade	46		
4.1.1. Lattice	46		
4.1.2. Magnets with associated new technologies	50		
4.1.3. Vacuum system	52		
4.1.4. RF systems	54		
4.1.5. Diagnostics	55		
4.1.6. Layout	57		
4.1.7. Injection into SR	59		
4.2. Photon Sources	61		
5. BEAMLINE TECHNOLOGY FOR THE FOURTH-GENERATION LIGHT SOURCE	64		
5.1.1. Optics	65	5.2. Planning the new beamlines	69
5.1.2. Optomechanics and controls	66	5.2.1. Range of technical parameters for long beamlines on IDs	70
5.1.3. Detectors	67	5.2.2. Range of technical parameters for Bend and Super-Bend sources	73
5.1.4. Sample environment	68	5.3. Upgrading existing beamlines	73
		5.3.1. Impact of the new sources on the ALBA beamlines	73
		5.3.2. Enhancing performance of the beamlines	74
		6. DATA MANAGEMENT STRATEGY	78
		6.1. Data Acquisition	81
		6.2. Data Analysis	82
		6.3. Collaborations on data management	84
		7. PARTNERSHIPS	85
		7.1. Joint Electron Microscopy Center at ALBA (JEMCA)	86
		7.2. In-CAEM (In-situ Correlative installation for Advanced Materials for Energy)	87
		7.3. Battery and catalysis laboratories (BATTlab, CATlab)	88
		7.4. Future opportunities: ASTIP	89
		7.5. League of European Accelerator-based Photon Sources	90
		8. ENVIRONMENTAL SUSTAINABILITY	91
		8.1. General framework	92
		8.2. Infrastructure development	93
		8.3. Energy Efficiency and Sustainability	94
		8.4. Impact on environment	95
		9. PROJECT MANAGEMENT	96
		9.1. Organization	97
		9.2. Cost	98
		9.3. Staff	99
		9.4. Timeline	99
		9.4.1. Timeline for Storage Ring upgrade	99
		9.4.2. Timeline for the beamlines	99
		9.5. Milestone Plan and risk analysis	101
		10. ECONOMIC AND SOCIAL IMPACT OF ALBA II	103
		10.1. Economic impact	104
		10.2. Socioeconomic impact	104
		ANNEX A ECONOMIC AND SOCIAL IMPACT OF ALBA II	106
		References	110
		List of figures and tables	116

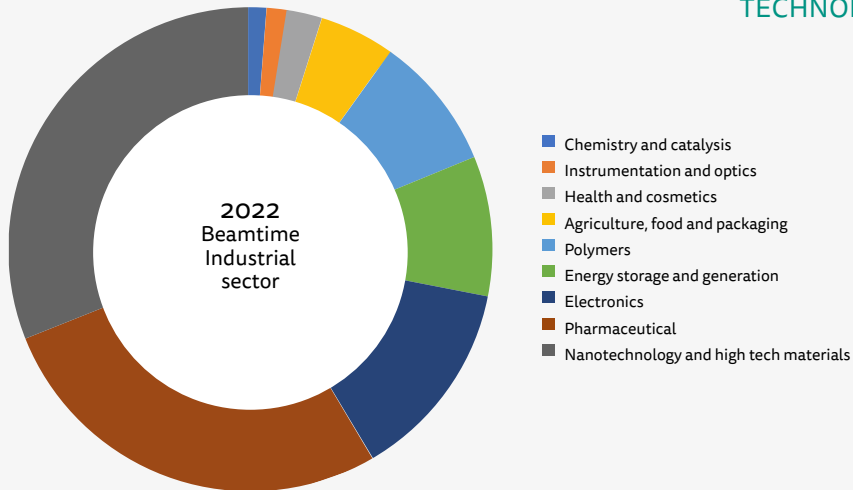
INDUSTRIAL SECTORS

 CHEMISTRY	 FOOD AND AGRICULTURE
 ADVANCED MATERIALS	 ENVIRONMENT
 NANOTECHNOLOGY	 AUTOMOTIVE AND AEROSPATIAL
 PHARMACEUTICAL	 ENERGY
 HEALTH	 CULTURAL HERITAGE & FORENSIC SCIENCES

75 companies
33 SMEs
51% national
49% international
532 industrial experiments

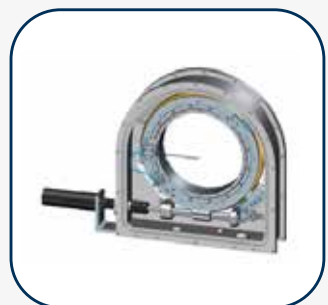
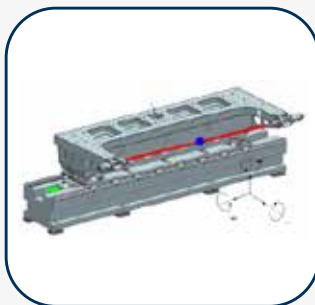
SERVICES
Beamtime
Data analysis
Sample preparation
Assistance during the experiment

TECHNOLOGY TRANSFER
18 Patents

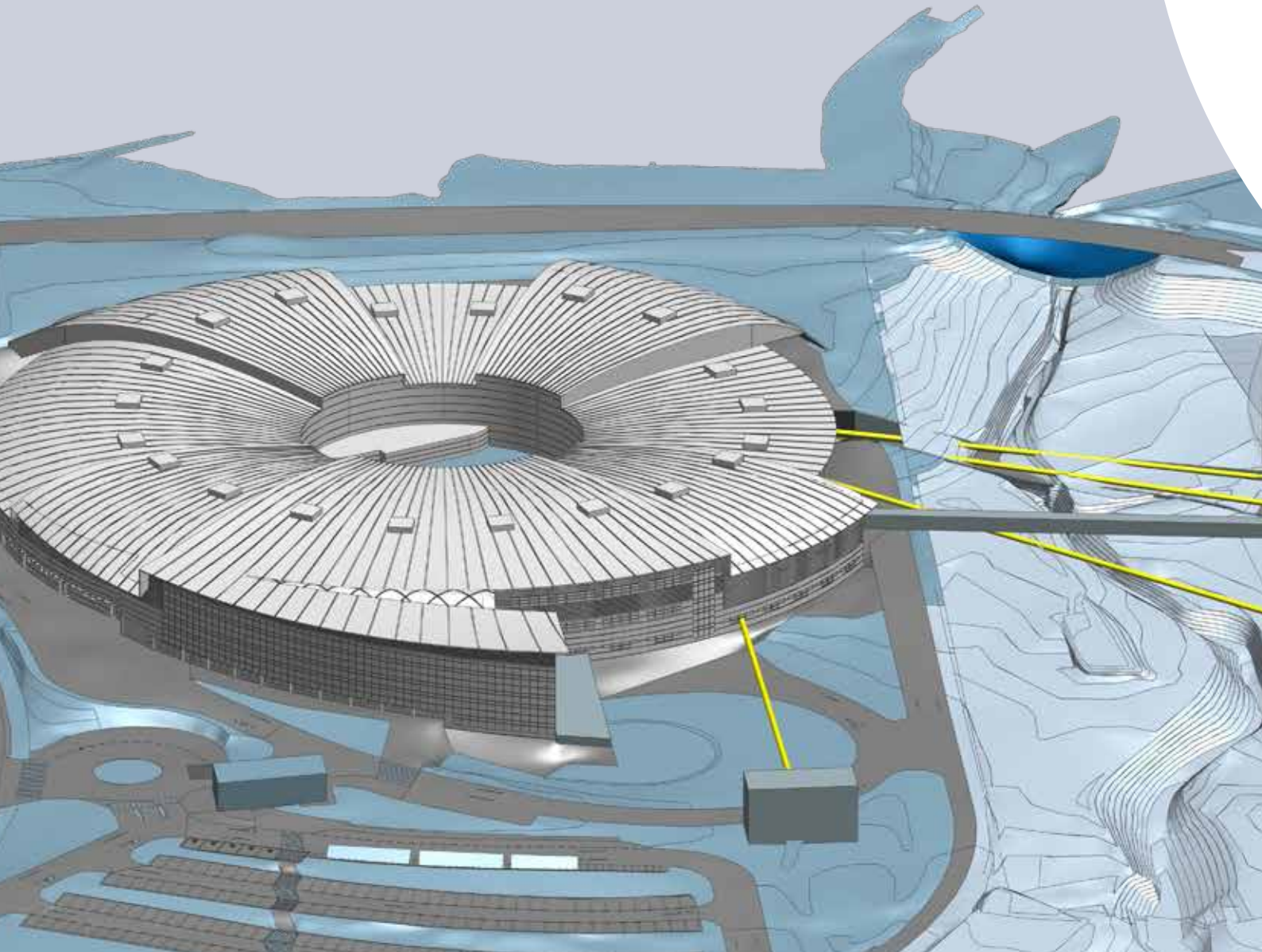


OPPORTUNITIES FOR INDUSTRY OF SCIENCE

- New viewport design compatible with high vacuum
- A new bench concept for measuring magnetic fields of big closed structure
- Variable speed UHV chopper
- Two rotation mechanism for a beam stop in vacuum
- Angular orientable sample parking for STM plates
- Motor device for actuating elements in ultra-high vacuum environments
- X-ray mirror adaptive optics system



1 Executive summary



ALBA Synchrotron¹, a 3rd generation light source facility, is an important pillar of the Spanish and European Research Area, providing extended research capabilities and a wide range of state-of-the-art instrumentation to academic and industrial users. ALBA scientific program addresses the mayor challenges society is facing and ALBA industrial program directly impacts the economic growth by showing industrial leaders of Spain new development opportunities and ultimately windows of innovation for their businesses. ALBA plays an influential role in science tutoring and education, contributing to dual professional training, preparing and enabling young scientists and engineers for their national and international career, providing role models to foster gender equality in STEM disciplines, promoting overall safety culture at all level of activities, and seeding the inquisitiveness for rational cognizance and the scientific perspective in the youngest generations. It delivers to the Spanish research and policy community another gate to the larger European research network and infrastructures from the active participation in LEAPS, the *League of European Accelerator-based Photon Sources*² and its positioning in the Horizon Europe programs. In other words, **ALBA has proven to be a resilient essential part of the Spanish research landscape** and ALBA staff has shown social and innovation responsibility corroborating ALBA as an important asset in Spain.

Significant progress in accelerator design, X-ray optics, detection technology, and Information Technology (IT) drives worldwide the evolution of synchrotron light sources to the **4th generation**, opening **new windows to the exploration of inner details of matter, devices, and their functionality**. Photon brilliance (photons per unit time, per unit area, per unit solid angle and per unit spectral bandwidth) and the coherent fraction of the photon flux are increased by orders of magnitude, providing the ground for unmatched analytics tools, ultimately leading to develop new approaches and technologies for a sustainable, clean and smart economy and a more efficient health system. The first 4th generation operating light source is MAX IV³ and all new synchrotrons in construction belong to the new generation. ESRF⁴ has been the first 3rd generation light source upgrading to the ESRF-EBS⁵ project, setting the example for many others, who will upgrade during the next decade their facilities.

¹ <https://www.albasynchrotron.es/en>

² <https://leaps-initiative.eu/>

³ <https://www.maxiv.lu.se/>

⁴ <https://www.esrf.fr/>

⁵ <https://www.esrf.eu/about/upgrade>

ALBA is ready to leap from the 3rd to the 4th generation and give birth to **ALBA II**, by combining the partial substitution of the accelerator with the upgrade of the existing instrumentation and the addition of new and fully optimized beamlines, thus maintaining the present position within the European and worldwide scenario and providing a crucial competitive advantage for the Spanish innovation ecosystem. The advantages brought by the future high brightness are boosted in terms of resolution and coherence with long optical path in the experimental beamlines. The opportunity of using the nearby plots for extending up to three fully new beamlines puts ALBA in a privileged position for developing state of the art instruments and at the same time providing them with exceptional large end station space and sophisticated infrastructures.

By building on ALBA culture, **ALBA II will provide answers for growing research demands caused by the ecological and economical challenges of the 21st century and the aftermath of the current health and social crisis.**

Upgrading the storage ring, the photon sources, and completing the optimized instrumentation will significantly **increase the number of photons on the sample and at the same time increase the spatial resolution**, it will push the usable energy range to higher energies, and will provide remarkable coherent flux in the tender to hard X-ray range. In the start-up of ALBA II, the number of **operating beamlines will be increased from the present 10 to 17**, proportionally increasing the number of beamtime hours provided to users. There will still be opportunity for further

increasing the number of beamlines up to a total of 26.

The parallel development, in collaboration with several partner institutions, of the center for electron-microscopy, JEMCA⁶ (Joint Electron-Microscope Center at ALBA), as well as InCAEM⁷ (Infrastructure for Correlative Analysis of Energy Materials), funded with Next Generation EU funds and funds from the Generalitat de Catalunya, within the program of Advanced Materials of the Complementary Plans⁸, contributes to enhance the multimodal instrumentation capacity for tackling complex scientific programs.

With regards to sustainability, ALBA II vision is twofold: providing tools to users to **develop green technologies**, and making the facility a **green infrastructure** itself. The holistic approach will include taking concrete action in relation to external cooperation, research programs and projects, and is aligned to national and international green policies with special attention to research and innovation related to health, environment and energy economy. **ALBA II will be positioned in Europe and worldwide as a positive example for a self-aware and environmental best practice facility.**

The space available for the long beamlines infrastructures (see Figure 1-1) can also host new institutes, as the proposed ASTIP⁹ (ALBA Science-Technology-Innovation Park). The combination of a large research infrastructure and a science park will foster research and create innovation and economic growth, and **a unique high-tech incubator for Spain and specifically for the Catalan area** will be provided.

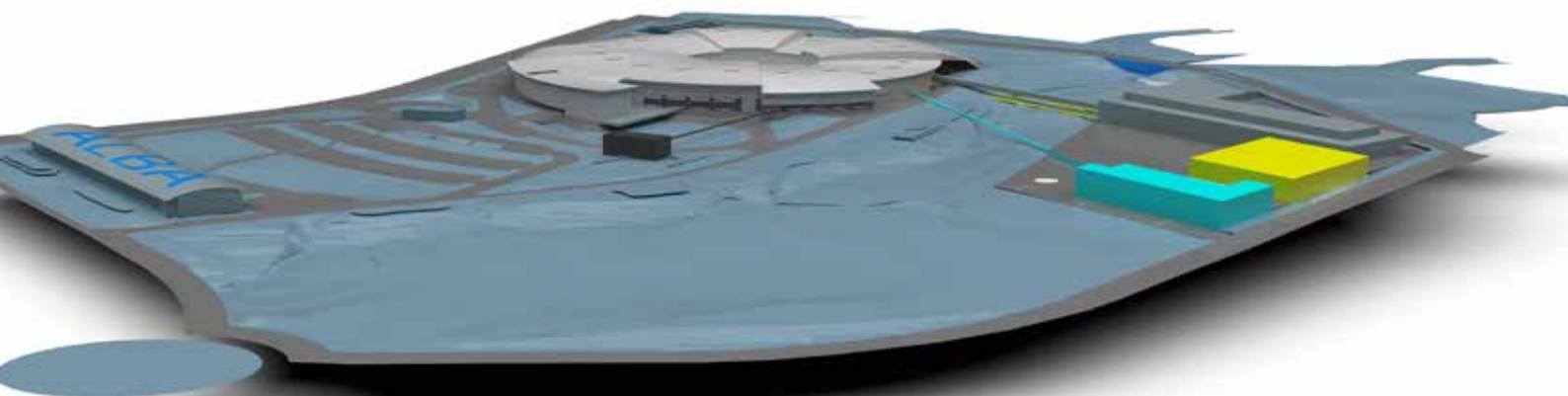


Figure 1-1: ALBA and future ALBA II extension.

⁶ <https://www.albasynchrotron.es/en/instrumentation/jemca>

⁷ <https://www.albasynchrotron.es/en/instrumentation/incaem>

⁸ <https://www.ciencia.gob.es/en/Estrategias-y-Planes/Plan-de-Recuperacion-Transformacion-y-Resiliencia-PRTR/Planes-complementarios-con-CCAA/Materiales-avanzados.html>

⁹ <https://www.albasynchrotron.es/en/media/corporate-publications/astip2021-a4.pdf>

Resumen Ejecutivo

El Sincrotrón ALBA¹, fuente de luz de tercera generación, es un pilar fundamental de la ciencia española y europea, que proporciona capacidades de investigación extendidas y una amplia gama de instrumentación de última generación para usuarios académicos e industriales. El programa científico de ALBA aborda los principales desafíos a los que se enfrenta la sociedad y el programa industrial de ALBA impacta directamente en el crecimiento económico al presentar a los líderes industriales nuevas oportunidades de desarrollo, en última instancia, ventanas de innovación para sus negocios. ALBA desempeña un papel influyente en la formación y educación científica, contribuyendo a la formación profesional dual, preparando y capacitando a jóvenes científicos e ingenieros para su carrera nacional e internacional, brindando modelos a seguir para fomentar la igualdad de género en las disciplinas STEM, promoviendo una cultura general de la seguridad en todos los niveles de actividades, y estimulando la curiosidad por el conocimiento racional y la perspectiva científica en las generaciones más jóvenes. Además, el Sincrotrón ALBA brinda a la comunidad científica y política española una puerta de acceso al resto de instalaciones científicas europeas a partir de su participación activa en LEAPS, la *Liga de Fuentes de Fotones Basadas en Aceleradores Europeos*² y su participación en los programas Horizonte Europa. En otras palabras, **ALBA ha demostrado ser una parte esencial y resiliente del panorama de investigación español** y el personal de ALBA ha demostrado responsabilidad social y de innovación ratificando a ALBA como un activo importante en España.

El progreso significativo de los últimos años en el diseño de aceleradores, la óptica de rayos X, la tecnología de detectores y la tecnología de la información (TI) está impulsando en todo el mundo la evolución de las fuentes de luz de sincrotrón a la **cuarta generación, abriendo nuevas ventanas a la exploración de los detalles internos de la materia, los dispositivos y su funcionalidad**. La brillantez del haz de fotones (fotones por unidad de tiempo, por unidad de área, por unidad de ángulo sólido y por unidad de ancho de banda espectral) y la fracción coherente del flujo de fotones aumentan varios órdenes de magnitud, proporcionando la base para herramientas analíticas inigualables, lo que en última instancia conduce al desarrollo de nuevos enfoques y tecnologías para una economía sostenible, limpia e inteligente y un sistema de salud más eficiente. La primera fuente de luz de cuarta generación operativa fue MAX IV³ y todos los nuevos sincrotrones en construcción pertenecen a esta nueva generación. ESRF⁴ ha sido la primera fuente de luz de tercera generación que se ha modernizado a fuente de luz de cuarta generación con el proyecto ESRF-EBS⁵, y ha sentado las bases para otros muchos proyectos, que actualizarán sus instalaciones durante la próxima década.

ALBA está lista para dar el salto de la 3ª a la 4ª generación y dar a luz a **ALBA II**, combinando la sustitución parcial del acelerador con la actualización de la instrumentación existente y con la construcción de nuevas líneas de luz especialmente optimizadas para ALBA II. De esta forma, ALBA mantendrá su posición actual dentro del escenario europeo y mundial y proporcionará una ventaja competitiva crucial para el ecosistema español de I+D. Las ventajas que aporta la alta brillantez, se potenciarán en términos de resolución y coherencia en las tres nuevas líneas de luz experimentales que tendrán una mayor longitud al poder utilizar parcelas adyacentes a ALBA. La utilización de estas nuevas parcelas, y la construcción de las líneas largas coloca a ALBA en una posición privilegiada para desarrollar instrumentos de última generación y, al mismo tiempo, proporciona a las nuevas líneas suficiente espacio para sus estaciones experimentales e infraestructuras necesarias.

ALBA II continuará el camino emprendido por ALBA y brindará **respuestas a las crecientes demandas de investigación causadas por los desafíos ecológicos y económicos del siglo XXI y las secuelas de la actual crisis social y de salud**.

Actualizar el anillo de almacenamiento, las fuentes de fotones y completar la optimización de la instrumentación **aumentará significativamente la cantidad de fotones en la muestra y, al mismo tiempo, aumentará la resolución espacial**, impulsará el rango de energía utilizable a energías más altas y generará una proporción notable de flujo de fotones coherentes en el rango de rayos X blandos a duros. Con la puesta en marcha de ALBA II, **se aumentará el número de líneas de luz operativas de las 10 actuales a 17**, aumentando proporcionalmente el número de horas de luz ofertadas a los usuarios. En el futuro, todavía habrá oportunidad de ampliar aún más el número de líneas de luz hasta un total de 26.

En paralelo, el desarrollo en colaboración con varias instituciones asociadas, del centro de microscopía electrónica avanzada, JEMCA⁶ (*Joint Electron-Microscope Center at ALBA*), así como InCAEM⁷ (*Infraestructura para el Análisis Correlativo de Materiales Energéticos*), financiado con fondos Next Generation de la EU y con fondos de la Generalitat de Catalunya dentro del programa de Material Avanzado de los Planes Complementarios⁸, contribuye a potenciar la capacidad de instrumentación multimodal para abordar programas científicos complejos.

Con respecto a la sostenibilidad, la visión del ALBA II es doble: **brindar herramientas a los usuarios para desarrollar tecnologías verdes** y hacer de la instalación **una infraestructura verde** en sí misma. El enfoque global incluirá la adopción de medidas concretas en relación con la cooperación externa, los programas y proyectos de investigación, y está alineado con las políticas verdes nacionales e internacionales, con especial atención a la investigación y la innovación relacionadas con la salud, el medio ambiente y la economía energética. **ALBA II se posicionará en Europa y en todo el mundo como un ejemplo positivo de instalación con las mejores prácticas ambientales y de responsabilidad social.**

El espacio disponible para las infraestructuras de las líneas experimentales largas (ver Figura 1-1) también podrá albergar nuevos institutos, como el propuesto ASTIP⁹ (Parque Científico-Tecnológico y de Innovación de ALBA). La combinación de una gran infraestructura de investigación y un parque científico fomentará la investigación y creará innovación y crecimiento económico, y **proporcionando a España y específicamente a Cataluña una incubadora única para empresas de alta tecnología.**

Resum Executiu

El Síncrotró ALBA¹, font de llum de tercera generació, és un pilar fonamental de la ciència espanyola i europea, que proporciona capacitats de recerca esteses i una àmplia gamma d'instrumentació d'última generació per a usuaris acadèmics i industrials. El programa científic d'ALBA aborda els principals desafiaments a què s'enfronta la nostra societat i el programa industrial d'ALBA impacta directament en el creixement econòmic en presentar als líders industrials noves oportunitats de desenvolupament i, en darrera instància, finestres d'innovació per als seus negocis. ALBA exerceix un paper influent en la formació i educació científica, contribuint a la formació professional dual, preparant i capacitant joves científics i enginyers per a la seva carrera nacional i internacional, brindant models a seguir per fomentar la igualtat de gènere en les disciplines STEM, promovent una cultura general de la seguretat a tots els nivells d'activitats, i estimulant la curiositat pel coneixement racional i la perspectiva científica en les generacions més joves. A més, el Síncrotró ALBA brinda a la comunitat científica i política espanyola una porta d'accés a la resta d'instal·lacions científiques europees a partir de la participació activa a LEAPS, la Lliga de Fonts de Fotons Basades en Acceleradors Europeus² i la seva participació en els programes Horitzó Europa. Dit en altres paraules, **ALBA ha demostrat ser una part essencial i resilient en el mapa de la recerca espanyola** i el personal d'ALBA ha demostrat responsabilitat social i d'innovació ratificant a ALBA com a un actiu important a Espanya.

El progrés significatiu dels darrers anys en el disseny d'acceleradors, l'òptica de raigs X, la tecnologia de detectors i la tecnologia de la informació (TI) està impulsant a tot el món l'evolució de les fonts de llum de síncrotró a la **quarta generació, obrint noves finestres a l'exploració dels detalls interns de la matèria, els dispositius i la funcionalitat**. La brillantor del feix de fotons (fotons per unitat de temps, per unitat d'àrea, per unitat d'angle sòlid i per unitat d'amplada de banda espectral) i la fracció coherent del flux de fotons augmenten diversos ordres de magnitud, proporcionant la base per a eines analítiques inigualables, cosa que en última instància condueix al desenvolupament de nous enfocaments i tecnologies per a una economia sostenible, neta i intel·ligent i un sistema de salut més eficient. La primera font de llum de quarta generació operativa fou MAX IV³ i tots els nous síncrotrons en construcció pertanyen a aquesta nova generació. L'ESRF⁴ ha estat la primera font de llum de tercera generació que s'ha modernitzat a font de llum de quarta generació amb el projecte ESRF-EBS⁵, i ha establert les bases per a molts altres projectes, que actualitzaran les seves instal·lacions durant la propera dècada.

ALBA està llesta per fer el salt de la 3a a la 4a generació i donar a llum a **ALBA II**, combinant la substitució parcial de l'accelerador amb l'actualització de la instrumentació existent i amb la construcció de noves línies de llum especialment optimitzades per a ALBA II. D'aquesta manera, ALBA mantindrà la posició actual dins l'escenari europeu i mundial i proporcionarà un avantatge competitiu crucial per a l'ecosistema espanyol d'R+D. Els avantatges que aporta l'alta brillantor, es potenciaran en termes de resolució i coherència a les tres noves línies de llum experimentals que tindran una major longitud en poder utilitzar parcel·les adjacents a ALBA. La utilització d'aquestes noves parcel·les i la construcció de les línies llargues col·loca ALBA en una posició privilegiada per desenvolupar instruments d'última generació i alhora proporciona a les noves línies suficient espai per les seves estacions experimentals i les infraestructures necessàries.

ALBA II continuarà el camí emprès per ALBA i **brindarà respostes a les demandes de recerca creixents causades pels desafiaments ecològics i econòmics del segle XXI i les seqüeles de l'actual crisi social i de salut**.

Actualitzar l'anell d'emmagatzematge, les fonts de fotons i completar l'optimització de la instrumentació **augmentarà significativament la quantitat de fotons a la mostra i, alhora, augmentarà la resolució espacial**, impulsarà el rang d'energia utilitzable a energies més altes i en proporcionarà una proporció notable de flux de fotons coherents en el rang de raigs X tous a durs. Amb la posada en marxa d'ALBA II, **s'augmentarà el nombre de línies de llum operatives de les 10 a 17 actuals**, augmentant proporcionalment el nombre d'hores de llum ofertes als usuaris. En el futur encara hi haurà oportunitat d'augmentar encara més el nombre de línies de llum fins a un total de 26.

En paral·lel, el desenvolupament en col·laboració amb diverses institucions associades, del centre de microscòpia electrònica avançada, JEMCA⁶ (Joint Electron-Microscope Center at ALBA), així com InCAEM⁷ (Infraestructura per a l'Anàlisi Correlativa de Materials Energètics), finançat amb fons Next Generation de l'EU i amb fons de la Generalitat de Catalunya dins del programa de Material Avançat dels Plans Complementaris⁸, contribueix a potenciar la capacitat d'instrumentació multimodal per abordar programes científics complexos.

Pel que fa a la sostenibilitat, la visió de l'ALBA II és doble: **oferir eines als usuaris per desenvolupar tecnologies verdes** i fer de la instal·lació **una infraestructura verda** en si mateixa. L'enfocament global inclourà l'adopció de mesures concretes en relació amb la cooperació externa, els programes i projectes de recerca, i està alineat amb les polítiques verdes nacionals i internacionals, amb una atenció especial a la recerca i la innovació relacionades amb la salut, el medi ambient i l'economia energètica. **ALBA II es posicionarà a Europa i a tot el món com un exemple positiu d'instal·lació amb les millors pràctiques ambientals i de responsabilitat social.**

L'espai disponible per a les infraestructures de les línies experimentals llargues (vegeu la Figura 1-1) també pot albergar nous instituts, com ara el proposat ASTIP⁹ (Parc Científico-Tecnològic i d'Innovació d'ALBA). La combinació d'una gran infraestructura de recerca i un parc científic fomentarà la recerca i crearà innovació i creixement econòmic i proporcionarà **a Espanya i específicament a Catalunya una incubadora única per empreses d'alta tecnologia.**

2 From ALBA to ALBA II

ALBA Synchrotron is managed by the Consortium for the Construction, Equipment and Exploitation of a Synchrotron Light Laboratory (CELLS) and is in exploitation since 2012. It is a member of the Spanish Map of *Infraestructuras Científico Técnico Singulares* (ICTS)¹⁰, and is a public entity participated, in equal parts, by the Spanish and Catalan Governments. The infrastructure includes the accelerator systems, where the 3 GeV electron beam produces synchrotron radiation (SR), the beamlines (BLs) where the synchrotron light is exploited, the Joint Electron Microscopy Center at ALBA (JEMCA), the Infrastructure for Correlative Analysis of Energy Materials (InCAEM), and several additional laboratories.

¹⁰ <https://www.ciencia.gob.es/Organismos-y-Centros/ICTS.html>

2.1. ALBA present

ALBA is fully committed to serve the Spanish and international user community with state-of-the-art instrumentation and services which are built on the use of synchrotron light and enable the research and development community to address the challenges of our time. As a national source, ALBA priorities are focused on the needs of the existing Spanish academic, industrial and entrepreneurial user community as well as developing potential new communities which can greatly benefit from the facility and create new opportunities for the Spanish society. To react on the increasing demands on analytical tools and on developing new research and innovation teams, ALBA sees also an increased role in facilitating networking between different communities and ultimately develop system solutions in concert with these communities largely benefitting the individual user, enabling their to react fast to the grand challenges, requiring minimum resources owned by the individual researcher. These enhanced services will be an essential part of a cost-effective development ecosystem and will specifically support the early researcher community by providing otherwise unreachable resources to fully develop their potential.

In a nutshell, this is expressed in ALBA mission statement:

- Contribute to the improvement of well-being and progress of society as a whole through provision of scientific instruments dedicated to solving societal challenges such as health, energy and communication.
- Act as a catalyst for regional and national collaborations addressing overarching societal challenges.

To achieve these tasks, the traditional understanding of a synchrotron facility as a provider of data is being developed to a next level which addresses important gaps in sample preparation capabilities, a development of user-friendly instrumentation and automatization including automatic data pipelines which allows non-expert user fast access to the data and for industrial user cost-effective access to even complex novel techniques. Ultimately, it also includes the development of methodologies which allow the use of multimodal datasets to understand the complex correlations between structure and function of matter and devices. Addressing these three major tasks efficiently requires to partner with the community for guiding the prioritization and integrating all services into the existing national research and development capabilities. ALBA is starting this transformational change by focusing on three areas: Health, Energy and Environment; and Information and Communication Technologies.

At the time of writing ten beamlines are in operation, two in

commissioning and two more in construction (see Table 2-1 and Figure 2-1), each of them covering wide scientific programs. They are grouped into three scientific sections which reflect their main utilization and which cover the three strategic areas: Life Science, Chemical and Materials Sciences, and Magnetic and Electronic Structure. In particular, the Life Science section is covering the health area, including food and environment, the Chemical and Materials Sciences section the energy and environment areas, and the Magnetic and Electronic Structure of Matter section the information technology area. Using these fields as pilot projects, ALBA prioritizes the development of tools which can be utilized by a broad user community and are enabler technologies. The embedding into the three scientific sections will also ensure the fast and easy role out of new services to the broad user community of ALBA. Following the development of JEMCA and In-CAEM (see Table 2-2), a new scientific section has been recently created, the Interdisciplinary & MultiModal (IMM) section, whose role is to develop all key technologies necessary to perform multimodal experiments with focus on multi-length scale imaging, addressing key problems in all focus areas of ALBA.

All beamlines are oversubscribed, with an average overbooking factor of 2. ALBA operates during 24 hours in 4 to 5 week runs all year long, accumulating almost 6,000 hours per year of operation (see Page 4).

The community of users served by ALBA has grown ten times from the start of operations reaching currently more than 6800 national and international users. The excellence of the top-notch instrumentation and the great level of collaboration with visiting scientists of the highly motivated staff, who provide also support and training for less-experienced users, are key element of the evolution of the community. The more visible outcome of that intense activity is a total of more than 2700 scientific publications, with a high average Impact Factor (IF).

The average number of papers reached per beamline is more than 38, and is outstanding when compared with sister facilities. Other important Key Performance Indicators (KPIs) are related to the average Impact Factor (IF) of the publications and to the percentage of publications above a given impact factor threshold, which for the synchrotron light sources is taken as 7. ALBA is among the best performing synchrotrons of Europe. During 2022 the average IF of the publications was 10 (6 is already considered excellent) and about 50% of the publications had an IF above 7 (30% is already considered excellent).

TABLE 2-1: MAIN TECHNIQUES OFFERED BY ALBA BEAMLINES

PORT AND NAME	SCIENTIFIC SECTION	MAIN TECHNIQUES AND STATUS
BL01 - MIRAS	Life Science	<i>Infrared Spectroscopy & Microscopy - in operation</i>
BL06 - XAIRA	Life Science	<i>Macromolecular Microcrystallography - in commissioning; in operation in 2024</i>
BL09 - MISTRAL	Life Science	<i>Soft X-ray Microscopy - in operation</i>
BL13 - XALOC	Life Science	<i>Macromolecular Crystallography - in operation</i>
BL31 - FAXTOR	Life Science	<i>Fast X-ray Tomography and Radioscopy Beamline - being installed; starting operation in 2024</i>
BL20 - LOREA	Electronic & Magnetic Structure of Matter	<i>Angle Resolved Photoemission Spectroscopy - in operation</i>
BL24 - CIRCE	Electronic & Magnetic Structure of Matter	<i>Photoemission Spectroscopy and Near Ambient Pressure Photoemission - in operation</i>
BL29 - BOREAS	Electronic & Magnetic Structure of Matter	<i>Resonant Absorption and Scattering - in operation</i>
BL04 - MSPD	Chemistry & Material Science	<i>Materials Science and Powder Diffraction - in operation</i>
BL11 - NCD-SWEET	Chemistry & Material Science	<i>Non-Crystalline Diffraction - Small/wide Angle X-ray Scattering - in operation</i>
BL15 - 3SBAR	Chemistry & Material Science	<i>Surface Spectroscopy and Structure at 1 bar - in construction; starting operation in 2026</i>
BL16 - NOTOS	Chemistry & Material Science	<i>Absorption, Diffraction, Instrumentation innovation and development - in operation</i>
BL22 - CLÆSS	Chemistry & Material Science	<i>Core Level Absorption & Emission Spectroscopies - in operation</i>
BL25 - MINERVA	Instrumentation & optics	<i>Metrology and instrumentation - in operation in 2023</i>

TABLE 2-2: ELECTRON MICROSCOPES OFFERED BY JEMCA AND InCAEM

NAME	SCIENTIFIC SECTION	MAIN TECHNIQUES AND STATUS
EM01-Cryo-TEM	Interdisciplinary & Multimodal section	<i>ThermoFisher Scientific, Glacios 200 kV transmission electron microscope equipped with a Falcon 4 direct electron detector. Owned by IBMB-CSIC¹¹ and shared among different partners, including ALBA. In operation since fall 2022</i>
EM02-METCAM	Interdisciplinary & Multimodal section	<i>ThermoFisher Scientific Spectra 300kV monochromatic transmission (scanning) electron microscope with double aberration correction. Starting operation. Owned by ICN2¹² and shared among different partners, including ALBA. First users in 2023</i>
InCAEM - TEM	Interdisciplinary & Multimodal section	<i>In construction, foreseen operation in 2025</i>
InCAEM - AFM/STM	Interdisciplinary & Multimodal section	<i>In construction, foreseen operation in 2025</i>

Dedicated and advanced proprietary services have strengthened the industrial community supporting its technological innovation (see Page 5). ALBA has served so far more than 70 different companies, of which 53% national and 47% international. Around 500 hours per year in average in the last 6 years have been provided to proprietary users. ALBA industrial users mainly belong to the pharmaceutical (43%), chemistry (14%), nanotechnology and high-tech materials (13%) and polymers (10%) sectors. Fueled by the strategic decisions of focusing on energy material research, the contributions of the battery industry are increasing, having reached now up to 6%. The total portfolio of unique proprietary clients at the time of writing is 75, of which about one third are small and medium enterprises (SME), which have been approached also thanks to the leadership role played by ALBA with the TAMATA access initiative implemented in the European CALIPSOplus¹³ and LEAPS-INNOV¹⁴ programs and that will be also implemented in the ReMade@ARI¹⁵ programme on circular economy. More than 500 experiments have come out.

ALBA has adopted the Open Science principles in all public research, and is a member of the European Open Science Cloud (EOSC¹⁶) Partnership, aiming at providing the computational infrastructure necessary for future data reanalysis. This will increase the scientific output of the experiments conducted by making the generated data and the analysis tools available to the scientific community.

An innovation impact study¹⁷ was carried out in 2018 within the framework of the H2020 RI-PATHS project¹⁸ and based on the CSIL¹⁹ methodology. The study analyzed the scientific impact and its spillovers into the society especially into the companies, unveiling that 372 patents worldwide cited ALBA publications in a direct or indirect way, covering a wide range of fields: Human necessities; Performing operations transporting; Chemistry Metallurgy; Mechanical engineering lighting heating; Physics and Electricity. Given the fact that the average time span between publication and patent is six years, we are here seeing the impact of a small part of ALBA activity, corresponding to the first years of its operation, and we expect this innovation impact to be strongly amplified in the coming years.

¹¹ <https://www.ibmb.csic.es/en/>

¹² <https://icn2.cat/en/>

¹³ <https://www.calipsoplus.eu/trans-national-access/>

¹⁴ <https://www.leaps-innov.eu/>

¹⁵ <https://www.remade-project.eu>

¹⁶ [https://ec.europa.eu/info/research-and-innovation/strategy/goals-research-and-](https://ec.europa.eu/info/research-and-innovation/strategy/goals-research-and-innovation-policy/open-science/european-open-science-cloud-eosc_en#what-the-european-open-science-cloud-is)

[innovation-policy/open-science/european-open-science-cloud-eosc_en#what-the-european-open-science-cloud-is](https://ec.europa.eu/info/research-and-innovation/strategy/goals-research-and-innovation-policy/open-science/european-open-science-cloud-eosc_en#what-the-european-open-science-cloud-is)

¹⁷ Catalano, G., López, G. G., Sánchez, A., & Vignetti, S. (2021). From scientific experiments to innovation: Impact pathways of a Synchrotron Light Facility. *Ann Public Coop Econ*, 1-26. DOI: 10.1111/apce.12322

¹⁸ <https://ri-paths-tool.eu/en>

¹⁹ <https://www.csilmilano.com/>

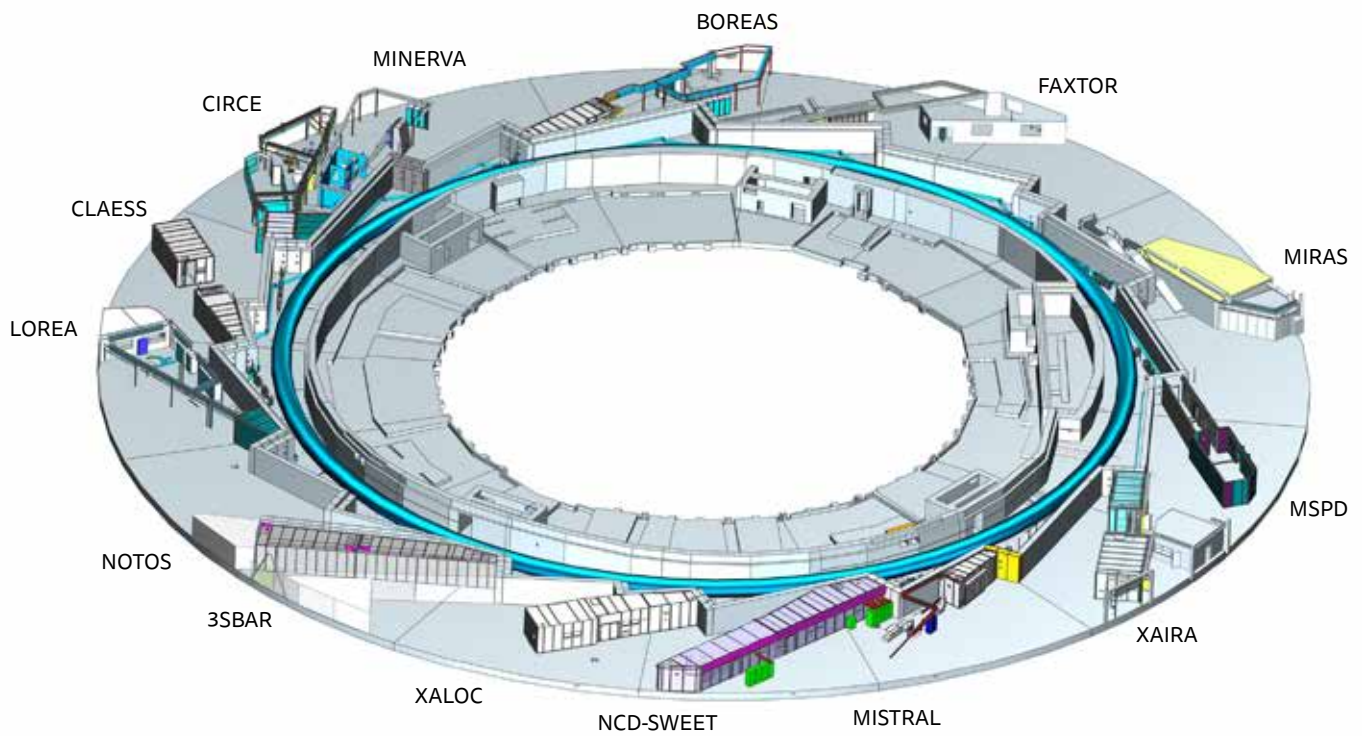


Figure 2-1: Layout of present ALBA Beamlines around the tunnel of the accelerators.

ALBA is an attraction hotspot for the general public and students, welcoming more than 55,000 visitors during the Open Days and the guided tours held during these years. The *Misión ALBA* program, born in 2018 and dedicated to children, has counted with more than 44,000 primary school students and 1,400 teachers from all the regions of Spain. Hundreds of vocational, university and PhD students performed stages at the different divisions of ALBA, upskilling their positioning in a privilege situation for accessing high-tech jobs.

A dynamic outreach program brings the ALBA scientific results closer to the society and shows how they can improve our lives. Efficient training and dissemination programs towards vocational students, school students, high school teachers, undergraduates and early stage researchers have been developed to raise curiosity and to better prepare the future scientists.

2.2. Evolution of synchrotron light sources

The world of synchrotron light sources is making the leap from the 3rd to the 4th generation. The essential difference between the two generations lies in the production of extremely concentrated synchrotron light, with such brightness that it provides advanced properties of resolution, coherence and speed of experimentation. This effect is achieved thanks to technological advances in recent years that allows to concentrate the electrons into volumes more than an order of magnitude smaller than previously. This, together with significant developments in X-ray optics, nanometre-level stability, detection technologies, data acquisition and analysis infrastructures, opens new windows to the exploration of the properties of matter. The coherence and resolution characteristics of the photon beam increase with the distance of propagation, so 4th generation sources also host experimental lines longer than 100 m, which represent the state of the art in synchrotron light methods. This increases resolutions and lowers detection limits to new levels, resulting in a substantial improvement in the capabilities of imaging, spectroscopy and diffraction techniques for unravelling the structure and composition of matter.

There are currently two newly built 4th generation synchrotrons in operation worldwide: MAX IV³ in Sweden since 2017 and Sirius²⁰ in Brazil since 2020. In fact, all new projects under construction

around the world are now 4th generation, as is the case of different projects in China, South Korea and Russia.

A major advantage of this new technology is that it is possible to convert 3rd generation sources into 4th generation ones, with a great cost and time efficiency, by using most of the existing infrastructures, replacing the accelerator structure and part of the instrumentation of the experimental lines. This renovation process culminates in state-of-the-art experimental lines designed to take advantage of the new source parameters and to complement the existing instruments.

The first synchrotron to carry out this transformation has been the European ESRF synchrotron in France, now ESRF-EBS⁵, in operation since the end of 2020, after only one year and a half of downtime to install and commission the new systems. The results of the renovation are excellent and ESRF-EBS is attracting an increasing number of users, who choose it as a reference centre. The ESRF example is being followed by virtually all existing third generation synchrotrons. Figure 2-2 shows the renovation plans of European synchrotrons, which are similar to those in the rest of the world, in particular in US, Canada, Japan, Australia, Taiwan and China. ALBA, being the youngest third-generation synchrotron, will also be among the last to be renewed. After 2030 most of European synchrotrons will belong to the fourth generation.

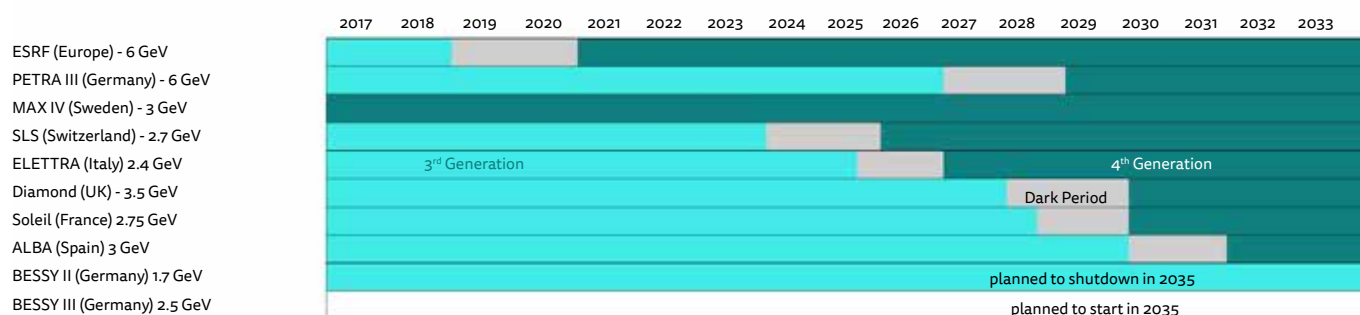


Figure 2-2: Renovation plans for European synchrotrons including a shutdown period of about two years for the installation and commissioning of the new systems.

²⁰ <https://lnls.cnpem.br/home/>

2.3. ALBA future

ALBA will maintain its relevance in the future research infrastructure landscape by upgrading to a 4th generation light source, ALBA II, which will have first users at the end of 2031. The design, construction and part of the installation will be carried out over the next seven years, while ALBA continues operating. This will allow ALBA to host users from the synchrotrons that are shutting down for renovation, which is a particularly interesting opportunity to expand the community of users, including industrial ones, and strengthen collaborative links with leading international experts. 2030 and 2031 will be dedicated to the installation and commissioning of the new light source.

ALBA has the opportunity to use adjacent plots for enlargement with up to three long experimental lines, as shown in Figure 23 plus a fourth one inside the original plot. The corresponding experimental stations are expected to be the seed for advanced centres for materials science, life sciences and innovation, in collaboration with other institutions.

The ALBA II project consists of four main actions:

- **Renovation of the accelerator structure and adaptation of the corresponding infrastructures.** The project includes the design, prototyping, construction of magnets, supports, vacuum chambers, diagnostics and insertion devices for the production of photons, and renovation of power supplies, electronics and conventional infrastructures.
- **Construction of long experimental lines.** The preliminary study, design, construction and installation are carried out while ALBA continues to operate. The commissioning of these lines is postponed until the time when the new source is available.
- **Renovation of the current experimental lines**, including the IT infrastructure, partly due to the fact that they will have been in operation for two decades and partly to adapt them to the new brighter photon beam.
- **Development of the capabilities** for simulation and prototyping, nanotechnology and advanced optics.

ALBA II will also offer the possibility of building other experimental lines within the experimental hall where other light ports are available, which opens the door to consolidate collaborations with other institutions that may be interested in developing joint projects. The maximum number of possible beamlines in ALBA II will be 26.

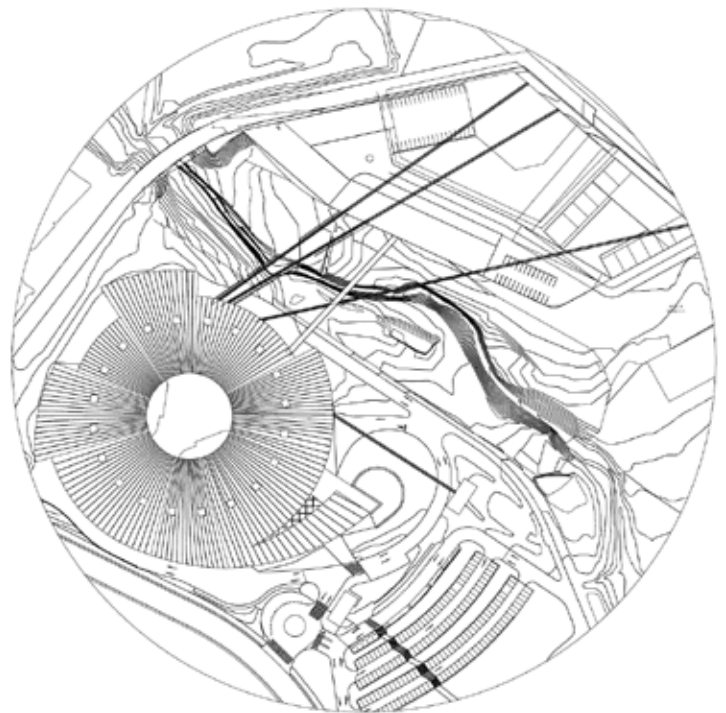


Figure 2-3: ALBA II Layout including long beamline paths.

Additional capabilities of ALBA II compared to present ones include, among many others, 3D imaging at atomic resolution achieved for macroscopic objects, such as CMOS (*complementary metal-oxide semiconductor*) processors, which are essential components of the digital transformation, or for complex materials applied to new technologies, such as quantum technology; experiments will be able to be performed with **extreme speed and efficiency** for different industrial applications; scientific data produced by experiments will increase a hundredfold; by exploiting new high-performance computing infrastructures, new analysis algorithms will be developed, allowing, for example, increased research into new molecular complexes that will greatly benefit the pharmaceutical industry in combating diseases and pandemics; a **multi-modal approach** with different instruments is essential in many technologies in the energy and environmental sector, including the development of catalysts, enablers for the chemical industry, where Spain plays a leading role, and energy storage, an important component of electric mobility and the integration of renewable energies.

By substantially contributing to ALBA II construction, the Spanish research instrumentation industry is provided with a unique opportunity to develop products and train their personnel in accelerator and X-ray technologies, positioning them at the European and global level as high-tech suppliers, entering a global growth market which is characterized by the struggle of satisfying the increased request caused by many simultaneous upgrade projects worldwide (see Page 7).

The ALBA industrial program promotes and makes available to the industrial sector all the potential of the synchrotron services and developments to boost the competitiveness of the industry and benefit the society. ALBA II will expand the portfolio of industrial clients by offering high end services, technological developments opportunities and advanced synchrotron techniques and by rising awareness of the industrial applications of those techniques for boosting innovation and competitiveness of the companies. The superior brightness and coherence of ALBA II photon beam will open advanced synchrotron techniques to tackle the industry challenges in sectors such as energy, pharmaceutical, health, transport, agri-food, advanced materials and quantum computing. The industry ecosystem will also benefit from the implementation of those enhanced techniques by supplying the required equipment or by new technological developments required to meet the demanding specifications of the new ALBA II equipment. All these interlinks will pave the way to the creation of a fruitful interwoven ALBA II-industry ecosystem from which innovation and research will be boosted.

The assessment of the socio-economic impact of ALBA II in the Catalan and in the Spanish environment, as will be shown in chapter 10, is the continuation of the previous studies, the *ex-ante* one in 2004²¹ and the *ex-post* one in 2010²², at the end of the construction. It demonstrates the increased profit of the new investments with respect to the past, thanks to the effectiveness of building-up the upgrade on the existing infrastructures.

In short

The existence of ALBA has generated a community of academic and industrial expert users in Spain who require the most advanced instrumentation for their research and product development. In the coming years, this instrumentation will be concentrated in those infrastructures that are moving towards the next generation.

The possibility of having a state-of-the-art infrastructure that takes advantage of most of the existing one is a very cost and time extremely efficient process and an opportunity which is not to be missed. This is the right time to start the renovation of ALBA so that its contribution to the country's science and industry remains at a high level.

ALBA II will expand its current user base, in particular the applied-science and industrial community, which will have a high impact on the economic potential of the region. The current proposal foresees the construction of three long lines, thus having 17 experimental lines in operation in 2031 and increasing the annual beamtime by 70% compared to today.

ALBA II will be an essential instrument to provide answers to the growing research demands caused by the ecological, energy, health and economic challenges of the 21st century and to achieve the goals of the society of the future. In particular, it will contribute to European programmes, such as those defined in the Next Generation Europe or Horizon Europe plan, to the Spanish programmes that may come after the current State Plan for Scientific and Technical Research and Innovation 2021-2023 and to the R&D policies of the Catalan government, such as the current RIS3CAT-2030, and will keep our scientific and industrial community at the frontier of knowledge and innovation.

²¹ José García Montalvo, Josep María Raya Vilchez, "Potenciant la nova economia a Catalunya", Coneixement i Societat: Revista d'Universitats, Recerca i Societat de la Informació, ISSN-e 1696-7380, N.º 9, 2005 and <https://www.cells.es/es/que-es-alba/transparencia/publicidad-activa/docs-planificacion/acb-impacto-sdv.pdf>

²² José García Montalvo, Josep María Raya Vilchez, LA FUENTE DE LUZ DE SINCROTRÓN ALBA: ANALISIS COSTE BENEFICIO Y ESTUDIO DE IMPACTO ECONOMICO, https://www.cells.es/es/que-es-alba/transparencia/publicidad-activa/docs-planificacion/informe-alba-2010_final_accept_changes-3.pdf

2.4. Bridging to the Spanish and European Research Area

The last decade has seen the flourishing of ALBA collaborations with national and international Research Institutions and Research Infrastructures (RIs), driven by the simultaneous maturity of an operating facility and its remarkable development capacity.

The in-house research program of the beamline scientific staff has developed towards solid collaborations with external entities and is the seed for participation in competitive calls open to answer the societal challenges. This provides means to extend the instrumentation capabilities beyond the basic funding from our stakeholders and to offer co-funded grants for PhD students and Post-Docs.

The active participation in LEAPS from its inception in 2017 has opened opportunities for advancements and developments to the full ALBA community, including its users. ALBA has been acting as LEAPS vice-chair during 2018 and 2019, chair during 2020 and 2021, and vicechair again in 2022. The recent publication of the ESAPS2022^{23,24}, European Strategy for Accelerator-based Photon Science, underlines the European breadth of the national facilities, among which is ALBA. ESAPS2022 charts a transformative route into the future that features environmen-

tally friendly technologies and research strategies to critically support solving societal challenges, while making a core contribution to keep Europe at the international forefront of research and development.

LEAPS-INNOV²⁵, the first proposal granted by the European Commission to LEAPS for a H2020 call, is dedicated to key technological developments in particular those related to the new generation of light sources. It is an example on how the public-private partnership can advance in exploring new approaches, and preparing the industry for being more competitive.

In 2020 a LEAPS initiative brought together all European Analytical Facilities and ARIE²⁶ (Analytical Research Infrastructures of Europe) was born, to profit from the complementarity of the different analytical tools in answering to the present and future societal threats and to develop a better environment for European citizens and the rest of the world.

The evolution towards ALBA II and the development of its environment with new scientific, technological and innovation institutions, will ensure not only maintaining but boosting the competitiveness at international level.

²³ C. Biscari et al., ESAPS 2022, https://leaps-initiative.eu/wp-content/uploads/2022/05/LEAPS-ESAPS-Broschure_final-20052022-3.pdf

²⁴ Abela, R., Biscari, C., Daillant, J. et al. The European strategy for accelerator-based photon science. *Eur. Phys. J. Plus* 138, 355 (2023)

²⁵ <https://www.leaps-innov.eu/>

²⁶ <https://arie-eu.org>



3 Science at ALBA II

The evolution of ALBA to ALBA II is driven by the need of solving pressing challenges of our future by developing methodologies, infrastructure and networks together with the national and international scientific community which can address the characterization needs on all relevant length scales of complex functional systems. Building on ALBA operational strength, its user communities, and the research needs demanded by the Green Deal and other political guidelines, we are presenting a scientific case, which pivots around three focus areas, namely, health, energy and environment, and information and communication technologies. The scientific case is clearly identifying the grand challenges in these fields and is translating these into a characterization challenge which will be mapped on the exceptional opportunities a 4th generation synchrotron source provides.

Our strategy is focusing on imaging structure and chemistry of heterogeneous systems on all relevant length scales and their study under working conditions, ultimately revealing the correlation between structure and function. This will be achieved by visualizing dynamics and the correlated changes of the materials during the essential processes in the systems of interest, exploiting novel correlative imaging techniques including high-resolution imaging methodologies and Transmission Electron Microscopy (TEM) as well as the possibilities that coherent radiation presents. An essential pillar of the strategy is also the implementation of big data research allowing on one hand the identification of the correlation between functionality and relevant chemical and structural changes as well as the acceleration of innovation. This is obtained by providing research results of basic science to applied fields of engineering and science in fields like medicine, energy storage, nanodevices or functional materials, including reliability, and lifetime prediction. We want to emphasize that, even if developed around the three focus areas, most of the tools will benefit the vast majority of the current and potential future Spanish user community, amplifying the return of investments for the Spanish research community as a whole.

ALBA II, with its focus on correlative imaging, timely providing statistically relevant data amounts, and optimized operando conditions, is the necessary step to grow ALBA to a facility which promotes and enhances innovation and sustainable economic growth based on the strong national and international research community. Implementing this multimodal approach in all aspects of policies, analysis and instrumentation will create sophisticated tools to address real world problems, giving to the Spanish industrial, entrepreneurial and academic user

community a unique platform for building and fostering a culture of innovation. Moreover, ALBA II will give to many Spanish innovation communities an important asset for linking with European partners, ensuring fast development of even extremely challenging solutions and ultimately long-term economic success.

ALBA mission statements, namely contribute to the improvement of well-being and progress of society as a whole through provision of scientific instruments dedicated to solving societal challenges such as health, energy and communication, and act as a catalyst for regional and national collaborations addressing overarching societal challenges, are built on this evolution of ALBA to ALBA II by routing innovation into the DNA of the facility.

As already mentioned, ALBA is starting this transformational change by focusing on three areas: Health, Energy and Environment and Information and Communication Technologies. Each of the three scientific sections of the Experiments Division with its instrumentation is covering and dedicated to one of these areas; in detail, the life science section is covering the health area, including food and environment, the chemical and materials sciences section the energy and environment area, and the magnetic and electronic structure section the information and communication technologies area. Developed for these three areas, serving as pilot projects for baselining and measuring the effectiveness, ALBA will prioritize the development of tools based on the general usability of a broad user community and their impact on the scientific and economic driver-technologies. By embedding the developments into the three scientific sections we will also ensure the fast and easy role out of new services to the broad existing user community of ALBA.

3.1. Health

The environmental, food and health emergencies, especially that of COVID-19, have put life sciences research into the center of the entire society. Life sciences research at ALBA is thus requested to help unravel the mechanisms of living organisms through basic research but also to provide effective tools to guide informed and rational policy making. Growing around our current strength and strategies to provide tools across the borders between tissue, cellular and macromolecular biology, the instruments and technologies available at ALBA II will enable to study life in a broader view, change the understanding of our intimate nature and provide new approaches for health care, disease control, food security and environment surveillance.

This broader view of the life science research oriented to effectively tackling societal challenges is multi-scale, integrative and multidisciplinary. Life organizes in different spatial scales,

each having characteristic complex structures as shown in Figure 3-1. Regardless the level is macromolecule, organelle, cell or tissue, the mechanisms of life that are taking place in a level reflect on the others sometimes in a seemingly chaotic way unless a set of techniques and data analysis are available to study several scales on the same system. The correlation between data from different techniques is compelling for a complete view of the studied processes or structures. Another important aspect to be carefully looked after is sample preparation and conditioning, as living and biological systems are better understood when the structural information is produced from the most preserved and fully networked, environment possible.

Many socially relevant topics can be studied using modern approaches: pathogen infections, antibiotic resistance, crop resistance to climate change, cancer and diseases, ultrastructure

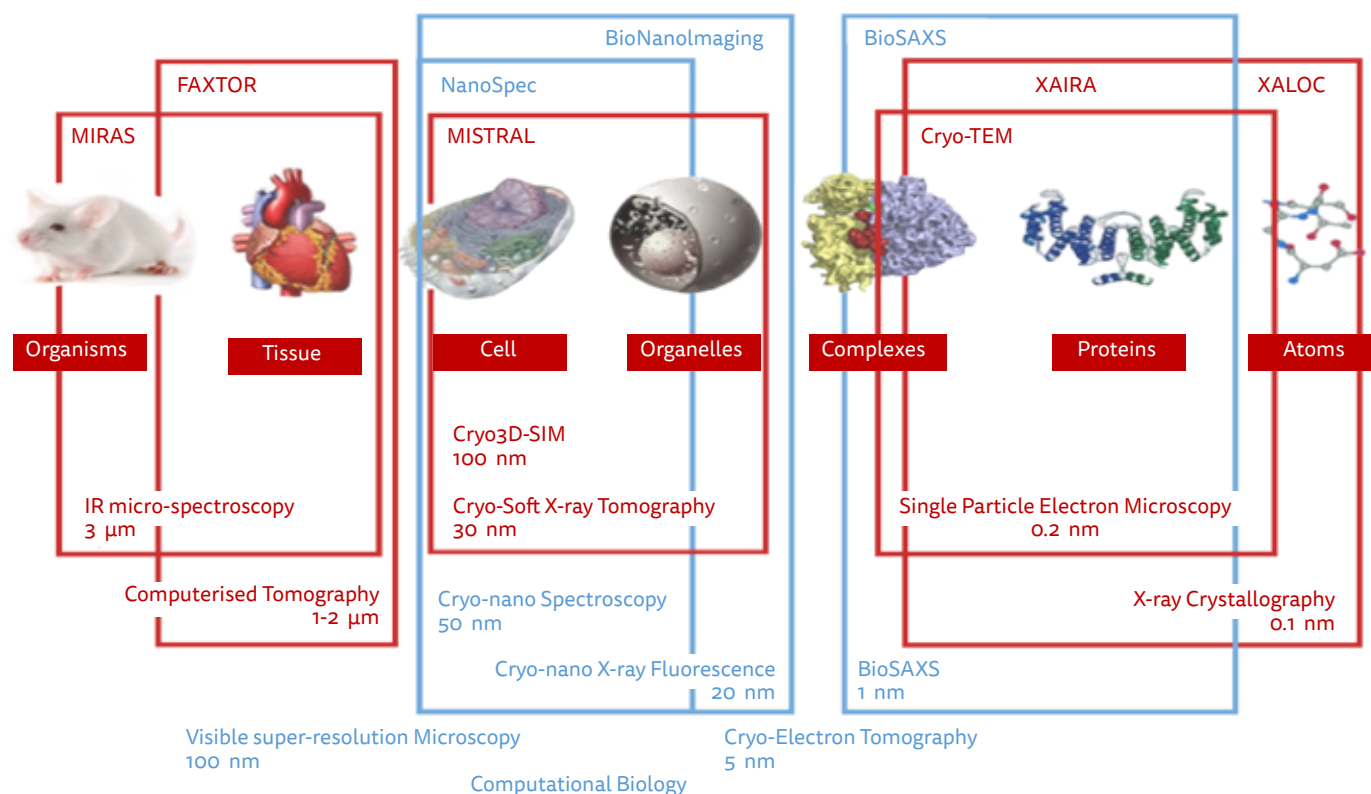


Figure 3-1: Multi-length scale approach of ALBA and the expected impact of ALBA II. The individual boxes indicate the role of the existing (in red) and expected (in blue) instruments. The boxes show the technique and typical resolution (bottom) achieved at the ALBA instrument (indicated at the top). Expected non-X-ray instruments or services are shown unboxed. ALBA II will not only strengthen the program of most existing beamlines by providing more photons on a smaller spot but most prominently will close the gap between the cellular and the macromolecular biology [adapted from Harkiolaki et al. DOI:10.1042/ETLS20170086].

of healthy and infected cells and tissues, drug delivery and distribution, bionanomaterials and structure-based time-resolved enzymology, among others. ALBA and increasingly ALBA II is and will provide not only the instruments portfolio appropriate to face these research challenges but also builds on the supporting infrastructure like sample preparation laboratories, non-X-ray tools like the cryo-EM platform or super-resolution visible light microscopies, computational capabilities and, perhaps most importantly, methodologies and expertise to integrate ALBA tools into the methods used by the corresponding communities. Some of these are already heavily using ALBA but others, especially in the area of cellular biology and the various biomedical disciplines are potential communities with high growth potential at ALBA II, a facility built around multi-length scale and correlative imaging.

The integrative study of such relevant systems requires the use of many synchrotron-light-based techniques, some of them are currently available at ALBA (Figure 3-1). Macromolecular crystallography (including serial- and micro-crystallography) is available and extensively used at ALBA for studies at macromolecular level. At cellular and tissue levels cryo soft X-ray tomography and infrared microscopy and spectroscopy experiments are also routinely performed, while hard X-ray computed tomography will become available soon. Still, in our multi-scale, integrative vision, life sciences studies combine these synchrotron-based techniques with others based on electron or visible light probes. Following this vision, ALBA has already developed a cryo-3D-SIM super-resolution microscope to correlate visible-light studies with soft X-ray tomography, and is hosting a cryo-electron microscope for single-particle analysis⁶. Moreover, all the above techniques can be coupled with advanced molecular and cell biology methods available at the level 2 biological laboratories.

The life science program of ALBA II will build on strongly interlinked state-of-the-art characterization tools, combined with supporting infrastructure for sample preparation and computation, necessary to promote multi-length scale and correlative imaging and to plug these highly innovative toolsets into the research portfolio of the existing and potential Spanish life science and health communities. To this aim, some important techniques still missing at ALBA are included in our upgrade strategy. At macromolecular level, small-angle scattering (BioSAXS) is essential for the study of macromolecules in solution. Nano-X-ray fluorescence tomography at cryogenic temperature (BioNanoImaging) provides 3D imaging and quantification of trace endogenous or exogenous elements, such as drugs or contaminants, at very high sensitivity in whole cells in close-to-native conditions or tissue sections at room temperature. The instrument also enables phase contrast tomography at sub-micron resolution, which reveals the ultrastructure of isolated cells, organoids or biological soft tissues. Last in the synchrotron-based techniques but not least, cryo-nano-spectromicroscopy (NanoSpec) unveils the chemical state of relevant elements within the cell. Combined with these synchrotron-based instruments, the upgrade plan foresees to strengthen the cryo-electron microscopy facility (JEMCA) to include advanced sample preparation tools and cryo-electron tomography.

Essential for being successful to serve this broad field, spanning the research on complex networks such as brain, lungs or cardiovascular systems, over gene therapy, drug delivery, to drug development, is the good balance of high throughput and

highly sophisticated ultra-high-resolution techniques. With the BioNanoImaging and the upgraded JEMCA capabilities, ALBA II will push the high-resolution tools of ALBA already existing imaging portfolio but will also strengthen with FAXTOR and an upgraded MISTRAL the medium- and low-resolution throughput capabilities, essential to provide statistically relevant sample sets and overcome the natural variability of the biological samples.

The future of structural macromolecular biology at ALBA II will fully build on the exciting current developments in this field and ALBA existing community. The program will cover the classical need of structural biology with abilities to extend the program to time-resolved studies, able to characterize meta stable conformations, crucial to understand the mechanisms of life. The strategy foresees XALOC beamline being focused on high throughput and broadening the methods of crystal delivery, and XAIRA beamline, a state-of-the-art micro-focus beamline with native phasing capabilities, focused on poorly diffracting crystals and fixed-target serial crystallography. Integrating computational biology in the workflow and including a new beamline focused on BioSAXS in combination with the new cryo-EM program will bring a complete toolset for advanced research and proprietary projects on structural macromolecular biology.

This joint effort in tissue, cellular and macromolecular biology gives hope to ultimately provide a full picture of biological processes, from organs and tissues down to the smallest building blocks, the atoms. Today nearly unimaginable, ALBA II as a package of enhancing brilliance and integrating multimodal concepts provides all ingredients to participate on this international grant challenge and race, empowering the Spanish community with competitive tools for the future and opening new opportunities like the integration of these tools in new response centers fit to find solutions for upcoming health and food security challenges.

3.1.1. DRUG DELIVERY (CORRELATIVE MICROSCOPY)

ALBA, in concert with its user community and international partner facilities, had played a pivot role in the development of a new correlative methodology allowing to image the location of a drug within cells, allowing to locate the drug within the individual organelles. This pilot project shows clearly the potential of high health and commercial impact on the development of future drugs and drug delivery systems; ALBA II will allow to bring this methodology from a pilot level to a readily available tool for the drug development community without the need to become experts in all required tools.

The so-called Iridium half-sandwich complex is an extraordinary anticancer compound, 15-250 times more powerful than the widely used cisplatin in a number of cell lines. Intracellular drug localization and quantification is a mandatory step to understand both on-target and off-target effects and so as to improve rational drug design. Until recently, no optimal approach was available. X-ray fluorescence microscopy is used to locate the target compartment, but it cannot image non-labelled structures, thus losing the whole cell context, and do not allow for quantification. Quantitative elemental analysis of cell fractions by means of Inductively Coupled Plasma Mass Spectrometry (ICP-MS) can help shed light, but it involves mechanical manipulation of the

cell sub-fractions, which can result in disruption of the – perhaps already compromised – organelle wall. Perturbations to avoid include chemical fixation and endogenous element leakage, labeling, and mechanical manipulation of the cells. In brief, the intracellular drug localization and quantification requires to gather structural and chemical information of near-native conditioned cells at nanometer scale.

Only recently the full picture could be attained by correlating data from different techniques taken from the same sample²⁷. The cryo soft X-ray tomography provided the structural information of the cryo-preserved cell while the X-ray fluorescence tomography enables the localization of the Iridium compounds within the cell. The experiments were performed at MISTRAL beamline in ALBA (at a resolution of ~40nm) and at ID16A beamline at the ESRF (at a resolution of ~100nm, for Ca, Cl, K, Mn, P, S, Zn and Ir edges), respectively. The methods for this correlative approach had to be developed in the framework of this collaboration. The experiments could be entirely done at ALBA II with the help of the expected Cryo-Nano-Imaging beamline.

This study identified unequivocally the intracellular fate of the potent iridium cytotoxic ACC25, which includes the Iridium half-sandwich complex ([Ir(η^5 - κ^1 -C₅Me₄CH₂py)(2-phenylpyridine)]PF₆) in the human breast cancer cell line MCF7 in close-to-native cellular context (Figure 3-2). The compound was localized unambiguously in mitochondria, and not in other cell organelles, relating its accumulation to cytomorphological alterations in MCF7 cells at nanometric resolution. The method workflow also included TEM experiments, from which the cytomorphological alterations related to cell death, and visible light cryo-epifluorescence, to select the best samples for the X-ray techniques.

This original correlative and quantitative method is of general interest as it combines element 3D localization with 3D cell structural information at high spatial resolution, and can be readily applied to help understand the intra-organelle trafficking of a number of elements related to a multitude of biochemical processes in the human cell.

Another good example of correlative multi-scale study is the one of the progressions of SARS-CoV-2 infection in the native cellular context combining serial cryoFIB/SEM volume imaging and soft X-ray cryo-tomography with cell lamellae-based cryo-electron tomography (cryoET) and subtomogram averaging²⁸. The study reports critical SARS-CoV-2 structural events in the context of whole-cell volumes which reveal drastic cytopathic changes. The events include viral RNA transport portals, virus assembly intermediates, virus egress pathway, and native virus spike structures. This integrated approach allowed a holistic view of SARS-CoV-2 infection, from the whole cell to individual molecules.

This inter-facility collaboration has been demonstrating the potential input of this methodology if it would be readily available to a larger non-expert community. ALBA II with its ability to provide a CryoNanoImaging probe with specifications at the top of the available instruments will allow to integrate a high-end optimized bio-nano probe with the corresponding complex sample preparation tools and cryo-EM imaging tools at one laboratory. The close proximity of all instruments will not only promote the effective collaboration of all required groups for developing protocols and even methodologies to be followed by non-expert

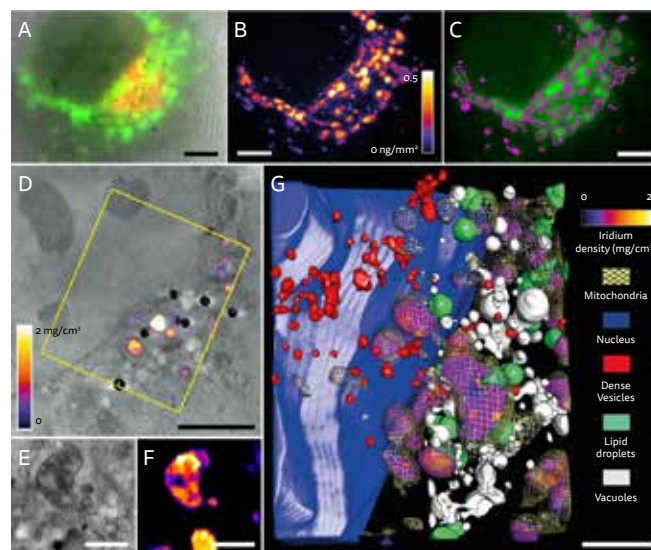


Figure 3-2: Determination of intracellular location of iridium in human breast cancer MCF7 cells. (a) -shows an image of an MCF7 cell treated with 1 μ M ACC25 for 12 h, which is an overlay of Soft X-ray microscopic imaging (grey) and epifluorescence signal (green, mitochondria; red, acidic organelles). (b) shows the Ir distribution imaged by 2D XRF on the same cell. (c) is an overlay of the epifluorescence mitochondria signal (green) with a mask generated using the Ir signal shown in (b). The two signals correlate to each other. (d) shows a selected area of the cell in (a), as an overlap of two reconstructed slices from the cryo-SXT and the XRF tomography, respectively (XRF acquisition area squared in yellow). Ir densities are shown. (e) and (f) compare slices across the mitochondria from the cryo-SXT and the XRF tomography results of the same area, illustrating the location and concentration of Ir signal inside mitochondria. (g) shows the 3D rendering of the yellow square area in (d) after segmentation of the organelles. The Ir signal is displayed with the same colour density scale as in (d) and (f), different organelles are displayed. Scale bars: (a)-(d) 5 μ m; (e) and (f) 1 μ m; (g) 2 μ m.²⁷

users but also allows a fast turnaround with optimized workflows providing statistically relevant sample sizes (in the number of investigated cells), both essential to make this methodology from one-of-a-kind to a high impact tool for the health system. The one-stop-all-shop approach, facilitated by one facility, will also act like a catalyst to make this toolset and methodology easily available so that a large community can benefit from these high-end tools.

3.1.2. INTEGRATIVE BIOLOGY AND TIME-RESOLVED ENZYMOLOGY

Integrative structure determination aims at modeling the structures of biological systems from different experimental data and theoretical methods. An excellent example of this approach is the structural elucidation of the yeast nuclear pore complex (NPC)²⁹. The NPC is a very large (50–100 MDa) macromolecular assembly consisting of ~500 copies of 30 different structured and partly intrinsically disordered proteins, known as nucleoporins (Figure 3-3). It is the only known conduit for trafficking between the nucleoplasm and cytoplasm, and mediates the active exchange of a large range of proteins and RNAs. NPC interacts with many different macromolecules in a large dynamic range from ultrafast (such as with transported macromolecules) to stable (such as between scaffold components). The structural determination of the yeast NPC is key for an insightful understanding of its functionality, which ultimately may lead to a rational control of its mechanisms.

As the toolbox of techniques and methods continue to improve, integrative structural biology will be increasingly applied not only to discover the basic mechanisms of life systems, but also to

²⁷ Conesa et al. *Angew. Chem.* 59, 1270–1278, 2020

²⁸ Mendonça et al., *Nat. Comm.* 12,4629, 2021

²⁹ Rout and Sali, *Cell* 177, 1384–1403, 2019

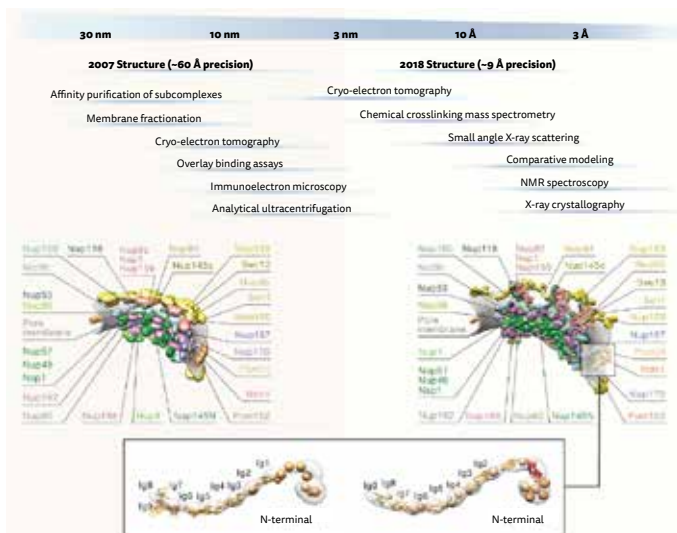


Figure 3-3: Techniques used for the structural determination of the yeast nuclear pore complex (NPC), as solved in 2007³⁰ and 2018³¹. The integration of a larger amount of more precise data led in turn to a structure with a higher precision. Shown in the inset is a comparison of the representative pore membrane nucleoporin Pom152 models.³⁹

drug discovery. As a result, it will enable to rationally target larger systems in addition to single proteins.

Life science studies do not only expand the knowledge in the different spatial scales, they also do it in the time domain. Time-resolved crystallography studies in 4th generation synchrotron and X-ray free electrons laser (XFEL) facilities are now available using serial crystallography methods. A good example is the study of structural changes of bacteriorhodopsin (bR), the protein in archaea responsible of absorbing light to produce a proton gradient which is subsequently converted into chemical energy³². Using the XFEL source, the early events in the proton pumping cycle were characterized, including the ultrafast process of photon energy capture through photoisomerization of retinal³³, and the proton release step from the retinal Schiff base toward the extracellular side of the membrane³⁴. Synchrotron source experiments could elucidate the changes from the first 5 ms after photoactivation. After 10 ms, large additional structural rearrangements up to 9 Å were observed on the cytoplasmic side, leading to the formation of a water chain.

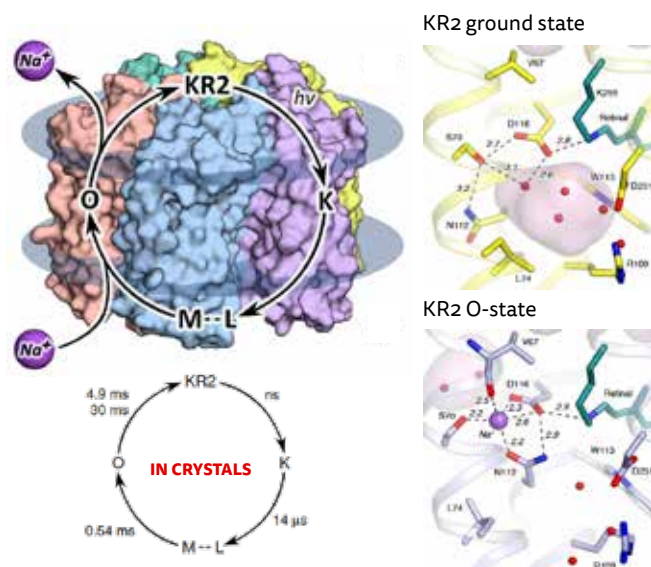


Figure 3-4: First time-resolved crystallography experiment at ALBA. Scheme and time scales of the light-driven sodium-pumping KR2 rhodopsin photocycle (left). The Na⁺ binding occurs transiently in the O-state, that was captured by photoactivation of crystals delivered by the XALOC jet-based injector. Detailed view of the Schiff base region of the ground and the O-states of KR2. (right) Cavities are marked in pink. The results allow to propose a pathway and molecular mechanism of the active light-driven Na⁺ transport.³⁵

Time-resolved studies are also being developed at ALBA. The jet-based serial crystallography setup at XALOC, together with a photoactivation system, has been employed to reveal an activated intermediate of the sodium-pumping rhodopsin KR2 from *Krokinobacter eikastus*, the only non-proton cation active transporter with demonstrated potential for optogenetics at a time resolution of few ms (Figure 3-4)³⁵.

ALBA II will enable in full extent the time-resolved synchrotron serial crystallography methods. The foreseen diffraction-limited source with higher flux density and the state-of-the-art optics and end-station instrumentation will optimize the X-ray beam and the sample conditions for high time-resolution experiments. Following the experiences of other facilities, potent nanosecond lasers integrated in the updated beamlines in combination with employing faster detectors enable a more precise time signature of the experiment. Altogether these factors may push in the near future the time resolution from the few milliseconds down to the lower microsecond range to cover the majority of biologically relevant protein dynamics.

³⁰ Alber et al., Nature 450, 683–694, 2007

³¹ Kim et al., Nature 555, 475–482, 2018

³² Weinert et al., Science 365:6448 61–65, 2019

³³ Nogly et al., Science 361, eaato094, 2018

³⁴ Nango et al. Science 354, 1552–1557, 2016

³⁵ Kovalev et al. Nat Comm 11, 2137, 2020

3.2. Energy and environment

In the area of energy, ALBA is focusing on needs resulting from the carbon neutral circular economy and that from energy storage with smaller engagement in energy production, e.g. polymer based photovoltaic systems. In the following, catalysis, as one of the enabling technologies for the carbon neutral circular economy, and batteries, as a specific example of storage, are used to explain how ALBA II will contribute to the overall problem as defined by the Green Deal. The examples will motivate the importance of the relevant technologies, identify key materials and their functionality enabling the technologies and finally derive the characterization challenges for developing new materials, the basis for the sustainable economy.

3.2.1. CATALYSIS

The relevance of catalysis for the society is highlighted by the European Green Deal, aiming among other points at the development of a prosperous sustainable full carbon neutral cycle economy, or in other words an economy which is based on carbon sequestration and valorization, or in other words removing or avoiding concentrations of warming gas from the atmosphere. FReSMe is a large-scale project for valorization of CO₂ on an industrial level and is a good example how these new technologies will benefit the Spanish economy and at the same time will effectively build a sustainable economy. The results obtained by this project, an European consortium led by a Spanish business (i-deal) and funded under the Horizon2020 program, had demonstrated that the existing technology for CO₂ to Methanol is mature enough to valorize CO₂ from a blast furnace of a steel production site, largely responsible for CO₂ emissions, and green H₂; it also developed a full business case for a CO₂ to methanol economy by using the produced Methanol as maritime fuel for a large-scale commercial ferry³⁶.

The industrial implementation, developed by ThyssenKrupp, currently in the test phase and classified as TRL7-TRL8, is another example for a full-scale circular economy, including key areas currently taken by fossil resources which shows the economic importance and at the same time the real-world challenges of turning carbon intense steel or cement production into a carbon neutral circular economy. By using the flue CO₂ gas in combination with green H₂, meaning the H₂ is produced with renewable energies, a hazardous greenhouse gas becomes an important resource for the chemical industry and fuels³⁷.

FReSMe and even more ThyssenKrupp's business model shows clearly that a Carbon neutral economy has to be understood as a system change and a challenge, requiring technologies for harvesting of renewable energies, the generation of green hydrogen using these renewable energies, efficient filtration and concentration of CO₂, and finally and most obviously, novel process technologies producing the value chain from synthetic fuels for transportation and combustion based energy production, over raw material production for the chemical industry to the existentially necessary production of fertilizers. Due to the decentralization of the energy production, these technologies have to be compatible and economic with smaller facilities. The development and optimization of existing catalysts, a field in which a wide range of ALBA existing user community are actively working and successfully engage with industry, is indispensable so that policy changes and the economic pressure can facilitate this life-saving economic transition.

Moreover, the large impact of catalysts on the environmental friendliness and cost effectiveness by providing increased selectivity, higher yields and lower energy consumption and the use of abundant materials for these new catalysts, makes these new developments often to true enablers for affordable and broad applicable technologies, essential for this transition; many real-world applications will not be either ecological compatible or economical sustainable without their availability, making their development a key for success. Synchrotron and TEM based characterization tools, as shown below, can help not only to systematically develop new classes of materials appropriate for these catalytic tasks, but also can accelerate the development to high TR-levels by elucidating on the mechanistic processes resulting in degradation and ultimately finding new strategies to overcome the degradation of the catalyst, essential for economic success. ALBA II with its integrated multimodal approach and the strengthening of high throughput and microscopy tools will allow a large ALBA user community, devoted to catalytic developments, to participate on this exciting race for economic growth and prosperity, ultimately strengthening Spain's importance and influence.

We will focus on three specific catalysts important to the circular Carbon neutral economy to understand which tools and services has to be provided by a future ALBA II; two of the catalysts are used to hydrogenate CO₂, one for complete oxidation of Synthetic Natural Gas (SNG) in combustion applications for avoiding the emission of potent CH₄ as greenhouse gas; one case offers insights

³⁶ <https://i-deals.es/project/fresme/>

³⁷ https://ucpcdn.thyssenkrupp.com/_legacy/UCPthyssenkruppBAISMicositePowertoX/assets.files/power-to-x/hydrogen-brochure.pdf

in the hydrogenation to make methanol, an important chemical which can either be used as a fuel or as an important raw material for the chemical industry, the other case in making methane which is referred as Synthetic Natural Gas (SNG) if produced from CO₂. All three catalysts are in the early development phase, show exceptional performance and require a complex structure on various length-scales to facilitate all intermediate reactions necessary to reduce the carbon of the CO₂ and ultimately perform the hydrogenation or oxidation. Currently lacking the full understanding of these important catalysts, these systems are good examples for defining the characterization challenges, the future ALBA II has to answer.

The Fundamental Challenge of Understanding the Reactivity of Catalysts: Heterogeneous Catalysis for Methanol Production

As used in the example of the FReSMe project³⁶, Cu-ZnO-Al₂O₃ is currently the most used catalyst for industrially produced methanol from CO₂ and hydrogen and is consequently studied by many researchers.^{38,39} However, the widely use of this catalyst, as necessary for the valorization of effluent CO₂ from industries with high carbon foot print and green hydrogen, may be seriously hampered by its pyrophoric character, resulting in safety concerns, and perhaps more importantly by its susceptibility to poisoning by water vapor, a necessary byproduct of the reaction, which results in ZnO agglomeration, Cu oxidation, sintering, and ultimately to degradation.^{38,40,41} In addition, there are concerns about the abundance of Zn within the next decade, especially important for the needs of large industrial quantities needed for the application⁴².

Within the set of alternative catalysts currently proposed, Mo/TiO₂ catalysts form an interesting class which is using abundant materials and is not poisoned by the water vapor. As Figure 3-5 shows, yield and selectivity are largely correlated to the choice of the TiO₂ substrate, more precisely the mixture between rutile and anatase phase of the substrate, the distribution of crystalline facets, and its exact structure, hinting the ability to optimize

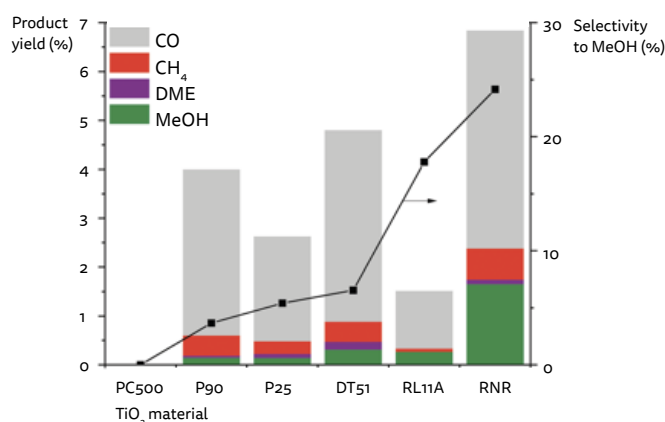


Figure 3-5: Effect of TiO₂ nature on product yields and methanol selectivity for 3Mo/TiO₂ catalysts at 275 °C under 30 bar of H₂/CO₂/N₂ (3/1/1), GHSV = 7500 mL g⁻¹ h⁻¹.³⁸

the structure for higher selectivity and yield³⁸. A closer analysis reveals however that there is no simple correlation between phase mixture and yield or selectivity. For example, the RL11A sample shows the highest selectivity but the lowest yield, whereas the RNR sample has one of the poorest selectivity but the highest yield, even if both samples use a 100% rutile TiO₂ substrate.

The high-resolution Scanning Transmission Electron Microscope (STEM) micrograph using a high-angle annular dark field (HAADF) detector, shown in Figure 3-6, gives a first hint on the origin of the catalytic activity. The structure of the surface of a 2.9 wt% of Mo loading on a 100% anatase phase of TiO₂ (3Mo/DT51D) is compared with that of a 2.9 wt% of Mo loading on a 100% rutile phase of TiO₂ (3Mo/RNR), which are the two samples from Figure 36 providing the highest yield. Both of these samples show, that Mo is growing either as a single atom or in small sub-nanometer 2D clusters.

To understand the chemical state of the Mo atoms, Near Ambient Pressure X-ray Photoelectron Spectroscopy (NAP-XPS) is employed which allows to characterize the valence state of Mo which is on the surface but also that which may be embedded into the TiO-matrix. Figure 3-7 shows the results of these investigations for the rutile (RNR) and the anatase (DT51D) sample for different process temperatures and under reaction conditions. Additionally, the data are compared with a third sample which uses an 80% anatase / 20% rutile phase substrate and a similar Mo load (2.8 wt%) and due to the applied preparation method shows a different facet-ratios than the other two samples³⁸. Clearly, the specific structure of the substrate impacts strongly the valence state of the Mo which ultimately is key to the active site itself, responsible for the specific reaction. Understanding the structure and chemical composition of the active site, which is most likely involving a set of atoms including specific defect sites, will be the prerequisite to rationally design an optimized catalyst which at the same time will show high yield and high selectivity.

ALBA II with its multimodal approach and the increased capabilities to provide correlative microscopy will be an essential asset to come closer to this goal. Using the example

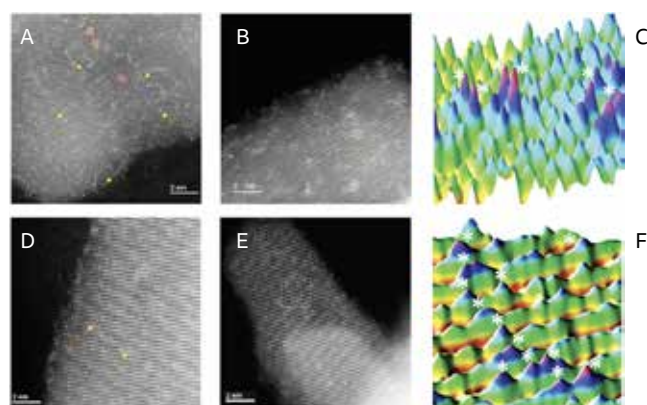


Figure 3-6: Representative aberration-corrected STEM-HAADF micrographs. (A and B) 2.9 wt% of Mo loading on a 100% anatase phase of TiO₂ (3Mo/DT51D); (D and E) 2.9 wt% of Mo loading on a 100% rutile phase of TiO₂ (3Mo/RNR). Arrows and circles in (A) and (D) show single Mo atoms and Mo clusters, respectively. (C and F) Color-map representation of the intensity in the 2 nm² yellow square represented in (B) and (E), respectively. The white stars indicate the Mo atoms.³⁸

³⁸ Green Chem., 2021, 23, 7259–7268, DOI: 10.1039/d1gc01761f

³⁹ Zhang X, Zhang G, Song C and Guo X (2021) Catalytic Conversion of Carbon Dioxide to Methanol: Current Status and Future Perspective. Front. Energy Res. 8:621119. DOI: 10.3389/fenrg.2020.621119

⁴⁰ B. Liang, J. Ma, X. Su, C. Yang, H. Duan, H. Zhou, S. Deng, L. Li and Y. Huang. Ind. Eng. Chem. Res., 2019, 58, 9030–9037.

⁴¹ O. Martin and J. Pérez-Ramírez, Catal. Sci. Technol., 2013, 3, 3343–3352.

⁴² Element Scarcity - EuChemS Periodic Table, <https://www.euchems.eu/euchems-periodic-table/>

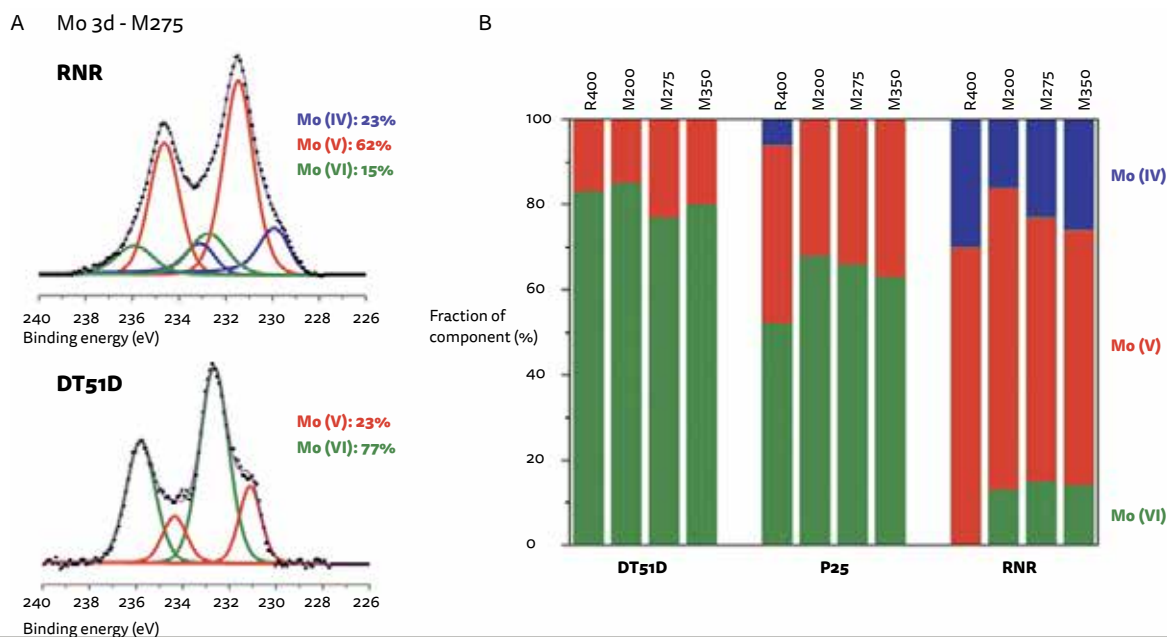


Figure 3-7: (A) Mo 3d NAP-XPS analysis at 275 °C under 2 mbar of a 3/1 H₂/CO₂ mixture on 3Mo/RNR (top) and 3Mo/DT51D (bottom). (B) Mo oxidation state distribution in 3 wt% Mo supported on DT51D, P25 and RNR TiO₂ determined from NAP-XPS (Mo 3d), during in situ reduction at 400 °C (R400), and exposure to the CO₂/H₂ reactant mixture (3/1) at 200 °C (M200), 275 °C (M275) and 350 °C (M350).³⁸

of another catalyst for the methanol production, a highly selective and at the same time high yield, macroporous Cu-ZnO-ZrO₂ (CZZ) catalysts visualize the full complexity, an active center can have. Current work shows clearly that the details of the complex three-dimensional ordered macro-porous (3DOM) CZZ catalyst largely determine yield, selectivity and process temperature^{43,44,45,46} more importantly, the structure-function correlation, or better the question “how does the catalyst work” can be revealed by the multimodal approach under operando conditions, which combines the functional and structural data sets.

The porous support structure of Copper is not only responsible for the transport of the feed- and reaction products throughout the system, provides an enormous effective surface, but also has a significant part on the chemical reactivity of the embedded nano particles. Operando InfraRed (IR) measurements, more precisely Diffuse Reflectance IR Fourier Transform Spectroscopy (DRIFTS) data, indicate that the Cu-ZnO and Cu-ZrO₂ interfaces are essential for providing the activated *H species, indispensable for the hydrogenation, whereas the ZnO-ZrO₂ interfaces promote the activation of the CO₂ and ultimately are responsible for the hydrogenation process.⁴⁷

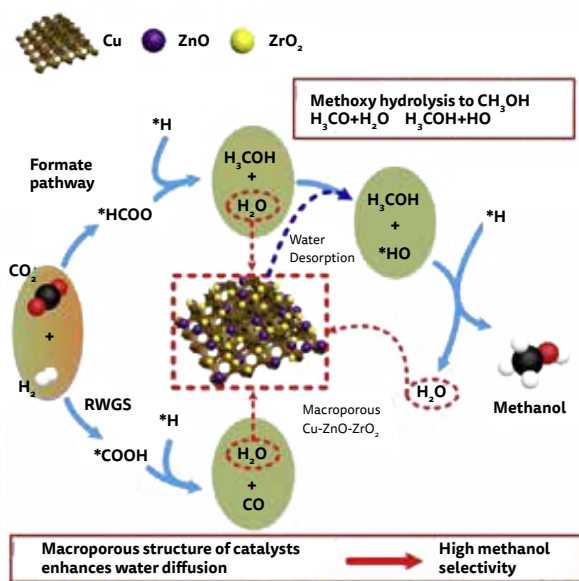


Figure 3-8: Graphical illustration of some of the most important intermediate reaction steps to form from CO₂ and H₂ Methanol.⁴⁸

Catalysis experiments in combination with “post mortem” and operando structural investigations applying various diffraction techniques, hard X-ray Absorption Spectroscopy (XAS), especially Extended X-ray absorption fine structure (EXAFS) measurements, and HRTEM has shown that selectivity, reaction temperatures, required Hydrogen pressure, and the reaction rates largely depend on the particle size and how well the particles are dispersed on the surfaces.⁴⁷

An established model of the structural necessities for the different interfaces involved and a clear picture of the intermediate reaction steps, as they are shown in Figure 3-8, is still not available; despite a large number of experiments had been performed over the past 15 years, mainly investigating various model systems with Near Ambient Pressure X-ray Photoelectron spectroscopy (NAP-XPS), and various forms of IR and Raman spectroscopy which probed the chemical changes during the reaction but missing the structural information on an atomic and mesoscopic scale during the reaction itself.⁴⁸

⁴³ Álvarez, A. et al. Challenges in the greener production of formates/formic acid, methanol, and DME by heterogeneously catalyzed CO₂ hydrogenation processes. *Chem. Rev.* 117, 9804 (2017).

⁴⁴ Bernskoetter, W. H. & Hazari, N. Reversible hydrogenation of carbon dioxide to formic acid and methanol: Lewis acid enhancement of base metal catalysts. *Acc. Chem. Res.* 50, 1049–1058 (2017).

⁴⁵ Kattel, S., Ramírez, P. J., Chen, J. G., Rodríguez, J. A. & Liu, P. Active sites for CO₂ hydrogenation to methanol on Cu/ZnO catalysts. *Science* 357, 1296–1299 (2017).

⁴⁶ Behrens, M. et al. The active site of methanol synthesis over Cu/ZnO/Al₂O₃ industrial catalysts. *Science* 336, 893 (2012).

⁴⁷ Yuhao Wang, Shyam Kattel, Wengui Gao, Kongzhai Li, Ping Liu, Jingguang G. Chen, Hua Wan, Exploring the ternary interactions in Cu-ZnO-ZrO₂ catalysts for efficient CO₂ hydrogenation to methanol, *NATURE COMMUNICATIONS* | (2019)10:1166 | <https://doi.org/10.1038/s41467-019-09072-6>

⁴⁸ Yuhao Wang, Wengui Gao, Kongzhai Li, Yane Zheng, Zhenhua Xie, Wei Na, Jingguang G. Chen, Hua Wang, Strong Evidence of the Role of H₂O in Affecting Methanol Selectivity from CO₂ Hydrogenation over Cu-ZnO-ZrO₂, *Chem Volume 6, Issue 2, 13 February 2020, Pages 419-430. <https://doi.org/10.1016/j.chempr.2019.10.023>*

Progress in computational chemistry, including code development and the availability of significant computational power, gives a first idea about the complexity of the structures which at the end facilitates the reaction. Figure 3-9 visualizes the results of density functional theory calculations which were used to determine the energy of the different configurations and optimize accordingly the structures. The large variety of the possible intermediates and competing reaction pathways gives a glimpse on the complexity of the characterization challenge, requiring the combination of imaging on the different length scales up to atomic resolution with understanding the functional behavior at a given site, e.g. investigating the electronic states correlated with the structure and identifying their role along the reaction coordinates.

The large number of active sites enabling different reaction pathways and their interdependence are forming the main obstacle to understand the reaction and rationally design a better catalyst. From the point of the characterization needs, it is also important to point out, that the electronic structure which results to an active site for a reaction, is not only dependent on the surrounding structure of the active site but is strongly impacted by the details of the structure over multiple nanometers requiring the knowledge of the various defects and interfaces. Further complicating is the influence of physisorbed gas molecules and atoms/ions on surfaces which will depend on the partial local pressures of the different gas contributions, other reactions and their active sites making the response of the catalyst dependent from the interaction between several distinct active sites, their reaction rates and the internal surfaces.

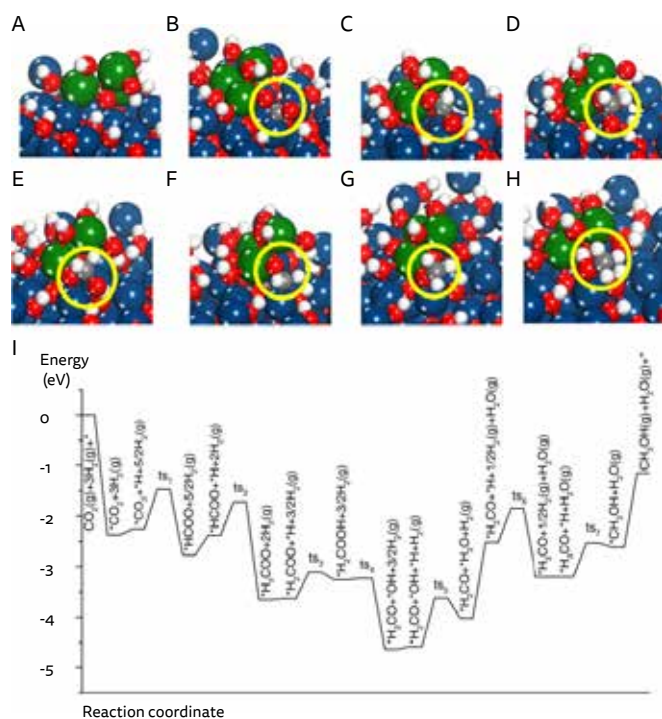


Figure 3-9: Density functional theory results describing the various possible intermediates and their energetic relationship to each other; the models illustrate the expected catalyst structure and the corresponding reaction steps: a-h DFT optimized configurations of a ZrO₂/ZnO(112̄0) and b *CO, c *HCOO, d *H₂COO, e *H₂COOH, f *H₂CO, g *H₂CO, and h *CH₃OH adsorbed at the ZrO₂/ZnO(112̄0) interface. *(X) indicates adsorbed species. The reaction intermediates are shown inside the yellow circle. Dark blue: Zn, green: Zr, red: O, gray: C and white: H. i Energy profile for CO₂ hydrogenation to CH₃OH at the ZrO₂/ZnO(112̄0) interface via the formate pathway. "ts" corresponds to the transition state.⁴⁷

Clearly, no single technique or characterization tool will be able to master this challenge. Combining imaging, ensemble averaging tools probing the composition and order as well as the electronic structure, and observing the sample under operating conditions will be key to identify the active species by verify models which can be provided by computational chemistry. At the same time, the same measurements will dramatically help to reduce the computational efforts by providing good assumptions for the structure model optimization.

From basic research towards innovation: Development of a new Ruthenium-Carbide catalyst for the Syngas Production.

Rationally designing a catalyst is a fascinating idea and is an old dream of basic science. However, none of the existing and commercially used catalysts were developed in this way but they were discovered more or less accidentally or by "intuition" and later refined over generations of engineers and scientists using combinatorial methods.^{49,50}

The Spanish contribution, centered around a novel RuC-based catalyst for Syngas production, is an excellent example for the discovery by "intuition", showing the different aspects of the development of a new system with the eye on fast commercialization. It also shows the crucial importance of Synchrotron light in this process and highlights the potential of the new multimodal and multi-length scale imaging capabilities of ALBA II.

The new catalyst facilitates the Sabatier reaction, discovered in the early 20th century, and originally using a Nickel-based catalyst to react CO₂ and H₂ to H₂O and CH₄ in a high temperature reaction. A wide range of different metal catalysts like Ni, Ru, Pd, and Rh,

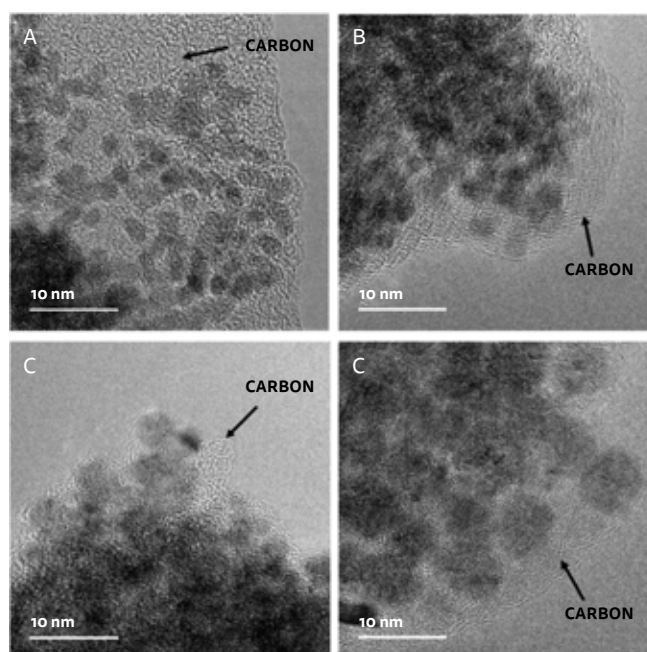


Figure 3-10: TEM images of RuC samples prepared by hydrothermal synthesis with different ratios of Ru/EDTA: (a) Ru@C-EDTA-6, (b) Ru@C-EDTA-12, (c) Ru@C-EDTA-20 and (d) Ru@C-EDTA-28.⁵¹

⁴⁹ Catalysts 2020, 10, 160; doi:10.3390/catal10020160.

⁵⁰ Combinatorial and High-Throughput Discovery and Optimization of Catalysts and Materials Edited By Radislav A. Potyrailo & Wilhelm F. Maier, Copyright Year 2007 ISBN 9780367390594 (2019), CRC Press.

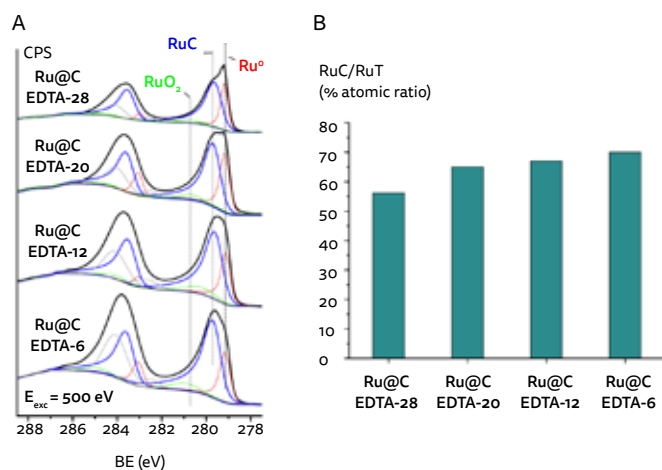


Figure 3-11: XPS data sets of four RuC catalysts prepared according various recipes. The data show a Ru-C contribution and various other compounds including a metallic Ruthenium and a Ru-O admixture.⁵¹

supported on various oxides were proposed in numerous patents, showing the strong economic potential of these facilitators of the Syngas production.⁵¹ However, all of these candidates fail in delivering a high-enough yield at ambient feed-gas pressure conditions and at low reaction temperatures (160C-200C) to make these catalysts commercially interesting for carbon-intense industries like steel and cement manufacturers to implement Syngas sequestration technologies into their production systems. The commercial and ecological success of such a catalyst is dramatically coupled on the reaction temperature requirements. The aforementioned catalysts work well in the temperature range of 300C to 500C; to reach these temperatures, additional energy has to be used, making the resulting Syngas extremely expensive and ecologically questionable due to additional fossil fuel consumption. In addition, the enhanced temperature creates additional challenges for the plant infrastructure and the catalysts lifetime, increasing additionally the economic and ecologic costs. A low temperature catalyst, however, capable to perform well in the temperature range between 160C and 200C benefits from the waste heat of the primary manufacturing process and together with the low feed-gas pressure requirement can be easily implemented in the existing industrial installations, guarantying acceptable production costs and high reliability for the Syngas production as a byproduct.

Early experiments from the 90's showed that RuC based catalysts have a similar and even slightly higher yield for the Sabatier reaction than conventional Sabatier catalysts; these experiments also hinted that the active site would contain Ru^{IV}-species which gave rise to the assumption that the active catalyst would be correlated with a Ruthenium-Carbide structure.⁵¹

Motivated by these experiments, the researchers focused on the development of low temperature grown Ruthenium-Carbide compounds using Ruthenium^{III} acetylacetonate dissolved in various organic solvents which were dried and ultimately went through a pyrolysis process. This mild hydrothermal method produced Sabatier catalysts without a sophisticated optimization process which already at this early stage of development showed excellent selectivity for the CH₄ production of 99,9%, an exceptional yield of 3.5 μmol_{CH₄}·s⁻¹·gcat⁻¹ at 160 °C and 13.8 μmol_{CH₄}·s⁻¹·gcat⁻¹ at 200 °C and at normal pressure of the feed-gases. This exceptional performance, outperforming the best current Sabatier catalyst by at least a factor 5, sparked the interest to visualize the atomic structure and identify the dominant active

sites ultimately allowing to optimize the material and reduce the required precious Ruthenium raw-material.

To elucidate the origin of the extraordinary performance, the team was using synchrotron-based spectroscopy (NEXAFS (L_{3/2}-edge), XPS, and EXAFS (K-edge)), HRTEM, and RAMAN-spectroscopy to visualize the complex inhomogeneous structure and identify the different phases of this material, essential for the catalytic reaction⁵¹.

Ex-situ XPS data provide a first glimpse in the composition of the particle, especially in the surface composition. A quantitative analysis of the different surface compounds is achieved by fitting reference spectra to the surface sensitive XPS data sets of the samples. As Figure 3-11 shows, the RuC contribution on the surface of the particles is significantly dependent on the details of the catalyst growth recipe. The fits also show some metal like and some Ru-O like contributions to the overall observed spectra. Figure 3-10 reveals also that the particles are surrounded by an amorphous Carbon layer; its thickness and morphology depend also strongly on the growth recipe. Figure 3-10 also gives a first hint that the catalytic particles are highly crystalline and not randomly partially oxidized, indicating that a new and unknown Ru-O-C phase may be the nature of the highly active catalyst.

At this point, it is important to stress the significance of using not only imaging tools, especially high-resolution ones, but ensemble averaging probes which characterizes all particles which may contribute to the catalytic performance. Only the combination of both ensures that the refined structure models describe the full sample system and avoids that some particles, which at the end may perform the main catalytic function are undetected and unrevealed.

Using the structural data of the average particles, the high-resolution electron microscopy images can be used to verify the model but also reveal the details on individual particles. A similar information to X-ray diffraction, e.g. the plane orientation, the plane spacing, and the plane indexing, can be obtained by forming a Fast Fourier Transformation (FFT) of the full or partial image, called Digital Diffraction Pattern (DDP). Even if the data don't allow to refine the structure like in a Rietveld approach, it clearly demonstrates that the individual particle is a single crystal with a high ordering. The Rietveld model can physically explain the distortion of the "RuO" nano particle and also explains the Carbon contribution of this area when Electron Loss Spectroscopy (EELS) is performed from the same area.

This example shows clearly how ALBA is currently contributing to the structure determination of novel materials and ultimately to the development of new functional materials like catalysts. Key to this approach is a multimodal approach; it also shows the current limitations: The speed in which the structure of such a complex structure can be revealed is driven by the practical limitations like the availability of beamtime at the time when needed but even more by the fact that current multi-modal approaches are fully "manual", in a sense that each analysis of a data set is performed independently from each other and has to be manually applied to each available data set whenever new results are available. However, this time-intensive approach brings limits to the quality of refinement missing out important opportunities.

ALBA II will at least partially overcome this limitation by developing a data infrastructure which will easily identify all

available data sets to an individual sample set and at the same time provide automatic analysis pipelines for the key probes allowing the automatic refinement of the models, or at least the automatic verification that a new structure model fits all available data sets better.

Another important contribution of ALBA II will be improved imaging capabilities. With strong investments in electron microscopy, the user will be able to combine the techniques as shown here even in a single visit accelerating the development process significantly. Moreover, the availability of high-quality operando experiments even in the HREM case will bring a new quality to understand the functionality of the catalyst. In this context one needs also to mention the new HEXPES-beamline 3Sbar. This instrument will be able to provide the XPS data not only depth-selective but also pushes the envelope of near ambient pressure XPS to the 1bar regime or higher, an important next step to provide full operando conditions during the experiment.

Besides multimodal methodologies and the improved operando capabilities, ALBA will also extend the X-ray imaging and nano spectroscopic and diffraction capabilities. These new capabilities could be hosted on one of the new long beamlines and will fully complement the capabilities of the new operando HREM microscope. With beam sizes down to the 10nm and achievable resolutions using coherent imaging techniques, the nano probe will not only be able to provide spectroscopic, e.g. the local electronic state, and structural information of the individual particle but also allows complex sample environments with relative low requirements to the sample preparation in comparison to TEM experiments. It will also be able to characterize complex system in which multiple particles

are intermingled and their functionality is depending on the details of the interface, like shown in the previous example.

To accelerate the development of the catalysts capable to be used in real industrial processes, ALBA II will need also to satisfy the needs correlated to combinatorial developments as well as fostering the innovation by "intuition". Both are essential if the original societal challenge of providing catalysts for an economic and ecologic sustainable circular carbon economy is the ultimate goal.

Tools appropriate for combinatoric developments require the fast and easy characterization of catalytic reactivity and, for systems with a basic understanding of the functionality, the characterization of structure and active sites. This requires the development of high throughput, fast schedulable ex-situ and operando measurements, and access modes which are compatible with the combinatoric iteration cycle. Remote access with all necessary staging laboratories, especially to allow remote operando experiments, and automatic data pipelines are key in providing the timely information for the next iteration cycle. Often used techniques include Hard X-ray spectroscopy, EXAFS, powder diffraction and IR-spectroscopy. Even if the latter two techniques are often used as laboratory probes, providing a synchrotron light-based service to the community will allow to increase the data quality especially for operando experiments, necessary to apply more sophisticated data analysis strategies, elucidating much richer details of structure and function.

A new and exciting building stone within the multimodal concept brings big data science and data analytics. A google search for the terms "big data catalysis" results over 6M hits, showing clearly the interest of the catalytic community on these new

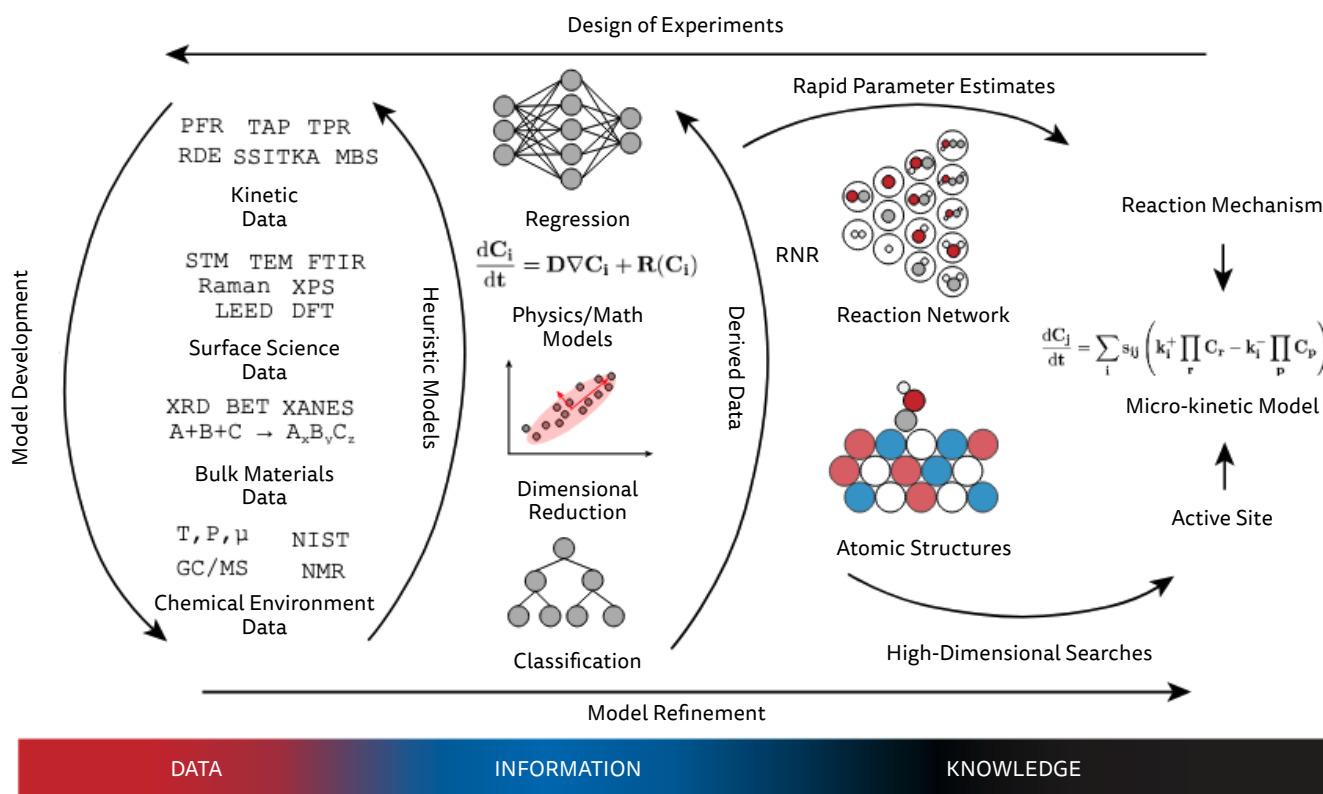


Figure 3-12: Graphical explanation of all necessary steps to optimize and understand a catalyst using big-data science. Models based on statistics and/or physics can be used to create derived data, to establish heuristic relationships between data, or to rapidly estimate parameters for reaction network or atomic-scale surface models. The reaction network and atomic-scale structure are high-dimensional structures that can be distilled to reaction mechanism(s) and active site(s) via high-dimensional searches. Ultimately this leads to design of experiments and refinement of micro-kinetic models based on the chemical master equation.⁵²

⁵² Andrew J. Medford, M. Ross Kunz, Sarah M. Ewing, Tammie Borders, Rebecca Fushimi, Extracting Knowledge from Data through Catalysis Informatics, ACS Catal. 2018, 8, 8, 7403–7429. <https://doi.org/10.1021/acscatal.8b01708>

tools. Figure 3-12 schematically shows, how structural models can be derived out of a multimodal data set, and how ultimately structure predictions are developed for optimized catalysts⁵². Data analytics is therefore the binding link between the basic science ansatz and the innovation driven combinatoric approach, benefitting both and from each other. For the combinatoric approach, data analytics can also contribute significantly to the “by intuition” original discovery of a new catalytic system. Moreover, the development of new analysis methods based on machine learning will also bring significant advantages in the area of data analysis of data sets from a single technique. It will allow to provide the fast analysis of large data sets as it is produced in powder diffraction⁵³, and will open a new way to extract structural information from spectroscopic tools.^{54,55}

To participate on these developments, ALBA II will largely invest in automatization of the data pipelines and integrating a metadata concept which is fully compatible with the operando concept. Of paramount importance is the development of the ALBA tools which will be compatible with the tools developed by the user community by building a FAIR data, metadata and data analysis platform. In addition, appropriate and customizable query tools will build the backbone of ALBA II.

The example of the development of 3DOM CZZ catalysts shows how imaging tools covering the different resolutions, ensemble structural and electronic probes, the operando concept, high throughput capabilities, and finally data analytics form a concept which not only allow to gain fundamental understanding in the functionality of complex catalysts, but also how the same tools will benefit the innovation community allowing to accelerate the technological readiness of new technologies.

ALBA catalysis community

ALBA current user community is highly active in this field of science covering the full width of catalytic systems required for an effective carbon neutral circular economy. This includes the areas of materials growth and the necessary process optimization like shown in ref⁵⁶ as well as the different aspects of the value chain. A good example is a work focused on a catalyst allowing complete oxidation of SNG in the effluent of combustion processes to avoid the contamination of the atmosphere with the extreme potent green greenhouse gas. Using a wide range of hard X-ray spectroscopy, NAP-XPS at different X-ray energy, providing depth sensitivity, and HRTEM microscopy, the structure and the active sites of a Pd-Pt catalyst supported on ceria was studied and, based on the results optimized⁵⁷.

3.2.2. BATTERY RESEARCH AND THE CORRELATED ECOSYSTEM

Whereas energy production by fossil fuels can be tuned to the temporal power needs of the grid, renewable energy production is

mostly independent from the demand, making the development of reliable, economic, and safe short and long-term storage capabilities essential for a consumer friendly and resilient economy. Batteries play here a key role for electro mobility and decentralized short-term storage; they are true enablers in combination with digitalization for automatic adjustment of the energy consumption according to energy availability and catalysis for the development of long-term chemical storage concepts including Syngas or Hydrogen production, as discussed above.

To support the research needs correlated with this transition, ALBA II will have to develop a broad portfolio of tools and services to enable our current and potential users to fully contribute to the emerging and new markets which go far beyond the needs of battery development itself.

A prominent example, which illustrates the extend of the needs, is the buildout of electromobility; it's requiring not only reliable light-weight solutions for the battery systems itself but also is changing the bill of critical materials on an European level, making economic and ecologic aspects of mining within our own communities to a major focus, is changing the value chain in car manufacturing industry, emphasizing the importance of power electronics and the underlying power management system, and is ultimately changing dramatically the requirements of our power distribution and the economics of it.

Most of these areas are correlated with research activities currently served by the synchrotron light community and will greatly benefit from the upgrade and the increased brightness; ALBA II will bring important new tools for many of these areas, especially the tailored multimodal approaches with the ability to zoom in into the interesting sample volume of complex and inhomogeneous samples using the enhanced imaging and microscopy capabilities. An example of applying various spectroscopic, diffraction and imaging techniques to solid-state batteries can be found in ref⁵⁸. Another obvious example is the visualization of power devices necessary for the power management including their integration with the Complementary Metal-Oxide- Semiconductor (CMOS) controls integration. As shown later, the enhanced imaging capabilities will allow to image relatively large volumes of a few cubic millimeter with a 3D-resolution of 20-30nm, which corresponds to a typically size of these devices and is good enough to resolve all individual building blocks, interconnects and interfaces of interest. The ease of sample preparation in combination with the relative fast data acquisition makes these microscopy tools to a great guide for high-resolution, post-mortem HREM investigation with atomic and subatomic resolution but allowing to probe only small areas with a few 100 square nanometer area.

The newly founded company Basquevolt⁵⁹, a spin-off from CICEnergigUNE⁶⁰, is a good example how Spain is addressing the new business opportunities of battery development by building on the strong local research capabilities. Pushing new solid-state battery concepts, the researchers aim to develop safe batteries with a significant higher power density, meaning that a device with equal weight can store much more energy and at the same

⁵³ Dong, H., Butler, K.T., Matras, D. et al. A deep convolutional neural network for real-time full profile analysis of big powder diffraction data. *npj Comput Mater* 7, 74 (2021). <https://doi.org/10.1038/s41524-021-00542-4>

⁵⁴ Matthew R. Carbone, Mehmet Topsakal, Deyu Lu, and Shinjae Yoo, Machine-Learning X-ray Absorption Spectra to Quantitative Accuracy, *Phys. Rev. Lett.* 124, 156401.

⁵⁵ Guda, A.A., Guda, S.A., Martini, A. et al. Understanding X-ray absorption spectra by means of descriptors and machine learning algorithms. *npj Comput Mater* 7, 203 (2021). <https://doi.org/10.1038/s41524-021-00664-9>

⁵⁶ *J. Mater. Chem. A*, 2021, 9, 8401.

⁵⁷ Divins, N.J., Braga, A., Vendrell, X. et al. Investigation of the evolution of Pd-Pt supported on ceria for dry and wet methane oxidation. *Nat Commun* 13, 5080 (2022). <https://doi.org/10.1038/s41467-022-32765-4>

⁵⁸ <https://doi.org/10.1002/cey2.131>

⁵⁹ <https://basquevolt.com/en>

⁶⁰ <https://cicenergigune.com/es>

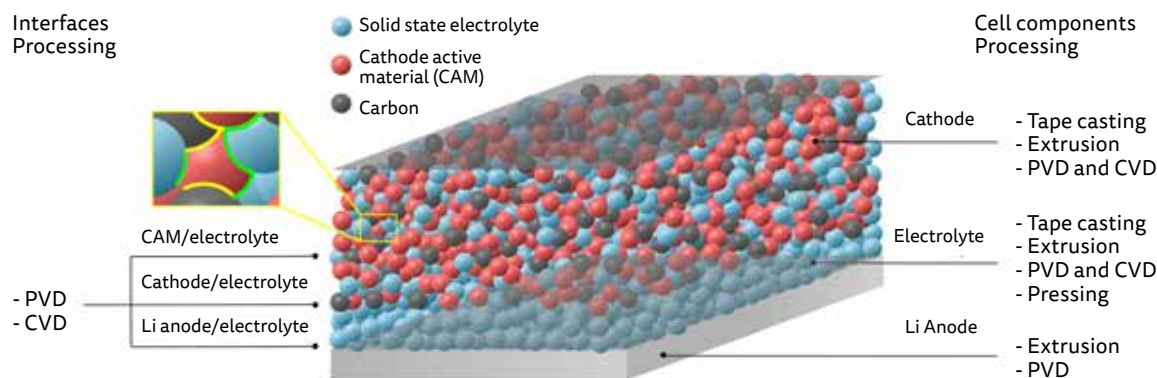


Figure 3-13: Schematic of a solid-state battery with a metallic Lithium anode and metallic current collector on top (grey plane). The solid-state electrolyte (blue) act not only as Li+ conductor but also as insulator for electrons. The cathode layer is a mixture of cathode active material (red), carbon (black) as electron conductor and the solid-state electrolyte (blue) for efficient Li+ transport. Left notations indicate the different process types available to create the interfaces whereas the right sight indicates processes for the initial raw materials.⁶¹

time show an unprecedented maximal current allowing high power applications like required during fast acceleration or for fast charging of Electric Vehicles (EV's). In other words, providing a platform which allows fast and comfortable electromobility with less energy consumption due to the reduced weight of the energy storage system. The business idea of Basquevolyt is to bring these technologies to the higher TR-levels, ultimately creating a European production facility on a large scale.

A schematic sketch of a solid-state battery using a metallic Lithium anode is shown in Figure 3-13. The challenges of developing solid state batteries are finding a solid-state electrolyte with high ionic but low electronic conductivity at room temperature, which shows a strong mechanical strength, an electrochemical stability and is not sensitive to moisture, can be easily processed, and is compatible with the other materials used in the battery, mainly the Lithium-anode and the cathode particles. On top, the full system should require a minimum on strategic materials and uses mainly easy to recycle and abundant raw materials.

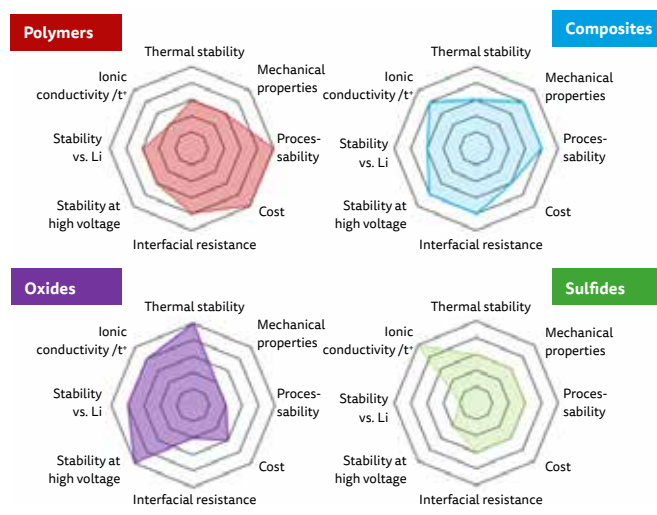


Figure 3-14: Radar chart presenting the most relevant properties of the polymer, composite, oxide and sulfide families of solid-state electrolytes.⁶¹

⁶¹ Nicola Boaretto, Iñigo Garbayo, Sona Valiyaveetil-SobhanRaj, Amaia Quintela, Chunmei Li, Montse Casas-Cabanas, Frederic Aguesse, Lithium solid-state batteries: State-of-the-art and challenges for materials, interfaces and processing, *Journal of Power Sources*, Volume 502, 2021, 229919, ISSN 0378-7753, <https://doi.org/10.1016/j.jpowsour.2021.229919>

⁶² Adams, Stefan, and Rayavarapu Prasada Rao. "Ion transport and phase transition in $\text{Li}_{7-x}\text{La}_3(\text{Zr}_{2-x}\text{M}_x)\text{O}_{12}$ ($\text{M} = \text{Ta}^{5+}, \text{Nb}^{5+}, x = 0, 0.25$)." *Journal of Materials Chemistry* 22.4 (2012): 1426-1434

⁶³ V. Thangadurai, H. Kaack, W.J.F. Weppner, Novel fast lithium ion conduction in garnet-type $\text{Li}_5\text{La}_3\text{M}_2\text{O}_{12}$ ($\text{M} = \text{Nb}, \text{Ta}$), *J. Am. Ceram. Soc.* 86 (3) (2003) 437-440, <https://doi.org/10.1111/j.1151-2916.2003.tb03318.x>

⁶⁴ R. Murugan, V. Thangadurai, W. Weppner, Fast lithium ion conduction in garnet-

Besides the intrinsic properties of the individual components, the interfaces between the individual grains and between the major components, anode, cathode and separator, are widely determining the functional performance of the device; these interfaces, their evolution over the lifetime of the device and the electrochemical stability of the electrolyte determines also the reliability and ultimately the safety of the battery.

A wide range of different solid-state electrolytes are currently under considerations. They can roughly be grouped in four categories: polymers, oxides, sulfides, and composites. Figure 3-14 provides an overview about the strength and weaknesses of these classes in respect to chemical stability and electrochemical performance (Ionic conductivity and transference number (t^+), stability against Li metal, stability against high voltage cathode, interfacial resistance), thermal and mechanical stability and cell integration towards manufacturing (described as processability and cost)⁶¹.

To support the development of such solid-state batteries, there will be four main trusts of research which needs to be supported by ALBA II. As described in the following, the facility has to develop a program which fully supports the 1) development of new materials, mainly in the area of Oxides and Sulfides, the 2) development of compound materials and their processing, the 3) processing of polymer-based electrolytes, and finally 4) the visualization of the grains within the battery including their interface with the neighboring morphologies:

- **Systematic development of new inorganic electrolytes:** This field is specifically identified as a focus area in the Battery2030+ roadmap and is widely based on computational and combinatorial approaches. To optimize the different properties as shown in Figure 3-14, the compound composition itself and the addition of dopants is systematically optimized for the known crystalline material classes, like the garnets and Li-stuffed garnets^{62,63,64,65}, Li-based perovskites^{66,67,68}, Lithium Superionic Conductors^{70,71}, Sodium Superionic Conductors⁷³,

type $\text{Li}_7\text{La}_3\text{Zr}_2\text{O}_{12}$, *Angew. Chem. Int. Ed.* 46 (41) (2007) 7778-7781, <https://doi.org/10.1002/anie.200701144>

⁶⁵ L. Xu, et al., Garnet solid electrolyte for advanced all-solid-state Li batteries, *Adv. Energy Mater.* (May 2020) 2000648, <https://doi.org/10.1002/aenm.202000648>

⁶⁶ V. Thangadurai, W. Weppner, Recent progress in solid oxide and lithium ion conducting electrolytes research, *Ionics* 12 (1) (May 2006) 81-92, <https://doi.org/10.1007/s11581-006-0013-7>

⁶⁷ T. Takahashi, H. I. E. Conversion, and undefined, *Ionic Conduction in Perovskite-type Oxide Solid Solution and its Application to the Solid Electrolyte Fuel Cell*, Elsevier, 1971

⁶⁸ Y. Inaguma, et al., High ionic conductivity in lithium lanthanum titanate, *Solid State Commun.* 86 (10) (Jun. 1993) 689-693, [https://doi.org/10.1016/0038-1098\(93\)90841-A](https://doi.org/10.1016/0038-1098(93)90841-A)

⁶⁹ Mara Olivares-Marín, Andrea Sorrentino, Rung-Chuan Lee, Eva Pereira, Nae-Lih

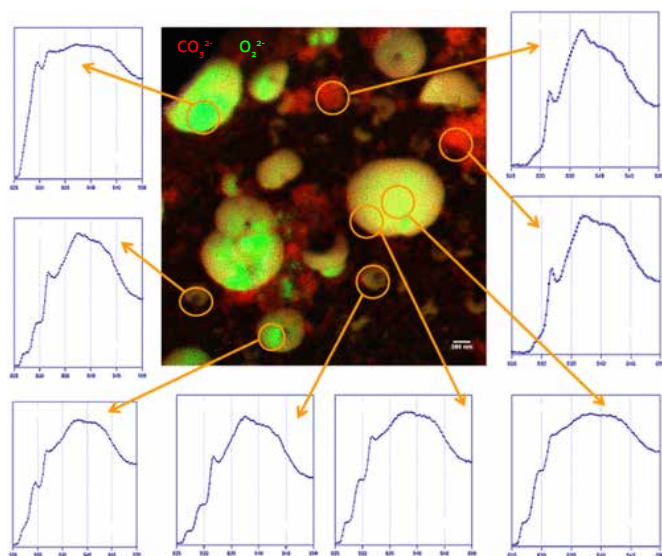


Figure 3-15: ALBA current imaging capabilities of interfaces and particles: Spectro-microscopy on a model system of a Lithium-Oxygen battery, revealing the speciations of Li depending on particle shape and size.⁶⁹

and Lithium Phosphorous Oxynitride⁷⁴ and the amorphous or glassy compounds like $\text{Li}_7\text{P}_3\text{S}_{11}$, $\text{Li}_{10}\text{GeP}_2\text{S}_{12}$, $\text{Li}_7\text{P}_2\text{S}_6$. This work can be well supported by providing Rietveld analysis of high-resolution powder diffraction data.^{75,76} In addition, the effects on the structure of stress factors like electrochemical cycling, the Li+ transport/storage itself, especially the corresponding volume changes, can be elucidated in operando and in-situ experiments.^{77,78,79} ALBA is already currently contributing to this field, however, the progress in digital materials laboratories and the increased combinatorial material output will require an optimization of the high-resolution powder diffraction program including automatic sample handling (robot and sample data base), automatization of data pipelines and access policy changes which will allow very fast and regular access to beamtime but also the connection of the data and analysis to the existing large materials databases. Key to have impact on the national development capabilities is the ability to understand the morphological and chemical changes of the new materials during the cycling making high throughput and fast access operando and in-situ experiments indispensable. In collaboration with the user community, ALBA II will address this new challenge by integrating specialized well equipped and staffed laboratories which will be able to assemble raw materials to test units following well defined protocols.

ALBA II with its new capabilities to improve the experimental conditions in the high-energy range above 40KeV will also significantly contribute to the future leading role of this program, allowing a wider range of operando environments and at the same time boosting the Pair Distribution Function capabilities (PDF), essential to characterize disordered materials. One should stress that this program will also support the cathode development and is geared to support not only the work of research centers and, to a smaller part, academic users but also the development departments of industry.

- Processing of polymer-based electrolytes:** Besides the tuning of the different polymer components⁸⁰ the processing including the use of additives is defining the functionality and reliability of the organic electrolytes and their interfaces with anode and cathode⁸¹. Specific attention has to be devoted to the surface and interface preparation. Details of the cleaning and termination of the surfaces on which the polymer is coated will determine the Li interface conductivity and ultimately define the chemical fate of the Li at the later interfaces⁶². GI-SAXS and GI-WAXS are the classical tools to probe these interfaces and the morphology of the resulting electrolyte film. In-situ and operando conditions play a major role in optimizing the process parameter and at the same time understand the morphology changes on interfaces and the electrolyte itself causing degradation of the system. ALBA II will improve slightly the GI-WAXS and GI-SAXS conditions due to the increased flux at a smaller footprint on the sample but will significantly improve the spectro-microscopic tools allowing not only resolving the interface layers itself but also characterizing the chemical compositions of the interface. The improved coherence properties will allow a new class of high-resolution microscopic tools which will bring a new imaging capability to the existing ensemble averaging tool set. Another important tool of ALBA II will be the beamline 3Sbar; this beamline will combine surface XRD with High Energy X-ray Emission Spectroscopy. 3Sbar will give unique understanding of the polymer chemistry in presents of the Lithium ions and the interface to the metallic anode or cathode by probing the surface morphology of the substrate and at the same time measuring the depth dependent electronic structure of the material and interface. The combination with HREM will complete the picture of the interface morphology down to the atomic resolution. The combination of relative slow and complex high-resolution imaging techniques with fast and ensemble averaging scattering techniques will give not only understanding of the interface chemistry of individual particles and surfaces with the electrolyte but at the same time allows fast data acquisition characterizing the full sample

Wu, and Dino Tonti, "Spatial Distributions of Discharged Products of Lithium-Oxygen Batteries Revealed by Synchrotron X-ray Transmission Microscopy", *Nano Lett.* 2015

- ⁷⁰ L. Zhou, A. Assoud, Q. Zhang, X. Wu, L.F. Nazar, New family of argyrodite thioantimonate lithium superionic conductors, *J. Am. Chem. Soc.* 141 (48) (Dec.2019) 19002-19013, <https://doi.org/10.1021/jacs.9b08357>
- ⁷¹ Y. Wang, et al., Design principles for solid-state lithium superionic conductors, *Nat. Mater.* 14 (10) (Oct. 2015) 1026-1031, <https://doi.org/10.1038/nmat4369>
- ⁷³ P. Knauth, Inorganic solid Li ion conductors: an overview, *Solid State Ionics* 180(14-16) (Jun. 2009) 911-916, <https://doi.org/10.1016/j.ssi.2009.03.022>
- ⁷⁴ J.B. Bates, et al., Fabrication and characterization of amorphous lithium electrolyte thin films and rechargeable thin-film batteries, *J. Power Sources* 43 (1-3) (Mar. 1993) 103-110, [https://doi.org/10.1016/0378-7753\(93\)80106-Y](https://doi.org/10.1016/0378-7753(93)80106-Y)
- ⁷⁵ Chen, J., Yang, Y., Tang, Y., Wang, Y., Li, H., Xiao, X., Wang, S., Darma, M.S.D., Etter, M., Missyul, A., Tayal, A., Knapp, M., Ehrenberg, H., Indris, S. and Hua, W. (2023), Constructing a Thin Disordered Self-Protective Layer on the LiNiO₂ Primary Particles Against Oxygen Release (*Adv. Funct. Mater.* 6/2023). *Adv. Funct. Mater.*, 33: 2370034. <https://doi.org/10.1002/adfm.202370034>
- ⁷⁶ Gorbunov, Mikhail V. et al. "Studies of Li₂Fe_{0.9}Mo_{1.5}O Antiperovskite Materials for Lithium-Ion Batteries: The Role of Partial Fe²⁺ to M²⁺ Substitution." *Frontiers in Energy Research* (2021) *ACS Appl. Energy Mater.* 2022, 5, 11, 13735-13750 Publication Date: October 19, 2022 <https://doi.org/10.1021/acsaem.2c02402>
- ⁷⁷ Anna Windmüller, Tatiana Renzi, Hans Kungl, Svitlana Taranenko, Emmanuelle Suard, François Fauth, Mathieu Duttine, Chih-Long Tsai, Ruoheng Sun, Yasin Emre

Durmus, Hermann Tempel, Peter Jakes, Christian Masquelier, Rüdiger-A. Eichel, Laurence Croguennec, and Helmut Ehrenberg, "Feasibility and Limitations of High-Voltage Lithium-Iron-Manganese Spinels", *Journal of The Electrochemical Society*, 2022 169 070518

- ⁷⁸ Christian Baur, Monica-Elisabeta Lacatusu, Maximilian Fichtner, and Rune E. Johnsen, Insights into Structural Transformations in the Local Structure of Li₂VO₂F Using Operando X-ray Diffraction and Total Scattering: Amorphization and Recrystallization *ACS Applied Materials & Interfaces* 2020 12 (24), 27010-27016 DOI: 10.1021/acsaami.0c02391
- ⁷⁹ Romain Wernert, Long H. B. Nguyen, Emmanuel Petit, Paula Sanz Camacho, Antonella Iadecola, Alessandro Longo, François Fauth, Lorenzo Stievano, Laure Monconduit, Dany Carlier, and Laurence Croguennec, "Controlling the Cathodic Potential of KVPO₄F through Oxygen Substitution", *Chemistry of Materials* 2022 34 (10), 4523-4535 DOI: 10.1021/acs.chemmater.2c00295
- ⁸⁰ Luca Porcarelli, M.Ali Aboudzadeh, Laurent Rubatat, Jijeesh R.Nair, Alexander S.Shaplov, Claudio Gerbaldi, David Mecerreyes, Single-ion triblock copolymer electrolytes based on poly(ethylene oxide) and methacrylic sulfonamide blocks for lithium metal batteries, *Journal of Power Sources* Volume 364, 1 October 2017, 191-199, DOI: 10.1016/j.jpowsour.2017.08.023
- ⁸¹ Andreas Bergfeldt, Laurent Rubatat, Daniel Brandell, Tim Bowden, Poly(benzyl methacrylate)-poly[(oligo ethylene glycol) methyl ether methacrylate] triblock-copolymers as solid electrolyte for lithium batteries, *Solid State Ionics* Volume 321, August 2018, 55-61, DOI: 10.1016/j.ssi.2018.04.006

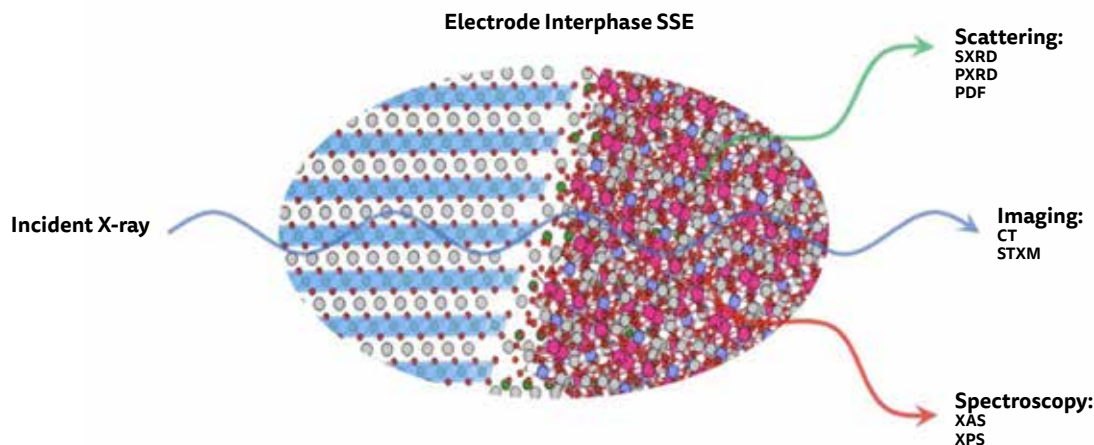


Figure 3-16: In situ synchrotron X-ray techniques used to study the interphase between electrode materials and solid-state electrolytes. Scattering can include conventional powder X-ray diffraction for identification of the crystalline phase in any solid-state battery format, including bulk and thin films, while surface X-ray diffraction is especially useful for extremely high-quality thin-film model systems. Spectroscopy techniques such as X-ray absorption and photoelectron spectroscopy can help to identify phases that lack crystallinity or are amorphous. Additionally, they can help to identify ligands, oxidation states, and composition. X-ray imaging methods are considered direct methods to visualize the morphology changes at the solid–solid interface. CT, computed tomography; PDF, powder diffraction file; PXRD, powder X-ray diffraction; SSE, solid-state electrolyte; STXM, scanning transmission X-ray microscopy; SXRD, surface X-ray diffraction; XAS, X-ray absorption spectroscopy; XPS, X-ray photoelectron spectroscopy.⁸³

system and enabling fast development cycles for processing and optimization of the polymer itself.

- **Development of compound electrolytes and their processing:**

As described above, the morphology and, correlated with it, the electrical behavior of the organic electrolytes depend largely on the processing parameter and the preparation of the surfaces which are in connection with the organic electrolyte. Obviously, including non-organic materials into the electrolytes is even more emphasizing this aspect. An example for the complex interaction between polymer and $\text{Li}_{7-x}\text{La}_3\text{Zr}_{2-x}\text{Ta}_x\text{O}_{12}$, including the change of composition on the interfaces to achieve charge compensation, is given in⁸². The authors were able to characterize the system on the different length scales by synchrotron-based X-ray fluorescence imaging (XRF) and Transmission X-ray Microscope (TXM) to image nanoscale chemical heterogeneity. Besides the structure of the interface, they could also observe the accumulation of LiI at the interface between the organic and the non-organic electrolyte explaining the degradational effects during the charging cycle. ALBA current soft X-ray TXM capabilities, as shown in Figure 3-15, are expected to be complemented at ALBA II by its long beamlines, enabling nano X-ray fluorescence imaging (XRF) as well as various high-resolution microscopy tools, empowering the researcher to investigate not only a broad range of materials under operando conditions, but also their 3D distribution of their chemical states. Coherent imaging, specifically Bragg-Coherent-Diffraction-Imaging but also other far and near field high resolution techniques, are other examples which can only be provided within the ALBA II project and are providing essential information on the full particle but also on the interfaces on the morphology and chemical composition of this highly inhomogeneous materials.

- **Visualization of grains within the battery including their interface with the neighboring grain and electrolyte:** Perhaps

the holy grail of understanding why a battery works or better why it fails is to visualize the morphology of the interfaces and monitor its changes and chemistry during the electrochemical cycling. Besides large local mechanical stresses on the compound material due to the large volume changes of anode and specifically cathode, the complex redox-chemistry on the interfaces result in degradation effects and determine the fire risk of the battery⁶². By using a wide range of additives and surface treatments before the battery assembly, the engineer can mitigate these negative effects. The visualization of the morphology, including crack formation, locally appearing chemical changes and ultimately understanding the current density on a nanoscopic level will help significantly to battle these changes and optimize the interface structure. As shown in Figure 3-16 Lucero et al. has demonstrated a multimodal approach allowing exactly this, using tools like 3Sbar or these, ALBA powder diffraction program is or will provide⁸³. ALBA II will benefit all of the mentioned techniques either by allowing a smaller footprint on the sample with increased flux in comparison to current ALBA conditions or by extending the high energy capability especially benefitting the pair distribution technique, specifically suited to describe the morphology of highly disordered small particles. The 3Sbar beamline, a true ALBA II beamline will combine in a unique way surface-scattering technique with depth profiling spectroscopy. A full new quality will bring a hard X-ray nano probe which will not only allow to image the overall morphology in 3D but also probe the crystalline structure and chemical composition of the areas. The use of coherent imaging techniques, an extension of the existing microscopy program, will allow to increase the resolution to the few nanometer-ranges for selected areas of interest. Together with the HREM capabilities of ALBA II, the user will find a set of tools which not only allow to drill down on structure and morphology on selected areas but also combine these models with fast and averaging tools allowing to probe the width of samples necessary to fast drive the development into the high TR-level range.

⁸² Tianze Xu, Chunrun Chen, Tianwei Jin, Shuaifeng Lou, Ruiwen Zhang, Xianghui Xiao, Xiaojing Huang and Yuan Yang, Chemical Heterogeneity in PAN/LLZTO Composite Electrolytes by Synchrotron Imaging, 2021 J. Electrochem. Soc. 168 110522

⁸³ Marcos Lucero, Shen Qiu, Zhenxing Feng, In situ characterizations of solid–solid interfaces in solid-state batteries using synchrotron X-ray techniques, Carbon Energy. 2021;3:762–783. DOI: 10.1002/cey2.131

3.3. Information and communication technologies

The development of *Information and Communication Technologies* (ICT) has been accelerated in the last century, boosting science, technology, and finally our economy, ultimately driving a complete transformation of our society and the way how we live. The ICT revolution has radically changed our lifestyle, among others the way, speed and scale at which we are communicating, learning, working and consuming. Moreover, ICT is the basis for Europe's digital strategy to transform workflows and processes for people and businesses and at the same time achieve a climate-neutral Europe.

Not astonishingly, the material science aspects and to some part the engineering aspects of ICT is in the center of a large user community of ALBA. An overview of the different technologies⁸⁴ is given in the road map shown in Figure 3-17. The following discussion will give an overview over the current state-of-the-art technologies and the corresponding characterization challenges, as well as an overview of the emerging technologies and the different levels ALBA II will provide tools: ALBA will contribute

to the evolutionary development of established technologies, and is also ready to support the development of disruptive technologies including Quantum, Spintronic and Neuromorphic (brain-inspired) technologies. The development of tool sets which serve both communities will fulfil ALBA role as an enabler for innovation and basic science, and at the same time, will help to integrate novel approaches within the established technologies.

3.3.1. AGE OF CMOS TECHNOLOGY

The increasing needs for higher information density and fast communication have pushed device size towards the micro- and nano-scale, continuing a scaling evolution that is often referred as *Moore's law*, meaning the number of transistors on an integrated circuit is doubling roughly every two years at constant cost⁸⁵. The technological scaling in which transistor shrinking drives improvement of performance and reduction of power consumption, area and cost (PPAC) has been applied for decades, with Moore's Law serving as a time guideline for companies to set the expectations for performance and at the same time resulting in an exponential pace of technology development.

At the basis of this success is the development and downscaling of the metal-oxide-semiconductor field-effect transistors (MOSFET) and posterior lower dissipation complementary-symmetry CMOSFET -or simply CMOS- transistor technology⁸⁶. CMOS is the basic semiconductor technology for memory and logic devices.

During the last decades of CMOS evolution, lithography has been the essential enabler for scaling, and consequently for the technology roadmap, by making it possible to reduce the dimensions of the transistors. In due time, signal routing, rather than the size of the transistor, became the limiting factor for integration⁸⁷. Among the main advances one may highlight: i) *strain engineering* the gate channel by embedding it in an architecture of different materials with mismatched lattice parameter like Germanium-Silicon, SiC, and SiN resulting in an increased carrier mobility within the gate channel, ii) *introducing highly dielectric*

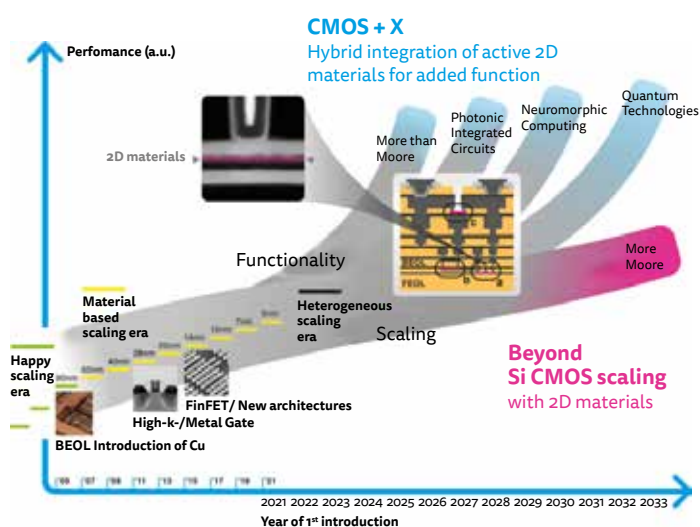


Figure 3-17: Road map prospect with branching on emerging conceptual technologies for solving the ICT challenges over the next 15 years, and potential role of 2D materials.

⁸⁴ Lemme, M. C.; Akinwande, D.; ... C. H.-N.; 2022, undefined. 2D Materials for Future Heterogeneous Electronics. nature.com.

⁸⁵ Moore, G. E. Cramming More Components onto Integrated Circuits, Reprinted from Electronics, Volume 38, Number 8, April 19, 1965, Pp. 114 Ff. IEEE solid-state circuits society newsletter 2006, 11 (3), 33–35.

⁸⁶ https://en.wikipedia.org/wiki/Field-effect_transistor

⁸⁷ Graef, M. Positioning More Than Moore Characterization Needs and Methods within the 2011 ITRS. AIP Conference Proceedings 2011, 1395 (1), 345–350. <https://doi.org/10.1063/1.3657913>

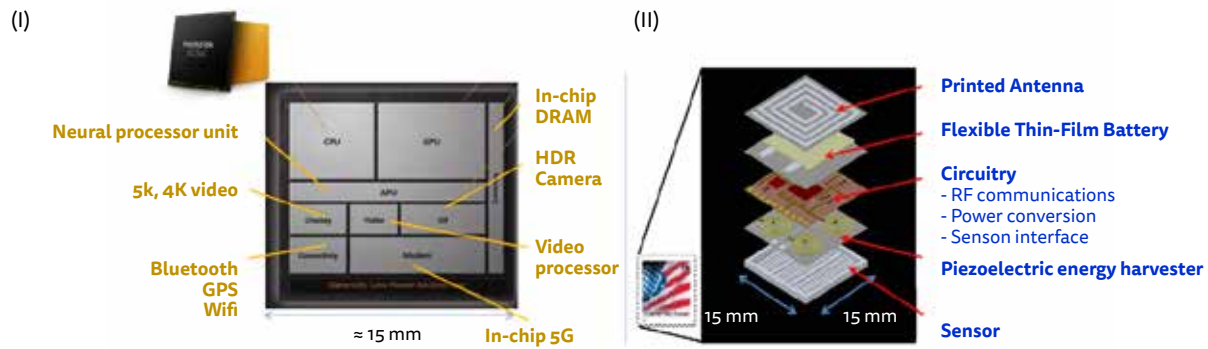


Figure 3-18: Examples of “More than Moore” systems-on-a-chip (SoC) for mobile devices, connectivity and IoT products. (I) Architecture of recent 5G, wifi-7 SoC for mobile devices designed by Taiwanese company Mediatek and manufactured by TSMC latest technology; (II) schematic of a stamp-sized self-powered wireless sensing and signal processing unit as would be needed in smart cities for a green and digital transition.⁸⁸

materials to achieve enhanced dielectric/metal gate structure allowing scaling down of the dimensions at controlled leakage currents, iii) *introducing multi-gate and 3D architectures* such as FinFET's to improve performance and reduce the footprint of the individual transistor, and more recently iv) simplification of mask processes and ultimate minimization of the structure dimensions of the transistor (about 20-30nm) and the interconnects (roughly 30-45 nm) by *using extreme ultra-violet (EUV) lithography* in the present '5nm' technology node. EUV is an optical lithography technology based on reflective that uses UV radiation with wavelength of 13.5 nm, and has become the standard light source in the advanced lithographic systems for present integrated circuit (IC) technology nodes (7 and 5 nm). While the theoretical resolution limit is 13.5nm, present resolution is limited to about 30 nm due to a blur of the pattern resulting from the escaping dimension of secondary electrons emitted by the absorption of the EUV light. Currently, only Dutch company ASML provides last generation EUV lithography systems. It is worthwhile to mention that in the last decade or so the node nomenclature, i.e. the label of the fabrication process like a *5nm process node*, does no longer refer to the smallest dimension achievable but is mainly a marketing term to indicate a next generation with improved performance. Key to this success was the fundamental understanding of materials and their growth often promoted by sophisticated imaging and functional characterization tools, evidencing the relevance of fundamental science and high-end characterization tools as enablers of solutions for technological challenges.

To overcome the fabrication limitations of the minimum structure size and still follow the guideline of Moore's Law, industry developed 3D design structures which integrate multiple layers of integrated circuitry separated by insulators and ground planes. Key to this technology is the ability to fabricate sub-micrometer vias or larger bonds in the micrometer level, which electrically connect the individual layers with each other and to bond the various layers in a defined way together with an alignment precision of sub-via dimensions. In this way, the performance gain of a device is no longer simply scaling with the density of transistors but results from the chip architecture complexity, with the integration of highly specialized subcomponents like memory, CPU, GPU, and other chips optimized for the specific tasks and interface units, not necessarily using the same node technology. This is illustrated in Figure 3-18. As shaped in the International Technology Roadmap

for Semiconductors in 2010, extrapolation and generalization of these ideas by researchers and technology experts has nucleated onto a broader perspective denominated “more than Moore” approach⁸⁸, envisaged as both complementary or alternative to a “more Moore” scaling. The more than Moore concept is and will be applied in the development of many devices needed for the planned green and digital transformation of our economy⁸⁹.

The required characterization needs of current and future Integrated Circuitry technology can be perceived when considering a device like shown in Figure 3-18. Panel II in the figure outlines a scheme for a solution to the remote sensing challenge⁸⁸, a necessary element of any smart and efficient digitalization strategy. The structure, with its 3D integration of various material families and diverse hierarchical levels, including but not only high-end CMOS technology, clearly shows the need of imaging the different length scales from the micrometer down to the nanometer regime of a large 3D volume with tens of cubic millimeters. Even if ALBA II novel concept of multiscale and multimodal approach and enhanced technique portfolio will provide the necessary comprehensive set of tools and services for tailoring an efficient, fast and ultimately cost-saving characterization of these kind of devices, directly addressing the needs of the emerging European industry and developers in the i+ community. The combination of tools and appropriate automatization could allow fast (up to about 10-20 devices per hour), non-destructive imaging of the full packaged device with medium resolution (roughly 1-5mm resolution) to visualize all building blocks, characterize major interconnects (like bump-bonds) or inspect the larger structures of the different device levels. By using different contrast mechanisms like absorption, phase but also diffraction it will enable to understand the strain distributions and get a first elemental distribution of the 3D-structure to understand reasons for failures and correlate it with the fabrication process or operation conditions.

In combination with the ultra-high-resolution X-ray and electron microscopy tools, ALBA II forms a characterization platform which will provide detailed images of all critical features from the system level to the smallest building block, including the smallest scale CMOS layers. To achieve highest sub-atomic or in some cases even nanometer resolution, the new instruments have to be combined with sophisticated sample preparation tools which will allow localization of the region of interest and the subsequent careful

⁸⁸ Arden, W.; Brillouët, M.; Coge, P.; Graef, M.; Huizing, B.; Mahnkopf, R. More-than-Moore White Paper. Version 2010, 2, 14

⁸⁹ Roy, K.; Jung, B.; Peroulis, D.; Raghunathan, A. Integrated Systems in the More-than-Moore Era: Designing Low-Cost Energy-Efficient Systems Using Heterogeneous Components. IEEE Design & Test 2013, 33 (3), 56-65

preparation of individual microscale thin-cuts using advanced ion-milling. Key to image structure and chemistry in these complex devices on all relevant length scales, essential to understand interdiffusion, strain maps, or other processes impacting the functionality of the device, is the multimodal imaging approach combining imaging techniques with different resolutions and sensitivities, sample preparation and advanced and automated data handling which is, next to the nanometer resolving X-ray microscopes, part of ALBA II DNA. One has also to stress the close relation and complementarity of these capabilities for device characterization with those previously mentioned in section 3.2 focused on Energy, for characterization of functionality and degradation of specific device layers like batteries or the piezo-electric energy harvesting layer by combining operando micro diffraction and spectroscopy.

3.3.2. NEW WAYS TO OVERCOME THE ENERGY CONSUMPTION CHALLENGE: SPINTRONICS

However, ICT, as we know it today, faces a fundamental problem despite the enormous progress made in improving performance of computing devices and including 3D technologies allowing to optimize systems for specific tasks like imaging processing or speech recognition already available in consumer electronics: The overall power consumption.

Today's energy consumption per CMOS logic operation is on the order of 50-100 pJ. According to an estimation⁹⁰ from 2015, as shown in Figure 3-19, the total required power for ICT will be about 21% of the world power production in 2030. This estimation is not

Share of Communication Technology of global electricity usage

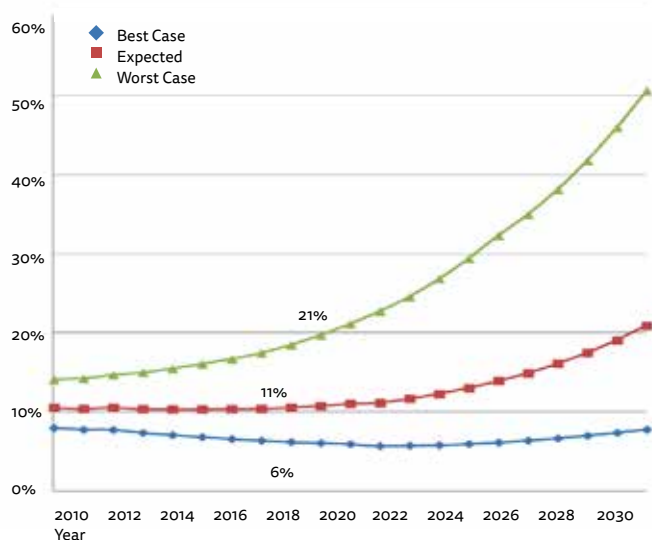


Figure 3-19: Share of communication technology of global electricity usage 2010-2030.

even considering the digital transformation and clearly shows a continuous, near to exponential growth of power needs in the years beyond 2030.

Further reduction of device size will not improve the situation since increasing tunnel currents, resulting in leakage current, will require even higher power to ensure reliable operation. Significant improvements may be found in integrating into the existing CMOS technologies new material classes with improved carrier transport, like carbon nanotubes, Graphene or other 2D materials. However, the minimum of energy consumption reduction is ultimately limited by the Boltzmann thermal distribution for electrons/holes for any kind of field effect transistors⁹¹. Another approach is the combination between CMOS and photonics structures which may allow to significantly increase the computation or encryption speed at similar energy consumption, an important special application which will be essential for providing secure communication and ecommerce in the future.

A much more radical approach with significant reduction of power per computation and a significant speed increase of the device is currently pursued by developing spintronic or spin-orbitronic technologies where the information is contained and transmitted by i.e. magnetic or ferroelectric domains or spin waves in atomically-thin films or nanotracks, and actuated by energy efficient and fast stimuli. A lot of effort is put to understand the basic science and to develop corresponding device structures for electrically controlling the magnetic behavior, i.e. via currents, spin currents, spin torques, directly applied voltage fields, ion motion or light stimuli, which present large efficiency and practical advantages over magnetic field^{92,93}. Such spin currents and magnetic domains, will have a much lower dissipation and faster speeds than charge currents. Related examples are the so-called spin-transfer torque memories (1st commercialized in 2012 by Everspin MRAM company), and spin orbit torque memories (whose commercialization is pursued by the French spin-off Antaios). These are magnetic RAM memories based on a tunnel magnetic junction (TMJ), but while on magnetic memories the writing is done via magnetic fields, on spin transfer and spin orbit torque memories it is done by a spin polarized current, requiring much less energy. Spin polarized currents and other spintronics-related concepts have the potential for broad application, hence spintronics role in ICT may go well beyond memories and includes a full spintronic, ferroelectric or magnetoelectric logic gate computing device (as opposed to CMOS transistor's logic)^{90,94,95}. Indeed, in a general abstraction, one could consider a device operating as a switch of any order parameter on a quantum material with non-linear input-output transfer (amplification), on which basis a "gate" logic is implemented⁹³. In such device the energy efficiency is dictated by the related energy barrier between the order parameter states used. Low dissipation could be also achieved in the occurrence of eventual breakthroughs such as discovery of room-temperature superconductors or topological insulators with non-dissipative conduction of electrical charge in the surface or edge states.

⁹⁰ Andrae, A. S. G.; Challenges, T. E.-; 2015, undefined. On Global Electricity Usage of Communication Technology: Trends to 2030. [mdpi.com](https://doi.org/10.1038/s41567-018-0101-4)

⁹¹ Manipatruni, S.; Nikonov, D.; Physics, I. Y.-N.; 2018, undefined. Beyond CMOS Computing with Spin and Polarization. [nature.com](https://doi.org/10.1038/s41567-018-0101-4) 2018. <https://doi.org/10.1038/s41567-018-0101-4>

⁹² Juge, R.; Je, S.-G.; Chaves, D. de S.; Buda-Prejbeanu, L. D.; Peña-García, J.; Nath, J.; Miron, I. M.; Rana, K. G.; Aballe, L.; Foerster, M.; Genuzio, F.; Mentis, T. O.; Locatelli, A.; Maccherozzi, F.; Dhesi, S. S.; Belmeguenai, M.; Roussigné, Y.; Auffret, S.; Pizzini, S.; Gaudin, G.; Vogel, J.; Boule, O. Current-Driven Skyrmion Dynamics and Drive-Dependent Skyrmion Hall Effect in an Ultrathin Film. *Phys. Rev. Appl.* 2019, 12 (4), 044007. <https://doi.org/10.1103/PhysRevApplied.12.044007>

⁹³ Huang, M.; Hasan, M. U.; Klyukin, K.; Zhang, D.; Lyu, D.; Gargiani, P.; Valvidares, M.; Sheffels, S.; Churikova, A.; Büttner, F.; Zehner, J.; Caretta, L.; Lee, K. Y.; Chang, J.; Wang, J. P.; Leistner, K.; Yildiz, B.; Beach, G. S. D. Voltage Control of Ferrimagnetic Order and Voltage-Assisted Writing of Ferrimagnetic Spin Textures. *Nature Nanotechnology* 2021, 16 (9), 981–988. <https://doi.org/10.1038/s41565-021-00940-1>

⁹⁴ Manipatruni, S.; Nikonov, D. E.; Lin, C. C.; Gosavi, T. A.; Liu, H.; Prasad, B.; Huang, Y. L.; Bonturim, E.; Ramesh, R.; Young, I. A. Scalable Energy-Efficient Magnetoelectric Spin-Orbit Logic. *Nature* 2019, 565 (7737), 35–42. <https://doi.org/10.1038/s41586-018-0770-2>

⁹⁵ Ramesh, R.; Royal, S. M.-P. of the; 2021, undefined. Electric Field Control of Magnetism. royalsocietypublishing.org 2021, 477 (2251). <https://doi.org/10.1098/rspa.2020.0942>

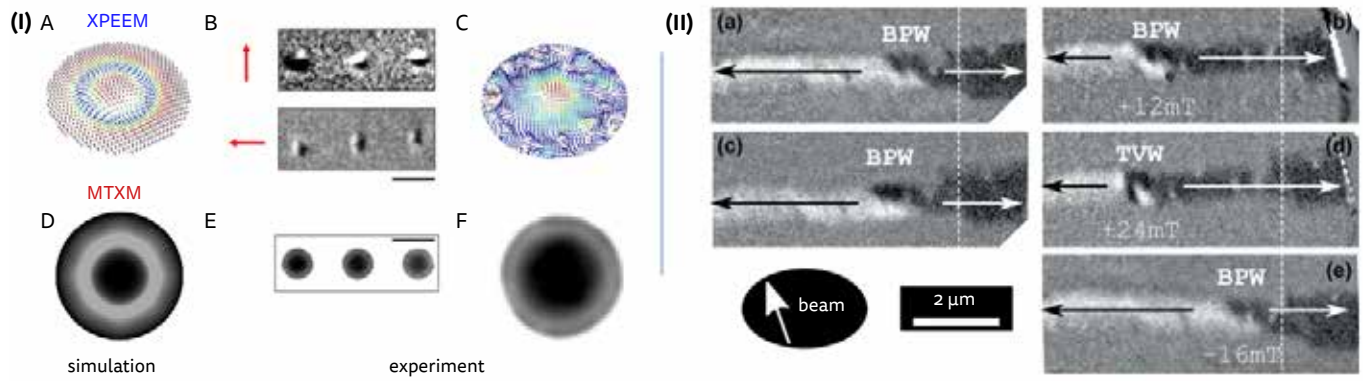


Figure 3-20 | 3-21: Synchrotron radiation imaging for novel spintronic concepts and devices. (I) First experimental confirmation of a novel magnetic topological texture, a magnetic hopfion⁹⁶. The image shows the simulated measured spatial patterns for XPEEM and Magnetic Transmission X-ray Microscopy (MTXM) experiments. The combination of techniques allowed to nail down ambiguities and claim that the objects correspond to the conceptual magnetic hopfion pattern; (II): Domain wall motion in a nanowire racetrack¹⁰¹. XPEEM shadow-technique microscopy in the investigation of DW motion on a 140-nm-diameter Permalloy (Fe₂₀Ni₈₀) nanowire, featuring a DW in its thin section. Arrows stand for magnetization in the domains, and the vertical dotted line indicates the diameter modulation. (a), (b) and (c), (d) are two sequences initialized with a first type of domain wall (Bloch) followed by the application of a quasistatic field with strength 12 and 24 mT, respectively, showing that in large fields the domain topology changes to a second type (tail-to-tail) whereas for small fields is preserved.

A large user community of ALBA is working already now on various aspects of spintronics, as was patent on the ALBA II workshops on “Spintronics with Synchrotron Radiation”⁹⁶ and “2D materials with SR”⁹⁷ with in total more than 300 participants including world-leading researchers. The spintronics community discussed novel concepts for magnetic memories and devices based on emergent magnetic concepts such as spin torque, chiral domain walls in ferrimagnets and antiferromagnets or other topological magnetic objects such as skyrmions^{91,92,98,99,100}. Figure 3-21 and Figure 3-22 show some examples of fascinating magnetic non-collinear

states, their topology and transformation with field, temperature or current. Following the fast dynamics of this growing field, it is obvious at this point, that studying the materials under device ‘operando’ conditions is essential, not only to understand the interaction between the different device components but also to observe the effects which are often not material but device or operando stimuli dependent; an example is shown in Figure 3-21 which elucidates the transformation of the magnetic topology of fast moving Domain Walls (DW).¹⁰¹

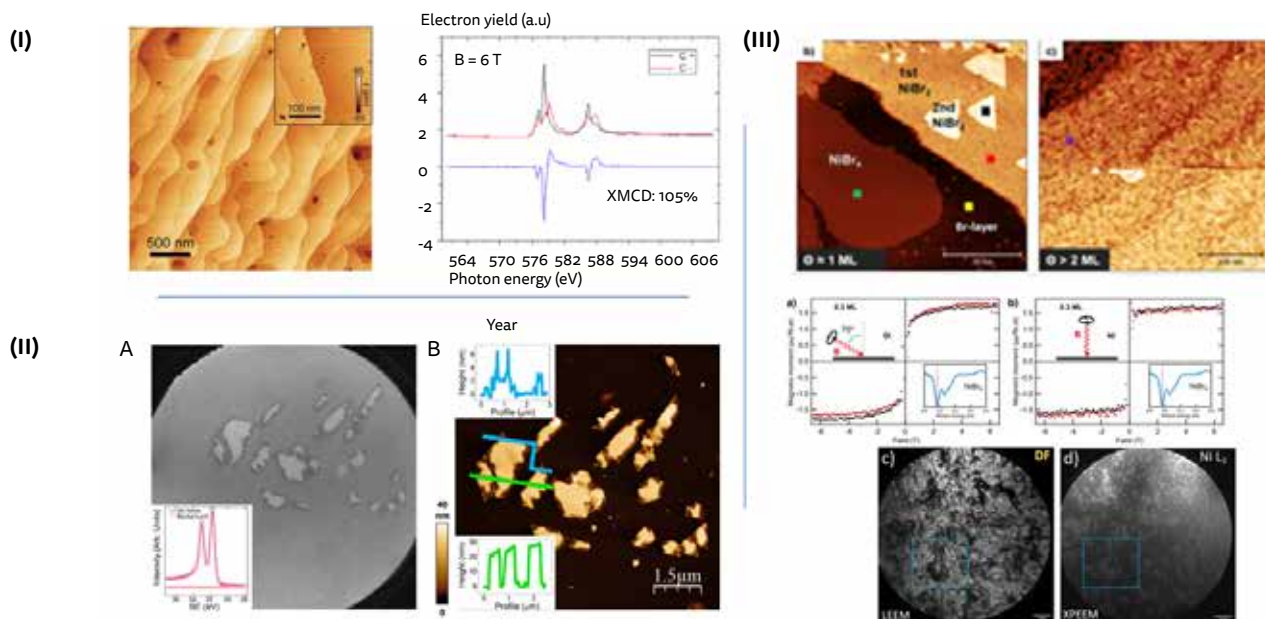


Figure 3-22: Examples of 2D van der Waals materials investigated at ALBA. Panel I: Discovery of novel XY 2D ferromagnetic class¹⁰². Images of single layer CrI₃ vdW grown by MBE on Graphene acquired by Scanning Tunneling Microscopy (STM), and corresponding XMCD at 2k and 6T (ALBA BL29). Panel II: Correlative imaging by X-ray PEEM (ALBA BL24) and Atomic Force Microscopy (AFM) on mechanically exfoliated flakes of few-layer (FL) antimonene¹⁰³. Correlative imaging of flakes of different thicknesses (2–40 nm) has allowed to establish the chemical and electronic properties via X-PEEM to the regions with morphological (i.e. thickness) properties determined via AFM. Panel III: Multimodal, multiscale investigation of NiBr₂ ferromagnetic 2D materials using STM and XMCD at ALBA BL29, and X-PEEM at ALBA BL24¹⁰⁴. The STM images (top) and LEEM/X-PEEM demonstrate the predominant single atomic layer morphology from the nano to the micron scale, whereas the XMCD (middle) evidence the magnetic nature and strong magnetic anisotropy of the system.

⁹⁶ <https://indico.cells.es/e/ALBAII/workshop-2D-materials>

⁹⁷ <https://indico.cells.es/event/373/>

⁹⁸ Kent, N.; Reynolds, N.; Raftrey, D.; Campbell, I. T. G.; Virasawmy, S.; Dhuey, S.; Chopdekar, R. V.; Hierro-Rodríguez, A.; Sorrentino, A.; Pereira, E.; Ferrer, S.; Hellman, F.; Sutcliffe, P.; Fischer, P. Creation and Observation of Hopfions in Magnetic Multilayer Systems. *Nat Commun* 2021, 12 (1), 1562. <https://doi.org/10.1038/s41467-021-21846-5>.

⁹⁹ Sanz-Hernández, D.; Hierro-Rodríguez, A.; Donnelly, C.; Pablo-Navarro, J.; Sorrentino, A.; Pereira, E.; Magén, C.; McVitie, S.; de Teresa, J. M.; Ferrer, S.; Fischer, P.; Fernández-Pacheco, A. Artificial Double-Helix for Geometrical Control of Magnetic Chirality. 2020, 1–19

¹⁰⁰ Ukleev, V.; Yamasaki, Y.; Morikawa, D.; Karube, K.; Shibata, K.; Tokunaga, Y.; Okamura, Y.; Amemiya, K.; Valvidares, M.; Nakao, H. Element-Specific Soft x-Ray Spectroscopy, Scattering, and Imaging Studies of the Skyrmion-Hosting Compound Co₈Zn₈Mn₄. *Physical Review B* 2019, 99 (14), 144408

¹⁰¹ Wartelle, A.; Trapp, B.; Staño, M.; Thirion, C.; Bochmann, S.; Bachmann, J.; Foerster, M.; Aballe, L.; Menteş, T. O.; Locatelli, A.; Sala, A.; Cagnon, L.; Toussaint, J.-C.;

Fruchart, O. Bloch-Point-Mediated Topological Transformations of Magnetic Domain Walls in Cylindrical Nanowires. *Phys. Rev. B* 2019, 99 (2), 024433. <https://doi.org/10.1103/PhysRevB.99.024433>.

¹⁰² Bedoya-Pinto, A.; Ji, J. R.; Pandeya, A. K.; Gargiani, P.; Valvidares, M.; Sessi, P.; Taylor, J. M.; Radu, F.; Chang, K.; Parkin, S. S. P. Intrinsic 2D-XY Ferromagnetism in a van Der Waals Monolayer. *Science* 2021, 374 (6567), 616–620. <https://doi.org/10.1126/science.abd5146>

¹⁰³ Ares, P.; Pakdel, S.; Palacio, I.; Paz, W. S.; Rassekh, M.; Rodríguez-San Miguel, D.; Aballe, L.; Foerster, M.; Ruiz del Álbor, N.; Martín-Gago, J. Á.; Zamora, F.; Gómez-Herrero, J.; Palacios, J. J. Few-Layer Antimonene Electrical Properties. *Applied Materials Today* 2021, 24, 101132. <https://doi.org/10.1016/j.apmt.2021.101132>.

¹⁰⁴ Bikaljević, D.; González-Orellana, C.; Peña-Díaz, M.; Steiner, D.; Dreiser, J.; Gargiani, P.; Foerster, M.; Niño, M. Á.; Aballe, L.; Ruiz-Gomez, S.; Friedrich, N.; Hieulle, J.; Jingcheng, L.; Ilyn, M.; Rogero, C.; Pascual, J. I. Noncollinear Magnetic Order in Two-Dimensional NiBr₂ Films Grown on Au(111). *ACS Nano* 2021, 15 (9), 14985–14995. <https://doi.org/10.1021/acsnano.1c05221>.

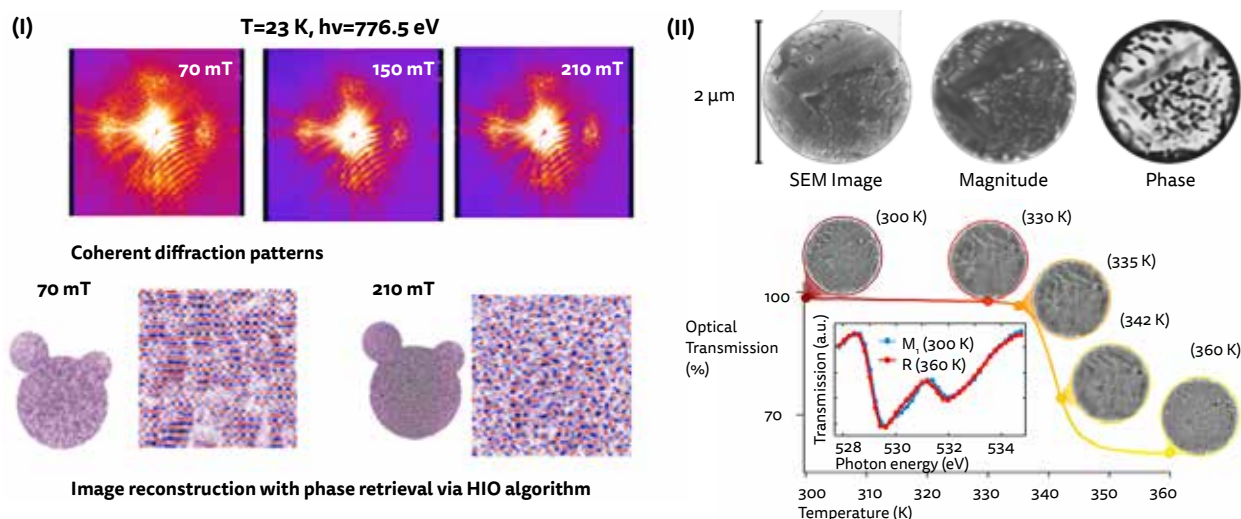


Figure 3-23: Nanoscale coherent imaging of magnetic and electronic phase transitions in Quantum Materials.

(I) Coherent diffraction imaging of topological magnetic domains at low temperature and under high applied magnetic fields on a $\text{Co}_{0.9}\text{Zn}_{0.1}\text{Mn}_4$ sample, using soft X-ray XMCD; the shown retrieval was taken at the $\text{Co L}_{2,3}$ edge ($E = 776.5\text{ eV}$) at different $T = 23\text{ K}$ under different applied magnetic fields of $B = 70\text{ mT}$ and 210 mT . The transformation of the elongated skyrmions to a smaller-size skyrmion phase takes place. The achieved resolution using a phase retrieval algorithm is roughly 30 nm .¹⁰⁰

(II) Coherent imaging by soft X-ray holography of metal and dielectric domains coexisting during the Metal-Insulator phase transition in VO_2 quantum material¹⁰⁵. Using soft X-ray spectroscopic linear dichroism contrast to exploit spectroscopical signatures of the high temperature metal (rutile) or low temperature insulating (monoclinic) phase, the X-ray holography enables to follow the evolution during the transition and evidence that the local heterogeneity results on phase coexistence at the nanoscale.

So called 2D materials form a new class of materials with large potential of application in the field of spintronics. In this new and exponentially fast-growing field, research ranges from materials growth and isolation, device development, to even engineering the band structure by adjusting the misalignment or twist between individual layers of 2D van der Waals monolayers (twistronics). Accordingly, the wide range of ALBA tools including powder diffraction, various hard and soft X-ray spectroscopies, XMCD, ARPES and PEEM come to employment. This is an area where the national and European research communities are strong, notably strengthened via the strategic Graphene EU Flagship that has also covered related 2D vdW materials. Numerous leading studies and discoveries have made use of ALBA techniques, as for the examples on Figure 3-22 below. Such correlative, in-situ, multiscale and multimodal investigations will be boosted and fully optimized in ALBA II.

ALBA II will bring here essential advantages to the community, with capabilities to decrease the spatial probe volume to the cubic-micrometer level, image buried interfaces and push the current imaging resolution from $30\text{--}50\text{ nm}$ to even few nanometers level by applying next generation of aberration-corrected XPEEM, scanning transmission X-ray microscopy and coherence-based imaging techniques.

The remarkable enhancement of coherence in the soft as well as in the hard X-ray range of ALBA II bring new exciting opportunities by developing coherence-based imaging tools, along tradition at ALBA; ALBA II coherence improvements will boost the contrast, allowing the 3D imaging of magnetic vector moments even on buried layers and all this on the nanometer and has a long tradition at ALBA.

Lensless coherent imaging experiments at ALBA have been key for visualizing the magnetic domain structure of $\text{Co}_8\text{Zn}_8\text{Mn}_4$ of interest in spintronics⁹⁹, and the Metal-Insulator phase transition in VO_2 ¹⁰⁵ of relevance for example in neuromorphic and brain-inspired artificial devices, as depicted in Figure 3-23.

An additional important component of ALBA II will be the improved laboratory infrastructure which will allow to assemble and optimize the devices directly at ALBA reducing the risk for failures and accelerating the development cycle. Part of this enabling and additional laboratory infrastructure is also other high-resolution microcopy technologies like TEM's, atomic force, and scanning tunneling microscopes, currently installed at ALBA in the framework of InCAEM bringing new ways for multi-length-scale and correlative imaging, currently developed as workflow within the InCAEM project. Last but not least, ALBA II high throughput capabilities will largely benefit the combinatoric development of diverse raw materials like the development of close to defect free 2D van der Waals materials.

3.3.3. NEUROMORPHIC AND QUANTUM COMPUTING

More efficient computing schemes such as brain-inspired neuromorphic computing or quantum computing could solve the challenges and enable further scaling up of data and processing power, providing orders of magnitude larger processing power and speed in energy saving technologies. Those schemes are sometimes referred to as *beyond Moore* paths for scaling of micro-processing, encrypting and computing. Indeed, those schemes are not antagonist but could merge in quantum neuromorphic computing¹⁰⁶.

Von Neumann computers are outperformed by the mammal brain in numerous data-processing applications such as pattern recognition and data mining. Neuromorphic engineering (or computing) aims to mimic brain-like behavior through the implementation of artificial neural networks based on the combination of a large number of artificial neurons massively interconnected by an even larger number of artificial synapses. In order to effectively implement artificial neural networks directly in hardware, it is mandatory to develop artificial neurons and

¹⁰⁵ Vidas, L.; Günther, C. M.; Miller, T. A.; Pfau, B.; Perez-Salinas, D.; Martínez, E.; Schneider, M.; Gührs, E.; Gargiani, P.; Valvidares, M.; Marvel, R. E.; Hallman, K. A.; Haglund, R. F.; Eisebitt, S.; Wall, S. Imaging Nanometer Phase Coexistence at Defects during the Insulator-Metal Phase Transformation in VO_2 Thin Films by Resonant Soft X-ray Holography. *Nano Letters* 2018, 18 (6), 3449–3453. <https://doi.org/10.1021/acs.nanolett.8b00458>.

¹⁰⁶ Spagnolo, M.; Morris, J.; Piacentini, S.; Antesberger, M.; Massa, F.; Crespi, A.; Ceccarelli, F.; Osellame, R.; Walther, P. Experimental Photonic Quantum Memristor. *Nature Photonics* 2022 16:4 2022, 16 (4), 318–323. <https://doi.org/10.1038/s41566-022-00973-5>

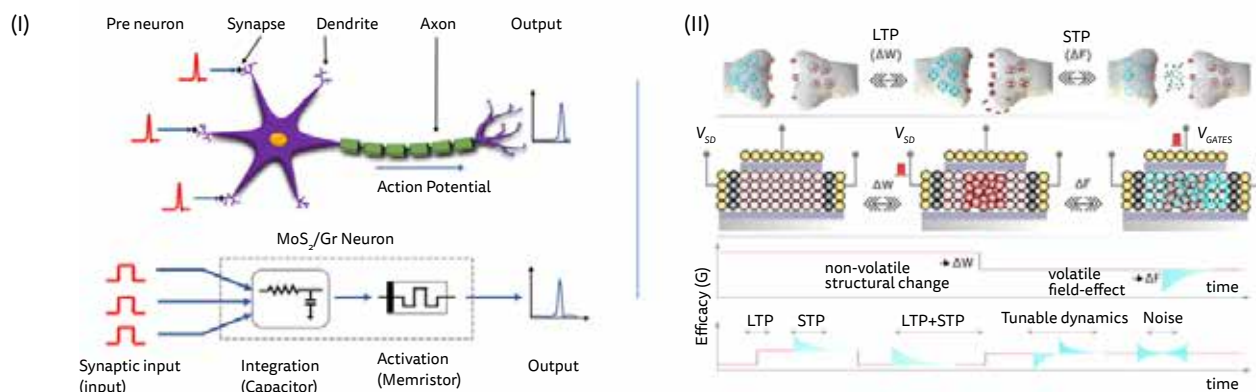


Figure 3-24: Artificial neurons for neuromorphic computing. (I) Implementation of an integrate-and-fire artificial neuron using a vdW memristor, in which vdW MoS₂ is used on a Graphene electrode to benefit from Synaptic Efficacy and Phase Change Memtransistors: The top panel is a representation of the biophysical long (LTP) and short (STP) plasticity mechanisms which change the strength of synaptic connections. The middle panel is an emulation of these mechanisms using our phase change memtransistive synapse. The bottom panel illustrates how by mapping the synaptic efficacy into the electrical conductance of a device, a range of different synaptic processes can be mimicked.

synapses which will require low power consumption and show a small footprint; hence, IC solutions to scale down the size and energy consumption, and spintronic energy-saving concepts are of high interest in this context¹⁰⁷.

Leading ICT companies have started using chip structures in their product line-up based on 3D CMOS architectures with embed neural modules specifically tuned for artificial intelligence tasks, such as speech and image processing. For example, IBM z16 Telum chip with integrated accelerator for AI with neural network, and the Apple-designed and TSM-manufactured M1 ultra chip. The M1 ultra chip uses advanced 3D packaging to create a more performant IC by integrating 2 previous generation M1 chips. It is based on 5nm node technology, packs 114 billion transistors, and an embedded 32-core neural engine capable of processing 22 trillion operations per second. Neural engines in mobile phones to speed-up speech and image processing, enabling for example fast face recognition for face unlocking, image processing and AI-enhanced video-photography or improved speech recognition. A promising advance has been made in recent years with the introduction of the components called memristors that might implement synaptic functions. More recently, advances in artificial neurons have implemented the basic functions of leaky integrate-and-fire of spiking neurons¹⁰⁸.

These new and more radical technology transformations will leave the typical CMOS landscape and design rules even if most developers expect that the devices have to be compatible with CMOS electronics. Their materials bill typically various and their functionality is strongly dependent on order/disorder on the nanometer scale.

To illustrate the advantages of these new structures one has to compare modern supercomputers with the brain: while supercomputer clusters can process similar or even superior number of instructions per second, have much larger storage capability, and pack a similar number of elements, the brain uses 1 million times less energy. Hence, the brain functions on a much more efficient scheme beyond Turing-von Neuman's reprogrammable

sequential processing, thanks among others to a massive number of parallel synapses, their analog nature and the complexity of the connections.

ALBA and its user community is already contributing to this emerging field by fundamentally studying the structural changes and their reversibility during the application of electrical fields using microscopy or spectroscopic tools^{104,109,110,111}; however, ALBA current characterization suite is not capable to visualize the complex three-dimensional structures and their changes on the relevant length scales in realistic devices, capable of performing the computation. This is key and basis for contributing in moving this innovative basic research to the application level and finally boosting economic growth. The characterization requirement for neuromorphic computing is driven by the typical 3D assembly, the component size and the interconnects characteristic sizes making high-resolution imaging techniques with chemical and an optional magnetic contrast to a must. ALBA II with its new enhanced microscopic tools based on the 4th generation source, mainly coherence-based imaging in the polarization dependent soft and hard X-ray regime and the subatomic resolution TEM capabilities, as well as its integrated approach of combining multiple imaging, spectroscopy and diffraction techniques, to create a truly correlative and multi length scale imaging approach, will image all necessary parameters on the relevant length scale for the device. In concert with the high throughput instrumentation and as already proven in the case of CMOS technology⁹⁸, it will not only contribute to the development of the device physics itself but will provide the basis for efficient and reliable production protocols essential for commercialization.

Quantum Informatics Systems (QIS) is a fundamentally different approach from classical machines: a classical bit is either $q=1$ or $q=0$, but a quantum bit, or qubit, is a superposition of both states typically represented with a vector.

Depending on the operator acting on the state, or as computing scientists would call it gate(s), the one qubit can now express multiple states, leaving the class $|q\rangle = \cos\frac{\theta}{2}|0\rangle + e^{i\phi}\sin\frac{\theta}{2}|1\rangle$

¹⁰⁷ Grollier, J.; Querlioz, D.; Camsari, K. Y.; Everschor-Sitte, K.; Fukami, S.; Stiles, M. D. Neuromorphic Spintronics. *Nat Electron* 2020, 3 (7), 360–370. <https://doi.org/10.1038/s41928-019-0360-9>.

¹⁰⁸ Stolar, P.; Tranchant, J.; Corraze, B.; Janod, E.; Besland, M. P.; Tesler, F.; Rozenberg, M.; Cario, L. A Leaky-Integrate-and-Fire Neuron Analog Realized with a Mott Insulator. *Advanced Functional Materials* 2017, 27 (11), 1604740. <https://doi.org/10.1002/ADFM.201604740>.

¹⁰⁹ Martins, S.; de Rojas, J.; Tan, Z.; Cialone, M.; Lopeandia, A.; Herrero-Martín, J.; Costa-Krämer, J. L.; Menéndez, E.; Sort, J. Dynamic Electric-Field-Induced Magnetic

Effects in Cobalt Oxide Thin Films: Towards Magneto-Ionic Synapses. *Nanoscale* 2022, 14 (3), 842–852.

¹¹⁰ Domain Wall Automation in Three-Dimensional Magnetic Helical Interconnectors | *ACS Nano*. <https://pubs.acs.org/doi/10.1021/acsnano.1c10345> (accessed 2023-01-18)

¹¹¹ Dawidek, R. W.; Hayward, T. J.; Vidamour, I. T.; Broomhall, T. J.; Venkat, G.; Mamoori, M. A.; Mullen, A.; Kyle, S. J.; Fry, P. W.; Steinke, N.-J.; Cooper, J. F. K.; Maccherozzi, F.; Dhési, S. S.; Aballe, L.; Foerster, M.; Prat, J.; Vasilaki, E.; Ellis, M. O. A.; Allwood, D. A. Dynamically Driven Emergence in a Nanomagnetic System. *Advanced Functional Materials* 2021, 31 (15), 2008389. <https://doi.org/10.1002/adfm.202008389>

multiple qubits can be superposed and entangled, meaning an operation on one qubit automatically acts on the entangled state. Perhaps the most important consequence of this is, that n qubits describe 2^n states per operation, whereas a classical computer can describe $2 \cdot n$ states with a bit-width of n and one operation.

Besides in classical computing, QIS play important roles in a nearly completely secure encrypting and decrypting of sensitive information or in the hacking of encrypted information, currently unthinkable to realize with classical computing systems.⁹⁹ Additionally, QIS enables sensing of ultrasensitive electromagnetic, optical, and chemical signals, an area also of high interest of the Spanish and European communities.^{100,101}

QIS devices are strongly dependent on the decoherence time of the different qubits, or in other words, the time in which the different states lose their quantum coherence. Losing the coherence results in not only losing the information but resulting in wrong results of the operation if not otherwise detected. The community is fighting this problem in two ways: they develop specific error correction methodologies⁹⁷ and they enhance the decoherence time by improving the device structure itself.

Technically, various different platforms exist which allow to realize qubits. Currently, the most "popular" systems are based on trapped ions, using the atomic states of the ion, the family of ultra-cold superconducting devices, using either charge, magnetic flux, or phase of the current⁹⁸, silicon quantum dots, the closed technology to CMOS and using the wave function of a single electron in a defined potential, topological qubits, and diamond (or diamond like) vacancies, which use the nuclear spin to encode the quantum state. Currently, trapped ion and superconducting devices are mostly explored for computing applications where diamond vacancies are mostly used for encryption in fiber-optic application. Silicon quantum dots are a fast-emerging technology and topological qubits promise a great future due to the large variety of available materials, but so far, no working device was demonstrated using this technology.

To fight the interaction with the thermal bath which ultimately results in the decoherence of the quantum state, most structures use either materials of a different isotope from the surrounding elements for the device itself or have to cool down the substrate to the milli-Kelvin regime. All of the devices are in common that they have a complex structure with precisely positioned multiple micro-electrodes; interface chemistry and the strain fields within the device itself and its surrounding are typically an important parameter which has to be controlled during the manufacturing process.

A specific case are the ultra-cold superconducting devices. Perhaps the most promising path with nearly all big commercial players developing prototypes, they exhibit various significant materials science problems which are mostly attributed to the interface between the superconducting layer and its substrate and imperfections, including strain effects in the area of the Josephson tunnel Contact.

3Sbar, a currently being designed and fully optimized beamline for ALBA II, is a good example how ALBA II is the enabler technology to bring insight in the quality determining interfaces and the device structures. Providing HEXPAS, a technique which allows to probe depth sensitive the chemical states and composition of thin films and their interfaces, in combination with surface diffraction allowing to probe the long-range structure, including strain and stress, defect structures of the substrate and their impact on the device structure, grown on top, is giving a unique tool for understanding the materials aspect of defects, interface chemistry and imperfections. Essential to understand the effects on the device structure level is the lateral probe size in the range of 1mm; this, combined with the vertical nanometer resolution gives the perfect tool to elucidate the effects of imperfection on the final device performance. The new beamline will start its operation still as an ALBA beamline, and will reach its optimal performance with ALBA II. Its performance will then be boosted because the horizontal beam size on the sample will be 10 times smaller and the horizontal transverse coherence length at ALBA II will be 10 times larger than in ALBA, allowing to exploit the large coherence fraction by performing X-ray surface photon correlation spectroscopy (monitoring the time dependence of the diffracted coherent scattering speckles) to investigate dynamical surface processes.

ALBA II with its highly brilliant beams and consequently the capability to perform spectroscopic as well as diffraction-based techniques on a micrometer and sometimes even on sub-micrometer level will be a game changer in performing characterization of these small and often highly diluted systems. The ability of building hard X-ray nanoprobe on beamlines which exceeds by far a length of 150m, allowing not only exceptional high coherent flux and beam sizes in the sub-device level at working distances which allows to implement complex RF, optics or cryogenic sample environments, plays here a specific role to identify and characterize the chemical and strain effects around defects and the device structures itself.

3.4. ALBA II: Essential enabler technology to empower the Spanish user community to address the grand challenges

Independent from the applied metric, ALBA has proven over the past 10 years of operation that the facility is a reliable partner for providing a broad scientific and industrial community with tools essential to be competitive in the European and worldwide context. With a solid characterization portfolio, operated with high operational excellence, ALBA has not only built a solid user community, representing a wide spectrum of the Spanish basic research landscape, but has also optimized instrumentation and provided services according to the user needs, resulting in an exceptional productivity, measured in number of publications and at the same time pushing the impact of the publication, measured in the average impact factor per publication.

Building on this excellence and network, ALBA II is the answer to the increasing demands on the scientific communities to contribute technical, economic and sustainable solutions to the overarching challenges ahead of us. At the core of ALBA II is the upgrade of the accelerator, the integration of big data and high throughput capabilities and equally important the focusing on sample environments which allows to characterize matter during performing a function, pushing the boundary towards applied research and innovation.

Part of ALBA II DNA is the integration of the new and complex tools like nano probes, HRTEM or microscopic probes of electronic structure into the proven characterization suite by providing the user multimodal and correlative methodologies. This will reduce the efforts for the community to employ the often significantly more complex new tools and at the same time brings the facility closer to make the transition from delivering solutions and not only data to complex characterization challenges.

Based on these technologies, ALBA II approach is to provide new 2D and 3D imaging tools with resolutions appropriate to characterize the different length scales relevant to the function of devices and organisms. Key to understand the complex structure function characterization is the correlative and multimodal Ansatz. High throughput, data mining and data analytics tools are the second pillar for this approach guaranteeing statistical relevant data sets essential for applied problems like medical research or the development of novel devices and optimized materials.



4 Accelerator and Photon Sources



4.1. Accelerators: storage ring upgrade

The main goal of the accelerator upgrade for ALBA II is the transformation of ALBA into a diffraction limited storage ring, which implies the reduction of the emittance by at least a factor of twenty.

The upgrade has been conceived as a cost and time effective process, to be realized before the end of the decade and profiting at maximum all existing infrastructures, in particular the building which is now hosting the facility. It has been decided that the storage ring (SR) upgrade will be done without any major modification of the concrete tunnel. Furthermore, the requirement of maintaining the Insertion Devices (IDs) as close as possible to their present position will preserve them operative for ALBA II and will imply minor modifications to the beamlines.

Another important decision has been the determination of the beam energy of ALBA II, which will be maintained at 3GeV, after having considered several factors, of which the continuation of the present successful scientific programs is the main one. On top of that the circumference of the SR is constrained to be about 270m in order to reuse the tunnel; and since we want to preserve also the IDs position, a sixteen-cell geometry is imposed. With these constraints the length of the arcs is too short for obtaining a substantial reduction of the beam emittance at higher beam energies, also considering that the emittance scales with the square of the energy. Another consideration is related to the injector: increasing the energy of the SR would require to replace the whole booster, which increases the cost of the project and lengthen its realization. On top of these, a higher beam energy would have implied a higher energy consumption and, most likely, an additional upgrade of the conventional service infrastructures and reinforcing radiation shielding systems.

An extremely optimized lattice design has been conceived, fitting all these goals and constrains. Its details are found in the section 4.1.1.

The optimization of the lattice, together with the constrains on space, makes that one of the main challenges of this upgrade is the design of the magnets, in section 4.1.2 a description of proposed magnets and technologies is presented.

The high magnetic field density requirements for the magnets, in order to comply with the requirements of the lattice, result on magnets with a very small bore-radius, and vacuum chamber with

very small diameter. In order to preserve the ultra-high vacuum requirements of the accelerator, the use of the new NEG coating technology is a must. In section 4.1.3 a brief description of the vacuum system challenges is outlined.

Section 4.1.4 is related to the requirement of the RF system, that due to the small beam sizes and reduced lifetime requires the addition of a 3rd harmonic system to the main system. Description and expected parameters of both RF systems are given on this section.

Diagnostics for this small beam size, highly stable, and compact accelerator is also a major challenge. Section 4.1.5 gives an overall overview of the different diagnostics components that will be required.

In Section 4.1.6, the implementation of all these systems in the present tunnel space is considered; and a consistent overall layout solution is proposed and shown in Figure 4-19.

Section 4.1.7 is related to the important aspect of the electron injection from the existing booster to the upgraded storage ring. Aspect that, also due to the compactness of the proposed solution, will require the development of a novel pulsed magnet device, the Double Dipole Kicker (DDK). The description of the injection scheme and of the new DDK device is presented on this section.

The upgrade will involve as well the actualization and renewal of the different support subsystems, as new power supplies, modern timing systems, upgrade of the equipment and personal protection systems, improvement on the infrastructure control system, and actualization of the radiation protection systems.

4.1.1. LATTICE

Linear lattice

The ALBA II lattice is based on a six bend achromat cell (6BA) configuration¹¹². The choice of a 6BA is the result of an optimization work aiming to balance the demand for a lower emittance with the geometrical constrains due to the available space and the fixed position of the insertion devices. The new 6BA optics allows for a reduction of the horizontal natural emittance by about a factor 25, while keeping the cell length identical to the present ALBA

¹¹² A distributed sextupoles lattice for the ALBA low emittance upgrade. G. Benedetti, M. Carlà, U. Iriso, Z. Martí, F. Pérez. [ed.] Jacow. Campinas, Brasil : s.n., 2021. IPAC21

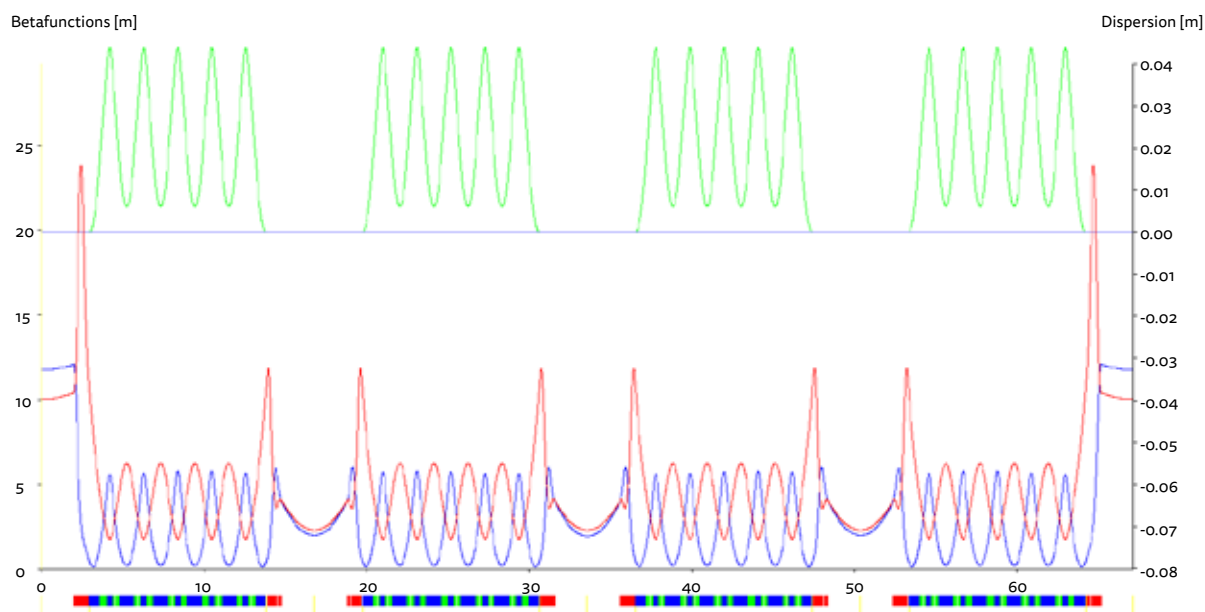


Figure 4-1: Optics functions for a machine quadrant. The first and fourth cell of each quadrant are of the high betas type and are matched to magnify the horizontal dynamic aperture at one straight section in order to accept the injected beam on a stable orbit. The betas at the ends of the unit cells instead are tuned to match the electron beam phase space as close as possible to the radiation emitted by the insertion devices and maximize the brilliance.

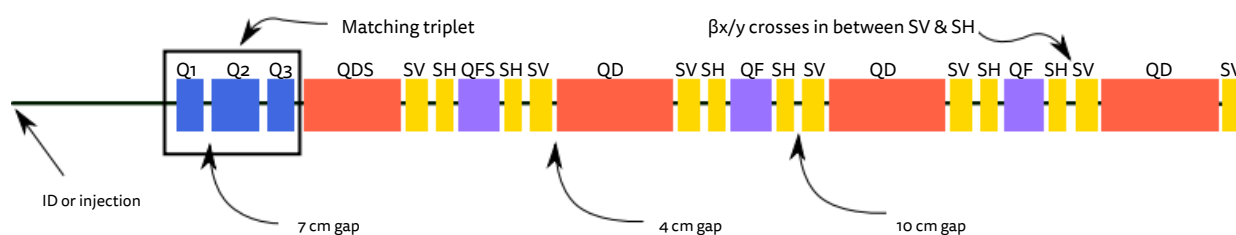


Figure 4-2: Arrangement of the magnets in a portion of a cell. Pure quadrupoles are shown in blue, the main dipole in red, the focusing quadrupoles with anti-bend field are purple while the sextupoles are yellow. The figure shows also the spacing between magnets.

cell length. The overall ring symmetry is preserved: the lattice is composed by 16 cells organized in four quadrants. All arcs have the same low-emittance lattice, and four straight sections have high-betas, see Figure 4-1. One of them is required for the injection, two more are for RF cavities and one is available for an ID.

The first and last dipoles in the arc section are shortened and tuned to act as dispersion suppressors. The bending magnets in the arc are interleaved with strong and compact focusing quadrupoles. Both the bending magnets and the focusing quadrupoles are combined function type, incorporating a bending field and a transverse linear gradient (quadrupole field), resulting in a very compact lattice (see Figure 4-2). To achieve the smallest possible equilibrium emittance a weak defocusing gradient is incorporated into the main bending magnets while a weak anti-bend component is required for the focusing quadrupoles. To avoid the isochronous condition and incur in head-tail instabilities triggered by the vanishing momentum compaction factor, an additional constrain was introduced during the optimization process, resulting in a final value momentum compaction factor of $0.8 \cdot 10^{-4}$ considered safe for standard operations. A preliminary comprehensive list of the parameters for the ALBA II lattice is shown in Table 41. Further studies are required in order to optimize the lattice considering the technical constrains.

TABLE 4-1: ALBA II LATTICE PRELIMINARY MAIN PARAMETERS

Horizontal natural emittance	180 pm-rad
Energy	3 GeV
Circumference	269 m
Number of cells	16
Betatron tunes	43.67 / 11.67
Natural chromaticity	-94 / -51
Momentum compaction factor	$0.8 \cdot 10^{-4}$
Energy spread	$1.0 \cdot 10^{-3}$
Energy loss per turn	843 keV
Damping times	3 / 6 / 6 ms

Round beam operations

Lifetime is expected to be dominated by the Touschek scattering due to the exceptionally small natural beam size, in particular the vertical emittance is foreseen to be of the order of a few pm-rad only. To limit beam losses and increase lifetime, a solution under investigation consists in leaking part of the horizontal emittance

on to the vertical plane by exploiting the coupling resonances. By matching the horizontal and vertical tune is thus possible to obtain a round beam with an effective horizontal and vertical emittance of around 115 pm-rad pm with a substantial improvement of the lifetime.

Intra-beam scattering (IBS)

The ultralow emittance of ALBA II, and so the small transverse dimensions of the beam, results on an enhancement of the Intra-beam scattering (IBS) effects which can blow-up the beam and deteriorate the effective emittance. This effect is diminished by enlarging the bunch length with the use of the 3rd harmonic RF system.

In Figure 4-3 the IBS effect is shown, in terms of percentage increase of the emittance, as a function of the bunch length for a beam of 300mA in multibunch mode, in full coupling, round beam. As can be seen, the effect is appreciable but small. With the foreseen bunch lengthening factor of 3, estimated in Section 4.1.4, the increase of the emittance due to the IBS effect is around 2%, as computed with the ZAP (2) code.

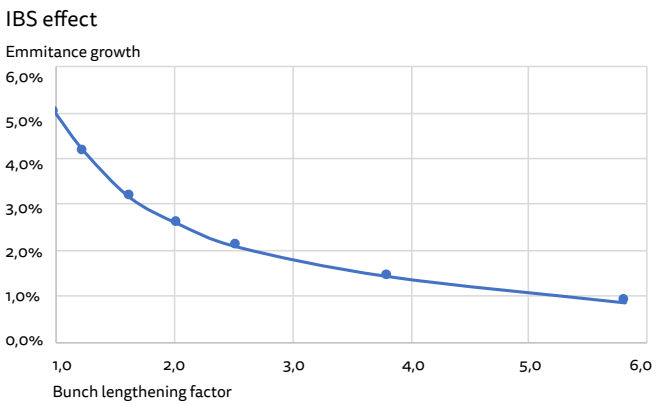


Figure 4-3: IBS emittance increase in %, as a function of the bunch lengthening factor, computed with the ZAP code.

Non-linear lattice

The initial chromaticity correction is based on a distributed two-families sextupole scheme. Horizontal and vertical sextupoles are paired and located in between each bending-magnet and focusing quadrupole, for a total of 10 horizontal and 10 vertical sextupoles per cell. In fact, the steep variation of the betatron functions, which cross in between bending-magnet and focusing quadrupole, provides two locations with a substantial separation of the betatron functions allowing for an effective correction of the chromaticity in both planes. The phase advance in the arc section

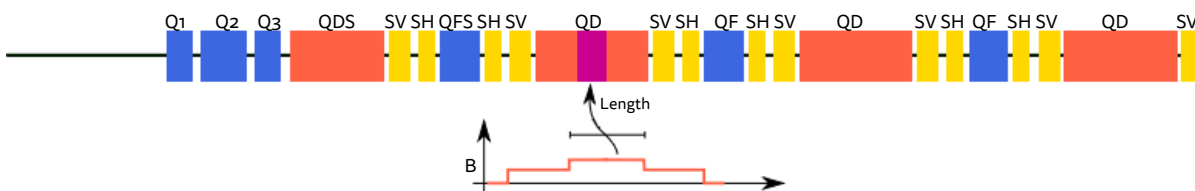


Figure 4-4: Typical cell of ALBA II, equipped with a super-bend magnet to provide hard X-rays for dipole-based beam lines. A small portion of a few cm at the center of a normal dipole is modified to provide very high field, the field in the rest of the dipole is lowered slightly to keep the nominal bending angle.

is tuned to obtain the cancellation of the geometric aberrations produced by the sextupoles to the first order, resulting in a large dynamic aperture exceeding ± 6.1 mm in the horizontal plane at the injection point, value compatible with the considered injection scheme, as per Section 4.1.7.

The required sextupole field strength to achieve zero chromaticity is close to the maximum achievable value, nevertheless some room is available for further optimization. By grouping the horizontal and vertical sextupoles in multiple families and allowing for some variation in strength an improvement of the dynamic aperture is expected. However, since the complexity of the problem does not allow for a systematic study of all the possible configurations, an alternative approach successfully applied for the optimization of many designs involves the use of genetic algorithm. The application of such approach to the optimization of the ALBA II optics is currently undergoing.

Super-bend solution for high energy dipole-based beamlines

Concerning the source for the dipole beamlines, many of the present beamlines would use the field of 1 T provided by the 6BA, with a critical energy of 6 keV; while for higher energy beamlines a super-bend solution would be preferred (see Figure 4-4). The impact on the lattice performance due to the insertion of very short high field region in the middle of the arc bends is shown in Figure 45. Considering that not all the cells will be equipped with a super-bend, the overall emittance degradation is found to be smaller than 10% and therefore totally acceptable.

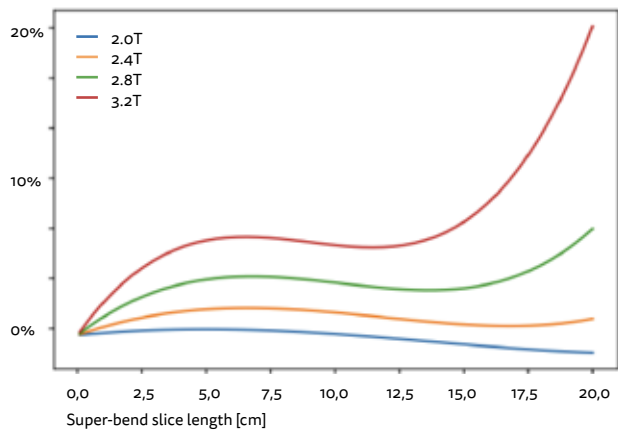


Figure 4-5: Impact on the performance due to the presence of a high field region (super-bend) in one dipole per cell. Four different field intensities have been considered in the high field region and the emittance has been evaluated as a function of the slice size (total of 16 super-bend in the ring). Note that if a smaller number of super-bends is installed in the ring the overall impact scales linearly.

Misalignment and linear errors: orbit, optics and coupling correction

The ALBA II lattice performance has been studied in the presence of realistic misalignment and field errors. The error sources detailed in Table 4-2 have been considered.

TABLE 4-2: REALISTIC ERROR SOURCES USED FOR THE SIMULATIONS

ERROR	RMS VALUE
Quadrupole gradient	0.1%
Magnet fiducial	23 μm
Magnet to girder	23 μm
Laser-tracker to grid	30 μm
Laser tracker to girder marker minimum	15 μm
Laser tracker to girder marker distance change	6 μm

Here we are assuming that the girder alignment can be performed based on measurements of the closest girder markers. The feasibility of such alignment strategy is under consideration.

In this study we have not included the beam position monitor (BPM) errors, the beam-based alignment of the magnets and the physical apertures.

A bunch lengthening factor of 3 generated by the 3rd harmonic RF cavity system is assumed in the lifetime calculations, see Section 4.1.4.

ALBA II aims to be operated at full coupling, but this circumstance is not considered so far, instead the coupling is corrected as much as possible but with a compromise with the total number of skew quadrupole correctors. In this sense, 8 skew quadrupoles per sector is found to be optimum. According to our studies, 9 BPMs and orbit corrector magnets (OCM) is also optimum. We found

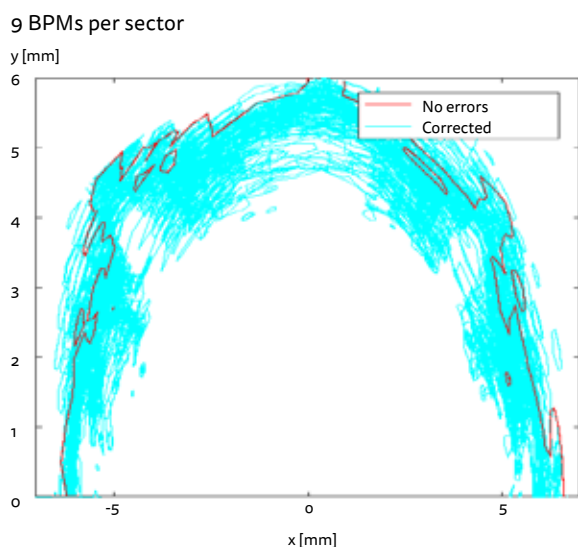


Figure 4-6: Dynamical aperture simulated for 500 turns. The red line corresponds to the bare lattice, while the cyan lines correspond to the individual lattices with errors and corrections.

that we need to be able to correct the quadrupole component of all the 10 families. Some of those families have also a dipole field which means that those magnets will need two different power supplies per magnet.

All the different configurations, namely the number of BPM, OCM, quadrupole and skew quadrupole correctors, have been tested using 100 different lattices with normal randomly distributed errors cut at the 1 sigma of the values given in Table 4-2. In the optimum conditions described above, the horizontal dynamical aperture is reduced on average by 0.2 mm and the lifetime is reduced on average by 2 hours (for the bare lattice it is 6 hours). Figure 4-6 shows the details of the resulting dynamical apertures for the 100 corrected lattices in the optimum case.

Insertion device effects

The effects of the existing insertion devices (ID) in the present machine have been studied in combination with the alignment and field errors described in the previous section.

ID effects are expected to be roughly the double with respect to the present storage ring, since those scale with the beta function value at their location. In the worst combination of ID settings, their effect would be around 1% and 3% RMS beta beating in the horizontal and vertical plane respectively. In that case, the horizontal dynamical aperture is barely affected while the lifetime is further reduced to around 3 hours.

Two different possible look-up tables correction schemes have been compared, namely correcting the optics effects at all the BPMs or only at the BPMs next to the beamline source points.

Aiming at correction in all BPMs reduces the horizontal dynamic aperture to 5.4 mm and the lifetime is partially recovered to 3.4 hours. If only the pure quadrupole magnets in the straight sections are used to correct the ID effect, a maximum of 14% and 8% correction strength is needed for the fixed and variable ID gap respectively.

Using optic correction only in the beamline BPMs actually reduces the performance. The horizontal dynamic aperture is reduced to 5.0 mm and the lifetime to 2.8 hours. In this case however, the maximum quadrupole strength need is 4.5% and 2.0% for the fixed and variable ID gap respectively.

Multipole effect

Due to the huge space of possible configurations, both random and systematic multipole components effects have been studied in the absence of any other source of error. In future, closer to definitive, versions of the lattice those effects would be combined. In this study the radius of reference has been set to 10 mm and we have used up to the 10th order multipole.

The random multipole components have been studied combining the multipoles following a uniform distribution at the radius of reference. Each error distribution has been scaled to produce a given maximum magnetic field variation at the radius of reference. If the maximum field error is kept below 5 Gauss the effect is a reduction of 0.03 mm in horizontal dynamical aperture and about

0.1 hours in lifetime. From there on, the degradation starts to be more significant.

A specialized GPU code for lattice optimization

The complexity of the optics under investigation is such that computational tools performance has become a dominant factor in the process of designing the lattice. A fully new code (named UFO), tailored toward high performance, was developed to assist the design of the ALBA II optics from a very early stage.

Two main strategies contribute to the performance of the new code: first, the execution flow follows a data parallel paradigm, very well suitable for GPU execution; second, the use of a just in time compiler allows to simplify the computation whenever the lattice allows for it (e.g. consecutive linear elements). At the core of UFO lies a single particle parallel tracking routine, structured in such a way to allow for parallel simulation of optics which differs in some parameters, such as magnets strength or alignment, but retain the same element ordering.

This reflects very much the scenario followed in the optimization process, where many optics differing for some parameter need to be evaluated to found the best candidate, or when dealing with magnetic or alignment errors, where many sets of errors need to be considered to evaluate the overall impact on the optics performances. Such approach allows to take full advantage of modern GPUs which yield the best performance when running tens of thousands of parallel threads with an overall performance comparable to a medium size cluster.

While the very first versions of UFO were developed with dynamic and momentum aperture computation in mind, it was found that the code could be easily extended to non-strictly tracking tasks such as the computation of closed orbit and linear optics function. The result is a versatile tool that allows for the optimization of complex optics, such as the one found in a next generation light source even on limited computational resources.

4.1.2. MAGNETS WITH ASSOCIATED NEW TECHNOLOGIES

The magnets required for ALBA II are defined by the lattice design presented in Section 4.1.1. The lattice is based on 16 identical 6BA cells consisting of 9 different magnet types, for a total of 592 individual magnets (for comparison purposes, the Storage Ring of ALBA has currently 264 magnets). The types and quantities of magnets are summarized in Table 4-3.

The lattice definition also includes a primary set of requirements in terms of field/gradient strengths and physical lengths for all the magnets. The parameters, which are presented in Table 4-4, have been determined assuming that the minimum distance between the yokes of adjacent magnets will be 70mm for magnets of the same type and 40mm for magnets of different type. In case that during the detailed design of the magnets some of these distances turn out to be too tight, it exists the possibility of reducing the magnet length and increasing its field/gradient strength accordingly.

The quadrupoles at both sides of the injection straight, labelled as IQ# in Table 4-4, operate at a different setpoint than the corresponding quadrupoles Q# at other locations, but they will share the same mechanical design.

In order to proceed with the design of the magnets, one of the most important parameters to define is their aperture diameter. Given a target value for the field/gradient strength, decreasing the magnet's aperture allows to reduce the required excitation currents and the associated power consumption in the case of electromagnets, or the required volume of permanent magnet material in the case of PM-based designs. In addition, in both cases the resulting magnet will operate more efficiently at a lower saturation level. However, it has to be considered that a reduction of the physical aperture increases the impact of geometrical errors on the field quality of the magnet and makes the design of the vacuum system more challenging. After considering all these factors, we have decided to adopt a minimum value for the aperture diameter of the magnets of 20mm. This aperture is compatible with a circular vacuum chamber with an inner diameter of 16mm, which is suitable to undergo NEG coating using standard procedures available to industrial manufacturers, and it is also consistent with choices made at other on-going upgrade projects with similar requirements.

Another key decision to be adopted is the technology that the magnets shall use: either conventional electromagnets (EM) with iron yokes and resistive coils or solutions that incorporate permanent magnets (PM) to inject magnetic flux into the system in an efficient and cost-effective way. In the latter case we can distinguish between solutions that rely purely on permanent magnets and do not incorporate any coils (pure PM designs) and those that combine permanent magnets and coils to provide some tunability to the system (hybrid designs). The different technological options are illustrated in Figure 4-8.

The benefits of using PM are diverse: (a) the removal (total or partial) of the coils reduces the longitudinal footprint of the magnets and enables more compact designs; (b) the simplification of the required services (power supplies and cables, cooling system, thermal interlocks...) reduces the capital costs associated to the system of magnets and facilitates its subsequent maintenance; and (c) the reduced power consumption (down to zero in the case of pure PM designs) cuts down the operational costs for the accelerator. However, the use of permanent magnets, especially in the case of pure PM designs, entails a loss of tunability of the resulting magnets that has to be compensated if one wants to recover the flexibility of the lattice. This is typically done by introducing additional correctors that take extra space from the lattice. In addition, there are still some concerns regarding the long-term stability of PM-based magnets due to potential demagnetization effects associated to radiation damage.

In the case of ALBA II, with its extremely compact lattice, a solution relying largely on pure PM magnets (like the ones that are being developed for the upgrades at SOLEIL¹¹³ and SLS¹¹⁴) is unfeasible due to the impossibility to accommodate the required correctors magnets (typically octupoles) inside an already overcrowded lattice. Therefore, as a first approach, we will adopt conventional electromagnets (EM) technology to define a baseline design for all 9 required magnet types, and in a second

¹¹³ SOLEIL Synchrotron, "Conceptual design report, synchrotron SOLEIL upgrade", SYNCHROTRON SOLEIL, l'orme des merisiers, 91190 saint-aubin. www.grouperougevif.fr - GROUPE ROUGE VIF - 26896 - Décembre 2020

¹¹⁴ A. Streun, M. Aiba, S. Bettoni, M. Böge, B. Riemann, V. Schlott, "SLS 2.0 Baseline Lattice", SLS2-SA81-004-17- 2021

TABLE 4-3: MAGNET TYPES AND QUANTITIES FOR ALBA II STORAGE RING

MAGNET DESCRIPTION	TYPES	# PER CELL	NUMBER IN SR
Bending with transversal gradient	QD	4	64
	QDS	2	32
Antibending with transversal gradient	QF	3	48
	QFS	2	32
Quadrupoles	Q1	2	32
	Q2	2	32
	Q3	2	32
Sextupoles	SH	10	160
	SV	10	160
Total	9	37	592

TABLE 4-4: CHARACTERISTICS OF THE DIFFERENT TYPES OF MAGNETS FOR ALBA II STORAGE RING

MAGNET DESCRIPTION	TYPES	LENGTH [m]	FIELD [TESLA]	GRADIENT (K_1) [T/m]	2 ND ORDER GRADIENT (K_2) [T/m ²]
Bending with transversal gradient	QD	0.8669	1.009	-15.41	
	QDS	0.6310	0.819	2.03	
Antibending with transversal gradient	QF	0.2972	-0.394	70.05	
	QFS	0.2972	-0.425	70.05	
Quadrupoles	Q1	0.2000		-31.54	
	Q2	0.3500		83.16	
	Q3	0.2000		-109.83	
Quadrupoles (injection)	IQ1	0.2000		89.71	
	IQ2	0.3500		-69.61	
	IQ3	0.2000		44.70	
Sextupoles	SH	0.2972			4936
	SV	0.6310			-4084

The definition of the gradient parameters is such that the magnetic field at the tip of the poles is given by $B_{ip} = K_1 r_0$ for quadrupoles and $B_{ip} = K_2 (r_0)^2$ for sextupoles, where r_0 is the magnet's aperture radius.

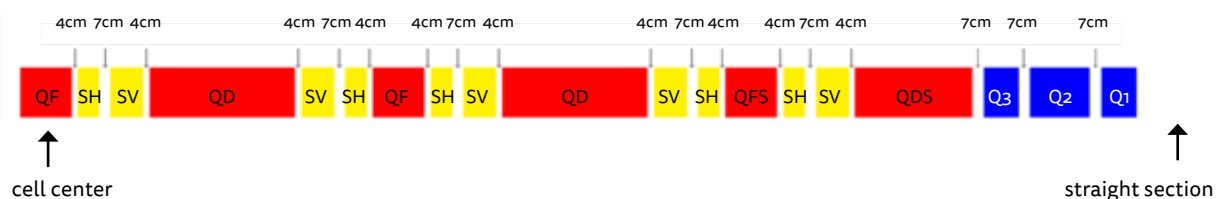


Figure 4-7: Schematic representation of half 6BA cell of ALBA II lattice, illustrating the assumed distances between magnet yokes.

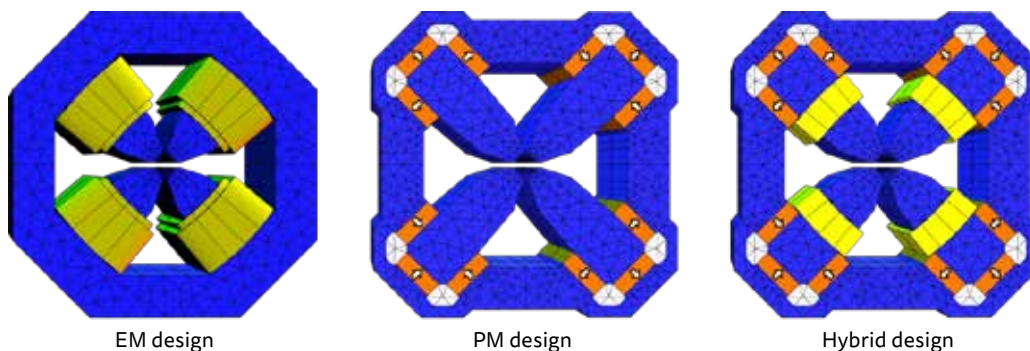


Figure 4-8: Technological choices for the magnets depending on the source of the magnetic flux: electromagnets (EM), pure permanent magnets (PM) or hybrid designs.

stage we will explore the possibility of using hybrid designs for some particular types of magnets. In connection with this prospect, ALBA participates in PerMaLIC collaboration¹¹⁵ within the LEAPS consortium, aimed to the development of permanent magnets for future, ultra-low emittance, light sources.

In the case of electromagnets, one of the main design criteria is the efficiency at which the magnets operate, defined as the ratio between the current value required to attain the target field/gradient strength and the ideal one that would be required by a yoke with infinite permeability. Efficiency provides a measurement of the degree of saturation of the iron yoke, and gives an estimation of the linearity of the magnet at the selected working point. Adhering to the guidelines developed for the upgrade at APS¹¹⁶ we have adopted the following design criteria:

- Single-function magnets (quadrupoles, reverse dipoles and transverse gradient dipoles) will be designed to operate at 90% minimum efficiency.
- Multi-function magnets (sextupoles with integrated correctors) will be designed to operate above 98% efficiency in order to minimize the crosstalk between different field configurations.

The development and verification of the magnets' designs by means of adequate prototypes will take place during the period 2022-25 within the framework of the funded project ALBA01-NGEU "Enabling technologies for ALBA II". The required magnetic modelling will be carried out using a diversity of software packages: RADIA¹¹⁷ as a versatile tool for geometry optimization; Maxwell package from ANSYS¹¹⁸, which offers optimization capabilities and a straightforward integration with thermomechanical calculations; and OPERA¹¹⁹ for the final verification of the obtained designs.

4.1.3. VACUUM SYSTEM

The vacuum is a crucial system for the proper operation of the new accelerator. The tight spaces, the large number of magnets, pumping difficulties and heat power removal among others topics makes the vacuum system design a really challenging project¹²⁰.

Requirements

The Vacuum system shall contend with many functionalities and performances, but the main requirements are the following:

- **Ultimate pressure:** A good portion of the synchrotron radiation will be absorbed on the vacuum chamber walls generating a significant PSD outgassing¹²¹, much of it in chamber segments without vacuum pumps. So, distributed pumping will be required in order to achieve vacuum levels of 1e-9 mbar or lower.
- **Synchrotron Radiation heat power removal:** All the heat power deposited on the vacuum chamber shall be removed. Since there is no space for the typical lumped absorbers, the cooling shall be directly coupled on the vacuum chamber where the radiation is hitting.
- **Image current:** The vacuum chamber shall allow a proper image current low impedance circulation along the ring at the inside and closest to the beam surfaces. In order to achieve a fluent image current circulation, it is needed to take special care of the chamber shape and design smooth transitions between chambers with different geometries.

Vacuum system preconception

Initial considerations assume that the smallest magnet aperture is 20 mm. In order to leave space for the magnets and chambers tolerances and drifts, a clearance of 1 mm between chamber wall and the magnets yokes is foreseen. Assuming 1 mm chamber wall thickness, the effective vacuum chamber diameter will be about 16 mm.

Preliminary CAD layouts, see Figure 4-9, shows that the tightest segments are the intersection between QD dipoles where there are four sextupoles and an anti-bending magnet. These intersections space will not allow for lumped pumps or many chamber size transitions, being the longest and smaller vacuum chamber segment.

At the bending magnets, which will have lateral aperture, it is foreseen to have a small antechamber where lumped pumps will

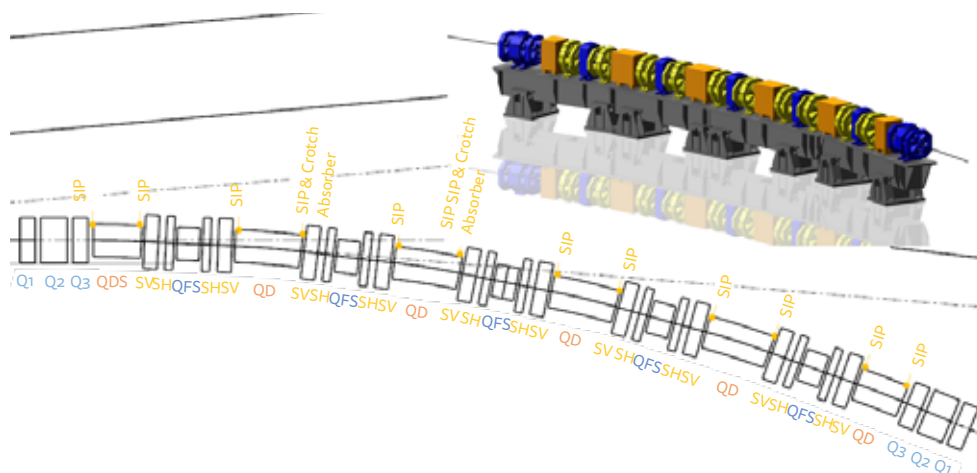


Figure 4-9: ALBA II Lattice Layout example.

¹¹⁵ Permanent Magnets LEAPS Internal Collaboration - <https://indico.cells.es/event/623/overview> - PERMALIC 1st Workshop -2021

¹¹⁶ Fornek, T. - Advanced Photon Source Upgrade Project, Final Design Report - APSU-2.01-RPT-003, 2019

¹¹⁷ www.esrf.fr/Accelerators/Groups/InsertionDevices/Software/Radia

¹¹⁸ www.ansys.com/products/electronics/ansys-maxwel

¹¹⁹ www.3ds.com/products-services/simulia/products/opera/

¹²⁰ E. Al-Dmour, et al., "Diffraction-limited storage-ring vacuum technology", *Journal of Synchrotron Radiation*, ISSN 1600-5775, Sept. 2014. DOI: 10.1107/S1600577514010480.

¹²¹ P. Chiggiato and R. Kersevan, "Synchrotron Radiation-Induced Desorption from a NEG-Coated Vacuum Chamber", in *Proc. 6th European Vacuum Conference (EVC-6)*, Vacuum 60 (2001): 67-72, Villeurbanne, France, Dec. 1999. DOI:10.1016/S0042-207X(00)00247-5.

Pumping Speed Effective
Effective Pumping Speed S_{eff} [l/s]

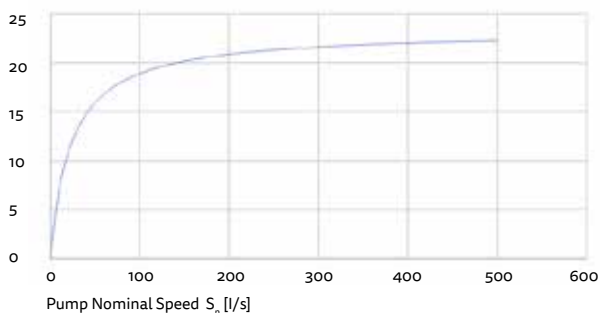


Figure 4-10: Small aperture vacuum chambers effective pumping speed.

be allocated, and where the extraction of the insertion devices radiation will be realized.

Since the chamber diameter between bending magnets, about 16mm, dominates the final conductance of this segment, it is considered that pumps of 75 l/s are enough, since larger pumps will not improve significantly the effective pumping, see Figure 4-10.

Dynamic Pressure

The extremely low conductance of the low-emittance storage rings is a common issue in the 4th generation light sources, requiring the use of distributed pumping along the chambers with non-evaporable getter films, NEG coatings. This kind of pumping assure not only an almost negligible thermal desorption rate, but pumping capacity on these chamber surfaces and, in addition, a substantial reduction of the photon stimulated desorption yield at impinged surfaces. The NEG coating along the ring shall be complemented by lumped pumps where space allows for it.

Simulations with Synrad+¹²² and Molflow+¹²³ have been done for the chamber segment between two QD bending magnets estimated to be, at this initial stage, the worst case. Simulations have been done with NEG coating yield at the irradiated surface and a sticking factor at the rest, assuming a negligible thermal

desorption with this treatment. The results are shown in Figure 411, where the vacuum profile is computed considering a global sticking coefficient for about 0.01^{124,125} and considering about 100Ah of conditioning. In these conditions, an average pressure of about 1e-9 mbar will be achieved.

Cooling

As a consequence of the compact design most of the synchrotron radiation coming from the bending magnets will be absorbed to the vacuum chamber wall. The ALBA Storage Ring is a relatively small ring but still the bending radius are quite large and the incidence angle at pipes wall quite small. The maximum power density is expected to be as large as 40 W/mm². In order to deal with the distributed power along the ring, a cooling tub welded at the radiation side of the chamber is proposed. See next Figure 4-12.

The cooling pipes have to be welded on the vacuum chamber with a continuous contact on the complete interfacing surfaces to ensure a proper thermal conductivity. This is typically solved by brazing. Chamber cooling diameter shall be small enough to pass through magnet yokes up to the end where water inlets and outlets would be installed.

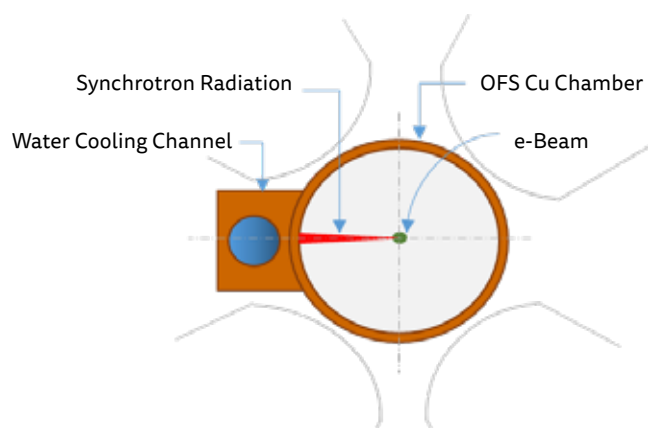


Figure 4-12: ALBA II chamber and cooling pipe.

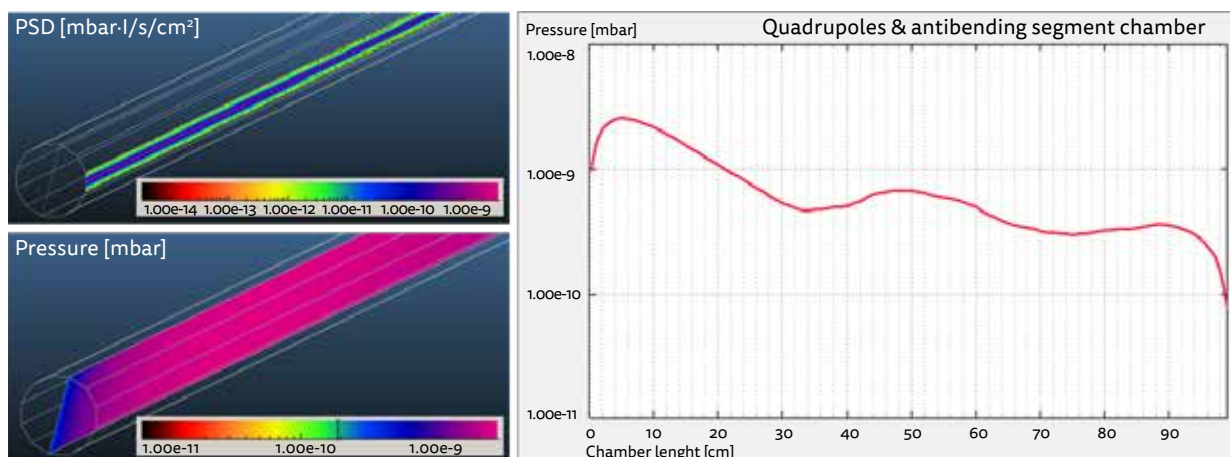


Figure 4-11: Left: Molflow+ PSD Desorption map and Dynamic pressure map. Right: Dynamic pressure (With NEG).

¹²² R. Kersevan and M. Ady, CERN, "Recent developments of monte-carlo codes Molflow+ and Synrad+", in Proc. 10th Int. Particle Accelerator Conf. (IPAC2019), Melbourne, Australia, May. 2019. doi:10.18429/JACoW-IPAC2019-TUPMP037.

¹²³ Molflow+, <https://molflow.web.cern.ch/>

¹²⁴ C. Benvenuti, "Non-evaporable getters: from pumping strips to thin film coatings", CERN, CH-1211 Geneva 23.

¹²⁵ C. Benvenuti, et al., "Vacuum properties of TiZrV non-evaporable getter films", in Proc. 6th European Vacuum Conference (EVC-6), Vacuum 60 (2001): 67-72, Villeurbanne, France, Dec. 1999. CERN EST/99-007 (SM). DOI:10.1016/S0042-207X(00)00246-3.

Other considerations

The main parameters of the ALBA II vacuum system have been approached in the previous chapters. These basic figures assure reaching a good ultimate dynamic pressure and effective cooling to absorb the synchrotron radiation power.

Nevertheless, the system requires on top of that, other functionalities and components. The following list shows the main characteristics to be developed during the design phase:

- **Mechanical Design:** The biggest project effort is on the mechanical design. Chamber geometry complexity, layout, supports, welding's and brazing's, vacuum connections (interfaces), integration with the magnets, girders and Front ends, etc
- **Supports and stress relieve:** The vacuum chamber and its components have to be properly supported on the girders, with supports stiff enough to maintain the chamber well centered inside the magnets but at the same time shall allow for the thermal expansions. Chamber movements have to be properly studied to guarantee that they will be in the magnet gap tolerances.
- **Beam extractions:** The beam from insertion devices and bending magnets feeding beamlines shall be conducted up to the Front End. The extraction channel through the magnets will require iterations with the magnets design.
- **Transitions:** The variations of the vacuum chamber along the ring in size and geometry have to be studied in order to assure smooth transition minimizing image current impedance.
- **NEG coating activation and bake out:** In-situ vs. Ex-situ activation bake out strategy will be analyzed.^{113,126}
- **Instrumentation and components:** The instrumentation like gauges, residual gas analyzers, valves, pumping ports, etc., all these have to be considered in the layout.

4.1.4. RF SYSTEMS

The main RF system of ALBA will be reused for ALBA II, since its operation parameters will be very similar. The nominal frequency will be kept at 500 MHz and the main upgrade of the system will be to replace the present IOT based transmitters by Solid State Power Amplifiers (SSPAs), taking profit of the good experience with this technology after more than four years of operation of the Booster transmitter.



Figure 4-13: 3rd harmonic cavity installed in the Bessy II ring for the performance tests.

But as mentioned in Section 4.1.1, the use of a 3rd harmonic system (3HS) is mandatory for increasing the bunch length of the beam in order to meet the lifetime specifications and to reduce the IBS effects. For this purpose, a RF system operating at 1.5 GHz will be installed in ALBA II. A prototype of the 3rd harmonic cavity has been designed and prototyped for ALBA, and it has been already tested with beam, and demonstrated its performance, in the framework of a collaboration with DESY and HZB. Figure 4-13 shows the cavity installed in the Bessy II ring.

Main RF system

The main RF system will be composed by six normal conducting HOM damped cavities, as ALBA. The six cavities will provide the required power to compensate the losses due to synchrotron radiation and the losses occurring at the 3rd harmonic cavities. Table 4-5 summarizes the main RF parameters for ALBA II.

In order to guarantee the redundancy of the system in case of a trip in one main cavity, and also in order to provide a minimum RF acceptance of 5 %, the total amount of voltage is set to 2.4 MV. This represents a 20 % of drop compared to ALBA in terms of voltage and a 36 % in terms of power dissipated in the cavity¹²⁷. Table 4-6 summarizes the main cavity parameters and Figure 4-14 shows the phasor diagram for the fundamental system.

TABLE 4-5: ALBA II MAIN RF PARAMETERS

PARAMETER	SYMBOL	VALUE	UNIT
Average current	I_{sr}	300	mA
Energy loss per turn*	U_o	1089	keV
Harmonic number	h	448	-
Revolution frequency	f_r	1.1	MHz
Momentum compaction factor	α_c	$0.8 \cdot 10^{-4}$	-
Natural bunch length	σ_{to}	5.47	ps
Natural synchrotron frequency	f_{so}	2.59	kHz

* Includes losses due to synchrotron radiation (magnets and IDs) and losses occurring at the 3rd harmonic cavities.

¹²⁶ M. Grabskia and E. Al-Dmoura, "Commissioning and operation status of the MAX IV 3 GeV storage ring vacuum system", Journal of Synchrotron Radiation, Volume 28, Part 3, Pages 718-731, May 2021, DOI: 10.1107/S1600577521002599.

¹²⁷ I. Bellafont, "Proposal of an RF System for ALBA II storage ring", internal ALBA document 2021-AC-RF-0001, 2021.

TABLE 4-6: ALBA II MAIN CAVITY PARAMETERS

PARAMETER	VALUE	UNIT
Cavity voltage	400	kV
Number of cavities	6	
Coupling factor	3.2	-
Shunt impedance	3.3	MOhm
Quality factor	29500	
Synchronous phase	159	°
Transmitter power	80.0	kW
Power to the beam	53.3	kW

3rd harmonic RF system

The beam lifetime is a key parameter for the performance of a synchrotron light source, a large lifetime reduces losses and the frequency of injections. For ALBA II the goal is to have a lifetime of several hours for 300 mA. Since the Touschek scattering lifetime is the dominating effect at ALBA II and it is proportional to the bunch length¹²⁸, enlarging the bunch length with a 3rd harmonic system become the proper solution¹²⁹.

A third harmonic system is foreseen to increase the bunch length by at least a factor of 3 when applying a total harmonic voltage

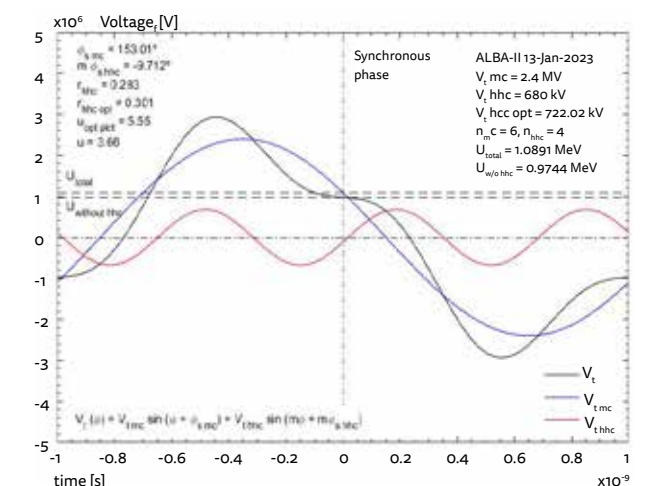


Figure 4-15: Main and harmonic voltage as function of time.

TABLE 4-7: ALBA II 3H CAVITY PARAMETERS

PARAMETER	VALUE	UNIT
Cavity voltage	170	kV
Number of cavities	4	
Coupling factor	0.4	-
Shunt impedance	1.1	MOhm
Quality factor	14000	
Synchronous phase	-9.5	°
Transmitter power	4.5	kW
Power to the beam	-8.6	kW
Bunch lengthening factor	3	

ALBA-II- Main RF cavity - Voltage phasor plot

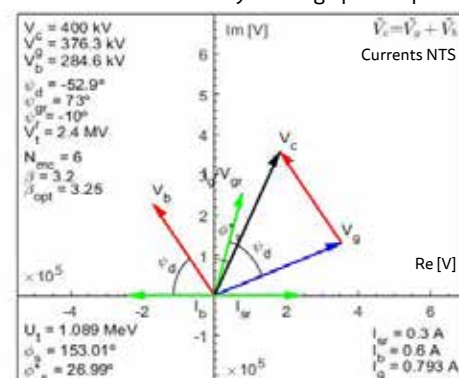


Figure 4-14: Main cavity phasor diagram.

of around 680 kV as shown in Figure 4-15. Table 4-7 summarizes the harmonic cavity parameters and Figure 4-16 shows the phasor diagram for the harmonic system.

4.1.5. DIAGNOSTICS

The upgrade of the ALBA machine will rely on state-of-the-art diagnostics and active feedback systems to an even larger degree to what ALBA currently does.

Table 4-8 summarizes the instrumentation that will be used to diagnose the electron beam at ALBA II to cope with the requirements from the beam dynamics needs.

Due to the lack of available space, the instrumentation listed in the table is to be distributed along the ring instead of being allocated in a single dedicated straight section (as it is the case in the current ALBA). Furthermore, since the cross-section of the ALBA II vacuum chamber is smaller, the mechanical designs of all diagnostics devices will need to be adapted.

Emittance Monitors

Using the X-ray fan from a bending dipole, the emittance measurements will be performed at two positions in the ring

ALBA-II- HH RF cavity - Voltage phasor plot

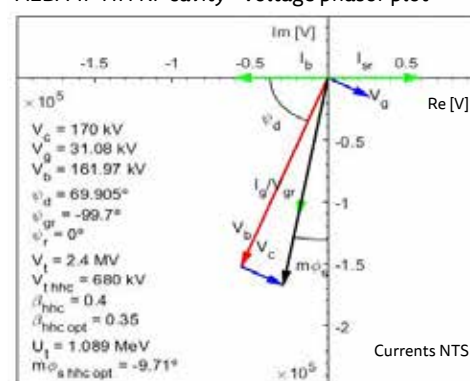


Figure 4-16: Main cavity phasor diagram.

¹²⁸ N. Carnignani, "Touschek Lifetime Studies and Optimization of the European Synchrotron Radiation Facility", Università di Pisa, 2014.

¹²⁹ B. Nash, F. Ewald, L. Farvacque, J. Jacob, E. Plouviez, J.-L. Revol and K. Scheidt, "Touschek lifetime and momentum acceptance measurements for ESRF," in Proceedings of IPAC 2011, San Sebastián, 2011.

using with the well-known technique of the pinhole camera¹³⁰. These two positions should have different dispersion values: one position with a high dispersion, and a second position with a low (or null) dispersion so that both transverse emittances (horizontal and vertical) and energy spread can be measured.

So far, two candidate positions are found with the required parameters. In these locations, the most challenging parameter corresponds to the horizontal electron beam (6 μ m), which is close to the minimum beam size measured in the current light sources with this technique¹³¹. In the preliminary studies, we have seen that the pinholes can achieve a magnification of a factor 2, therefore we are confident regarding this particular challenge.

This technique relies on a direct beam image analysis. In this regard, due care should be taken to operate at an acquisition rate and robustness suitable for a possible coupling feedback system, especially if ALBA II is to operate in full beam coupling mode.

Beam Position Monitors and Beam Stability

ALBA II beam stability will be obtained thanks to Beam Position Monitors (BPMs) and Fast Orbit Feedback (FOFB) system.

Each BPM block will be composed by 4 RF buttons at a 45 degree geometry. To fit the BPM block in a 16 mm vacuum chamber could

be problematic due to the possible interception of the buttons by synchrotron radiation produced upstream. Studies on the synchrotron radiation trajectory will be carried out to confirm or discard this necessity. A solution, already foreseen for several machines, is to use a larger diameter vacuum chamber for the BPM block.¹³⁹ In this scenario, a vacuum pipe of 20 mm diameter, a 5 mm button diameter with 300 μ m gap can be considered appropriate for an accurate position measurement.

Furthermore, boundary element simulation will be carried out to verify the linearity of BPMs block and the possible tolerances on button pickup misalignment. The BPM Lab code¹⁴⁰, developed in house, will be used for these purposes as well as to calculate possible polynomial position calculation options to be used instead of the standard Δ/Σ formula.

Simulations of BPMs feedthrough interaction with the electromagnetic field of the beam have also to be performed to study power distribution and trapped modes inside the buttons to minimize the impact on the beam.

A new BPM readout electronics system is foreseen for ALBA II due to obsolescence of the present Libera Brilliance system. The new electronics must maintain turn by turn position measurements capability and has to provide fast 10 KHz data stream for orbit correction. Commercial Libera Brilliance+ system is nowadays under investigation together with a pilot-tone based hybrid

TABLE 4-8: LIST OF DIAGNOSTICS COMPONENTS FORESEEN FOR ALBA II

DIAGNOSTIC	INSTRUMENT	PURPOSE	QTY
Beam Current Measurements	DC Current Transformer	It uses two transformers cascaded in a common feedback loop ¹³² . Its precision reaches 1 μ A rms (~0.01%)	1
	Integrated Current Transformer	Alternative current measurements. It consists of a capacitively shorted transformer designed to measure the charge with 1% accuracy ¹³³	1
Filling Pattern Measurements	Annular Electrode	Filling pattern measurements, with 1% precision	1
	PhotoMultiplier Tube (PMT)	Using the Time Correlated Single Photon Counting, achieve bunch purity precision down to 10 ⁻⁵ . ¹³⁴	1
Bunch Length Measurement	Streak Camera	Use visible light at the Diagnostics beamline. The present technology reaches an accuracy of 2ps, which should be enough for the bunch length in ALBA II. ¹³⁵	1
Transverse Emittance	X-ray Pinhole Camera at low dispersion	Measure horizontal and vertical emittances in a low dispersion dipole. ¹³⁶	1
	X-ray Pinhole Camera at high dispersion	Combined with previous X-ray pinhole, measure both emittances and energy spread.	1
Beam Loss Monitors	Scintillators + PMT	By detecting beam losses with this technique, and using a fast electronics read-out, we wish to detect beam losses even in a turn-by-turn basis, and potentially use them for fast beam lifetime measurements and injection optimization. ¹³⁷	32
Scrapers	Locate and control beam losses	Introduce aperture limits in a variable and controlled way to locate beam losses in specific locations avoiding radiation damage to other components (like Insertion Devices).	Hor (1) Ver (2)
Tune Measurement	Stripline	The stripline will be used to excite the beam so that the beam tune can be measured. Later, the beam position oscillations are read with a BPM (see below).	1
Multi-bunch feedback	Transverse feedback kickers	Cure fast transverse bunch-by-bunch instabilities combining a stripline kicker and using state of the art electronics. ¹³⁸	Hor (1) Ver (1)
Beam Position	Beam Position Monitors (BPMs)	10 BPMs/cell will be used to keep the orbit controlled within the required limits	160

¹³⁰ P. Elleaume, C. Fortgang, C. Penel, E. Tarazona. "Measuring Beam Sizes and Ultra-Small Electron Emittances Using an X-ray Pinhole Camera". Journal of Synchrotron Radiation, 1995.

¹³¹ U. Iriso, "Emittance Monitors for Low Emittance Rings", <https://agenda.infn.it/event/20813/>. Low emittance Ring Workshop 2020, Roma (Italy).

¹³² <https://www.bergoz.com/dcct>

¹³³ <https://www.bergoz.com/ict>

¹³⁴ L. Torino and U. Iriso, "Filling pattern measurements at ALBA using TCSPC", Proc. Of IBIC'14, Monterrey (USA).

¹³⁵ U. Iriso, M. Alvarez, A. Nosych and A. Molas. "Streak Camera Calibration Using RF Switches", Proc. Of IBIC'16, Barcelona (Spain).

¹³⁶ U. Iriso, "Emittance Monitors for Low Emittance Rings", <https://agenda.infn.it/event/20813/>. Low emittance Ring Workshop 2020, Roma (Italy).

¹³⁷ L. Torino, "New Beam Loss Detector System for EBS-ESRF", Proc. Of IBIC18, Shanghai (China).

¹³⁸ A. Olmos, U. Iriso, J. Moldes, F. Perez, M. Abbott, G. Rehm, I. Uzun. "Integration of the Diamond Transverse Multibunch Feedback system at ALBA", Proc. Of IBIC'15, Melbourne (Australia).

¹³⁹ https://indico.cern.ch/event/1096767/contributions/4692953/attachments/2383768/4073382/ESRW22_N-HUBERT.pdf

¹⁴⁰ A. Nosych, U. Iriso, J. Ollé. "Electrostatic Finite-Element Code to Study Geometrical Nonlinear Effects in BPMs", Proc. Of IBIC'15, Melbourne (Australia).

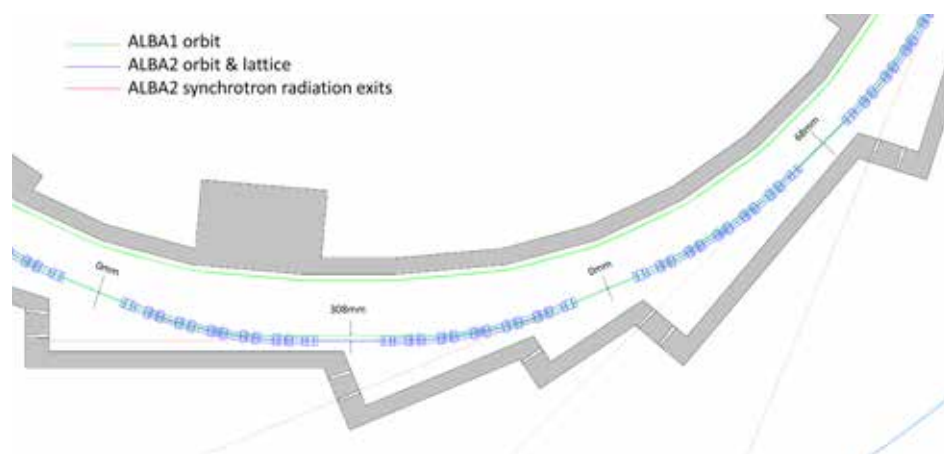


Figure 4-17: View of a section of the accelerator with ALBA and ALBA II orbits.

readout system proposed by Elettra¹⁴¹. Developments of BPMs readout electronics from other labs will also be considered for the future choice.

The BPM system will be composed by a total of 160 BPMs distributed in 10/cell. In each cell, 9 BPMs will be used for orbit correction (together with 9 horizontal and 9 vertical correctors). A spare BPM is left in each cell for beam diagnostics purposes and/or possible beamline demands. The BPM distribution is shown in Figure 4-18.

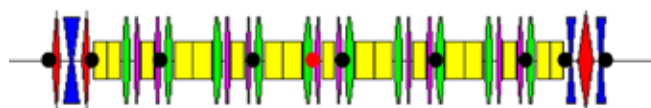


Figure 4-18: Distribution of the 9 BPMs in a ALBA II cell: 9 BPMs are used for orbit correction (black dots), while a spare BPM (red dot) is left for diagnostics purposes.

Beam stability better than 10% of the beam size will be guaranteed from a Fast Orbit Feedback (FOFB) system which will use the 10 KHz data stream from 144 BPMs around the ring. Four BPMs will be located before and after the matching triplet to ensure stable beam in straight section, five other BPMs will be distributed evenly inside the arc to stabilize bending magnet beamlines. XBPMs will also be located in each frontend and the possibility of using them into the FOFB will be studied upon demand of the corresponding beamline.

Corrector magnets will be implemented as extra winding in sextupoles, to keep the system as compact as possible. The effects of eddy currents in the vacuum chamber has to be studied and considered in the feedback calculation and implemented in corrector power supplies. Thanks to the ALBA II optics, the photon flux in the beamlines will increase and the experiments aim to use detectors faster than the current ones, therefore the desired overall bandwidth of the FOFB should exceed the 100 Hz of the current system. To do so, studies on latency of BPMs electronics and feedback processing will be investigated.

Finally, tune variation related with IDs gap movement will be addressed using lookup tables. Possibility of implementing tune and coupling feedback has to be considered for full coupling operation.

4.1.6. LAYOUT

One of the key factors of the ALBA II upgrade is taking advantage of ALBA as much as possible. This will be accomplished keeping the tunnel, the injector (LINAC and Booster), the infrastructures (technical building, water cooling and electrical power stabilization) and maintaining the beamlines at the same position.

Trying to keep the same source points for the beamlines adds

some constraints in the lattice design that are: having sixteen cells and a similar Storage Ring length. Still, it is not possible to have all the sixteen straight sections (where Insertion Devices are installed) at the same position as the present lattice. In ALBA not all the cells have the same configuration and thus, not all the straight sections are at the same distance with respect to the center of the Storage Ring. On the other side, ALBA II requires sixteen identical cells to maximize the symmetry keeping an optimum emittance and so, all the straight sections will have the same distance to the center. The ALBA II lattice has been designed to minimize the movement of the existing beamlines, with the result of having eight straight sections with zero displacement, four straights displaced by 68mm and four displaced 308mm, as shown in Figure 4-17. These last ones have no beamline in ALBA, so there is no impact.

The bending magnets beamlines have also been studied. From the present ports at ALBA, thirteen bending magnets beamlines can be re-used in ALBA II; including the four ones already in use. The other six bending magnet ports cannot allocate a beamline due to interactions of the light exit with equipment, use for Accelerator diagnostics or space in the Experimental Hall. In addition, due to the change of the accelerator lattice, some sources points of these thirteen beamlines are displaced: seven of the exit lines have zero displacement but six have a $\pm 2.5^\circ$ displacement, see Table 4-9. In the case of using as bending source a superbend, see Section 4.1.1.5, the orbit is displaced 1mm at the center of the bending. This option can be chosen by any of the beamlines.

All the proposed modifications needed to accommodate the new ALBA II magnetic lattice and RF systems will have an impact on the beam loss scenarios; type and occurrence rate, which correlate directly with the expected dose rates in the surrounding areas. Consequently, the behaviour of the current shielding buildings will be re-evaluated and a dedicated commissioning will be on place to ensure the compliance of the Nuclear Safety Council regulations.

¹⁴¹ L. Torino, U. Iriso. "Performance of BPM Readout Electronic Based on Pilot-Tone Generator and a Modified Libera Spark", Proc. Of IBIC'21, Pohang (Korea).

TABLE 4-9: ALBA II BEAMLINES DISTRIBUTION

INSERTION DEVICE BEAMLINES				
Port	Straight	Displ. [mm]	Use in ALBA	Foreseen use in ALBA II
02	SR01	0	BL - Free	Long BL
04	SR02	68	BL - MSPD	Long BL
06	SR03	0	BL - XAIRA	BL - XAIRA
08	SR04	308	BL - Free	Long BL
11	SR05	0	BL - NCD	BL - NCD
13	SR06	68	BL - XALOC	BL - XALOC
15	SR07	0	BL - 3Sbar	BL - 3Sbar
17	SR08		ACC - RF	ACC - RF
20	SR09	0	BL - LOREA	BL - LOREA
22	SR10	68	BL - CLAESS	BL - CLAESS
24	SR11	0	BL - CIRCE	BL - CIRCE
26	SR12		ACC - RF	ACC - RF
29	SR13	0	BL - BOREAS	BL - BOREAS
31	SR14	68	BL - FAXTOR	BL - FAXTOR
33	SR15	0	BL - Free	BL - MSPD
00	SR16		ACC-Injection	ACC-Injection

BENDING MAGNET BEAMLINES		
Port	Displ. [deg]	Foreseen use in ALBA II
01	0	BL - MIRAS
03	0	Long BL
05	0	BL - Free
07	+2.5	BL - Free
09	-2.5	BL - MISTRAL
10		Blocked
12		Blocked
14	-2.5	BL - Free
16	+2.5	BL - NOTOS
18		Blocked Truck entrance
19	0	BL - Free
21		ACC - Pinhole2
23	-2.5	BL - Free
25	+2.5	BL - MINERVA
27		Blocked
28	0	BL - Free
30	0	BL - Free
32	0	BL - Free
34		ACC - Pinhole1 & XANADU

13 Insertion Device beamlines (3 free + 10 in use);
 13 Bending Magnet beamlines (9 free + 4 in use).

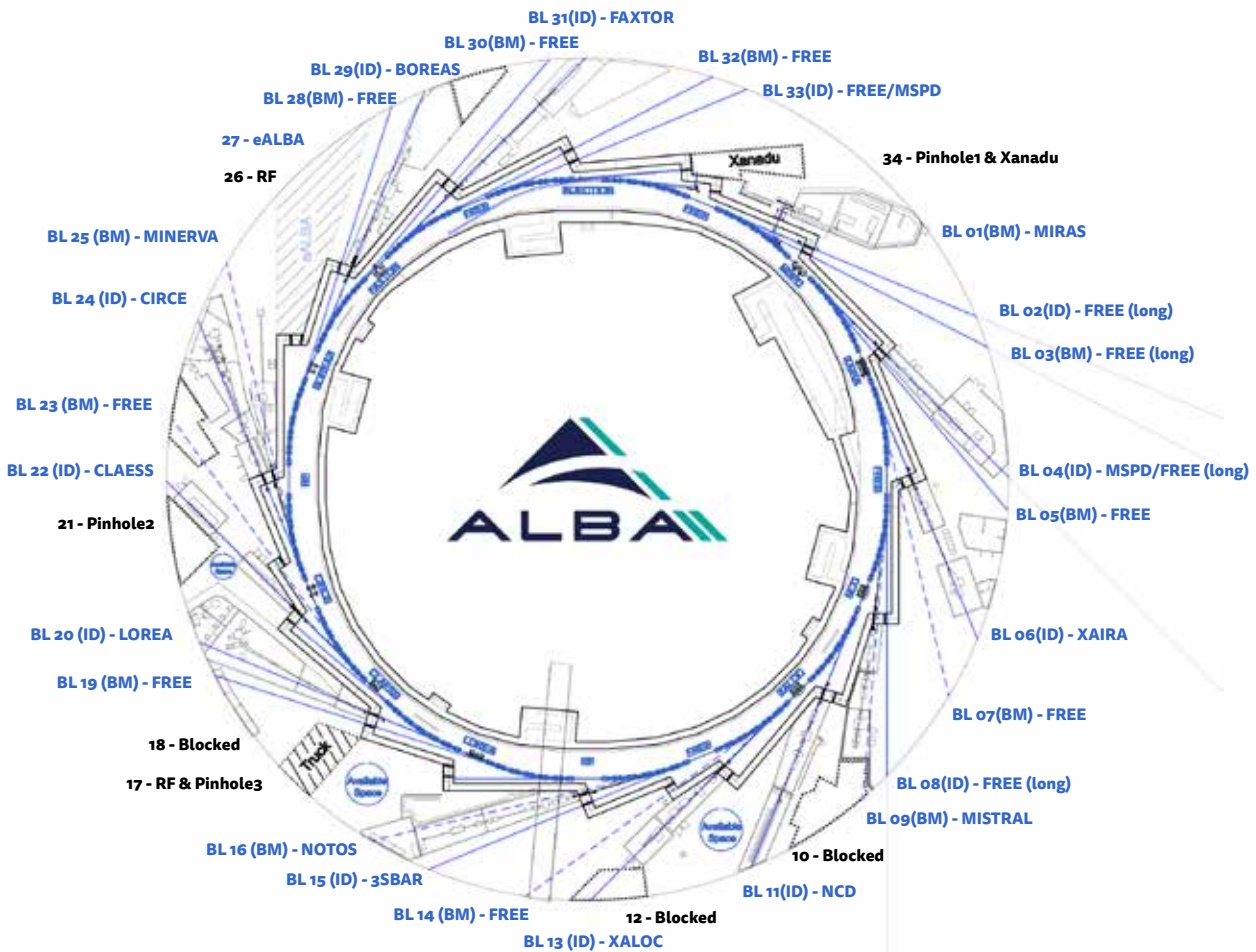


Figure 4-19: ALBA II Layout. The ALBA II lattice and exit lines have been integrated in the present tunnel.

Regarding the equipment for the accelerator, one straight section is reserved for the injection and two for the radiofrequency (RF). All three are high beta straight sections. The injection is maintained at the same location as ALBA. Each of the two sections for the RF will allocate three main cavities and two 3rd order harmonic cavities. Other accelerator equipment, like the diagnostic elements, will be distributed along the Storage Ring. In Table 4-9 and Figure 4-19, the use of the ALBA II straight sections and existing ports is summarized.

4.1.7. INJECTION INTO STORAGE RING

The existing ALBA injector, thanks to its large circumference and innovative design, delivers a beam emittance as small as 9nm-rad, already suitable for the injection into the upgraded storage ring.

Injection into the upgrade storage ring will be much more difficult compared to the existing ring, mainly due to the strong reduction of the horizontal dynamic aperture from ± 20 mm to ± 6 mm with similar betatron functions. A second factor that complicates the process is that in the new lattice the injection straight section is reduced from 8 m to 4 m.

The best scheme that fulfills these conditions is injecting with a single fast pulsed multipole kicker magnet installed in the same straight section as the septum magnet. This choice, besides avoiding to employ the present four dipole kickers scheme that could not be arranged any more in a 4 m section, has several advantages concerning both the transparency of the injection in terms of stored beam position stability and the reduced number of elements involved in the process.

In a multipole injection kicker, the magnetic field is zero at the center where the stored beam is traveling through, while it exhibits a high field value off-axis, where the injected beam is kicked and captured into the Storage Ring. The pulse of the kicker is a semi-sinus that lasts less than two turns, $T = 1.75 \mu\text{s}$, so that the injected beam is kicked only at the first passage, while at its second turn the field is off.

The arrangement of the injection straight section is sketched in Figure 4-20. The incoming beam from the Booster Ring is injected off-axis with a horizontal angle at the septum exit. To be captured, it's kicked by the multipole kicker in order to reduce its large oscillations within the dynamic aperture.

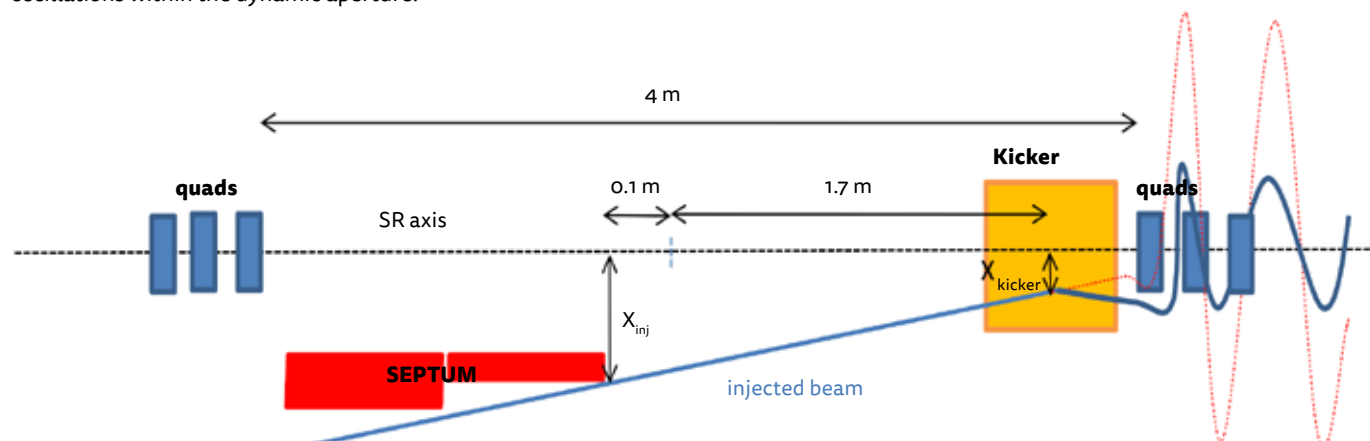


Figure 4-20: Sketch of the pulsed magnets and injection trajectory in the 4 m long injection section.

The multipole kicker under study for ALBA II is a modified design of the BESSY II non-linear kicker (NLK) and the MAX IV/SOLEIL multipole injection kicker (MIK) that are based on an octupole-like magnet. Instead, the proposed pulsed magnet will be based on a double dipole kicker (DDK) where 8 conductor rods are arranged in order to produce a sextupole-shaped zero field at the stored beam position and a field peak at the injected beam position (Figure 4-21).

Such topology allows producing an almost pure dipole field when only 4 out of 8 rods are powered, so that can be used for on-axis injection for the first beam turn in the ring during the commissioning. This is a very useful choice, since the ALBA II injection straight section has reduced space to install all the other necessary devices (scrapers, diagnostics...), hence combining two kickers (dipole and multipole) in one element is a convenient space saving option.

The DDK will be a 400 mm long in air kicker, composed of 8 conductor rods fixed on a ceramic vacuum chamber, titanium coated on the inner surface. The rods positions are determined as to preserve the vertical aperture of the vacuum chamber and to produce a peak close to the horizontal position of the injected beam.

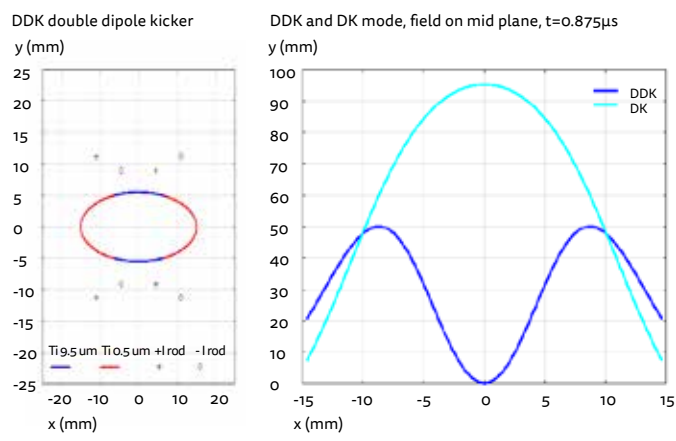


Figure 4-21: The prototype DDK.

a) cross section with the conductor rods and the vacuum chamber profile with two different titanium coating thicknesses of $9.5 \mu\text{m}$ (top and bottom wall surfaces) and $0.5 \mu\text{m}$ (side walls surface)

b) the magnetic field profile along the horizontal mid plane for the multipole mode and the dipole mode.

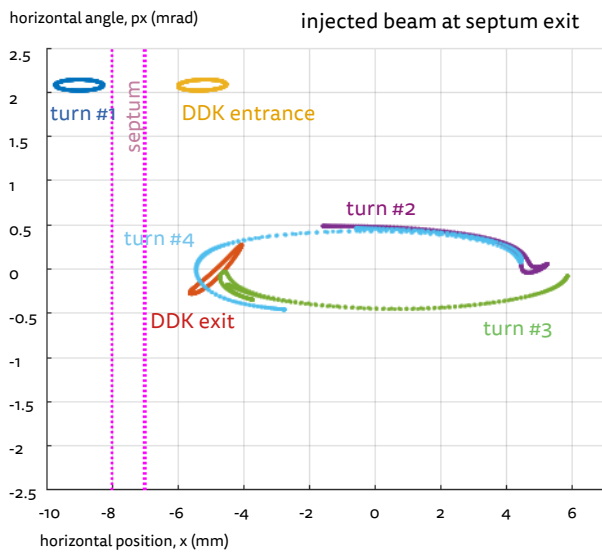


Figure 4-22: Simulation of the horizontal position and angle of the injected beam at the septum exit for the first three turns without errors. The septum blade, DDK entrance and exit have been superimposed for convenience.

A prototype of the DDK to be installed and tested in the existing ALBA ring is under design process. Figure 4-21 shows the prototype cross section of the rod positions and the magnetic field both for the multipole (8 powered rods) and for the dipole mode (4 inner rods switched off).

In order to minimize both the heat dissipation due to the image currents generated by the stored beam and the orbit and emittance stability disturbed by the eddy currents fields, the thickness of the metallic coating must be carefully shaped and its effects evaluated. A design with two different titanium coating thicknesses on the top/bottom wall surfaces and on the side walls surface is proposed to produce zero induced field on the stored beam.

The rod mechanical positioning tolerances should be less than $20\ \mu\text{m}$ to guarantee defect field and gradient on the stored beam smaller than $35\ \mu\text{T}$ and $0.35\ \text{T/m}$ in both planes. Since this tolerance is technologically unfeasible on a ceramic chamber, the inner and outer coils will be powered by two independent pulsers, by adjusting differentially both pulsers the defect field due to the mechanical position errors will be corrected.

Injection dynamics have been analyzed and the first turns in the horizontal phase space are shown in Figure 4-22. Simulating a booster beam ensemble of particles distributed at $\pm 3\sigma$ on a 6D hyper-contour and not considering errors, the injection efficiency is 100%.

4.2. Photon Sources

The portfolio of beamlines available at ALBA, both in operation or currently under installation, is shown in Figure 4-23. One of the aims of the ALBA II upgrade project is to keep all the Insertion Device (ID) beamlines already installed or currently under design at their present locations. Therefore, on day one ALBA II will make use of the current set of IDs, listed in Table 4-10. As explained in Section 4.1.6, in ALBA II all 16 straight sections will have the same length, 4 meters, which is identical to the length of the middle straight sections currently accommodating the IDs at ALBA, making straightforward the integration of the existing IDs into the new machine.

From the point of view of the beam optics, the straight sections will also be identical ($\beta_x=1.98\text{m}$, $\beta_y=2.30\text{m}$) with the exception of the injection straight and those at 90° intervals from it (thus keeping the 4-fold symmetry of the Storage Ring), which will have higher beta values ($\beta_x=11.74\text{m}$, $\beta_y=10.02\text{m}$) in order to enable injection. As shown in Table 4-10, after taking the current occupancy of IDs and the requirements for injection and RF, four straights will be available at ALBA II for the installation of additional IDs, three with “standard” low beta values and one with the higher ones.

From the point of view of the photon delivery performance, the existing IDs will benefit from the foreseen 25-fold decrease of the electron beam emittance. Figure 4-24 shows a comparison

between the spectral brilliance calculated for the undulator-type IDs in the present and the upgraded machines. It can be seen that the expected brilliance increase will depend strongly on the photon beam energy: from a factor 6 at 100eV, passing through a factor 13 at 1keV, and up to a factor 20 at 10keV.

In a similar way, the change in the transverse coherent fraction, which measures how close the source is to the diffraction limit, is shown in Figure 4-25. The improvement in the coherent fraction will range from a factor 2 at low energy up to a factor 30 at high energies.

In the case of wiggler-type IDs, the gain in brilliance is smaller, and strongly dependent on the effective source size as determined by the amplitude of the electron beam oscillations inside the device. Figure 4-26 shows the spectral brilliance curves calculated in wiggler approximation for the 3 wiggler-type IDs at ALBA.

Up to this point we have evaluated the benefits of the upgrade on the existing IDs. However, the reduction of the horizontal beam size will make it possible to install round vacuum chambers in the straight sections, opening the door to IDs with magnetic material surrounding the electron beam, as Delta-type¹⁴² or APPLE X¹⁴³ undulators.

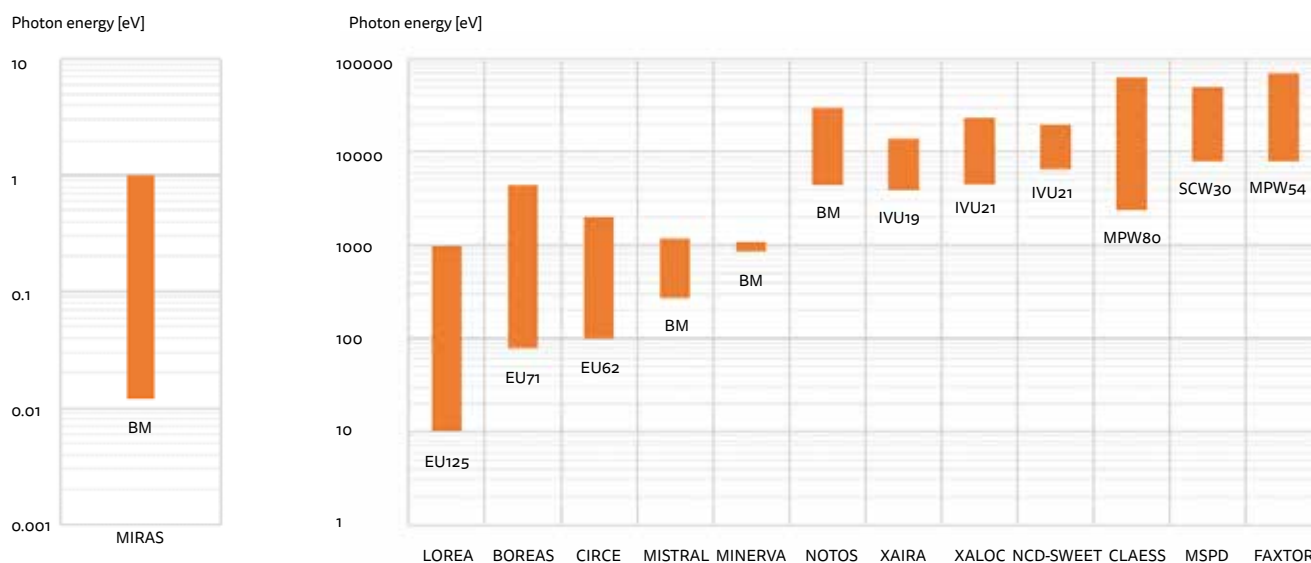


Figure 4-23: List of beamlines at ALBA, indicating the corresponding operating energy range and the associated photon source (BM stands for bending magnet beamlines, and the other labels indicate different types of insertion devices). MIRAS beamline, operating in the infrared region, is shown in a separate plot for convenience.

¹⁴² A. B. Temnykh, “Delta undulator for Cornell energy recovery linac”, Physical Review Special Topics - Accelerators and Beams Vol.11, 120702 (2008)

¹⁴³ T.Schmidt and M.Calvi, “APPLE X Undulator for the SwissFEL Soft X-ray Beamline Athos”, Synchrotron Radiation News, Vol.31, p 35 (2018)

TABLE 4-10: EXPECTED OCCUPANCY OF STRAIGHT SECTIONS FOR ALBA II

STRAIGHT#	PORT #	BEAMLINE	ID SOURCE	[MM]	N_p	K_{MAX}	OPTICS
1	02	Free					Low beta
2	04	Free					Low beta
3	06	XAIRA	IVU19	19.9	116	2.17	Low beta
4	08	Free					High beta
5	11	NCD-SWEET	IVU21	21.6	93	1.60	Low beta
6	13	XALOC	IVU21	21.6	93	1.75	Low beta
7	15	3Sbar	IVU	tbd	tbd	tbd	Low beta
8	17	RF					High beta
9	20	LOREA	EU125	125.0	16.5	13.14	Low beta
10	22	CLÆSS	MPW80	79.93	12.5	11.65	Low beta
11	24	CIRCE	EU62	62.36	27.5	5.2	Low beta
12	26	RF					High beta
13	29	BOREAS	EU71	71.36	22.5	6.40	Low beta
14	31	FAXTOR	MPW54	54.0	5.5	11.5	Low beta
15	33	MSPD	SCW/SCU	tbd	MSPD	SCW/SCU	Low beta
16	34	Injection					High beta

Including the legacy beamlines from ALBA (white), those that are not available for IDs (dark gray) and the available ports for the installation of additional IDs (light gray). For each ID, the period length (λ_u), the number of periods (N_p) and the maximum value of the deflection parameter are indicated.

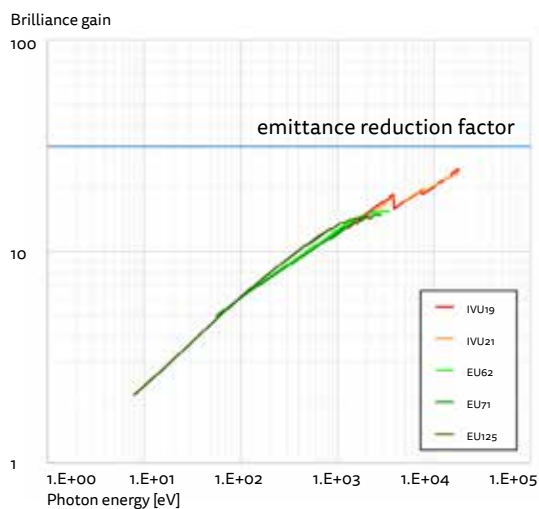
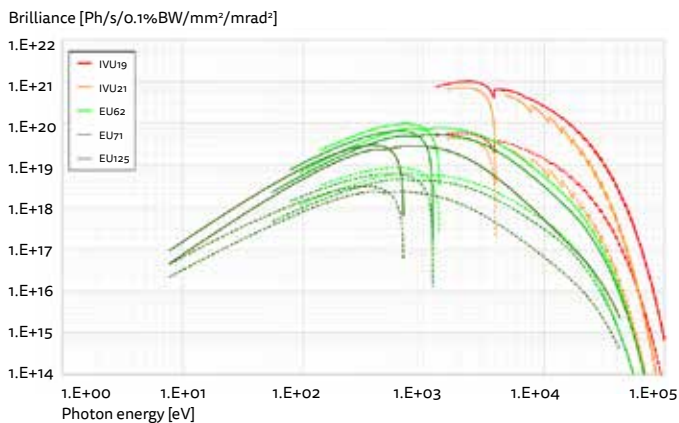


Figure 4-24: Left: Comparison of the spectral brilliance for undulator-type ID sources operating in the present (ALBA, 1% coupling, dashed lines) and the upgraded (ALBA II, 100% coupling, solid lines) storage ring, for an electron beam current of 250mA. Right: Gain in brilliance for each undulator operating at ALBA and ALBA II. Results obtained using SPECTRA.

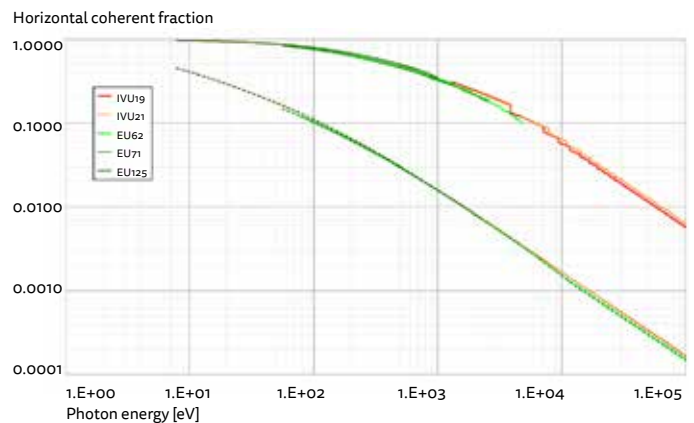


Figure 4-25: Evolution of horizontal coherent fraction with ALBA upgrade. Dashed lines correspond to present storage ring (ALBA, 1% coupling) and solid lines to the upgraded one (ALBA II, 100% coupling). Results obtained using SPECTRA.

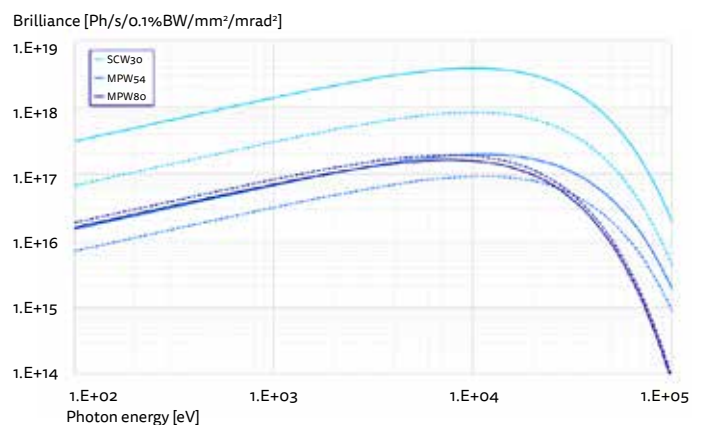


Figure 4-26: Spectral brilliance in wiggler approximation from wiggler-type IDs operating in the present (ALBA, 1% coupling, dashed lines) and the upgraded (ALBA II, 100% coupling, solid lines) storage ring, for an electron beam current of 250mA.

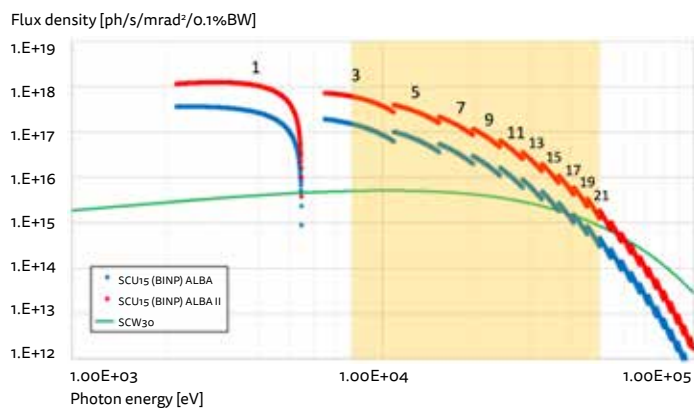


Figure 4-27: Spectral flux density of a SCU of a period length of 15mm as compared to the present SCW of a period of 30mm

On top of this, we have also started to explore the development of superconducting undulators¹⁴⁴ for pushing the delivered spectral range to higher energies, and improving the spectral flux density.

As a first case, we have analyzed the effect of using this technology for the MSPD beamline, replacing the superconducting wiggler (SCW) by a superconducting undulator (SCU). In Figure 4-27 the spectral flux density of a SCU of a period length of 15mm is compared to the present SCW of a period length of 30mm, where the improvement -in the usable range of the beamline, 8-50keV- is evident. The development of such a SCU prototype will take place during the period 2022-25 within the framework of the funded project ALBA01-NGEU "Enabling technologies for ALBA II"

The modification of the lattice of ALBA, with an increased number of dipoles of lower magnetic field, will have a major impact on the already existing bending beamlines. More precisely, the magnetic field will decrease from 1.42 T in ALBA dipoles down to 1.01 T in ALBA II QD magnets, corresponding to a 30% reduction of the critical energy of the generated radiation, from 8.5keV down to 6.05keV. The effect of this change on the spectral distribution of the brilliance is shown in Figure 4-28.

Those bending beamlines operating at photon energies below 4keV (BLO9-MISTRAL and BL25-MINERVA, see Figure 4-23) will benefit from the reduction in critical energy of the source, but for those beamlines operating at higher energies (as per today, BL16-NOTOS) an alternative source will have to be devised. One of the

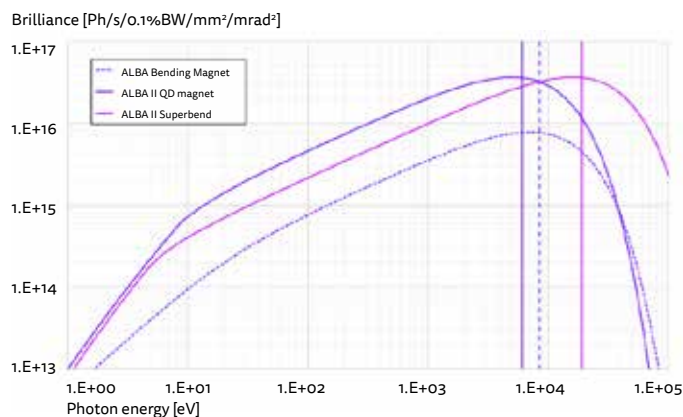


Figure 4-28: Spectral brilliance of dipoles at ALBA and of the proposed dipolar sources at ALBA II. Vertical lines indicate the critical energy for each source.

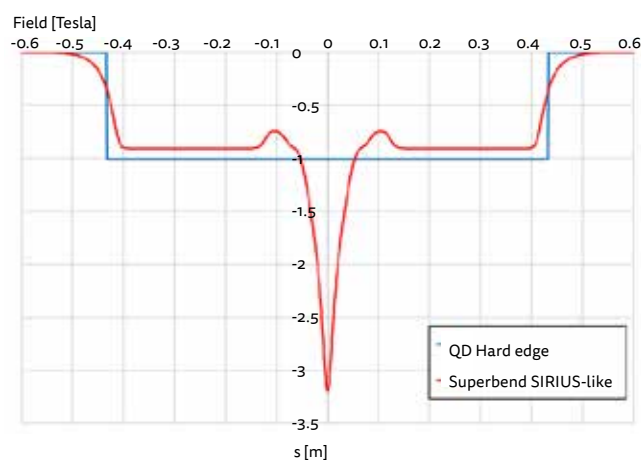


Figure 4-29: Field profile for the proposed 3.2T superbend compared with the standard QD magnet for ALBA II.

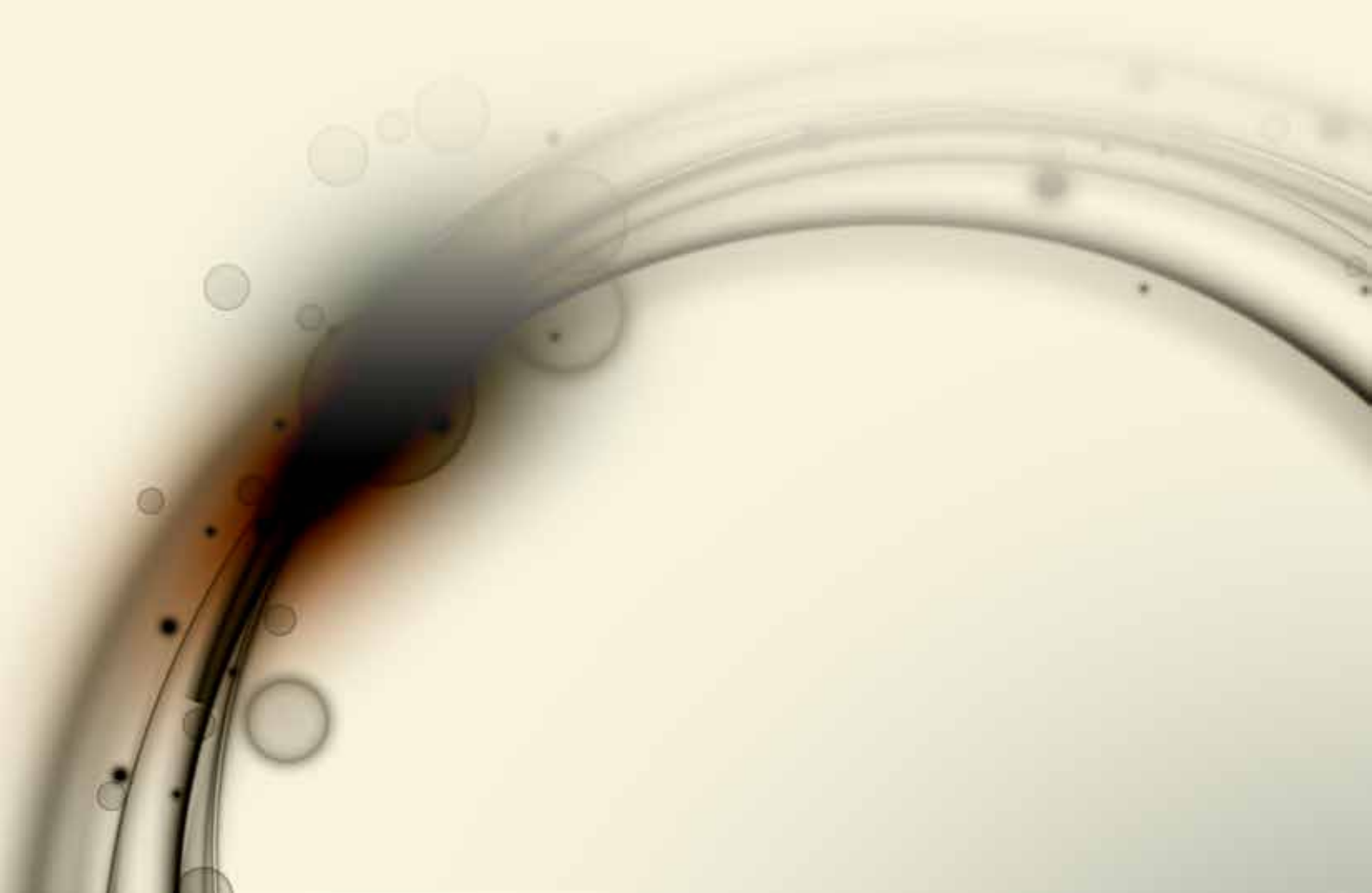
candidates under consideration is a 3.2T superbend based on the PM design developed at SIRIUS.¹⁴⁵ The original SIRIUS design, with a length of 0.92m and a deflection angle of 4.3deg, can be easily adapted to replace one of the QD magnets at ALBA II, with a length of 0.867m and a deflection angle of 5.0deg. The resulting magnetic field profile is presented in Figure 4-29, with two low field regions and a high field central pole. The corresponding photon spectrum is shown in Figure 4-28, together with the one for the conventional dipole sources.

¹⁴⁴ J. Bahrtdt, E. Gluskin, "Cryogenic permanent magnet and superconducting undulators", Nuclear Instruments and Methods in Physics Research, Section A, V.907, 149 (2018)

¹⁴⁵ J. Citadini et al. "Sirius-Details of the new 3.2T permanent magnet superbend", IEEE Transactions on Applied Superconductivity, Vol.28, 4101104 (2018)

5 Beamline technology for the fourth-generation light source

The small emittance of the electron beam in the new Storage Ring will allow for higher brilliance and for increased transversal coherence at the beamlines. The optical source size for most photon sources will be smaller, and this will allow focusing the X-ray beam into smaller spot sizes, with the corresponding increase of photon flux density (see Figure 5-1). The divergence of the beam will also be reduced, and this means that, in some cases, a larger fraction of the beam will fit within the acceptance of current beamlines. This will contribute to an increase in the flux on the sample, and on the detector.



The other feature of the new source is the increase of transversal coherence for the emitted beam. For Insertion Devices beamlines, the coherent fraction of flux will increase by almost an order of magnitude at 1 keV. In addition, the availability of long beamlines will allow exploiting transverse coherence also at higher photon energies.

To benefit from the features of the new source, the present beamlines will need to be upgraded to a higher level of performance in many aspects. For instance, most optical elements currently installed at the ALBA beamlines have surface errors exceedingly large for ALBA II, and keeping them would limit the spot size and the photon flux density achievable on sample, and would introduce significant structures and inhomogeneities in the photon beam. In addition to better optical surfaces, beamlines and experimental stations will require more accurate and stable positioning systems, as well as faster scanning systems. For instance, the higher photon flux will be useful only if detectors and monochromators are fast enough, and the much smaller beam size will require a much tighter control of vibration induced instability and of drifts caused by fluctuations on the environment.

In this section we discuss the main aspects of beamline technology that will be boosted or developed to guarantee that the scientific program of ALBA II benefits from the features of the new source.

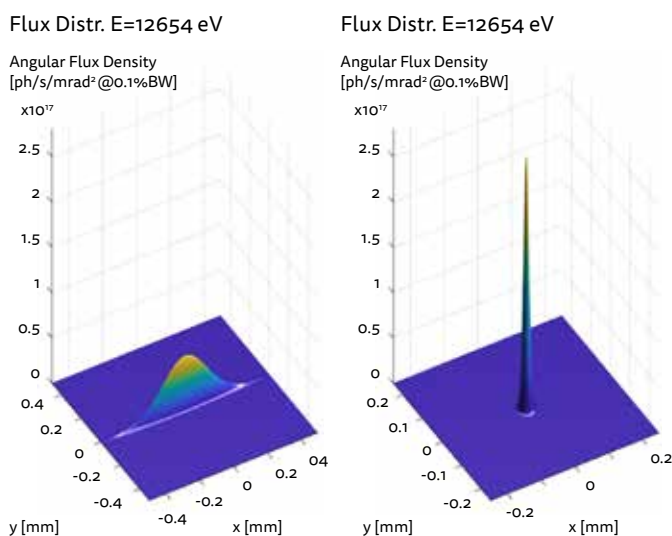


Figure 5-1: Increase of the angular flux density of the source for a photon energy of 3 keV

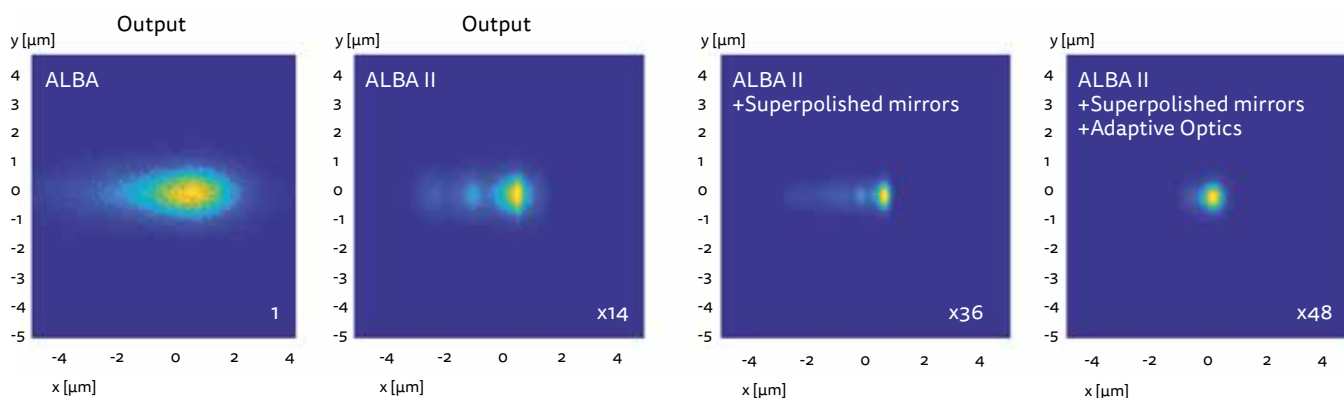


Figure 5-2: Simulation of the beam spot at the sample position of BL06-XAIRA considering different scenarios. The numbers indicate the gain in brilliance with respect to the current configuration. From left to right: a) using the beam parameters of ALBA, and the current optical elements, b) using the beam parameters of ALBA II, without changes in the optics, c) using ALBA II parameters, and replacing optical elements by super-polished mirrors, and d) using ALBA II parameters, super-polished mirrors, and considering wavefront correction with adaptive optics.

5.1.1. OPTICS

ALBA II beamlines will require optical elements with very low surface errors, as the tolerance to these is proportional to the source size, and therefore, a smaller source requires smaller slope errors (see Figure 5-2). In addition, there are many applications in which the sample or the detector must work out of the focal plane. In those cases, the requirements on the surface errors of optical elements are even tighter, since the distortions of the wavefront provoke striations on the intensity profile of the beam, as well as speckles and interference fringes, especially at low photon energies where the high coherence enhances the contrast of any interference effect.

The surface accuracy of commercially available mirrors has experienced a tremendous improvement in the last decade due to the development of deterministic polishing and of the required metrology feedback. Nowadays, some suppliers can produce mirrors with figure errors around one nanometer and below, for a wide variety of curvatures.

Nevertheless, the simple replacement of the mirrors at the existing beamlines by new, more accurate ones is not straightforward, since the mirror at the beamline is often subject to conditions that introduce a deformation of the substrate, which will have much tighter tolerances in ALBA II. Typical causes for such deformations are residual stress induced by the mirror clamps, parasitic deformations of benders, stress induced by the cooling pads, or simply the thermal bump or the gravity sag. While all these aspects need to be addressed at the beamlines of ALBA II, special attention is required for cooling schemes and for benders, or more generally for active optics.

In particular, mirror cooling is challenging since it requires assuring the thermal contact of the mirror with the coolant at the same time it requires minimal mechanical contact, to avoid deformations of the mirror substrate. In general, one goal goes against the other, and a tradeoff must be made, with the additional difficulty that the thermal contact between mirror and coolant cannot be easily evaluated at the laboratory. Additional difficulties come from the mechanical boundaries of optical elements, its stability requirements, as well as from the fact that the total power, and the power distribution at the mirror is not constant at the beamline, since it depends, for instance, on the gap of the undulator, while the geometry of the cooling cannot be changed.

Facing these challenges with guarantee requires investigating new cooling schemes, and developing capabilities to test their effectiveness.

The other technology concerning mirrors that requires some effort is adaptive optics (see for example Figure 5-3). The term refers to optical elements that allow modifying the X-ray wavefront deterministically, remotely and dynamically, as required by the beamline. In almost all cases, adaptive optics is based on mirrors whose optical surface topography can be modified by a number of high-resolution motorized actuators that introduce a controllable deformation of the substrate. ALBA has already developed and implemented an active optics system, capable of controlling the figure of the mirror in operation conditions with high resolution and high stability. The system is also very scalable from a basic configuration to a system with many motorized actuators, for better control of the mirror optics. The system is installed and working at some beamlines, although it can be improved in several aspects, like figure feedback, control of parasitic motions, or cooling. Some of these improvements require prototyping independently of any beamline project.

The development of photon-based feedback techniques is an essential component required for the proper exploitation of active optics elements. Tools and methods used to determine the distortions of the X-ray wavefront at a given position of a beamline, which are used to provide feedback to the active optics elements installed at the beamline, and that compensate wavefront



Figure 5-3: Example of adaptive optics system installed at the XAIRA beamline at ALBA. It includes two bending actuators and two adaptive correctors, used to correct the thermal bump. The system includes also the water cooling of the mirror.

aberrations appearing during the operation of the beamline. There is a number of technologies that are being developed for such operation, from the use of Hartmann-sensors, talbot gratings or speckle tracking techniques, Figure 5-3 reproduces one such example.

In a wider scope, photon diagnostics are all the methods and devices used to determine the characteristics of the photon beam. Among them there are systems used to determine the shape, position and size of the photon spot, as well as the flux, intensity, energy and energy resolution of the beam delivered to the station. For example, the smaller spot size allows for X-ray beams below the micron, which are not measurable with usual fluorescent screen microscopes, in positions where a wire scan or a knife edge scan are difficult to integrate, due to interaction with the experimental station.

While mirrors are the most common optical element in X-ray beamlines, some applications will require other types of optics, like compound refractive lenses, or diffractive elements, like multilayer Laue lenses, bent Laue crystals, Fresnel zone plates, Kino-form lenses, etc. Those elements are not so frequently used in beamlines, but sometimes are the optimal solution for a beamline design. Therefore, the basic technical test facilities, as well as the competences for a reliable design, use and maintenance of such components will need to be maintained.

In order to properly control the quality of the optical elements that go to the beamlines, the existing laboratory of optical metrology needs to be kept at the highest level of performance. In addition to validating the characteristics of the purchased optical elements, the laboratory plays a key role in the installation of the optical elements in their holders or benders, as well as in their full characterization. The use of adaptive optics at the beamline must be preceded by a thorough characterization of the components at the laboratory, where each component can be measured independently, in a quick and accurate manner. Optical metrology is also one essential platform to sustain the developments in cooling systems and active optics required by the beamlines of ALBA II.

5.1.2. OPTOMECHANICS AND CONTROLS

The increased flux on sample of ALBA II will allow collecting data with sufficient statistics using shorter acquisition times. As a consequence, the sensitivity limit of many experimental stations will increase leading to new scientific opportunities. To take advantage of this, the beamline, including mechanics,

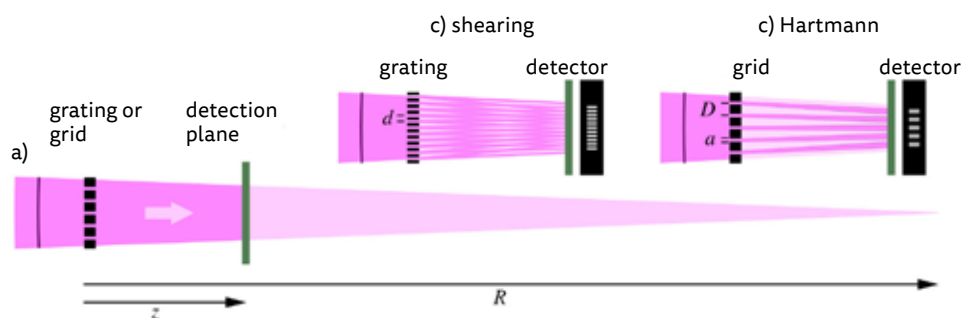


Figure 5-4: Optical scheme used in the single-grating shearing interferometry and Hartmann wavefront, assuming an expanded converging beam. Reproduced from.¹⁴⁶

¹⁴⁶ Goldberg, K.A.; Wojdyla, A.; Bryant, D. Binary Amplitude Reflection Gratings for X-ray Shearing and Hartmann Wavefront Sensors. *Sensors* 2021, 21, 536. <https://doi.org/10.3390/s21020536>

detectors and control system, will have to work synchronously at much higher speeds than at the present beamlines. For instance, scanning systems of some beamlines, like monochromators or diffractometers, will have to be capable of operating at high speeds, yet maintaining the alignment within tight limits, and without introducing any measurable vibrations. In addition, the reduced dimensions of the beam will lead to tighter stability requirements, not just on scanning components, but on every component interacting with the beam. Finally, the higher acquisition rate at the experimental station, will require the beamline to be free of mechanical resonances in a wider range of frequencies than for ALBA; for which moderately high frequencies are not visible for being averaged by relatively long integration times.

Those increased demands for speed, accuracy and stability will require some improvements in many beamline components. From a mechanical design perspective, systems will need to be more compact, with simpler kinematic chains, and the implementation of close loops feedback from encoders and interferometers to correct errors will be mandatory. Continuous scans at high speed, synchronizing multiple axes during the experiment will be the routine mode of operation. These aspects are described in detail in the following paragraphs.

The vibration stability, and the lowest vibration mode of common optomechanical systems, like mirror positioning systems, monochromators or slits are often limited by the long kinematic chain of their positioning systems, which usually consist on in-air stages connected to in-vacuum platforms by long rods through vacuum ports and sealed with bellows. Almost always, the kinematic chain between the fixed support, solidly anchored to the floor, and the point of interaction with the beam (the mirror, crystal or slit) is distributed between air and vacuum. This limits the performance of the systems in several ways.

To start with, the clearance required by the motions around the rods that connect the atmosphere and vacuum sides of the mechanics, sets a minimum length for the bellows, and thus a minimum distance between the motion stages and the point of interaction. This distance amplifies all the mechanical errors produced at the stages and limits the frequency of the lowest vibration modes of the system. In some occasions, the required motion ranges, require rods unacceptably long, and it is better to have some motion stages at the in-vacuum side. Although this allows for a more compact air-to-vacuum transfer, it also increases the weight on top of some motion stages and leads to a design consisting on a stack of stages, which is prone to errors and vibrations.

Another source of errors comes from the vacuum forces within the kinematic chain, which cause parasitic deformations. In order to minimize them, the designer must dimension the stages accordingly, what leads to massive mechanics, which unavoidably have resonances at low frequency.

As a result of all that, positioning systems are often very heavy and relatively weak, with low resonance frequencies (rarely above 70 Hz), and not really fit for fast scans or fast correction.

In order to allow for higher vibration stability and better dynamic behavior, the positioning systems of ALBA II must have more compact arrangements, with shorter kinematic chains,

minimizing the weight and size of the moving parts. This will lead to a higher use of in-vacuum actuators, and direct drives, i.e. without transmission between the motor and the point of interaction. The needs for speed and resolution will also require a precise selection of the type of motor. Torque-motors are already quite widespread for spectroscopy monochromators, and their use will be extended to other applications, too. And for many other components, like slits and diagnostics, motion stages based on stepper motors and transmission, will tend to be replaced by direct piezo-electric actuated drives, which are inexpensive, compact, light and accurate.

The accuracy requirements will also push for designs including a mechanic-independent metrology frame. This is, a mechanical structure solidly anchored to the base, independent of the motion stages, that provides a fixed reference for the position feedback sensors, namely encoder reading heads, interferometers sensors, or sensors of any other kind. Accuracy needs will also push for a more extended use of close loop operation, which will be used to control the motion, but also to correct the guidance errors along the scan, caused by limited guidance accuracy, or by dynamic deformations. The complex system described will require the integration of many different actuators and diagnostics in a common control system that ensures that time and accuracy requirements are met. When tight time constraints are required, customized electronic and software designs will be required to guarantee deterministic behavior. Finally, a comprehensive set of tools for monitoring each action and response will be required to ensure a continuous diagnosis of the performance.

5.1.3. DETECTORS

The detectors measure the interaction of the X-ray beam with the sample and are the main source of experimental data. Therefore, tailoring them to each scientific case is crucial to guaranteeing the scientific excellence of the experiments. Of course, a myriad of commercial detectors is available. However, they cannot be directly used in a synchrotron light source as most of the sensors are not detecting X-ray wavelengths, and, on many occasions, the key performance parameters of the sensors that have been optimized are not the ones required. For example, reducing the pixel size and the energy consumption or measuring multiple wavelengths simultaneously are crucial in the market. In contrast, achieving huge dynamic ranges or reducing dark noise are more critical for a synchrotron beamline.

In the past, indirect detection with scintillators was a common mechanism to adapt seamlessly sensors designed for other photon energy regimes. But now, tailor-made detectors for X-rays, mostly based on semiconductors, have surpassed their performance by far. In particular, semiconductor hybrid detectors have demonstrated achieving excellent results. They consist of two elements: the first, an array of sensors that absorbs photons generating charges, and the second, closely bound to the first, processes these charges and transmits the results to the backend. This architecture allows adapting the sensors depending on the photon beam's characteristics and reusing the processing part for different applications.

In ALBA II, new detectors will be installed, also using new materials in the sensors. The semiconductor material most commonly used is silicon but, since, its absorption coefficient

drops above 20keV, a thicker sensor is necessary to detect the photons, but, in practice, producing silicon thicknesses above 1mm is technically very complex and costly. Hence, a different semiconductor with a higher absorption coefficient will be necessary. Several High-Z semiconductors meet the requirements: cadmium telluride, germanium, gallium arsenide and others. Each of them has challenging properties, in R&D phase: strict cooling requirements at very low temperatures, uniformity problems or high defect rates. In addition, the availability of the production chain represents a further complexity. These materials are not widely used on the market, and the technology required for their production and quality assurance is complex. In practice, very few manufacturers can deliver high-quality materials, and accessing them is not simple.

The second big challenge is that detectors will receive a flux increased up to 30 times in intensity. This implies major changes in all the detector designs. For example, one mature technology in X-ray detectors is photon counting. Each pixel can discern when a photon hits the sensor and transmits this event to the backend. Currently, one pixel in the latest detectors can discriminate up to 10^7 photons per second. But a complex detector has about 10^7 pixels. In this case, the bottleneck comes from the backend processing capacities as the maximum rate of concurrent event processing is quickly reached. For ALBA II beam, detectors will greatly exceed these limits, and major developments are foreseen to make significant progress.

On the other hand, recently, there have been promising results using integrating detectors. These detectors accumulate the load generated in each pixel and measure its evolution over time. This concept is not new, but using the latest semiconductor technologies has reduced the noise level, allowing the detection of single photons. Theoretically, all these analogue signals can be used to determine the position of the photon hits with a precision exceeding the pixel size. Of course, the system complexity is enormous: 10 million analogue signals must be acquired and processed at extremely high rates. Different architectures to optimize this process are evolving, and soon, their first results will compare their performance with detectors with digital discrimination.

The need for photon detection in ALBA II will be wide-ranging. For instance, spectroscopy detectors constitute another fundamental type. In this case, these detectors must precisely determine the incident photon energy. Such detectors will be widely used as primary or complementary detectors. In this field, the use of drift detectors is well established. There are more performing options based on measuring the tunnel effect at extremely low temperatures. But the lower production cost of the drift detectors makes it possible to integrate several heads and to obtain unrivalled sizes in the total area of the detector.

The ALBA II detectors will produce a massive data flow, what is known as the deluge of data. Its impact will deeply affect many components in the beamline: the control and acquisition hardware and the data storage, bandwidth and processing capabilities. Custom software designs will be tailored to digest the deluge. This will be further detailed later.

Developing detectors is resource demanding. A high-level project requires many years, a massive budget and a large team of specialized designers. In most cases, ALBA II will collaborate with other institutes and private companies to develop and integrate them smoothly. A key to success will be to define the requirements far enough in advance. All of the above will need to be pulled together to guarantee that the highest-performing detector is available when the first photons of the ALBA II will hit the sample.

5.1.4. SAMPLE ENVIRONMENT

Ultimate understanding of materials properties and the factors governing their behavior and performance requires studying all their relevant properties in realistic conditions and at different length scales. This multi-modal, operando and multi-scale approach is expected to strongly accelerate the ability to design better materials in many critical fields such as catalysis, electrochemistry, photovoltaics or novel low consumption devices. Using in situ or operando conditions allows insights into structure–property relationships, which might not be observable by ex situ characterization, and a multi-scale approach is mandatory in order to link for example formulation, pore structure, binder properties, particle size and chemistry.

X-ray microscopy, diffraction and spectroscopy are powerful tools to determine structural and electronic properties, and the spatial resolutions achievable at micro and nanoprobe beamlines make them an ideal complement to high-resolution transmission electron microscopy studies in a multi-length-scale analysis approach. The advent of Micro-ElectroMechanical Systems (MEMS) based on in situ cells has enabled atomic resolution TEM studies at relevant conditions, such as reaction cell pressures of up to 1 bar and temperatures of up to 1000°C. The implementation of operando cells for catalysis and electrocatalysis is foreseen at ALBA in the frame of the InCAEM infrastructure⁷. An important aspect of this development is the ability to move these operando sample environments between instruments and thus offer the possibility of studying the same sample under well-controlled identical conditions using multiple techniques, making complementary experiments truly comparable and allowing for well-defined registration between the instruments to correlate results on the same region or particle of the sample. The lower emittance of ALBA II is very well matched to the need for micro- and nanofocus beamlines with high brilliance, as is necessary to use operando cells compatible with electron-based microscopies and also with the lower-energy X-rays, as these have very limited thickness and thus amount of sample, as well as to ensure an overlap of the sampling volume between techniques. In addition, the increased X-ray coherence is an excellent opportunity to develop lensless imaging approaches where there are fewer restrictions for advanced sample environments as compared to nanoscale scanning (limited space, maximum weight, thermal stability, etc.). Finally, the cryogenic systems are particularly important for many life sciences techniques to mitigate the radiation damage on the sample. These systems are required to be included from the initial design phase of the end station and the sample environment to foresee their associated spatial restrictions and positioning errors.

5.2. Planning the new beamlines

The new footprint of ALBA II opens the opportunity for enlarging the infrastructure in setting up the for the future facility. The involvement of the user community is strategic in such a process and has been encouraged from the very start-up of the project, via a series of colloquia, workshops, and finally open calls for proposals for the new beamlines.

The ALBA II capacity, as explained in chapter 4, offers up to 26 photon ports, of which 13 correspond to Insertion Devices (IDs) and 13 to Bending Magnets (BMs), four of them allowing extra-long beamlines.

A first call for proposals was launched in 2021 for the definition of a beamline to be built inside the present experimental hall, with the successful result of having now in the construction phase the 3Sbar beamline, as already mentioned, dedicated to surface diffraction and spectroscopy at 1 bar, which was shortly described in paragraph 3.2.

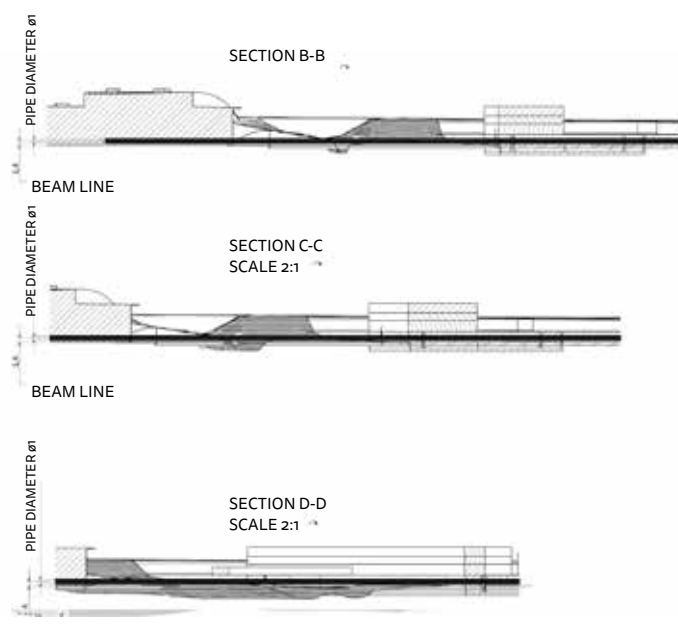


Figure 5-5: Profile of the three long beamlines with experimental stations in the new plots.

TABLE 5.1: LONG BEAMLINES TECHNICAL PARAMETERS SUMMARY

PORT	UNIT	BL02	BL03	BL04	BL08	NOTE
Source type		Undulator	Superbend	Undulator	Undulator	
Length available for ID	m	2	N.A.	2	2	1) 2)
Source Size X	$\mu\text{m rms}$	14	7.7	14	34	1) 3)
Source Size Y	$\mu\text{m rms}$	15.1	24.8	15.1	31.4	1) 3)
Source Divergence X	$\mu\text{rad rms}$	7.1	< 2000 ⁷⁾	7.1	2.9	1) 3)
Source Divergence Y	$\mu\text{rad rms}$	6.5	< 310 ⁸⁾	6.5	3.1	1) 3)
Beamline length at the Far Exp. Hall	m	134-249	141-255	173-292	85-125	1) 5)
Position stability	%	10	10	10	10	1) 6)

Notes:

- 1) All the parameters in this table may be slightly changed as a result of the refinement of the design of the ALBA II accelerator complex and buildings.
- 2) ID length is relevant since the given value allows allocating one ID, but not a tandem of IDs.
- 3) The specified values correspond to the rms spot sizes of the electron beam. For low photon energies, the actual size and divergence are dominated by the diffraction of the photon beam.
- 4) The beamline has some space available at the experimental hall of the main building of ALBA. That space can allocate part of the optical components, or some experimental station, if the design allows for it.
- 5) The space available for the beamline at the far experimental hall, allow installing components between the minimum and maximum distances given here.
- 6) The position of the electron beam is stabilized by an active correction system up to 100 Hz. The target stability tolerance is 10% of the electron beam size. The same stability criterion is maintained for the photon beam on sample, although there may be cases for which physical limitations of beamline components prevent from reaching this stability value.
- 7) The horizontal divergence of the superbend magnet is limited by the acceptance of the beamline optics. Typical values do not exceed 2 mrad, limited by available length of mirrors or the resulting aberrations in sagittal focusing systems. A larger fan can be accepted in absence of such limitations.
- 8) The provided value corresponds to the vertical divergence at 1 keV.

During 2022 a new call was open, this time for instruments which can be hosted in the nearby plots corresponding to the new and long beamlines. The call is, at the time of writing, in the first step of the evaluation process, aiming at having the prioritized list of the new instruments defined by summer 2023. The four long beamlines will be hosted in ports 2, 3, 4 and 8. Their layout is shown in Figure 2-3, while Figure 5-5 shows their profiles and Table 5-1 summarizes their main technical parameters.

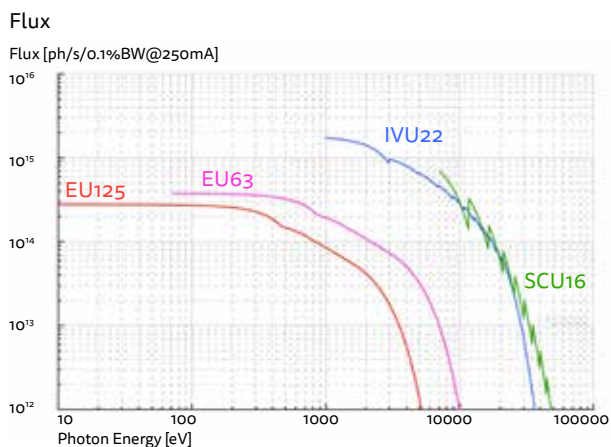


Figure 5-6: Flux emitted by different undulators within the energy range of ALBA II.

5.2.1. RANGE OF TECHNICAL PARAMETERS FOR LONG BEAMLINES ON IDs

A preliminary performance analysis is made for these beamlines based on examples of existing instruments, and typical optical designs. The examples provided in this section are not optimized for any particular scientific case, and the performance values are to be considered only as an indication.

The flux emitted by the different types of undulators which will be used in BLO2 and BLO4 is shown in Figure 5-6. We consider four state-of-the-art undulators, with periods that allow covering the energy range between 10 eV to about 40 keV.

To a first order approximation, the source size and divergence for undulators depend only on the energy and the characteristics of the machine accelerator. The values expected taking the full available length of the straight sections are given in Figure 5-7. The plots indicate the contributions of the electron beam size and divergence (constant dashed lines) and of the diffraction limit (wavelength dependent).

The finite size of the electron beam leads to a reduction of the coherent fraction of the emission. The horizontal coherence fraction of light is given in Figure 5-8.

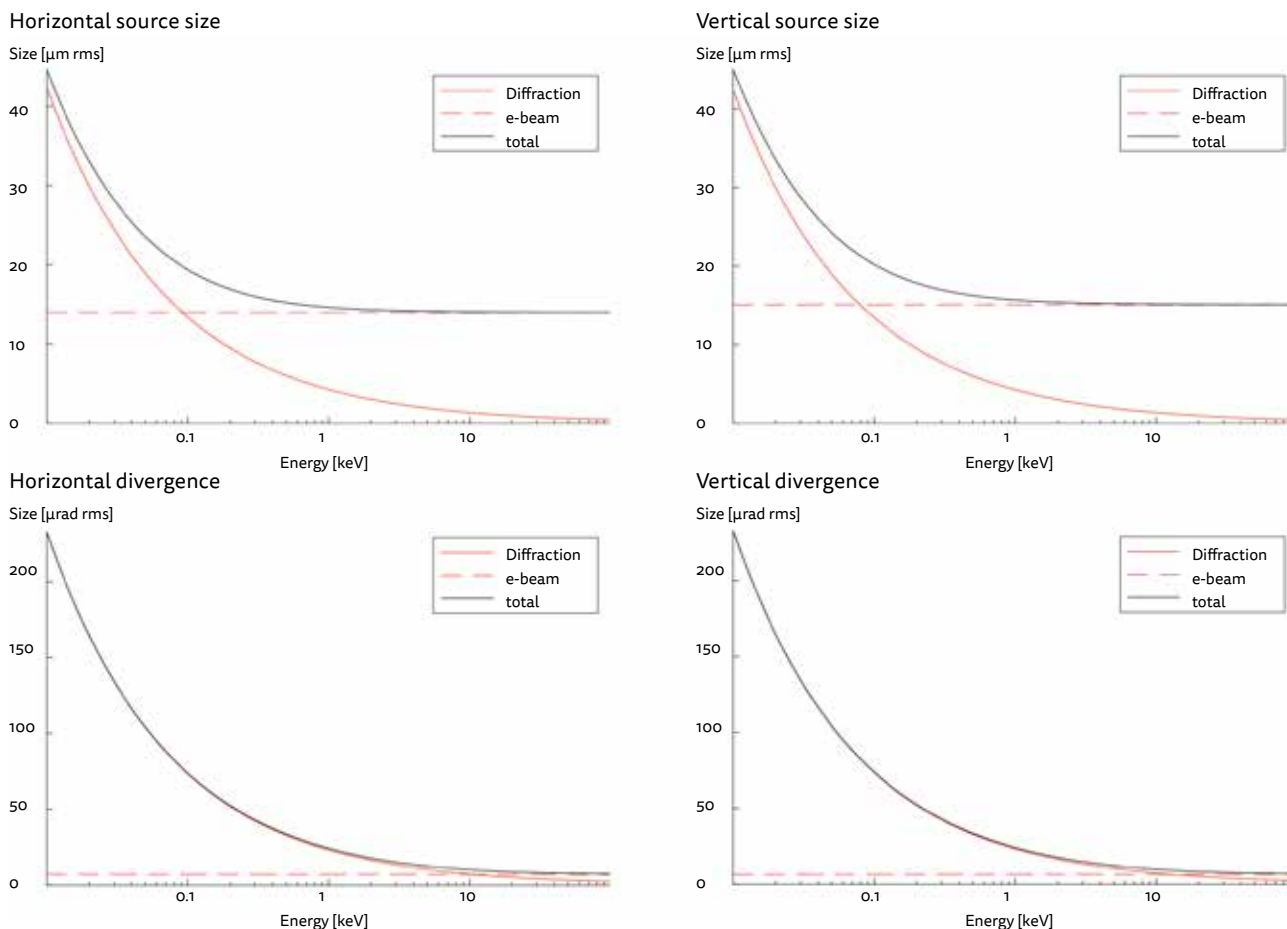


Figure 5-7: Source size and divergence for ALBA II ports BLO2 and BLO4.

BLO8 corresponds to a straight section, too, with the same length available for IDs as the other ports at ALBA, so total flux is exactly the same as for BLO2 and BLO4. Nevertheless, the source characteristics of this straight section are different. The beam is more collimated while the source is larger. The sizes and divergences for a source installed at BLO8 are given in Figure 5-9.

The different source characteristics yield to a slightly different coherent fraction, slightly lower than for the mini-beta straight sections

All the three considered ports feed beamlines with lengths ranging from 125 m to 292 m. The available length can be used to obtain nanometer scale focus. The achievable spot size depends on the used technology: mirrors, capillaries, Fresnel zone plates, etc. Here we consider only reflective optics. Also in this case, the results depend strongly on the distance to sample, and on the photon energy. Some reference values of the achievable RMS spot size are given in the following plot. The provided values are to be considered only for reference, since the actual achievable spot size depends on many other parameters, like coating, incidence angle, flux acceptance, surface errors or allowable curvature radius.

Horz. Coherent fraction

Horz. Coherent fraction

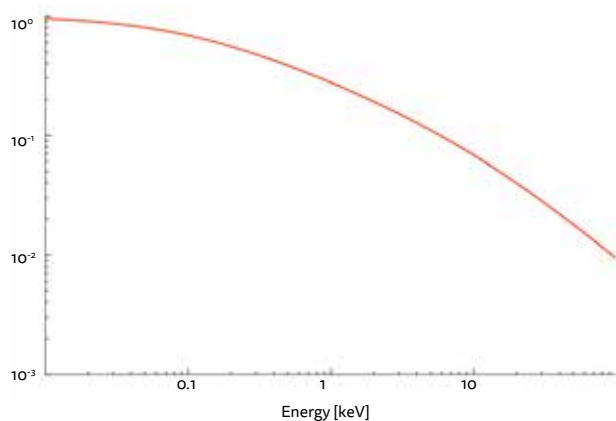
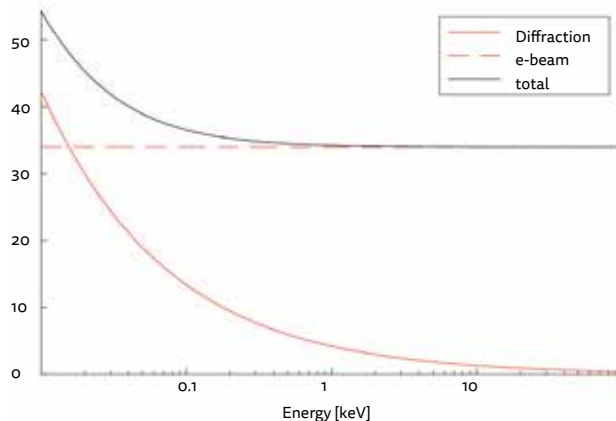


Figure 5-8: Horizontal coherent fraction of the sources of ports BLO2 and BLO4, for ALBA II.

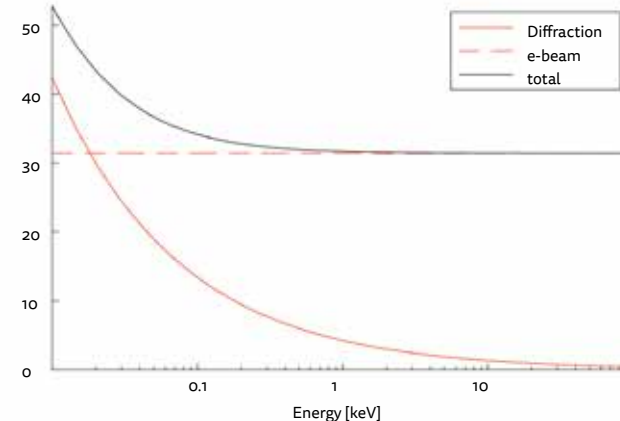
Horizontal source size

Size [$\mu\text{m rms}$]



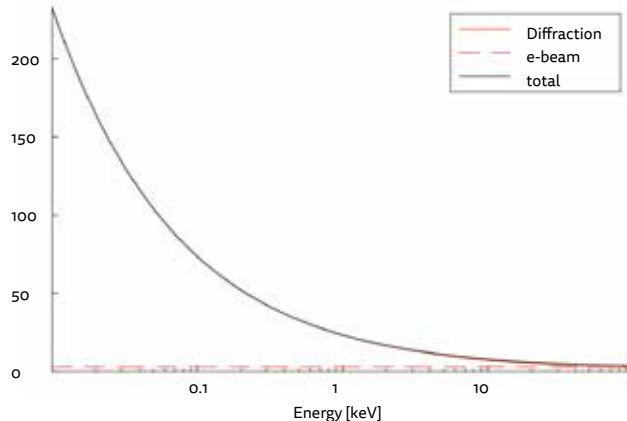
Vertical source size

Size [$\mu\text{m rms}$]



Horizontal divergence

Size [$\mu\text{rad rms}$]



Vertical divergence

Size [$\mu\text{rad rms}$]

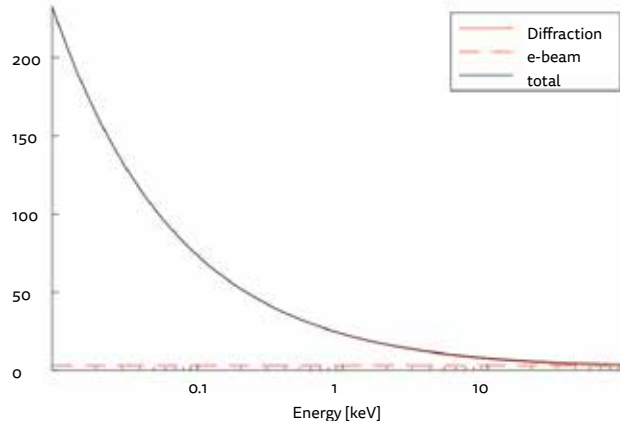


Figure 5-9: Source sizes and divergences for an undulator source installed at BLO8.

Horz. Coherent fraction

Horz. Coherent fraction

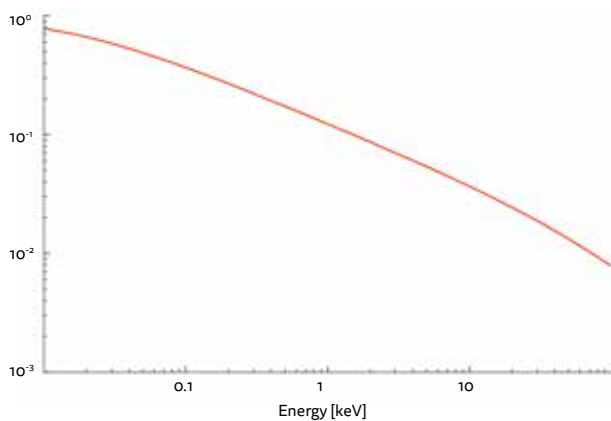


Figure 5-10: Coherent fraction of the flux emitted by an undulator installed at BL08.

BL length 150 m

Spot Size [nm]

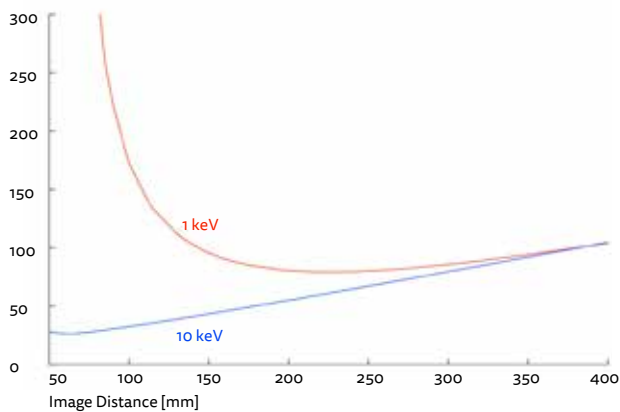


Figure 5-11: Achievable spot size as a function of the image distance to the sample for low and high photon energies.

5.2.2 . RANGE OF TECHNICAL PARAMETERS FOR BEND AND SUPER-BEND SOURCES

The new lattice provides two kind of sources from dipole magnets, as explained in chapter 4 with critical energy of 6 keV for the standard bending magnets, and up to 20 keV for the superbend. Among the available ports, four correspond to superbends, and five correspond to regular bending magnets.

The flux emitted by the standard bending magnets and the superbends at ALBA II is shown in Figure 5-12.

Spectral Flux (1 mrad H)

Flux [ph/s/0.1%BW]

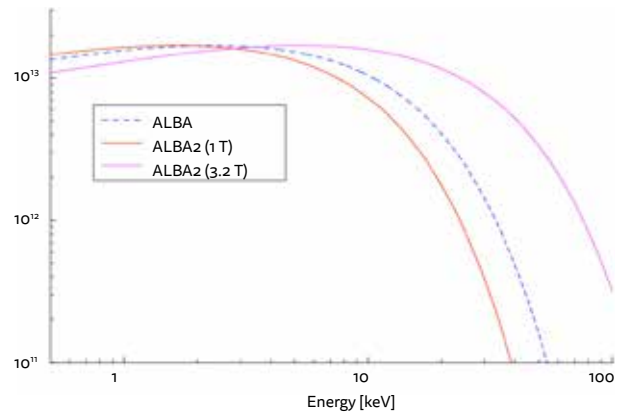


Figure 5-12: Flux emitted by the bending magnets of ALBA II, assuming acceptance of the full vertical divergence and 1 mrad of horizontal acceptance.

Vertical divergence

Divergence [μ rad rms]

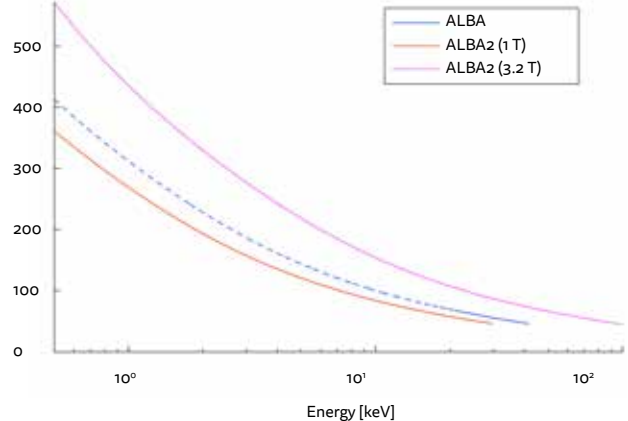


Figure 5-13: Vertical divergence of the beam emitted by the bending magnets of ALBA II.

The horizontal divergence of the beam is normally limited by the acceptance of the beamline. The vertical divergence is mostly contributed by the diffraction limit of the photon source, both for standard BMs and superbends. Its value is given as a function of energy in Figure 5-13.

One of the available superbends will feed BL03, which corresponds to a long footprint beamline. While the beamline is yet to be defined, the source and length offer an excellent opportunity for full-field, high-resolution tomography, with large sample volumes, and mostly dedicated to high energies.

5.3. Upgrading existing beamlines

As shown in Figure 5-14, half of the beamlines have now been in operation for more than one decade, creating an urgent need for upgrading individual aging instrumentation to avoid main failure of the corresponding user program and to adjust to the changing user demands independent of the optimization of the beamlines within the ALBA II context. Therefore, we will implement a 4-step upgrade project for all existing beamlines, which will satisfy the most urgent needs to ensure operational excellence and also addresses investments to benefit from new opportunities in the field under ALBA and ALBA II conditions.

The upgrade of the beamlines considers the following four different stages:

- **Essential ALBA:** Absolute essential upgrades or the current program will no longer be competitive or even is in risk of main failure.
- **Enabling ALBA:** Upgrades necessary to be state-of-the-art or to reorient the program opening new scientific opportunities.
- **Essential ALBA II:** Absolute essential upgrades or the program cannot be executed at ALBA II.
- **Enabling ALBA II:** Upgrades necessary to be state-of-the-art on a 4th generation source or to reorient the program under consideration of the opportunities ALBA II will bring.

The four categories will allow dynamic and fast actions to respond to rapid changing frame conditions but still allow to keep the

overview on the impact of the decisions. We note that this detailed analysis is an ongoing process at this time and consequently, we will only present details on a few beamlines and some broad ideas on the rest.

Updated radiation shielding calculations will be done for the present ALBA beamlines to ensure the performance of the existing shielding structures under the new beam conditions, except for the newest beamlines (FaXToR and 3Sbar), for which the shielding has already been designed considering ALBA II conditions. The beamlines upgraded optic elements with changes on the beam path will probably need adapted local shielding elements. Those Bending Magnet beamlines migrating to SuperBend magnets, with a significantly harder photon spectrum, ask for complete re-evaluation of the structural shielding elements.

5.3.1. IMPACT OF THE NEW SOURCES ON THE ALBA BEAMLINES

As a 3rd generation light source, ALBA was designed to accommodate insertion devices (IDs) as the main X-ray sources. At the moment of starting ALBA II, ALBA is providing light from 10 IDs and 4 Bending Magnet ports. Generally speaking, ALBA II will largely benefit the undulator beamlines by allowing smaller spot

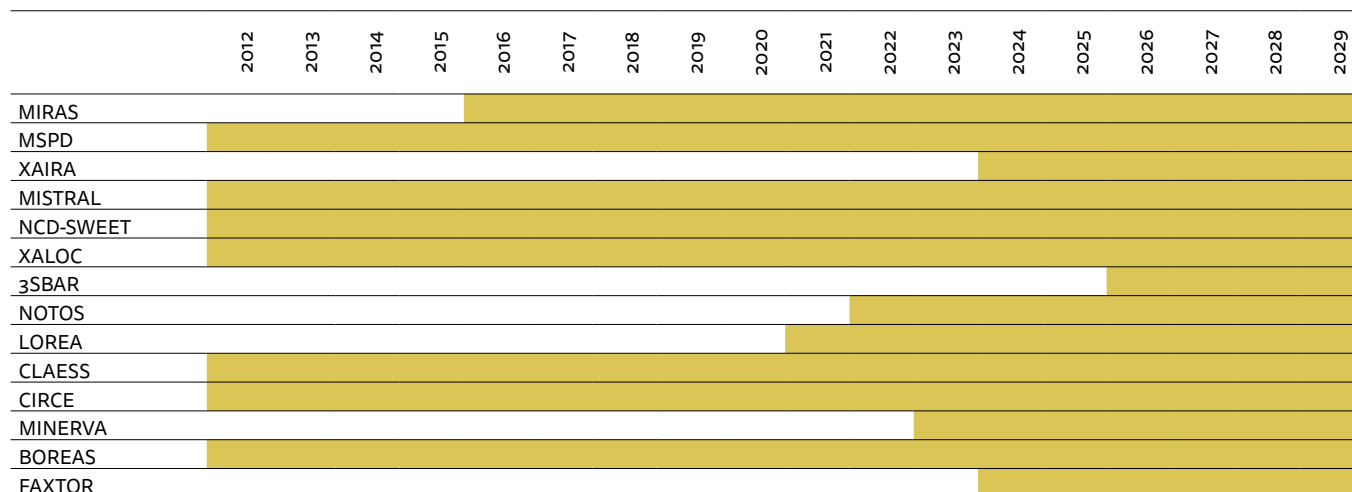


Figure 5-14: Chronogram showing when the different beamlines came into operation at ALBA.

sizes at similar or higher flux on the sample and bring a harder spectrum for bending magnet beamlines which will be upgraded with superbend or insertion devices.

Specifically, BLO4-MSPD will benefit at ALBA II from a new superconducting undulator to reach higher photon flux and a significantly smaller spot size (from $20 \times 15 \text{ mm}^2$ to about $2 \times 2 \text{ mm}^2$) that will largely benefit the micro-focus program. The present bending magnet beamline BL16-NOTOS will be moved to a superbend, enhancing the diffraction program and at the same time extending the spectroscopy range of the beamline to the 35 keV range, and it is under discussion whether BL31-FaXToR which at ALBA gets light from an in-vacuum multipole wiggler should be moved to a different photon source, either a superbend or an insertion device.

As mentioned in paragraph 4.2, all beamlines with undulators will benefit from the brilliance increase as well as from the increase in the transverse coherent fraction. In the case of wiggler-type IDs, the gain in brilliance is smaller, and strongly dependent on the effective source size as determined by the amplitude of the electron beam oscillations inside the device, this is one of the reasons why BLO4-MSPD will be moved to a SCU, and we are studying to exchange wigglers by undulators or superbends.

5.3.2. ENHANCING PERFORMANCE OF THE BEAMLINES

This section presents a short review of the evolution of the operational beamlines based on the four stages indicated above.

MSPD

The Materials Science and Powder Diffraction beamline BLO4-MSPD is devoted to high angular resolution Powder Diffraction (PD), and Micro Powder Diffraction (MD) at high energy, mainly used by a strong High Pressure (HP) Powder Diffraction program using Diamond Anvil cells up to 50 GPa. To accommodate the various experimental techniques, the beamline has two experimental end stations, one devoted to high angular resolution powder diffraction and the second one dedicated to high pressure and micro diffraction experiments at high energy. The position sensitive 1D detector which is operating up to 40 keV is likely unique in the world, while the 2D detector on the high pressure and micro powder diffraction is outdated, and is in danger to fail what would imply a significant damage to the HP program and will need to be replaced even before the dark period.

MSPD is located at port 04, one of the four possible long beamlines in ALBA II. In addition, MSPD is equipped with a superconducting wiggler (SCW) that has caused operational problems in the past. While moving MSPD to a new port, to free the space for a long beamline, a new ID will be procured for this beamline.

The decision has been taken to replace the SCW by a superconducting undulator (SCU) that will bring the following benefits to MSPD:

- Energy range up to 50 keV
- Higher flux at high energies (30-50 keV)
- Smaller spot size (from $20 \times 15 \text{ }\mu\text{m}^2$ to about $2 \times 2 \text{ }\mu\text{m}^2$)

In addition, the moving of MSPD to a new port offers the opportunity to move the standard high-resolution program of the beamline to a super bend beamline allowing to fully optimize MSPD for micro-focused diffraction and at the same to provide optimal conditions for the productive high-resolution program of the beamline. It is essential to invest already under ALBA into a state-of-the-art area detector to reduce the risk of failure and at the same time building and promoting the micro-focus program.

To enable ALBA, instruments will have to be adapted for in situ, operando techniques and high throughput.

CLAESS

CLAESS is a multipurpose hard X-ray Spectroscopy wiggler beamline providing simultaneous access to absorption and emission spectroscopy beamline (XAS, XES) in the tender to hard X-rays region. Most of its publications, up to 65% are related to catalysis and to energy related investigations. The beamline is well equipped with several sample environments. The beamline has a gas management system to perform measurements of XANES/EXAFS during chemical reactions under conditions close to industrial catalysis. A Core Level Emission Analyzer and Reflectometer (CLEAR) instrument, in-house developed, allows to energy-analyze the emitted fluorescence. Spectra on a single-shot basis can be collected thanks to the combined use of a Mythen unidimensional detector and a silicon diced analyzer.

To keep a good performance of the beamline until the dark period the monochromator will have to be replaced. This will allow to also optimize the data acquisition system for fast acquisition fully supporting the need of the catalysis community. This will be accompanied with a fast and automatized on line data analysis pipeline to boost the in-operando concept. These are essential ALBA upgrades. Common laboratories that allow a standardization of catalysis and battery setups to strengthen multi-modal approach in the different ALBA beamlines are currently under construction and will contribute to the enable ALBA approach.

Being served by a multipole wiggler, CLAESS would not greatly benefit at ALBA II from the accelerator upgrade. However, CLAESS could take over the role of the micro-spectroscopy beamline in ALBA II portfolio if the wiggler could be changed with an appropriate undulator which would still allow for fast scanning. Based on current technology, this would come with a reduction of scan speed; however, it is expected that progress in device and controls will significantly improve this issue. A final decision will be taken later in the process.

NOTOS

NOTOS is devoted to X-ray Absorption Spectroscopy (XAS), X-ray Diffraction (XRD) and instrumentation tests. It allows studies in situ and operando in chemistry, catalysis, energy science, nanomaterials, condensed matter and environmental science, by providing two experimental end stations: (i) a multipurpose station consisting of a wide table for preset or custom sample setups and (ii) a two-circle diffractometer station, both of them combine XAS and XRD. A third end station, in the Optics Hutch,

will allow beamline instruments improvement by using white, pink or monochromatic beam. The beamline operates between 4.5 and 30 keV (Bending Magnet source) with a beam spot size in the sample down to $100 \times 100 \mu\text{m}^2$.

NOTOS has entered in operation in 2022 and as such there is no need for an upgrade before the dark period. To expand on the current program, what we call enabling ALBA, a 2D acquisition for non-homogeneous XRD will be required.

Source of NOTOS at ALBA II will be a superbend which will bring the opportunity of increasing the energy range and the photon flux reaching the sample.

NCD-SWEET

The beamline allows the simultaneous recording of SAXS and WAXS (Wide Angle X-ray Scattering) which results in the capability to test length scale which ranges from a few microns to a few angstroms. It also provides Grazing incidence SAXS (GiSAXS) and Grazing incidence WAXS (GiWAXS) allowing characterization of biological systems, such as fiber systems, membrane systems or cellular organelles, samples in solution, polymers and nanotechnology systems including nanoparticles on substrates. The photon energy range is 6.5 - 13 keV. The beam spot size can be varied, the minimum value being $2.6 \text{ (H)} \times 2.5 \text{ (V)} \mu\text{m}^2$ with the current setup.

The scientific program for NCD-SWEET has been slowly shifting from life sciences towards energy related materials and catalysis, and as such the beamline is becoming a key contributor to the investigations related to solar cells and electrolytes.

A state-of-the-art SAXS detector was installed in 2017, as one of the actions of a general upgrade of the beamline during 2017-18. Before the dark period the WAXS detector will have to be replaced as part of the essential ALBA to keep the scientific program competitive.

ALBA II will enable new opportunities at the NCD-SWEET beamline coming from a smaller spot size and larger coherence fraction providing the opportunity to add a time correlation program to ALBA II portfolio.

BOREAS

BOREAS provides polarization dependent spectroscopic investigation on advanced materials. It is equipped with two end-stations. The first experimental end station (HECTOR) is dedicated to XAS, XMCD and XMLD with a spot size from $80\text{-}100 \times 20 \mu\text{m}$ up to mm size for studies of advanced magnetic materials under magnetic fields of up to 6T along the beam axis and 2T in the plane perpendicular to the beam. The second end station (MaReS) is dedicated to RMXS and reflectivity, also to coherent imaging with a spot size from $250 \times 80\text{-}100 \mu\text{m}$ up to mm size. This instrument is based on an ultra-high vacuum reflectometer for the research of magnetic anisotropies on magnetic surfaces, thin films, nanostructures and bulk single crystals.

The beamline covers an extended energy range from 100 to 4000 eV and it is one of the leading instruments for 4d-TM XAS-XMCD

experiments. Over the past years, the beamline has added an additional and growing coherent imaging program of magnetic structures. When going to ALBA II the beamline will benefit from a much stronger coherent and scattering program together with a higher flux and high submicron-spectroscopy making the instrument to a corner stone within the magnetism program for micro spectroscopy and high-resolution imaging of magnetic structures with nm resolution for materials development applications and the increasing growing need for characterization of devices.

Essential upgrade for ALBA contemplates going cryogen free particularly on the HECTOR magnet. The scattering end station requires a new and faster 2D detector for more efficient data collection. The replacement of the 2D detector will also reduce the risk of complete failure of the detector which shows already significant degradations.

Essential upgrade for ALBA II aims at the exploitation of coherence in ALBA II in combination with the smaller spot size, by means of upgrading the mirror system to allow for 1st harmonic rejection, and replacing the single Kirkpatrick-Baez (KB) mirror by two mirrors, optimized for each end station.

CIRCE

CIRCE is a variable polarization soft X-ray beamline dedicated to advanced photoemission experiments. A plane grating monochromator covering the energy range 100 - 2000 eV is shared between two independent branches with dedicated experimental end stations: PEEM (photoemission electron microscopy) and NAPP (near ambient pressure photoemission). A pair of deflecting mirrors directs the beam to one branch or to the other. On the PEEM branch, relevant results have been obtained in XPS-PEEM, XMC(L)D-PEEM, IV-LEEM and u-LEED modes, combining state of the art spatial resolution with spectroscopic measurements (spectromicroscopy). Several in operando environments, in particular with electric and magnetic signals are available to the users. To keep the actual program ongoing, the detector needs to be replaced to increase its sensitivity and there is an increasing need to automatize and provide data analysis in real time to the users. The PEEM will benefit from the smaller spot size of ALBA II, and will see its spatial resolution increased as the space charge will be reduced.

The Near-Ambient Pressure Photoemission (NAPP) end station is an Ultra High Vacuum (UHV) set up equipped with a hemispherical electron energy analyzer for X-ray Photoelectron Spectroscopy that can operate at a sample pressure range from UHV up to 25 mbar. Therefore, the usual characterization capabilities of XPS are extended to the study of gas-solid and gas-liquid interphases, with applications for in situ characterization of heterogeneous catalysts, corrosion processes, wetting, fuel cells, photovoltaics, etc. Near Edge X-ray absorption (NEXAFS or XAS) is also possible either in Total Electron Yield mode (measuring sample current) or in Auger mode using the electron energy analyzer. It is one of the few instruments with these characteristics open to users in Europe.

The ALBA essential upgrade for NAPP requires replacing the aging instrumentation, while to further develop the program, i.e. enabling ALBA will be achieved by enhancing the energy range

from 0.1-1.5 keV to 0.1-3.0 keV. NAPP will benefit greatly from the smaller spot size in ALBA II that in combination with the enhanced energy range, will allow pushing the sample conditions towards higher gas pressure and allowing much more realistic sample conditions for classical electrochemical applications.

LOREA

LOREA is a beamline specified for the investigation of band structure of solids by means of Angle Resolved Photo-Emission Spectroscopy (ARPES). The beamline operates in the photon energy range 10-1000 eV with tunable linear and circular polarizations produced by an APPLE II helical undulator. Thanks to the energy range and the high photon flux, LOREA is suitable for high resolution VUV ARPES investigations in the 10-200 eV range, while it is feasible to extend the ARPES measurements in the 200-600 eV energy range (soft X-ray ARPES). In addition, core level photoemission, resonant photoemission and X-ray absorption spectroscopies will be accessible in the whole energy range. LOREA is also equipped with a spin-detector to perform spin-resolved ARPES (SR-ARPES) experiments.

The beamline opened for users in October 2021. Essential upgrade for ALBA contemplates going cryogen free. There is no need for any essential for ALBA II, but the scientific program of the beamline will benefit enormously from the smaller spot size in the sub-micrometer range, making LOREA in concert with the PEEM instrument at CIRCE and the imaging capabilities at BOREAS the key for studying new materials and enable the extension to the device level. It is also worthwhile to note that this concept will also benefit widely from the new non-X-ray probes provided by InCAEM (HRTEM and STM's) and the corresponding laboratory infrastructures, making the program as such unique in Europe. The smaller spot size will require some modifications on the optics, a zone plate or a single bounce capillary would be needed.

MISTRAL: soft X-ray tomography and spectromicroscopy

MISTRAL aims at imaging the near-native structure of cells at a resolution of 30nm half pitch in a volume of $16 \times 16 \times 12 \mu\text{m}^3$ by means of cryo soft X-ray tomography (cryo-SXT). The observed frozen, hydrated cells do not need to be sliced or chemically modified, preserving the native structure. The region of interest is selected using an on-line visible light epifluorescence microscope for correlative, low-resolution 2D imaging. Most of the experiments are dedicated to health (pathogenic infections, cancer and several other diseases), biomineralization, nanoparticles internalization, drug delivery or characterization of particular organelles or structures inside the cell.

MISTRAL is equipped with a TXM which is one of five existing worldwide. It was developed as a prototype back in 2012, and as such, issues have been identified that need to be solved to keep the main program running. Currently, the essential upgrade at MISTRAL is the replacement of the TXM including the sample delivery system and the integration of cryo 3D CLXT (3D cryo correlative light and X-ray tomography) to keep competitiveness. To enable ALBA II operation and benefit from the higher brightness and better spectral emittance, the beamline optics will need to be

replaced, introducing ALBA benders and cooling in some of the beamline optics, and optimizing the diagnostics at the beamline. These improvements will result in a higher beamline performance.

MIRAS: infrared micro-spectroscopy

MIRAS beamline is devoted to Fourier Transform Infrared (FTIR) spectroscopy and microscopy. Its wavelength range is from about $1 \mu\text{m}$ to $\sim 100 \mu\text{m}$ with a spectral region between 2.5-14 μm . The beamline is able to map non-destructively the state of bio macromolecules in their natural environment at a spatial resolution of $\sim 3 \mu\text{m}$ by means of infrared micro-spectroscopy and becomes increasing importance for material science application to study the interface between hard and soft mater like essential for the electrolyte-cathode interface in batteries or the gas solid interface in heterogeneous catalysis. Output data is delivered either as spectral analysis (spectroscopy mode) or as images (microscopy mode). The beamline includes user friendly control system and provides a service of remote access of users to data analysis software.

IR light is collected from two bending magnets (edge radiation and constant field radiation) with large opening angles of 43 mrad horizontal and 25.17 mrad vertical that goes through a 3mm slotted mirror placed downstream the magnet. A specific vacuum chamber with larger vertical aperture is needed to collect the IR light. There are concerns whether this will be possible in the new ALBA II lattice, where the accelerator is much compact and the small diameter vacuum chamber intercepts most of the low energy photons. The solutions under consideration at SOLEIL¹⁹⁶ will be used as the basis to study a feasible solution for ALBA II.

In the trend towards multimodal research, the IR beamline will play a fundamental role providing complementary results to BL31-FaxToR and BLO9-MISTRAL. It is also complemented with the nano-Raman system currently under development within the InCAEM project, providing as such a worldwide unique characterization suite.

XALOC: macromolecular crystallography

XALOC, built as a multipurpose macromolecular crystallography (MX) beamline, provides a powerful tool to reveal the molecular machinery of life at atomic level. The 3D structures at atomic resolution of proteins, oligonucleotides and protein, DNA or ligand-protein complexes can be determined using Molecular Replacement or wavelength-dependent phasing methods. The beamline is currently offering oscillation, jet-based serial crystallography and in-plate techniques, which allow cryogenic and room temperature experiments.

The MX program requires a high-throughput, easy-to-use instrument to keep competitive and in parallel to attract new users, particularly from industry. The present equipment and software at the beamline limit the throughput. A major refurbishment of the beamline is already ongoing to secure the scientific program of XALOC. A new detector, a new sample changer and a replacement for the goniometer should boost the productivity at the beamline attracting new users and especially new industrial users.

XALOC will benefit from the increase in flux and reduction in beam size brought by ALBA II. Essential ALBA II will require changes in some of the beamline optics, like the mirror system and the monochromator allowing to optimize the beamline for high flux at the 20-25 keV range, widely seen as a sweet spot to minimize sample damage and at the same time optimize the achievable resolution.

This upgrade of optimizing the beamline is possible due to the construction of XAIRA which will take over more time-consuming experiments including native phasing, fixed-target serial crystallography and time-resolved experiments.

Beamlines in commissioning and in construction

There are four beamlines which at present are under construction or commissioning. BL31-FaXToR and BL14-3Sbar are still under construction, while BL06-XAIRA and BL25-MINERVA are under commissioning and should receive first users in 2023-24. For this set of beamlines, it is sensible to consider that no upgrade for ALBA will be required and any upgrade for ALBA II will come after the rest of upgrades.

6 Data management strategy

ALBA II pursues an improved understanding of our world. This is achieved through scientific experiments, which lead to capturing better knowledge. Nowadays, the path to knowledge is unique by retrieving information from processed data. Therefore, data, and, more precisely, how they are acquired, stored, processed, curated, and shared, is a key element of the ALBA II project.

The value of data is nowadays universally recognized. The days when the scientific community saw it as a by-product of the experiments are far behind in the past. Today, data is understood not only as a way to ensure the validity of a result, but, also, as the unique and comprehensive compilation of information from which to extract knowledge. Experimental data, in addition, provide an invaluable fountainhead for future knowledge: through future re-analysis using data analytics or as a valuable resource for machine learning, deep learning or other artificial intelligence algorithms. Data, in summary, is the outcome of the experiment, and there is no sound scientific result without proper data to hold it.

At ALBA II, the volume and the complexity of the data generated will be unprecedented. This will imply a complete redesign of IT infrastructure, information management systems and most software applications. An ambitious investment plan will be built for the necessary IT infrastructure and to sustain its operation. Its deployment and the development of all the necessary software on top will also require creating numerous highly specialized teams. In addition, they will allow exploiting emerging knowledge extraction techniques such as complex data analytics or artificial intelligence algorithms. The ALBA II aims at becoming a reference institution among the existing national computing research infrastructures.

ALBA II will embrace *Open Science*¹⁴⁷. ALBA is a member of the EOSC Association and a declared service provider in the future cloud. The precepts of *Open Data* imply the adoption of the FAIR

principles. The data must be Findable, Accessible, Interoperable and Reusable, not only by the ALBA II users but also by the entire scientific community. The end goal is to maximize the scientific results of all experiments carried out at ALBA by adopting these principles. Adopting the FAIR data principles will entail extending computing services to our users and the entire scientific community.

Given the priceless value of data, implementing an appropriate data management strategy is crucial to any scientific project. It seeks different objectives. First, identify and quantify all data sources. Second, define a storage strategy for the entire data life cycle, that is, not only during its inception but also during its future distribution, sharing and use. The goal is to guarantee its preservation and its capacity to extract value from it. Third, define the data package that guarantees future reusability and set rules for future data access. Fourth, develop guidelines for data processing that ensure traceability and reusability. And finally, establish, manage and communicate information management policies to use data effectively and ethically.

Data management strategy entails most of the computing infrastructure, information management systems and software applications. Designing and precisely sizing the IT infrastructure. Next, defining and building an adequate architecture for the data acquisition, control systems and online data analysis pipelines. And, finally, providing proper post-processing tools to the scientific community; documented enough to hold future use after the experiment execution. In summary, the purpose of developing a

Estimated Annual Data Production (Petabytes)

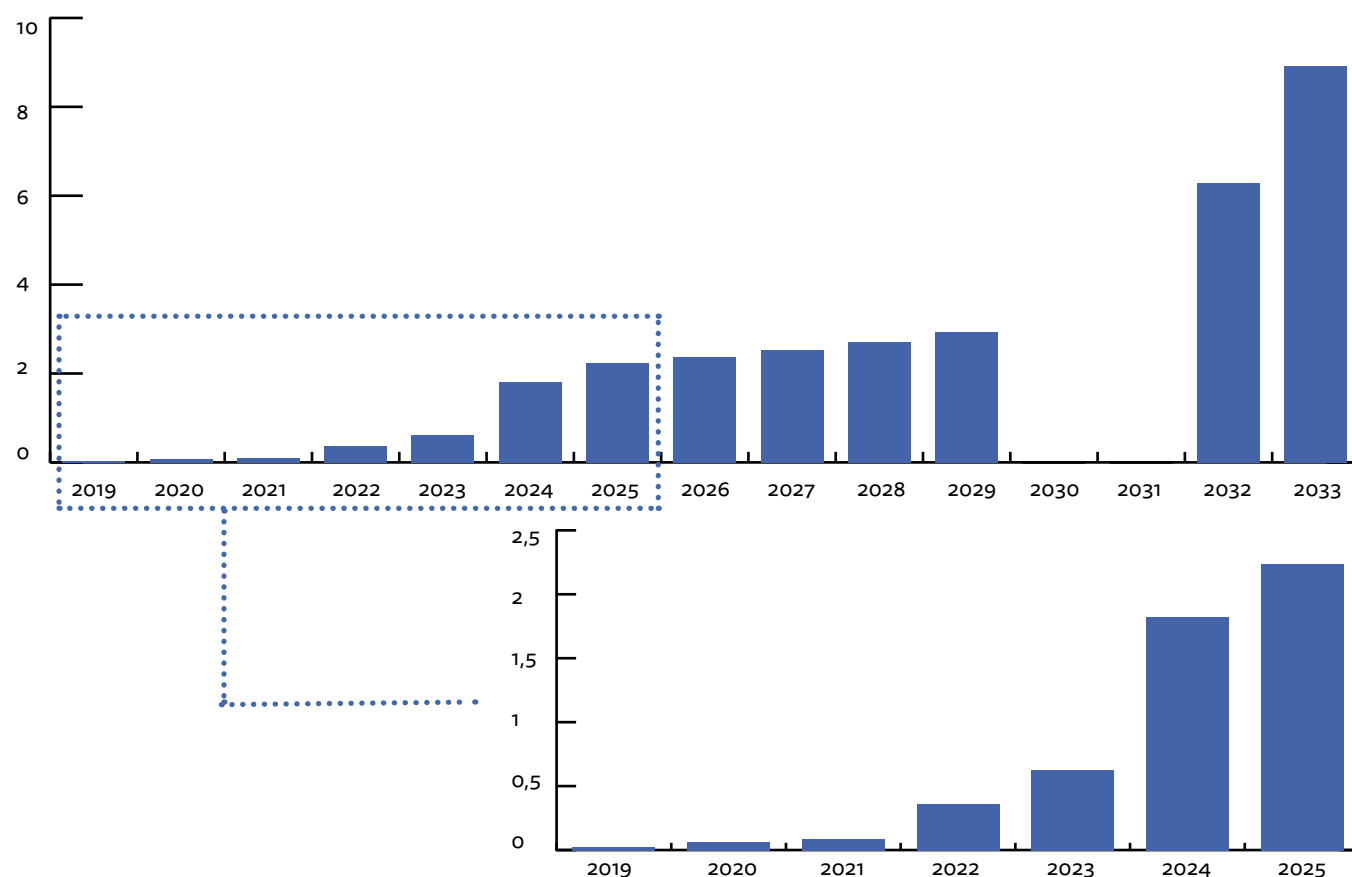


Figure 6-1: Estimated progression of annual data production at ALBA beamlines.

¹⁴⁷ https://research-and-innovation.ec.europa.eu/strategy/strategy-2020-2024/our-digital-future/open-science_en

data management strategy is to ensure that all data are stored, exposed, documented and processed in a way that allows it to be used, shared, stored and transferred easily and efficiently.

At ALBA II, the amount of data generated in the beamlines will increase by several orders of magnitude. The much higher X-ray beam intensity, combined with the hundreds of kHz frame rates attained by the latest detectors, will lead to a data explosion. The ability to process this amount of data has clear implications when defining the ALBA II IT infrastructure capacity. However, this deluge of data has more hidden and far more important aspects than the resizing of the infrastructure. The scientific community and the ALBA II users will not be able to store or process the outcome of the experiments using standard computers. Guaranteeing their scientific success will require providing them with external access to the data and to the High-Performance Computing clusters needed for processing it, and, just as necessary, adequate software applications to exploit these types of infrastructures.

The predicted data explosion also entails the potential fact that future beamlines would have to adapt their capabilities to

the available computing resources. In other words, computing bottlenecks may restrict their full scientific development. To this end, serving the required IT infrastructure and the proper software design must be considered an integral part of any future beamline construction.

However, future challenges are not just due to higher data volumes. Proper metadata ingestion will be necessary for future reuse and completeness of the information. And this will require the design of numerous automated processes to obtain such information during data collection. Consequently, the data structure from the experiments will become inherently more complex. Finally, the completeness of information will allow scientific community to perform data analysis and process data analytics from different data sources. Hence, data pipelines will need to process a greater variety of data sources requiring custom software design to enable it.

A thorough analysis of the computing needs from the data acquisition phase to the scientific community's final processing of the data is necessary to guarantee the scientific success of ALBA II.

6.1. Data Acquisition

At a synchrotron beamline, multiple instruments contribute to adjust the X-ray beam characteristics and ensure its perfect conditions when reaching the sample. The sample environment is complex and highly dependent on the experimental technique. The sample is positioned or rotated accurately, even excited by external stimulus or under a controlled environment. Finally, the detectors are precisely positioned and triggered for data acquisition at the exact timing. A distributed Control System orchestrates all this complex scheme that guarantees the experiment's perfect performance and is responsible for controlling and measuring all these attributes during the experiment which will be crucial for future analysis of the detectors' results.

At ALBA II beamlines, all these processes will be as automated as possible using artificial intelligence algorithms, industrial automation and robotics. The objective is to guarantee the perfect execution of the experiments and, also, to maximize the remote operation of the beamline by the users. The remote operation approach involves fundamental changes in the current internal architecture of the Control Systems. Currently, the interaction with the system is done by ALBA scientific staff using local servers. In the future, non-expert users will benefit from using automated processes and exportable graphical interfaces via web-based technologies. In addition to developing all the software required to execute the data acquisition, developing and implementing automated sample management processes will be used. A central database will track the life cycle of each sample: providing a unique identifier to each, enumerating its characteristics and registering all actions in it until the measurement is completed and the sample is returned to its owner.

Once the experiment is performed, a centralized federated data catalogue will provide a unique Data Object Identifier (DOI) for the measurement. It will include the sample information, the raw data from the detectors and all the relevant metadata from the beamline instrumentation. The scientific data catalogue will be a central part from which all future data processing, data analysis and scientific publications will be linked.

A key election is the format in which the data will be stored. This decision will determine the availability and performance of the data processing tools and their storage efficiency. A desirable goal is to use a standard open format for the majority of the experimental techniques. This would allow the development of common tools for data visualization and ensure the future reusability of the captured data. ALBA II, aligned with the rest of the synchrotron research infrastructures, will boost the usage of the file format HDF5 (Hierarchical Data Format) using Nexus conventions. This format enables compression, effective storage and transfer of large multi-images data files.

Some of the new beamlines at ALBA II will produce vast amounts of data. In some cases, a continuous throughput of tens of gigabytes per second is expected. These rates require the use of specialized storage buffers to ingest them. Since the cost of these systems is very high, they will be tailored to each specific use case.

Sustaining the continuous storage of such a deluge of data has a massive impact on the budget required for the IT infrastructure. Various strategies will, thus, be necessary to reduce such volume. The first obvious option is to run industry-standard lossless algorithms on the fly before writing the data to the disk. Even if this requires specific processing servers, the investment is worth considering the savings it brings in. However, the reduction factor of these systems is far behind what is needed. Two more strategies will be applied to achieve higher factors: The first is implementing lossy algorithms. In practice, lossy algorithms preserve the part of the data that will significantly contribute to the scientific result and discard the rest. These algorithms must be designed and tailored to specific experimental techniques and pre-defined use cases. The last strategy for reducing the amount of data is through validation. Once the data is acquired, automated data analysis pipelines will be executed, showing the experiment's first results. This will allow the scientists to discard irrelevant data for the experiment objective. And, most importantly, it will help to guarantee the scientific success of the experiment and to increase the beam time productivity. In the future, machine learning and deep learning algorithms will enable complex pattern recognition to assist during the data-triage process.

6.2. Data Analysis

Once the automated data processing is finished in the buffer, data will be transferred to a High-Performance Storage system with enough bandwidth to handle the still huge data rates. This process leans on the implementation of a clustered file system.

Data analysis is much more heterogeneous and requires wide scientific knowledge. The end goal is to extract the final findings of the experiment. A High-Performance Computing (HPC) cluster will also run customized data analysis pipelines connected to the clustered file system. These HPC clusters have shown that they can handle massive calculations in a much shorter time than standard servers. Exploiting their inherent capabilities requires designing specific software to distribute their functionality in concurrent processes using multiple CPUs or GPUs. The implementation and development of all these systems require highly experienced computing skills.

These powerful solutions are expensive in terms of budget and time required to optimize new implementations, execute operational maintenance, and control their performance. They must, therefore, be used only when use cases with undoubted benefits arise. A layered-tiered storage system will be created to efficiently tackle all cases. The first level will be the hot High-Performance Storage from which the most complex computing works can be launched. A second, cold, level background storage will follow it at a lower cost. Once the data stored at the hot level is no longer processed, it will be transferred to the cold side. All the data not requiring HPC performance will also be stored there.

Finally, as custodians of the scientific data, ALBA must preserve the data for future needs and enable its re-usability, with a cost-effective solution for long-term data storage. Currently, the cheapest technology available is tape-based solutions. They allow low-cost, long-term data storage with limited bandwidth data transfer. To avoid potential data transfer bottlenecks, the specific moment when data must be moved from the storage to the tape will be carefully selected: just when the probability of needing to retrieve the data back is very low.

The diagram of Figure 6-2 shows the different IT infrastructures that the data will use during its life cycle. In some cases, data processing will have strict timing requirements, for example, during the acquisition or the online data analysis. As a result, suited tailoring of the IT infrastructure will be needed to ensure the required systems availability and optimal performance are served. In other cases, such as during the post-processing, it will extend over weeks. Even occasionally, scientists may need to retrieve the data to reprocess it using the HPC Cluster.

Furthermore, the previous scheme will be repeated in all the running beamlines. In some cases, even with different needs from one day to another within each. Therefore, a centralized, agile architecture of the IT resources will be designed to overcome this challenge. Most modern virtualization, containerization and orchestration techniques will be deployed in critical IT infrastructures. That will also ensure future expansions when new scientific cases emerge with increased computing needs.

All of these processes executed within ALBA facilities will require the deployment of high-speed networks. In addition, certain identified links will be parallelized to handle increased data rates. However, the post-processing of the data will take place long after the departure of our users from the ALBA facility. Nor should we forget the objective of promoting experiments performed remotely. In all these cases, ALBA will provide access to computing services to external users, with far-reaching implications for IT security.

Since many of our users will not have sufficient computing power in their home facility to handle large volumes of data, nor access to the required software to analyse it, the IT infrastructure will extend its services over time to ensure users' scientific success. First, making available a robust and user-friendly way to securely download data. To do so, a high-speed connection to the GEANT network¹⁴⁸ will be used. In addition, ALBA II users will have granted access to a Data Analysis as a Service Platform (DAaaS). It will give them access to the data and metadata available in the federated catalogue and the required IT infrastructure with the appropriate data analysis software.

A solution to overcome the existence of peaks in computing needs will be using Cloud Computing infrastructure. Currently, its cost is decreasing but is still much higher than operating local IT infrastructure. Moreover, cloud costs are not directly assessed because different fees apply to each provider according to the total volume of data stored, data transfer, data processing, security assurance, etc. A smart definition of the different data processes can lead to significant savings. In all cases, the design of services using virtualized architectures will make easier to transfer them to cloud computing infrastructures. Being in the cloud or through local IT infrastructure computing services are costly. A trade-off between providing sufficient computing resources and budget sustainability will necessarily create a Computing quota per experiment. This quota will also be needed for the future EOSC that ALBA II will provide to the scientific community.

¹⁴⁸ <https://network.geant.org>

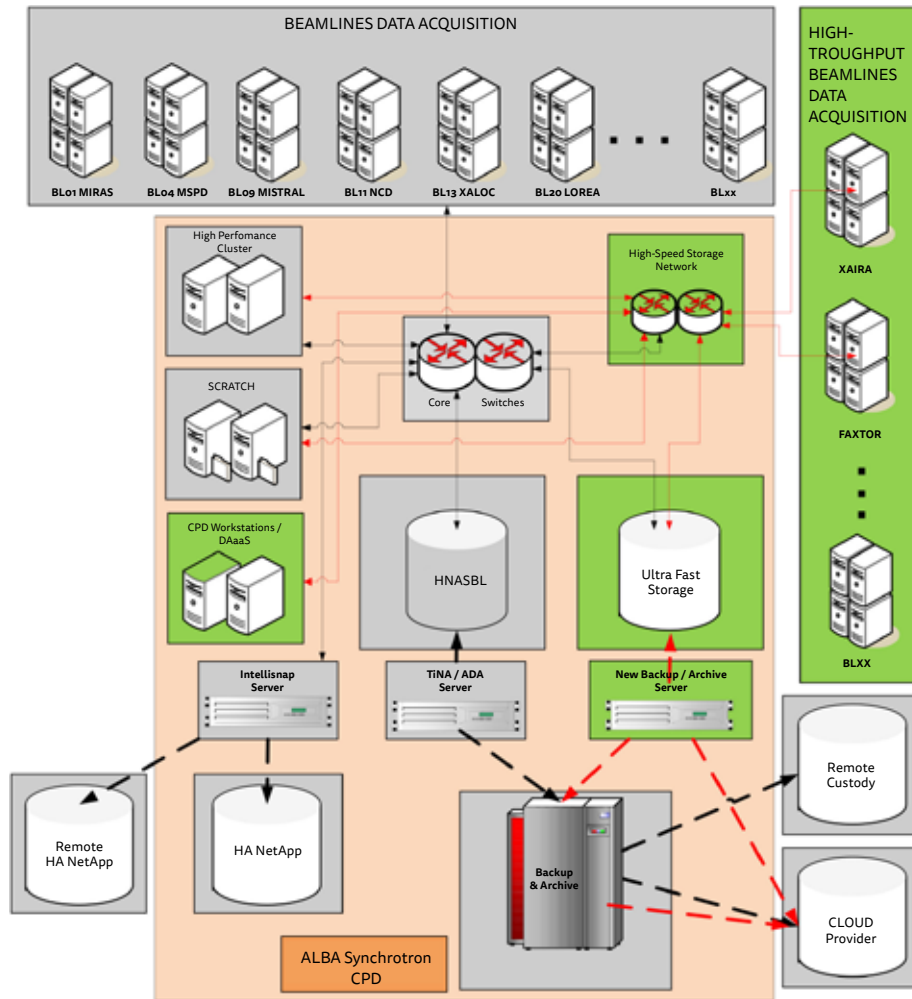


Figure 6-2: Diagram of foreseen IT infrastructures.

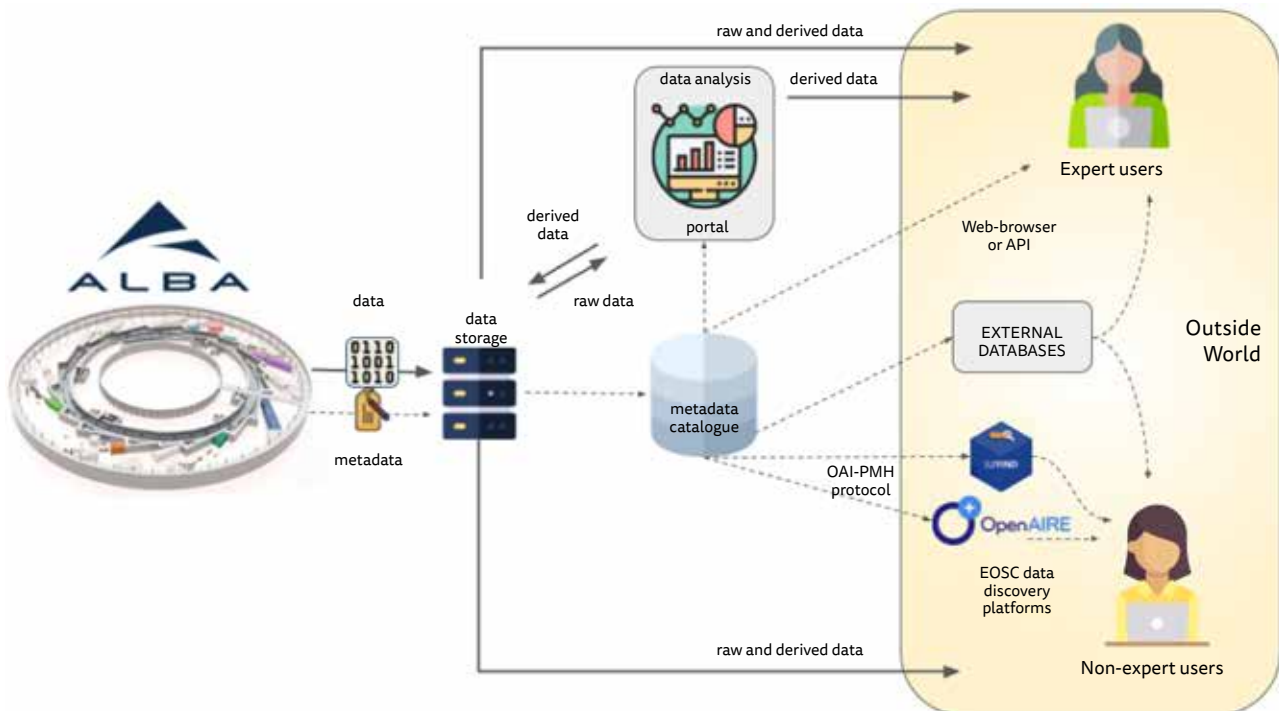


Figure 6-3: Sketch of future ALBA II data service to users.

6.3. Collaborations on data management

The whole scenario outlined requires broad expertise in many areas. Most of them are domain-specific and continuously need to evolve with the latest developments. Sustainability is ensured with synergies involving different players in the research area. Since its foundation, ALBA has built a robust network of collaborations and partnerships with multiple institutes, as for example in scientific instrumentation (IcePAP¹⁴⁹, Em#¹⁵⁰), Distributed controls systems (TANGO¹⁵¹), Data Acquisition and Visualization Building blocks (Sardana¹⁵², Taurus¹⁵³, Silx¹⁵⁴), Complex Data Collection Software (MXCuBE¹⁵⁵), scientific data catalogue and metadata management (ICAT¹⁵⁶), user federation and data service platform (umbrellaID¹⁵⁷, CALIPSOplus JRA2¹⁵⁸,

ExPaNDS¹⁵⁹, PaNOSC¹⁶⁰) or laboratory information management system (ISPyB¹⁶¹). Lastly, multiple contributions to domain-specific data analysis software are shared continuously with the scientific community.

At the same time, some of the future challenges of data management and IT infrastructure are common to other institutes within the national computing research network. In this sense, ALBA is an active member of RedIRIS community and among the few Spanish members of the EOSC Association¹⁶². Moreover, greater synergies will be sought with other computing centres to optimize the use of publicly funded IT infrastructures.

¹⁴⁹ <https://www.esrf.fr/Instrumentation/DetectorsAndElectronics/icepap>

¹⁵⁰ <https://accelconf.web.cern.ch/icalcps2017/papers/tuaplo4.pdf>

¹⁵¹ <https://www.tango-controls.org>

¹⁵² <https://www.sardana-controls.org>

¹⁵³ <https://www.taurus-scada.org>

¹⁵⁴ <http://www.silx.org>

¹⁵⁵ <https://mxcube.github.io/mxcube/>

¹⁵⁶ <https://icatproject.org>

¹⁵⁷ <https://www.umbrellaid.org>

¹⁵⁸ <https://www.calipsoplus.eu/joint-research-activities-jra/jra2-daas/>

¹⁵⁹ <https://expands.eu>

¹⁶⁰ <https://www.panosoc.eu>

¹⁶¹ <https://ispyb.github.io/ISPyB/>

¹⁶² <https://eosoc.eu>

7 Partnerships

A user facility is a composite system where research activities not only coexist with technological developments of cutting-edge instruments, but nurture them with a rich exchange of ideas, needs, and innovative solutions. Such an environment offers opportunities of establishing partnerships between the Research Infrastructure and Research Institutions or Universities, reinforcing their links, sharing resources, and finally being more efficient in solving societal challenges. The evolution of ALBA towards ALBA II foresees a renewed attention to partnering with national and international institutions. Some of the initiatives are already in progress and they are briefly mentioned here, highlighting how they will become a strong net of connections which will make ALBA II and its environment an essential character of the European Research Area.

7.1. Joint Electron Microscopy Center at ALBA (JEMCA)

Electron microscopy is a powerful imaging technique converted, thanks to its recent spectacular evolution, into an essential tool to unveil matter details down to few-nanometer resolution, both for life and material sciences. Its complementarity to synchrotron light experimental techniques makes a synchrotron facility the perfect environment for hosting the microscopes, allowing users to employ different instruments for the same project, with an optimized use of common services, as sample preparation laboratories or data management.

A Microscopy Platform in Catalunya has been funded in 2020, through the use of competitive ERDF grants granted by the Generalitat de Catalunya, and the concerted participation of several institutions. The Platform consists of two centers, one hosted at the Technical Services of the University of Barcelona, and another one, the JEMCA (Joint Electron Microscopy Center at ALBA), hosted at ALBA.

The JEMCA initially includes two microscopes, one dedicated to Life Science and one to Material Science, and has the capacity for other instruments, as well as sample preparation labs and data services.

The life science instrument is owned by the Molecular Biology Institute of Barcelona, IBMB¹⁶³, a research center of the Consejo Superior de Investigaciones Científicas (CSIC)¹⁶³, with contributions from the Institute for Research in Biomedicine (IRB)¹⁶⁴, the Center for Genomic Regulation, CRG¹⁶⁵, and the Universitat Autònoma de Barcelona, UAB¹⁶⁶. It consists of a 200-kV electron cryo-microscope for biological applications, which allows to observe the structure of biomolecules at atomic scale without the need to crystallize them. It is a microscope for the screening of biological samples and for obtaining structural data at the atomic level of large molecular and cellular complexes, for example the external structure of coronavirus, as responsible for the COVID-19 pandemic, or of the receptors it uses to enter cells. The microscope is hosting users since September 2022.

The material science instrument is owned by the Catalan Institute of Nanoscience and Nanotechnology, ICN2¹⁶⁷, with the contributions of the CSIC, the Institute of Materials Science of Barcelona, ICMA-B-CSIC¹⁶⁷, and the UAB. It consists of a Transmission Electron Microscope, 300 kV with Monochromatic Aberration Correctors, dedicated to material science, now in commissioning in the JEMCA, expecting users during 2023. It is complemented by a Focused Ion Beam (FIB) equipment to cut samples into very thin sheets and study them with atomic resolution, installed at ICN2.

¹⁶³ <https://www.csic.es/>

¹⁶⁴ <https://www.irbbarcelona.org/es>

¹⁶⁵ <https://www.crg.eu/>

¹⁶⁶ <https://www.uab.cat/>

¹⁶⁷ <https://www.icmab.es/>

7.2. In-CAEM

The *Complementary Plans* is a program designed by the Ministry of Science and Innovation in coordination with the different regional governments, aimed at establishing collaborations within the Spanish Autonomous Communities (CCAA) in R&D&I actions that have common objectives based on interests reflected in the state and regional Smart Specialization Strategy (RIS3)¹⁶⁸.

With the purpose of building territorial synergies, the Complementary Plans contemplate the participation of several CCAA in each of eight thematic programs, with the possibility of participating in several of them. Each program is partly funded by Next Generation Funds and partly by the regional Governments.

ALBA is participating as coordinator of the Catalan contribution to the program on Advanced Materials. In this program there is the contribution of eight CCAA: Aragón, Castilla y León, Castilla la Mancha, Cataluña, Madrid, Navarra, País Vasco and Comunidad Valenciana, this last acting a coordinator of the full program. The program aims at integrating and promoting research and innovation in Advanced Materials in these regions, supporting scientific leadership in strategic lines and enhancing collaborations. The use of unique capacities and infrastructures, together with the possible participation of companies is part of the program, which will have a duration of 3 years, with co-financing commitments and co-governance mechanisms, promoting territorial economic transformation.

The program foresees the development of a facility dedicated to research in the field of advanced materials to address the scientific challenges of the European Green Deal and to help promote a more sustainable European Union economy.

The In-situ Correlative installation for Advanced Materials for Energy (In-CAEM) will allow in-situ correlative experiments, combining (S)TEM (Scanning Transmission Electron Microscope), AFM/STM (Atomic Force Microscope / Scanning Tunnel Microscope) instrumentation with synchrotron radiation at different beamlines of the ALBA Synchrotron. In-CAEM is also the evolution of the JEMCA (see 7.1).

In-CAEM is foreseen as a key tool to meet the challenges of advanced characterization, down to the atomic scale, of new materials analyzed under conditions of work in-situ and in operating mode, under certain conditions in gaseous or liquid media. It is a unique opportunity in the research landscape in Spain and puts this facility among the most advanced poles in Europe in the field of development for sustainable energy and other fields of materials science. The complementarity between the new instruments and the already existing ALBA beamlines will be further developed with the new ALBA II beamlines.

The main collaborators of the In-CAEM are the ICN2, ICMAB, the Institute of High Energy Physics, IFAE¹⁶⁹, UAB and the Technological Center Eurecat¹⁷⁰.

The infrastructure will be set-up before the end of 2025. Its usage envisages open and competitive access, plus dedicated time to specific collaborations, nurtured by the whole program on Advanced Materials of the Planes Complementarios.

¹⁶⁸ <https://www.ciencia.gob.es/home/Estrategias-y-Planes/Plan-de-Recuperacion-Transformacion-y-Resiliencia-PRTR/Planes-complementarios-con-CCAA;jsessionid=6F2731C4ECD8DA056A7A96167F66C56A.1>

¹⁶⁹ <http://www.ifae.es/eng/>

¹⁷⁰ <https://eurecat.org/es/>

7.3. Battery and catalysis laboratories (BATTlab, CATlab)

As thoroughly explained in the document, the evolution of the synchrotron facility towards analyzing always more complex systems, more numerous (*high throughput*), and in real conditions (*In situ, Operando*), is highly visible in battery- and catalysis-oriented research lines, nowadays subject of intense support by governmental agencies and/or industries and strategic research lines at ALBA.

Within this context, more attention is put in sample preparation, characterization and conditioning before running synchrotron experiments, possibly to be conducted in ALBA premises with no need of supporting travel or shipment, and ultimately tested offline using the same equipment as installed on synchrotron beamline.

The battery case is a perfect example of this evolution. In view of so-called *Operando* experiments, electrochemical cells (batteries) have to be freshly prepared in order to minimize negative side effects (e.g. self-discharge, shortcuts, time instability...) which could hamper the success of the experiment. Chemical contents of most batteries are hazardous and/or air sensitive materials subject to restrictive transport conditions and requiring very strict storing regimes. Finally, ancillary equipment and sample environment used for running synchrotron experiments are often specific to ALBA, either because developed in-house or to be modified, and not accessible to users at their home institutes.

A Battery Laboratory (BATTlab) has been realized thanks to the collaboration with ICMAB, and its successful application in early 2021 to a CSIC grant call which allowed acquisition of equipment to

be used in battery research field. The battery laboratory includes equipment to prepare cells (Glove box, crimping tools for coin cells preparation, pouch cells press, balance, ...) and characterize them offline (16 channels potentiostat). ALBA has built the infrastructure (room, fume hoods, benches, gas distribution lines) and is in charge of the organization of the user access. The laboratory will be open to all ALBA users as well for long stay researchers (PhD, PostDoc), and is scheduled to be available in spring 2023.

Similar to what has been realized for the battery field, it is foreseen building an equivalent catalysis laboratory (CATlab) which will allow ALBA users to practice either brought equipment or In House designed and built sample environment, prior to effective synchrotron experiment.

This one is built in collaboration with the Institute of Chemical Technology, ITQ¹⁷¹, who was also granted by CSIC for the equipment to be installed. Also, other interested institutes are encouraged to contribute.

Both BATTlab and CATlab projects evidence the necessity of strong collaboration between ALBA and external users, the latter having the valuable expertise in "home laboratory" practices that ALBA staff might not necessarily have since essentially focused on synchrotron radiation instrumentation.

Both projects appear as model for ALBA II for which contribution by ideas and resource of all institutes in Spain and abroad will be vital for maintaining the highest scientific and technical level.

¹⁷¹ <https://itq.upv-csic.es/>

7.4. Future opportunities: ASTIP

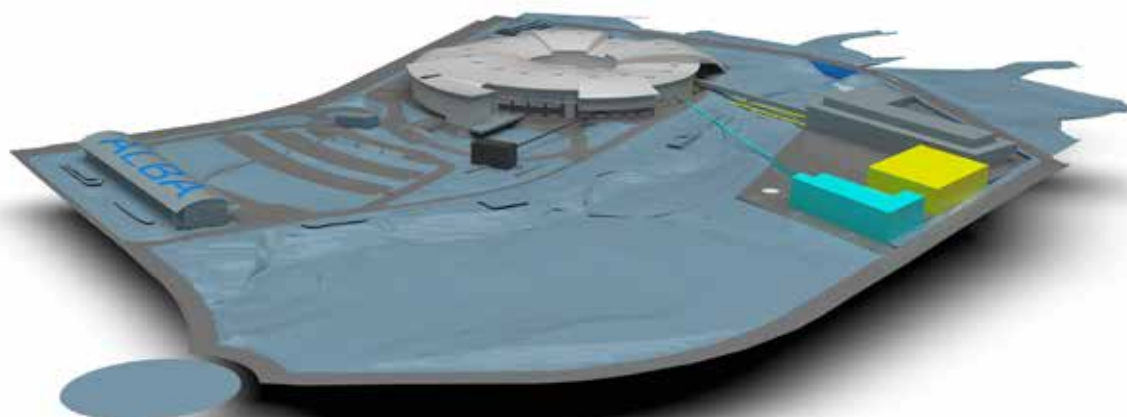


Figure 7-1: ALBA II and ASTIP preliminary layout. The four long beamlines paths are sketched for showing all the future possibilities.

The proposal of developing a new scientific and technological center in the vicinity of ALBA aims at activating the evolution from the original synchrotron facility to a center of excellence for synchrotron radiation science with enhanced capacities in research and innovation.

ALBA Science, Technology and Innovation Park purpose is the establishment of an ecosystem where scientific research, technology development and industrial innovation are integrated to create a resilient, resource-efficient and competitive environment focused on green energy, digital transition and health. ASTIP would nucleate around the ALBA Synchrotron and its upgrading to ALBA II, enclosing the key actors involved in the innovation value chain located in the Barcelona area, including several leading research institutions, the UAB and the EURECAT technology center.

ASTIP is thought as an interdisciplinary innovation hub that blends a unique combination of imaging and characterization tools for complex materials and for biological systems, material growth and detector and device fabrication facilities, big-data and data-mining capabilities with innovation driving synergies. ASTIP shall not only spearhead its own research programs, but shall provide various user modes tailored to, and accessible for, the experienced and early-career scientific researcher and, at the same time, the innovating developer. It will be a portal of access for the industry to these singular scientific and technological capabilities, accelerating knowledge-based innovation and targeting the local and national industrial ecosystem.

ASTIP can be located in a new complex adjacent to the ALBA Synchrotron (see Figure 7-1), within the Parc de l'Alba¹⁷² and has the support of ALBA Synchrotron, of the UAB with its departments

and institutes, of the Cerdanyola del Vallès City Council and of the institutions with which the participant centers are associated, in particular CSIC, CERCA¹⁷³ and BIST. The initial list of research institutions includes IBMB, ICMB, ICN², UAB, CSIC, CNM, and IFAE, which includes the PIC¹⁷⁴. ASTIP is meant to be inclusive and open to more national and international institutes who can profit from the proximity of the research environment to a large research infrastructure.

The original ASTIP proposal includes three new centers and the new ALBA II beamlines which enhance ASTIP scientific reach. The centers are the Complex Materials and Technologies Center (COMTEC), the Advanced Multiscale Bio Imaging Center (AMBIC), and the Innovation Hub (SYNDUSTRY, Synchrotron light-based R&D towards new industrial applications). Combining the optimization of already existing resources with state-of-the-art instrumentation fully profiting of the enhanced properties of the synchrotron, will make this center almost unique worldwide. One example is the fully integrated biosafety level-3 environment connected to one of the new beamlines, enclosing the imaging and sample preparation instrumentations and a strong data-driven bio-computational: it will allow *in-situ* infection studies, essential to understand all steps of the infection pathway and will provide insights in the pathological changes of cells, tissues and even organs, empowering clinical researchers for a fast response to health threats or crises. The evolution of this original proposal is presently on-going.

The center will exploit existing local and urban infrastructures and boost the research and training vocation of Cerdanyola del Vallès to a new level and will include a large auditorium and a guest house. ASTIP possible construction schedule and costs are not included in this document.

¹⁷² <https://www.parcdelalba.cat/>

¹⁷³ <https://cerca.cat/>

¹⁷⁴ <https://www.pic.es/>

7.5. LEAPS

LEAPS – the League of European Accelerator-based Photon Sources² is a strategic consortium initiated by the Directors of the Synchrotron Radiation and Free Electron Laser user facilities in Europe in 2017. Its primary goal is to actively and constructively ensure and promote the quality and impact of fundamental, applied and industrial research carried out at each facility to the greater benefit of European science and society.

ALBA has been actively participating to LEAPS development since its inception, including chairing the League in 2020 and 2021.

During the years of the COVID-19 pandemic, the relevance of this new research consortium has become particularly visible, as all LEAPS facilities made available their experimental stations to virologists and hospitals for precision structural analyses. Among the future challenges we will have to solve in Europe, combatting vexing diseases and climate change will remain predominant issues.

The unique analytical capabilities at LEAPS facilities in the molecular design of drugs and vaccines as well as of new materials for future carbon-free energy systems and for a future circular economy will therefore be of paramount European, even global importance.

The European Strategy for Accelerator-based Photon Sources (ESAPS 2022²³) is a coherent plan addressing the future challenges and needs of the new era in research and innovation, designed to put Europe in a global leadership position in this important technology of the future. It encompasses:

- the expansion of service provision to speed-up emerging research for societal challenges enabling new strategic long-term cooperation with European Partnerships (also increasing resilience)
- the coordinated upgrade of synchrotron radiation facilities implementing a disruptive high-brilliance electron lattice
- continuous development of FELs
- joining forces to enhance facility operation by implementing new digital technologies (an inclusive coordinated development of key enabling (AI-assisted) technologies will integrate all European stakeholders from academia and industry)

ALBA II will be fully embedded in the European landscape, maintaining the relevance within the Spanish and the European communities, as a motor of the Spanish Research and Innovation Area.



Figure 7-2: LEAPS scheme, highlighting its members.



Environmental sustainability



8.1. General framework

The aims of the Research and Innovation for the European Green Deal¹⁷⁵ are well reflected in ALBA II science case, and in parallel they are contemplated in the general environmental sustainability framework for ALBA II. The related Horizon Europe mission of fostering new technologies for sustainable and disruptive innovations, and spreading successful new solutions across Europe and the world is inherent to ALBA II strategies and operation.

ALBA II will be first of all an enabler and deployer of Research and Innovation **contributing to environmental sustainability**, as already explained in the chapter dedicated to the Science case and in the Industry dissemination and sectorial strategies, and will also be an **ambassador for environmental and social responsibility** and awareness, in its internal and external communication plans.

ALBA II will be designed, implemented and operated in such a way that the **environmental impact is reduced to the minimum**. We distinguish two types of impacts, the one produced by the construction of the new facility, and the difference in impact between the present and the future operation of the facility.

During its design and construction, ALBA II, **as responsible procurer**, will put attention in environmentally sustainable procurement strategies and criteria and innovative procurement strategies to contribute to enhanced relevant technologies with sight on footprint and impact reduction. This will take place at the highest level by contributing to the definition of buildings (number and height of buildings, grouping of different functions in the same building...) and services (parking, logistics, waste management), while at a lower level with specific requirements on call for tenders or detailed specifications of the constructive design.

Furthermore, **as responsible consumer**, will develop strategies for Energy Efficiency and sustainable energy generation, for the responsible use of materials and resources, and for sustainable mobility.

The resulting impact in terms of use of environmental resources should be brought into balance with the societal and environmental advances generated directly or indirectly by operating and developing ALBA II. Also, the European Commission's strategies and targets are important elements to be considered.

ALBA II will count on internal structures empowered to assume and coordinate these different strategies. A detailed gap analysis will be made which will identify areas in which to focus the sustainability efforts in the mid and long term as well as in relation to the ALBA II infrastructure development.

¹⁷⁵ https://ec.europa.eu/clima/eu-action/climate-strategies-targets/2030-climate-energy-framework_en

8.2. Infrastructure development

Environmental sustainability will be incorporated in the ALBA II design and construction at different levels.

In order to minimize the impact produced by the new constructions of ALBA II, the first step is to take consciousness about the environment surrounding the existing facility.

The experimental hall of ALBA II will be extended to a new building in the new plot of land nearby the plot of land where ALBA sits nowadays. Between these two plots of land, there is a little stream bordered by rich vegetation. This green path is a natural track for wild animals to move around a not fully urbanized area between a highway and the Collserola hills at the west side of Barcelona City. The design of ALBA II will include the three long vacuum chambers crossing this green path, part of the long beamlines. A very low impact approach will be adopted, by running just the minimal structure over the little river (just the vacuum chamber itself). The outer skin of the chamber will be made of stainless steel to protect environment from the lead shield required for radiological protection.

Among many others, the following list points out some of the foreseen complementary specifications/requirements directly derived from the sustainability approach:

In the design phase:

- Use of sustainable construction materials (recycled materials or carbon-neutrally manufactured)
- Efficient heating, cooling and ventilation systems.
- Water-saving plumbing fixtures.
- Windows placed strategically to maximize natural light.
- Energy-efficient lighting fixtures and appliances (full LED).
- Rainwater harvesting.
- Greywater reuse.
- Landscaping with native vegetation.
- Green-like roofs where possible (by storing and delaying rainwater drainage) to improve cooling in summer.

In the tendering and construction phases:

- Include sustainability as a technical criterion in the public tenders
- Treatment of waste and debris during the construction
- Impact on surrounding environment during the construction
- Use of local construction materials to reduce transportation distance and costs.

In addition, a thoughtful radiological characterisation of all the machine elements that will be dismantled during the ALBA Storage Ring deinstallation phase will be carried out, and where needed actions will be taken to ensure a safe decommissioning.

8.3. Energy Efficiency and Sustainability

Dwindling resources together with rising energy costs and climate change are challenges faced by all the next generation research infrastructures.

Although the enhanced performance of ALBA II will not come with significant increase on power consumption, the expansion of the experimental hall to a new building in nearby plots of land will carry some unavoidable energy consumption increase that will be kept below the initially installed electrical power supply at the ALBA site, meaning that for ALBA II the electrical capacity is already in place, as well as most of the energy-related existing technical installations.

At ALBA we aim for sustainable development and we will rely on mid and long-term strategies for reliable, affordable and carbon-neutral energy supplies and for this reason, we will identify the challenges, best practices and policies to develop and implement sustainable solutions at our infrastructure. This includes the increase of energy efficiencies, energy system optimizations, storage and savings, implementation and management issues as well as the review of challenges represented by potential future technological solutions and the tools for effective collaboration with other similar facilities. The following aspects will be thoroughly revised during the detailed design phase of ALBA II aiming at developing new solutions for efficiency maximization:

- Energy management
- Sustainability of equipment, materials and resources
- Energy-efficient technologies
- Energy-efficient technology research

More specifically, the design of ALBA II includes:

- Generation of photovoltaic energy. ALBA II will consider the use of its own photovoltaic generation where possible. This technology will be considered in connection with our goal to make mobility more sustainable. There are plans to install photovoltaic roofs on the car parking as well as on the roof of the technical buildings with which to supply electric or PHEV cars and partially the energy required in the office building. Furthermore, there are already existing plans towards the full electrification of our little fleet of vehicles (and the complete elimination of diesel trucks and vans).
- Construction of new thermal energy storage facilities closer to the consumption points.
- Cold water used by ALBA comes from a thermal store located about 800 m away from the facility. The new design will study the benefit of having several smaller local storage facilities much closer to the consumption points. These new storages would be also more efficient by taking advantage, if possible,

of the excess of thermal (cold) energy coming from the existing cryogenic network (mostly liquid nitrogen storage and distribution).

Other aspects are also being considered, as for example the reuse of hot water coming from the accelerators de-ionized water-cooling circuit to improve heating efficiency for the whole facility.

Concerning Energy Efficiency, the original ALBA approach is already very efficient. The use of a co-generation plant provides fully transformed thermal energy at a low cost. This thermal energy is a secondary product of electricity generation, making optimal exploitation of the potential energy of the natural gas used as fuel. For ALBA II, this efficiency shall be traded-off with the carbon print. The right mix between co-generation (and its associated efficiency for a high thermal energy consumer like ALBA) and carbon-neutral sources, shall be found. This mix would be not constant along time but could evolve together with the energy market.

Concerning carbon-neutral sources, a thorough study about the different possibilities will be included in the design phase of ALBA II. The first attempt would be to reach carbon-neutral sources (by tendering the purchase of energy for suppliers able to certificate the carbon-neutral origin of the energy they supply) but more ambitious strategies could also be considered in the future.

During the first years of operation of ALBA II, we would envisage the parallel use of co-generation and of carbon neutral certified energy with the aim to move to 100% renewable energy in the future.

The difference of the impact produced by the operation of the extended facility will be also minimal. ALBA II, just like ALBA, will be quiet, will produce almost no direct emissions and will produce no debris or waste coming from its normal operation.

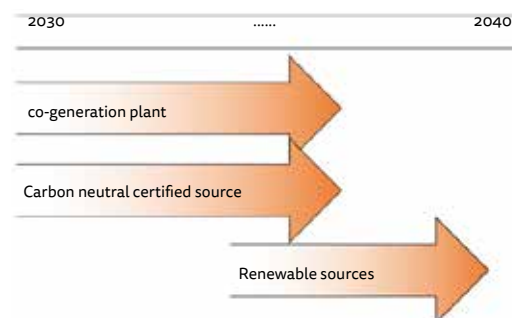


Figure 8-1: Sketch of energy efficiency evolution.

8.4. Impact on environment

ALBA II will be designed and implemented in such a way that the environmental impact is reduced to the minimum. We distinguish two types of impacts, the one produced by the construction of the new facility, and the difference in impact between the present and the future operation of the facility.

In order to minimize the impact produced by the new constructions of ALBA II, the first step is to take consciousness about the environment surrounding the existing facility.

The experimental hall of ALBA II will be extended to a new building in a new plot of land nearby the plot of land where ALBA sits nowadays. Between these two plots of land, there is a little stream bordered by rich vegetation. This green path is a natural track for wild animals to move around a not fully urbanized area

between a highway and the Collserola hills at the west side of Barcelona City. The design of ALBA II will include three long vacuum chambers crossing this green path (almost orthogonally) to connect the photon sources (in the main existing building) with the end stations (in the new experimental hall to be built). A very low impact approach will be adopted, by running just the minimal structure over the little river (just the vacuum chamber itself). The outer skin of the chamber will be made of stainless steel to protect environment from the lead shield required for radiological protection.

The difference of the impact produced by the operation of the extended facility will be also minimal. ALBA II, just like ALBA, will be quiet, will produce almost no direct emissions and will produce no debris or waste coming from its normal operation.

9

Project management

ALBA II is developed in parallel with the operation of the present ALBA facility, and with the upgrade of the existing beamlines and construction of new ones. The project management considers this interplay by optimizing the organization of the human resources and of the budget of the institution.

9.1. Organization

The organization for ALBA II is based on the methodology that has been successfully applied at ALBA for the design and construction of every new beamline. Following this previous experience, the ALBA II has been divided into 5 main programs, which are sub-divided into projects, these further sub-divided into work packages (WPs). For each WP a WP Leader is appointed. Each program has a coordinator and each project has a project manager. This organization benefits from a matrix organizational structure in which the work package leader and staff associated to a given

work package report hierarchically to one division while working on a project which is under the umbrella of another division.

The ALBA II project management is assisted by the Coordination Office on matters concerning scheduling, change management, budget control and documentation. The organization structure for ALBA II is shown in Figure 9-1. The project status will be regularly reported to the Advisory bodies, as well as to the representatives of the funding institutions.

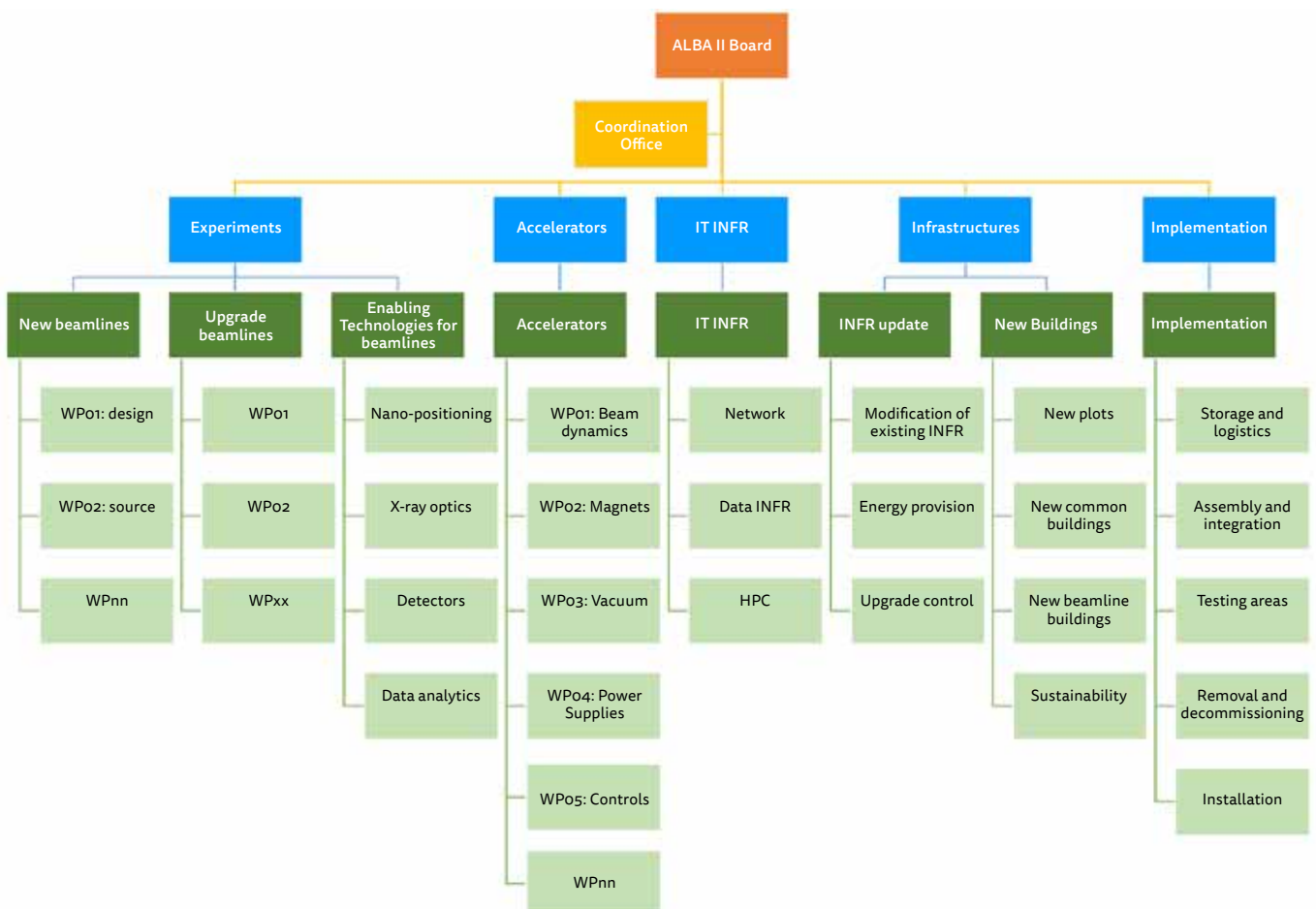


Figure 9-1: ALBA II Organization Structure.

9.2. Cost

The definition of the ALBA II project cost is of course linked to the overall cost of the operation and development of the facility for the coming years. A detailed financial plan for the period 2024-2038 is currently under assessment by ALBA funding bodies, and is expected to be approved along 2023.

We consider that ALBA II cost is the difference between the total budget that would be needed in the absence of the upgrade (ALBA operation and staff, 40 M€ for maintenance and/or renovation of obsolescent systems, construction of three more beamlines inside the present experimental hall) and the budget which include the ALBA II upgrade, integrated from now to the ALBA II operation start-up. This difference has been estimated as 130 M€.

In particular:

- The accelerator upgrade, including the refurbishing of the civil and technical infrastructure, and the dismantling and installation processes, has been estimated as 88 M€ (would be 10 M€ without the upgrade).
- 7 M€ for extra staff dedicated to the design and construction of the upgrade, part of which may be reused after the start-up for the continuation of the future ALBA II developments.
- The construction of two long beamlines, with their infrastructures and the buildings required to host the corresponding end stations, plus one short beamline, and the modification of the MSPD beamline amounts to 57 M€ including new personnel during construction phase.

- 80 M€ for the specific upgrade program of the existing beamlines and laboratories, which includes the required upgrade on the optics, detectors and, in some cases, the photon sources, as well as the fact that after running for 20 years some part of the beamline instrumentation needs to be replaced (equal with no upgrade program).
- 10 M€ for the necessary facility and lab extensions to the new plots.
- 16 M€ for the new plots (already assigned)

The proposed model for upgrading ALBA into ALBA II is a **high cost-effective model**, as the cost of transforming ALBA into ALBA II, 130 M€, represents only a 20% increase with respect to the cost of operating ALBA as a 3rd generation light source between 2023-2032 and adding three beamlines to our beamlines portfolio.

The development of further beamlines is planned to continue after the dark period to bring the facility to the maximum number of possible beamlines, the necessary resources not being included here.

9.3. Staff

Staff resources will be shared between the operation of ALBA and the ALBA II project. It is expected that the staff of ALBA will increase by about 70 FTE in the next decade. Figure 9-2 shows the expected ALBA staff evolution which covers both the upgrade and also the natural growth of the facility as the number of beamlines and services offered to the scientific community increases. There is an increase in the years dedicated to design and construction, then almost constant during the dark period, and then again a smooth increase corresponding to the operation with a larger number of beamlines. External experienced technical support will be added during the dark period for the testing of components and the removal and installation of the new accelerator, like has been done at other facilities.

Staff for operation and development

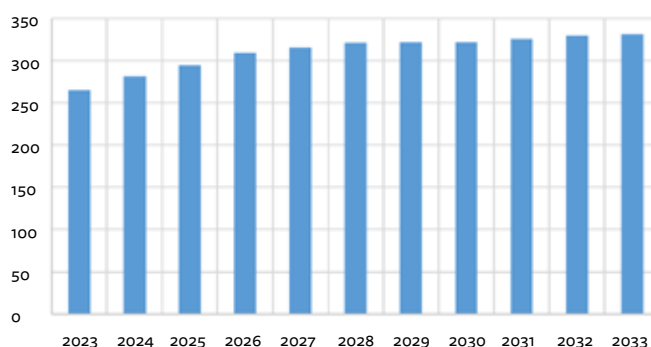


Figure 9-2: shows the ALBA staff evolution from 2023 to 2033.

9.4. Timeline

ALBA II will be developed in parallel with the operation of the present ALBA facility. The project spans from 2021 to 2031 and includes the full upgrade of the Storage Ring, selected upgrades on the operating beamlines, three new beamlines and the necessary upgrades on the infrastructure. The project is divided in several phases, which are different for the beamlines and for the accelerator, hereby shortly described.

9.4.1. TIMELINE FOR STORAGE RING UPGRADE

The Technical Design Report will be prepared between 2023 and 2025, and the procurement of the new storage ring will start in 2026. ALBA staff will produce reference designs and

procurement specifications but no detailed designs which will be produced by the manufacturers. The construction of the different parts and the pre-installation of the Storage Ring girders should finish in 2029, to proceed in 2030 with the installation into the tunnel and in 2031 with the commissioning, aiming at having first users within 2031.

9.4.2. TIMELINE FOR THE BEAMLINES

The definition of the new beamlines for ALBA II started with a first phase in 2021: a call for proposals for projects of beamlines to be built inside the present experimental hall gave as result the selection in Spring 2022 of the 3Sbar beamline, which is funded through NGEU funds and that shall be completed by 2025. Its design is fully optimized for ALBA II, even if it will enter into

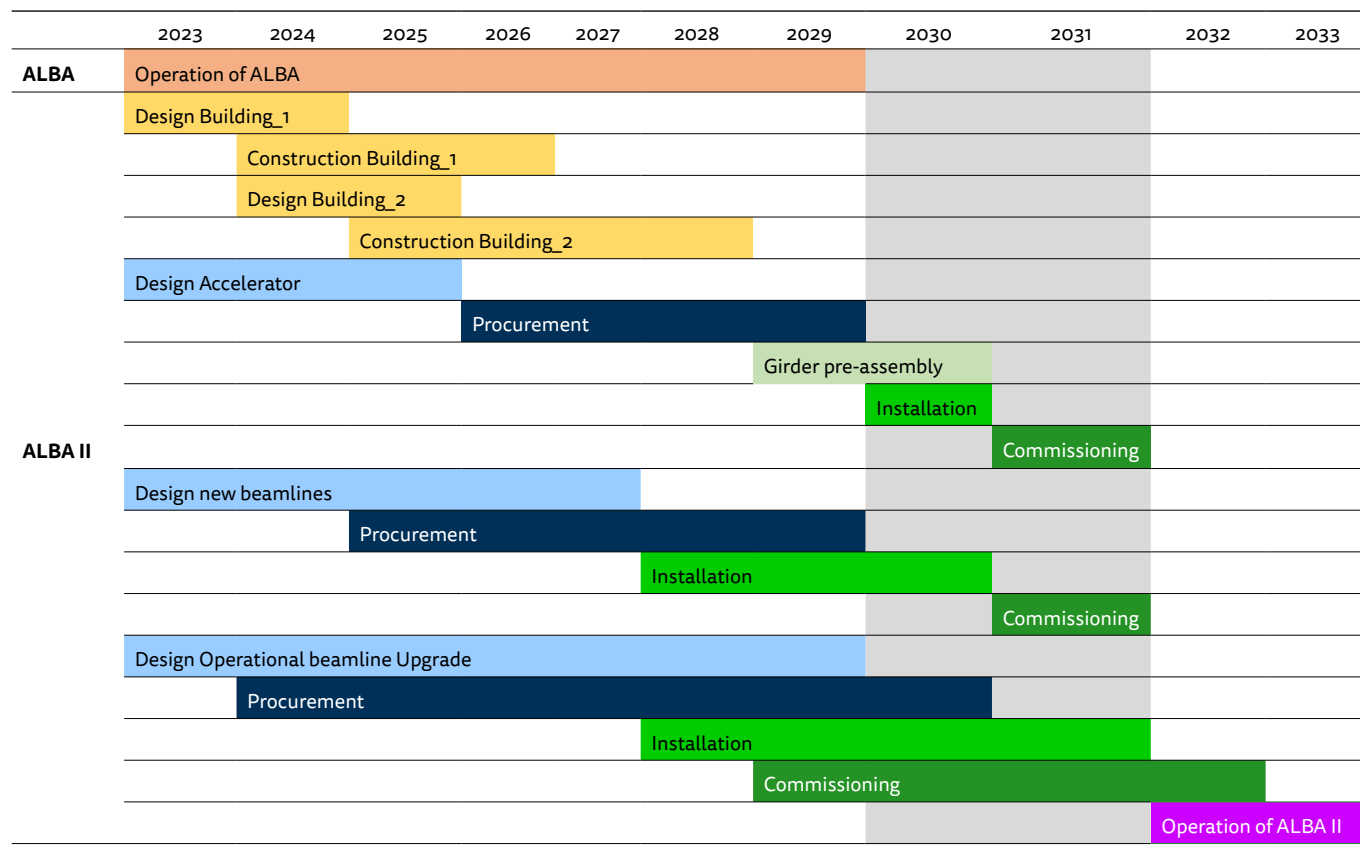


Figure 9-3: ALBA II Timeline.

operation in ALBA, before the shutdown. A second beamline project, CALIMA, dedicated to BioSAXS, has been also chosen and could be started as soon as the funding is available.

A new call for long beamline preproposals has been launched in Autumn 2022, aiming at choosing by mid-2023 the projects whose construction will start in time for being in operation together with ALBA II.

The Gantt Chart in figure 9-3 shows ALBA II timeline.

During the dark period the next beamline construction phase for 5 more Beamlines (until a portfolio of 22 beamlines in 2037) shall be started taking advantage of the well-established project management structures and a significant part of the personnel resources created during ALBA II. This synergy effect will make the mentioned following construction phase particularly efficient.

9.4. Milestone Plan and risk analysis

TABLE 9-1: MILESTONE PLAN AND ASSOCIATED RISKS

MILESTONE	MILESTONE TYPE	INDICATOR	FORESEEN DATE	RISK	PRELIMINARY MITIGATION PLAN ^{a)}
MS-0: Approval of the ALBA II Program	Directive	Agreement of the Governing Bodies of CELLS	16/12/2020 (CR-40)	No risk, already achieved.	
MS-1: Approval of final financial plan for ALBA II	Financial	Agreements signed with funding Administrations	2023	Budget constraints.	Detailed cost planning and justification of necessity and suitability of each cost item.
MS-2: White Paper			Q2/2023		
MS-3: Technical Design Report	Technical	TDR documentation	Q1/2025	Lack of resources. Unforeseen technical challenges	Close follow up by ALBA II Board
MS-4 End of user operation and start of dark period	Technical	Reception of all hardware and compliance with technical specifications	Q4/2029	Lack of resources, for hardware procurement follow up. Longer deliveries.	Close follow up during the construction phase
MS-5 Start of accelerator commissioning	Technical	All hardware installed	Q4/2031	Complex installation	Well defined implementation Plan
MS-6 Start of beamlines commissioning	Technical	Compliance with accelerators specifications	Q3/2031	Storage Ring commissioning longer than expected, not achieving specifications	Well defined commissioning plan with realistic day one achievements
MS-7 Start of user operation	Technical	Compliance with beamlines specifications	Q2/2032	Beamlines commissioning longer than expected, not achieving specifications	Well defined technical requirements for day one operation

^{a)} Detailed mitigation plans will be developed by the project management teams

TABLE 9-2: IDENTIFICATION OF GENERAL RISKS

RISK	DESCRIPTION	MONITORING	PRELIMINARY MITIGATION PLAN ^{b)}
Technical	Design problems or failures require unforeseen review or modification of work plans	Through Project Management structure, methodology and documentation.	Close follow up by MAC/SAC, and specific internal and external review committees
Schedule / Timeline	Deviation from the foreseen schedule or timeline	Through Project Management structure, methodology and documentation.	Continuous follow up of schedule
Budget	Missed budget targets due to uncertainties on the cost estimates	Coordination office and Administration monitor budget execution, staff- procurement forecasts on monthly basis.	Agile planning of priorities and contingencies.
Safety	Construction of new infrastructures with the participation of several external companies adds safety issues to those already present in normal operation.	ALBA Own Safety Service monitor all safety aspects and procedures during the design and during the construction phases	Reinforcement of follow-up, of training, including external resources where needed
Staff and recruitment	Difficulties in retaining and/or recruiting qualified personnel	Through contracting plans, selection process documentation and current staff lists and statistics.	Continuous internal and external communication actions. Continuous development of personnel policies.
Conjunctural / Macro economic	Macroeconomic factors affect the ALBA II program resulting in the materialization of one or several of the above risks.	General monitorization of the closer and wider economic context of ALBA, in close collaboration with the funding administrations.	Through the before mentioned mitigation plans.

^{b)} Detailed mitigation plans will be developed by the project management teams. They shall also assess the impact of the concrete risks, when they occur.

10 Economic and Social Impact of ALBA II

In 2003, when ALBA was approved, an economic and social impact assessment study for the infrastructure was commissioned to Jose García Montalvo and Josep Ma. Raya from the Pompeu Fabra University²¹. The same expert group was commissioned to perform a follow up study in 2010, just before the start of the operation²², and in 2022 the same analysis for ALBA II has been charged to the same team. This chapter has been written in collaboration with Jose García Montalvo and Josep Ma. Raya and a more extended description of the study can be found in the Annex A. The objective of the present study is to make an approximation to the economic impact (in terms of production, Gross Value Added (GVA) and employment), to the social impact of the investment that will represent transforming ALBA into ALBA II, and assessing aspects such as the effects of ALBA II on research and training.

All the analysis is applied to the 2023-2055 period which covers the period in which the investment and the start-up of ALBA II will take place and covers as well an approximate period of 25 years of ALBA II operation. Given the distribution of incomes and costs, increasing the time horizon implies increasing the profitability of the investment.

10.1. Economic impact

The methodology adopted to calculate the economic impact is the input-output model. The economic impact is considered in three magnitudes: production, added value and employment. For each magnitude a social accounting matrix is used to separately calculate the direct, indirect and induced impacts. The same multipliers, ratio of the sum of the direct, indirect and induced economic effects to the direct economic effects, calculated in 2010 have been used for the present study.

The analyzed items generate an impact of 983 million euros (multiplier of 1.9) on the production, an added value of almost 305 M€ (multiplier of 1.94) and 318 full-time jobs (and multiplier of 4.34).

These figures are very similar to those obtained in 2010, except in the case of the employment multiplier, which is even higher. The multiplier of 1.9 of production and value added is indicating that for every euro dedicated to ALBA II, the territorial economic impact almost doubles and the impact on employment is multiplied by 4.

10.2. Socioeconomic impact

To calculate the socioeconomic impact, the methodology in this proposal follows the principles set forth in ^{21,22} and ¹⁷⁶. The basis is the calculation of the net discounted value of the investment in ALBA II. The basic scenario considers an inflation rate of 2% and a discount rate of 3% (although inflation is currently higher and core inflation exceeds 2%, the sensitivity analysis shows that an increase in inflation increases the project's NPV and IRR, because the income flow is greater than cost).

The financial analysis in the basic scenario results in a net present value (NPV) of 209 million euros, Benefit-Cost ratio (B/C) of 1.17 and an internal rate of return (IRR) of 9.8%.

Thus, the annual return of ALBA investment is 9.8% and the ratio between the net present value of benefit and costs is 1.17.

These figures include only the value of access of users and the industrial value, i.e., exclude external factors and non-tangible incomes. The results are higher than those obtained in 2010, the reason being that the income is higher due to the increase number of beamlines in ALBA II compared to ALBA and the costs are lower, since an important part of the infrastructure investment was already made before 2010.

The economic analysis considers corrections to the financial results in order to consider external factors like the energy cost and the conversion into market prices of goods and services acquired under non-competitive conditions as indicated in Table 10-1.

TABLE 10-1: LIST OF KEY INDICATORS

IMPACT	KEY INDICATORS	SOURCE	INCOME (€)
Industrial	Income from industrial use	ALBA accounts	22,346,170
Users	Hours of use of ALBA	ALBA	1,213,325,872
Patents	Number of patents per year Number of citations per year	ALBA	59,166,909
Papers	Number of papers per year Number of citations per year	ALBA	193,117,750
PDB ⁹	Number of PDB per year	ALBA	41,250,000
Human capital (training)	Number of doctoral students, PhDs, post-docs per year	ALBA	57,780,093
Social capital (seminars...)	Number of seminars, courses, workshops and conferences per year	ALBA	47,707,319
Network (contacts from expenditures...)	Expenditures of ALBA in purchases	ALBA accounts	67,358,784
Other impacts (media, visits...)	Visits on ALBA from students, companies... Media news in TV, radio, newspapers Social media impacts: followers, interactions, leads.	ALBA	15,191,407

As a whole, the economic analysis in the basic scenario provides a net updated value of 460 million euros and an internal rate of profitability of 18.4%. That is, every euro of investment has a social return of 1.18 euros per year.

In summary, from the economic impact exercise we conclude that **ALBA II represents an important economic push for the different sectors of the region**, since the economic impact is twice the investment in terms of total production.

In addition, from the cost-benefit analysis a social return on investment in ALBA II of 18% per year has been obtained. This double-digit annual return is much higher than any alternative investment, and confirms the results obtained in 2010 and is possible thanks to the initial investment in ALBA.

TABLE 10-2: RESULTS OF THE ECONOMIC ANALYSIS

NPV (Income - Investments)	460,853,817 €
IRR	18.4%
B/C	1.39

⁹ The value of Protein Data Bank (PDB) at ALBA is publicly available (116 in 2021 and 873 from its beginning). The value of every PDB is calculated as in Technopolis (2021)

ANNEX A

Economic and Social Impact of ALBA II

(Jose Garcia Montalvo, Josep Maria Raya, UPF)

In 2003, when ALBA was approved, an economic and social impact assessment study for the infrastructure was commissioned to the group which has now received the same request for ALBA II.

Two studies of the economic and social impact of ALBA were carried out: one in 2004 before the construction started²⁰ and another one in 2010 before the start of the operation²¹. It is quite interesting to compare predictions and results with the future development of the facility into ALBA II.

The objective of the present study is to make an approximation of the economic impact (in terms of production, GVA and employment) and social impact of the investment that transforms ALBA into ALBA II, assessing aspects such as the effects of ALBA II on research and training, that were not included in the previous studies.

All the analysis is applied to the 2023-2055 period: period of investment and start-up of ALBA II and its exploitation. The period used is the minimum horizon that has been found in the literature on investment projects in technological infrastructures (25 years) since the launch of ALBA II, scheduled after the 2030. Given the distribution of incomes and costs, increasing the time horizon implies increasing the profitability of the investment.

A1 ECONOMIC IMPACT

The methodology adopted to calculate the economic impact is the input-output model, using a social accounting matrix to separately calculate the direct, indirect and induced impacts. The multipliers calculated in 2010 have been used. The economic impact on three magnitudes is considered: production, added value and employment. The starting point is the demand vector calculated from the allocation to the different economic sectors of the expenses obtained according to the 2023-2037 expense budget. These expenses have excluded personnel and user items and other transfers. The rest of the items (investments, current, operating and financial expenses) account for almost 60% of the

budget. The results can be seen in Table A1. The analyzed items generate an impact of 983 million euros (multiplier of 1.9), an added value of almost 305 M€ (multiplier of 1.94) and 319 full-time jobs (and multiplier of 4.35).

These figures are very similar to those obtained in 2010, except in the case of the employment multiplier, which is even higher. The multiplier of 1.9 of production and value added is indicating that for every euro dedicated to ALBA II, the territorial economic impact almost doubles and the impact on employment is multiplied by 4.

A2 SOCIOECONOMIC IMPACT

To calculate the socioeconomic impact, the methodology in this proposal follows the principles set forth in ^{21,22} and ¹⁷⁶. The basis is the calculation of the net discounted value of the investment in ALBA II. The basic scenario considers an inflation rate of 2% and a discount rate of 3% (although inflation is currently higher and core inflation exceeds 2%, the sensitivity analysis shows that an increase in inflation increases the project's NPV and IRR, because the income flow is greater than cost).

The financial analysis in the basic scenario results in a net present value (NPV) of 209 million euros, Benefit-Cost ratio (B/C) of 1.17 and an internal rate of return (IRR) of 9.8% (see Table A2). Thus, the annual return of ALBA investment is 9.8% and the quotient among net present value of benefit and costs is 1.17. These figures only include the value of access of users and the industrial value, i.e., these figures do not include externalities. The results are higher than those obtained in 2010, the reason being that the income is higher (because instead of 7 experimental beamlines, between 10 and 17 are active during the period) and the costs are lower, since an important part of the infrastructure investment was already made before 2010. Income from industrial use and costs have been obtained from the ALBA accounts. The financial income obtained by the hours of use of ALBA by the researchers has been obtained in a similar way to that calculated in 2010, but now with the information on the costs of ALBA. The income for each shift (eight-hours operation period) is updated using the same inflation rate (2%) and is reduced as the number of experimental

TABLE A1: ECONOMIC IMPACT OF ALBA II (€)

PIB 2023-2037	DIRECT	INDIRECT	INDUCED	TOTAL
Agriculture, livestock, fishing and extractive industries	5,000	14,880	227,246	247,126
Industry, construction & energy	464,632,271	115,074,039	300,788,997	880,495,307
Services	53,691,497	6,706,125	42,274,427	102,672,049
Total Amount	518,328,768	121,795,044	343,290,670	983,414,482

EMPLOYMENT (#jobs)				
Agriculture	0.0	0.00	0.0	0.0
Industry, construction & energy	53.6	70.6	129.5	253.7
Services	19.6	11.6	34.4	65.6
Total Amount	73.2	82.2	163.9	319.3

ADDED VALUE				
Agriculture	0	0	0	0
Industry, construction & energy	124,129,965	25,870,727	93,993,953	243,994,645
Services	32,943,848	4,052,149	23,962,125	60,958,122
Total Amount	157,073,813	29,922,876	117,956,078	304,952,767

lines increases until in 2032 the seventeenth line is saturated. Regarding the use of the facility, it is calculated assuming a use of 98% -practically saturation- which is the current use (4410 shifts). This use is increasing from the current 10 beamlines to 17, assuming that each new line is saturated in 2 years, which is the maximum observed to date.

The economic analysis considers corrections of the financial results in order to consider externalities and the conversion into market prices of goods and services acquired under non-competitive conditions. This implies a monetary valuation of aspects such as: the generation of knowledge (patents and publications), the development of human capital (doctors and post-docs), the development of social capital (conferences, visits), the benefits for suppliers or the benefits for the image of Barcelona, and also the environmental costs. In all cases, the social benefit is calculated for the year for which information has been analyzed (2021) and said benefit is projected into the future considering the change in the number of experimental lines, the discount rate and the inflation rate. This approach is conservative, especially in those aspects where it is logical to expect exponential growth (as it has happened up to now), as this is the case of the value of the aspects related to research. The main ones and how they have been calculated are discussed below.

Florio et al.¹⁷⁷ recommend calculating the *benefit for the development of new products* from the economic value of patents. In the case of ALBA, the number of patents is currently 16, an average

TABLE A2: RESULTS OF THE FINANCIAL ANALYSIS

NPV (Income - Investments)	209,267,413 €
IRR	9,8%
B/C	1.17

of 2 per year. We put the figure in context. According to data from the Spanish Patent Office, Catalan universities applied for a total of 298 patents in the last decade. In other words, in 7 years (2015-2021) ALBA alone has requested more than 5% of them. The value of these patents is linked to the number of citations received subsequently. As these patents are recent, it is difficult to assess this aspect with this route. Following ref¹⁷⁸ patents are valued at €300,000, although in ref¹⁷⁹ opts for a more conservative value (€85,000) taken from the European Investment Bank (2013).

Other businesses can also *benefit from the network of knowledge and contacts* that the business relationship with ALBA entails. To make this calculation, the average multiplier of the sectors has been taken by the profitability of each sector using the SABI database that contains 1.7 million Spanish companies and all the accounting data and economic-financial ratios. The weighted average of EBITDA over sales has been taken. With a turnover value of 1.43 and a 14.7% return in 2019, this component has a contribution of 1.8 million in 2021.

The benefit of research is one of the main social benefits of scientific

¹⁷⁷ Social benefits and costs of large scale research infrastructures, Volume 112, November 2016, Pages 65-78, <https://doi.org/10.1016/j.techfore.2015.11.024>

¹⁷⁸ Ceccagnoli, M., Gambardella, A., Giuri, P., Licht, G., & Mariani, M. (2005). Study on evaluating the knowledge economy—What are patents actually worth? The value of patents for today's economy and society. European Commission, DG Internal Market, Tender No. MARKT/2004/09/E, Final Report for Lot, 1

¹⁷⁹ Sartori, D., Catalano, G., Genco, M., Pancotti, C., Sirtori, E., Vignetti, S., et al. (2014). Guide to Cost-Benefit Analysis of Investment Projects. Economic Appraisal Tool for Cohesion Policy 2014–2020. Brussels: European Commission.

infrastructures. The benefits are considered from the citations of the articles by scientists who do not belong to ALBA. As usual, citations have grown from the birth of ALBA (40 in 2011) to the present (around 10,500 in 2021). The usual way of calculating the value of each citation includes the cost of the researcher's time, from downloading the paper to its citation. This cost is evaluated at the average salary of researchers in the field. Thus, the value obtained for 2021 is 63,862 €. As citations increase exponentially as the synchrotron's life progresses, this benefit will also increase exponentially throughout the life of the infrastructure.

It is clear that a scientific infrastructure such as ALBA is instrumental in the development of *human capital*, that is, the creation of knowledge, skills and competencies that are necessary outside the strict scope of research. Research infrastructures are fundamentally a hub of talent. Students do not pay a fee for their training in a research infrastructure but may receive training from third party resources (grants, etc.). In this way an externality is created. The techniques of the economics of education allow to obtain the increase in the human capital available to society. Human capital contributes to the growth and productivity of the economy. Thus, doctoral students and postdocs have access to learning by doing by having access to large research infrastructure singular opportunities. The salaries reflect these skills obtained during the stay in a large scientific infrastructure. The benefit of doctoral students' training is calculated by their higher future salary, duly discounted, (return on education) by the positive externalities of working at ALBA. This parameter is calculated as is standard in the literature (assuming that they retire at age 65). This bonus for having worked at ALBA- around 5% - applies to the set of students of professional education, pre-docs, doctorates and post-docs. The final amount for 2021 is 2.25 million euros.

Regarding the development of social capital, throughout the year researchers organize academic seminars, workshops, courses and conferences that attract a group of visitors from all over Europe. For example, in 2019-2020 and 2021 they are strongly influenced by the pandemic situation - 1,225 people visited ALBA either as guest speakers or as participants in seminars and workshops. Visitors' willingness to pay is calculated using the travel cost method (adding the costs of transportation, accommodation, registration, and the opportunity cost in terms of those days of attendees' wages). Assuming an average willingness to pay of 2,000 euros (Sartori et al, 2017). The result for our project is 1,856,000 € in 2021.

Finally, other additional benefits considered in this approach to the socioeconomic assessment of ALBA II are the benefit for visitors or the value for the image of the territory. Other possible benefits such as the value of "non-use" have not been calculated because for this it is necessary to have surveys with a questionnaire in order to obtain the willingness to pay for having the infrastructure (whether it is used or not). In the case of the Large Hadron Collider, Florio et al. (2016) estimate that it compensates 24% of the total costs.

Throughout the year ALBA is visited by schools, companies, staff from other universities. For example, in 2019 these visitors were around 17,000. These visitors are beneficiaries of ALBA insofar as their willingness to pay for the visit is higher than the price they actually pay (the visit is free). As in other recreational activities, the best way to approximate the willingness to pay is through

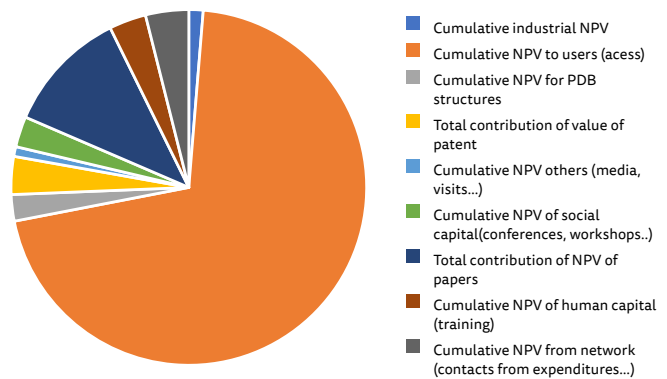


Figure A1: Distribution of the income NPV.

the trip cost method¹⁸⁰, which assumes that the financial and economic costs of the visitor make it possible to approximate the availability to turn off. Following a conservative approach, we have used the data from the mobility survey of the Barcelona area in 2018. This implies assuming that the trips come from that area and represent around 16.70 euros per visitor, assuming that they do not incur any additional expenses. For 2021, this implies a benefit for visitors of 117,240 €. Additionally, other visitors make a virtual tour of the ALBA through the website or through social networks. Likewise, there is the benefit for the image of the destination ALBA's notoriety is another benefit to the territory, in particular to Barcelona, Catalonia and Spain. A common way of measuring this notoriety is through the news that is generated in the media, whether traditional-press, radio, TV-or digital-social networks, website. This news can be understood as advertising impacts that implicitly increase the notoriety of the territory and are usually valued through clipping. In 2021, this value was 342,055 €.

Finally, regarding social costs, it is estimated that the value of the environmental cost of ALBAII, the cost is obtained by applying the price per ton of 86.6 €¹⁸¹, to the consumption of 48 GWh/y to the weighted average of CO₂ emissions per kWh of Spanish electricity companies (0.30 kg/kWh).¹⁸² The environmental cost in 2021, therefore, is estimated at 932,453 €.

Figure A1 and Table A3 summarize the impacts aforementioned. ALBA II will have a cumulative monetized impact of at least €1.72 billion during the period 2022-2055, based on the evidence captured at this relatively early stage of the facility's operations. Bearing in mind that not all activities, outputs and outcomes can be precisely monetized at this stage, this already compares very favorably with the €1.26 billion investment in the facility. Main contributors of VPN are the value for users (access) and the value of the papers.

As a whole, economic analysis in the basic scenario provides a net updated value of 460 million euros and an internal rate of profitability of 18.4%. That is, every euro of investment has a social return of 1.18 euros per year.

We can therefore conclude that the rate of return on investment in ALBA II is very high. To put it in context, it is more than double the rate obtained in ALBA, which was already high, since it is not usual for rates of return to exceed two digits. This is due to the

¹⁸⁰ Economics of Outdoor Recreation by Marion Clawson, Jack L. Knetsch, doi.org/10.4324/9781315064215

¹⁸¹ <https://www.sendeco2.com>

¹⁸² Comisión nacional del Mercado de la Competencia, <https://www.cnmec.es/>

TABLE A3: LIST OF KEY INDICATORS

IMPACT	KEY INDICATORS	SOURCE	INCOME (€)
Industrial	Income from industrial use	ALBA accounts	22,346,170
Users	Hours of use of ALBA	ALBA	1,213,325,872
Patents	Number of patents per year Number of citations per year	ALBA	59,166,909
Papers	Number of papers per year Number of citations per year	ALBA	193,117,75
PDB ^a	Number of PDB per year	ALBA	41,250,000
Human capital (training)	Number of doctoral students, PhDs, post-docs per year	ALBA	57,780,093
Social capital (seminars...)	Number of seminars, courses, workshops and conferences per year	ALBA	47,707,319
Network (contacts from expenditures...)	Expenditures of ALBA in purchases	ALBA accounts	67,358,784
Other impacts (media, visits...)	Visits on ALBA from students, companies... Media news in TV, radio, newspapers Social media impacts: followers, interactions, leads.	ALBA	15,191,407

TYPE OF INVESTMENT	KEY INDICATORS	SOURCE	INVESTMENTS (€)
Personnel	Costs from personnel	ALBA accounts	551,155,099
Investments	Costs of investments	ALBA	344,540,005
Operational Costs	Operational Costs	ALBA	337,485,852
Financial costs	Financial Costs	ALBA	3,749,733
Environmental costs	Consumption in Kw/h	ALBA	23,968,121

fact that the new investment in ALBA II takes advantage of a large part previous already beneficial investment in ALBA, increasing its positive impact. In addition, as has been mentioned, the assumptions that have been made are absolutely conservative. Figure A2 shows the evolution of the NPV throughout the analyzed period. As can be seen, once ALBA II is put into operation (2031) the NPV has a clearly growing trend that would continue if the time horizon is extended (something that could easily happen until 2050) and would offer much higher returns on investment. The years with negative NPV are years of important investment in new lines which will return later in important positive NPV.

To sum up, from the economic impact exercise we can conclude that ALBA II represents an important economic drag for the different sectors of the region, since the economic impact is practically double the investment in terms of total production. From the cost-benefit analysis we obtain a social return on investment in ALBA II of 18% per year. This double-digit annual return is much higher than any alternative investment, confirms the results obtained in 2020 and is possible thanks to the initial investment in ALBA.

TABLE A4: RESULTS OF THE ECONOMIC ANALYSIS

NPV (Income - Investments)	460,853,817 €
IRR	18.4%
B/C	1.39

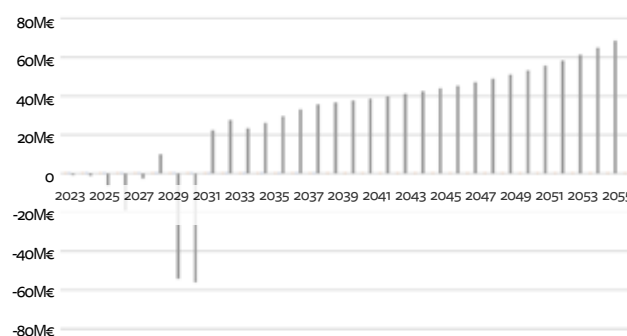


Figure A2 NPV (Income-Investments) evolution 2023-2055

^a The value of Protein Data Bank (PDB) at ALBA is publicly available (116 in 2021 and 873 from its beginning). The value of every PDB is calculated as in Technopolis (2021)

References

- ¹ <https://www.albasynchrotron.es/en>
- ² <https://leaps-initiative.eu/>
- ³ <https://www.maxiv.lu.se/>
- ⁴ <https://www.esrf.fr/>
- ⁵ <https://www.esrf.eu/about/upgrade>
- ⁶ <https://www.albasynchrotron.es/en/instrumentation/jemca>
- ⁷ <https://www.albasynchrotron.es/en/instrumentation/incaem>
- ⁸ <https://www.ciencia.gob.es/en/Estrategias-y-Planes/Plan-de-Recuperacion-Transformacion-y-Resiliencia-PRTR/Planes-complementarios-con-CCAA/Materiales-avanzados.html>
- ⁹ <https://www.albasynchrotron.es/en/media/corporate-publications/astip2021-a4.pdf>
- ¹⁰ <https://www.ciencia.gob.es/Organismos-y-Centros/ICTS.html>
- ¹¹ <https://www.ibmb.csic.es/en/>
- ¹² <https://icn2.cat/en/>
- ¹³ <https://www.calipsoplus.eu/trans-national-access/>
- ¹⁴ <https://www.leaps-innov.eu/>
- ¹⁵ <https://www.remade-project.eu>
- ¹⁶ https://ec.europa.eu/info/research-and-innovation/strategy/goals-research-and-innovation-policy/open-science/european-open-science-cloud-eosc_en#what-the-european-open-science-cloud-is
- ¹⁷ Catalano, G., López, G. G., Sánchez, A., and Vignetti, S. (2021). From scientific experiments to innovation: Impact pathways of a Synchrotron Light Facility. *Ann Public Coop Econ*, 1-26. DOI: 10.1111/apce.12322
- ¹⁸ <https://ri-paths-tool.eu/en>
- ¹⁹ <https://www.csilmilano.com/>
- ²⁰ <https://lnls.cnpem.br/home/>
- ²¹ José García Montalvo, Josep María Raya Vílchez, "Potenciant la nova economia a Catalunya", *Coneixement i Societat: Revista d'Universitats, Recerca i Societat de la Informació*, ISSN-e 1696-7380, N.º 9, 2005 and <https://www.cells.es/es/que-es-alba/transparencia/publicidad-activa/docs-planificacion/acb-impacto-sdv.pdf>
- ²² José García Montalvo, Josep María Raya Vílchez, LA FUENTE DE LUZ DE SINCROTRÓN ALBA: ANALISIS COSTE BENEFICIO Y ESTUDIO DE IMPACTO ECONOMICO, https://www.cells.es/es/que-es-alba/transparencia/publicidad-activa/docs-planificacion/informe-alba-2010_final_accept_changes-3.pdf
- ²³ C. Biscari et al., ESAPS 2022, https://leaps-initiative.eu/wp-content/uploads/2022/05/LEAPS-ESAPS-Broschure_final-20052022-3.pdf20
- ²⁴ Abela, R., Biscari, C., Daillant, J. et al. The European strategy for accelerator-based photon science. *Eur. Phys. J. Plus* 138, 355 (2023).
- ²⁵ <https://www.leaps-innov.eu/>
- ²⁶ <https://arie-eu.org>
- ²⁷ Conesa et al. *Angew. Chem.* 59, 1270-1278, 2020
- ²⁸ Mendonça et al., *Nat. Comm.* 12;4629, 2021
- ²⁹ Rout and Sali, *Cell* 177, 1384-1403, 2019
- ³⁰ Alber et al., *Nature* 450, 683-694, 2007
- ³¹ Kim et al., *Nature* 555, 475-482, 2018
- ³² Weinert et al., *Science* 365:6448 61-65, 2019).
- ³³ Nogly et al., *Science* 361, eaat0094, 2018
- ³⁴ Nango et al. *Science* 354, 1552-1557, 2016
- ³⁵ Kovalev et al. *Nat Comm* 11, 2137, 2020
- ³⁶ <https://i-deals.es/project/fresme/>
- ³⁷ https://ucpcdn.thyssenkrupp.com/_legacy/UCPthyssenkruppBAISMicositePowertoX/assets.files/power-to-x/hydrogen-brochure.pdf
- ³⁸ *Green Chem.*, 2021, 23, 7259-7268, DOI: 10.1039/d1gc01761f
- ³⁹ Zhang X, Zhang G, Song C and Guo X (2021) Catalytic Conversion of Carbon Dioxide to Methanol: Current Status and Future Perspective. *Front. Energy Res.* 8:621119. doi: 10.3389/fenrg.2020.621119
- ⁴⁰ B. Liang, J. Ma, X. Su, C. Yang, H. Duan, H. Zhou, S. Deng, L. Li and Y. Huang. *Ind. Eng. Chem. Res.*, 2019, 58, 9030-9037.
- ⁴¹ O. Martín and J. Pérez-Ramírez, *Catal. Sci. Technol.*, 2013, 3, 3343-3352.
- ⁴² Element Scarcity - EuChemS Periodic Table, <https://www.euchems.eu/euchems-periodic-table/>.
- ⁴³ Álvarez, A. et al. Challenges in the greener production of formates/formic acid, methanol, and DME by heterogeneously catalyzed CO₂ hydrogenation processes. *Chem. Rev.* 117, 9804 (2017).

- ⁴⁴ Bernskoetter, W. H. & Hazari, N. Reversible hydrogenation of carbon dioxide to formic acid and methanol: Lewis acid enhancement of base metal catalysts. *Acc. Chem. Res.* 50, 1049–1058 (2017).
- ⁴⁵ Kattel, S., Ramírez, P. J., Chen, J. G., Rodriguez, J. A. & Liu, P. Active sites for CO₂ hydrogenation to methanol on Cu/ZnO catalysts. *Science* 357, 1296–1299 (2017).
- ⁴⁶ Behrens, M. et al. The active site of methanol synthesis over Cu/ZnO/Al₂O₃ industrial catalysts. *Science* 336, 893 (2012).
- ⁴⁷ Yuhao Wang, Shyam Kattel, Wengui Gao, Kongzhai Li, Ping Liu, Jingguang G. Chen, Hua Wan, Exploring the ternary interactions in Cu–ZnO–ZrO₂ catalysts for efficient CO₂ hydrogenation to methanol, *NATURE COMMUNICATIONS* | (2019)10:1166 | <https://doi.org/10.1038/s41467-019-09072-6>
- ⁴⁸ Yuhao Wang, Wengui Gao, Kongzhai Li, Yane Zheng, Zhenhua Xie, Wei Na, Jingguang G. Chen, Hua Wang, Strong Evidence of the Role of H₂O in Affecting Methanol Selectivity from CO₂ Hydrogenation over Cu–ZnO–ZrO₂, *Chem Volume 6, Issue 2, 13 February 2020, Pages 419–430.* <https://doi.org/10.1016/j.chempr.2019.10.023>
- ⁴⁹ *Catalysts* 2020, 10, 160; doi:10.3390/catal10020160.
- ⁵⁰ *Combinatorial and High-Throughput Discovery and Optimization of Catalysts and Materials* Edited By Radislav A. Potyrailo & Wilhelm F. Maier, Copyright Year 2007 ISBN 9780367390594 Published October 18, 2019 by CRC Press.
- ⁵¹ *J. Am. Chem. Soc.* 2019, 141, 49, 19304–19311. <https://doi.org/10.1021/jacs.9b07088>
- ⁵² Andrew J. Medford, M. Ross Kunz, Sarah M. Ewing, Tammie Borders, Rebecca Fushimi, Extracting Knowledge from Data through Catalysis Informatics, *ACS Catal.* 2018, 8, 8, 7403–7429. <https://doi.org/10.1021/acscatal.8b01708>
- ⁵³ Dong, H., Butler, K.T., Matras, D. et al. A deep convolutional neural network for real-time full profile analysis of big powder diffraction data. *npj Comput Mater* 7, 74 (2021). <https://doi.org/10.1038/s41524-021-00542-4>
- ⁵⁴ Matthew R. Carbone, Mehmet Topsisakal, Deyu Lu, and Shinjae Yoo, Machine-Learning X-ray Absorption Spectra to Quantitative Accuracy, *Phys. Rev. Lett.* 124, 156401.
- ⁵⁵ Guda, A.A., Guda, S.A., Martini, A. et al. Understanding X-ray absorption spectra by means of descriptors and machine learning algorithms. *npj Comput Mater* 7, 203 (2021). <https://doi.org/10.1038/s41524-021-00664-9>
- ⁵⁶ *J. Mater. Chem. A*, 2021, 9, 8401.
- ⁵⁷ Divins, N.J., Braga, A., Vendrell, X. et al. Investigation of the evolution of Pd–Pt supported on ceria for dry and wet methane oxidation. *Nat Commun* 13, 5080 (2022). <https://doi.org/10.1038/s41467-022-32765-4>
- ⁵⁸ <https://doi.org/10.1002/cey2.131>
- ⁵⁹ <https://basquevolt.com/en>
- ⁶⁰ <https://cicenergigune.com/es>
- ⁶¹ <https://doi.org/10.1016/j.jpowsour.2021.229919>
- ⁶² Nicola Boaretto, Iñigo Garbayo, Sona Valiyaveetil–SobhanRaj, Amaia Quintela, Chunmei Li, Montse Casas–Cabanas, Frederic Aguesse, Lithium solid-state batteries: State-of-the-art and challenges for materials, interfaces and processing, *Journal of Power Sources*, Volume 502, 2021, 229919, ISSN 0378–7753, <https://doi.org/10.1016/j.jpowsour.2021.229919>
- ⁶³ Adams, Stefan, and Rayavarapu Prasada Rao. “Ion transport and phase transition in Li_{7–x}La₃(Zr_{2–x}M_x)O₁₂ (M= Ta⁵⁺, Nb⁵⁺, x= 0, 0.25).” *Journal of Materials Chemistry* 22.4 (2012): 1426–1434
- ⁶⁴ V. Thangadurai, H. Kaack, W.J.F. Weppner, Novel fast lithium ion conduction in garnet-type Li₅La₃M₂O₁₂ (M = Nb, Ta), *J. Am. Ceram. Soc.* 86 (3) (2003) 437–440, <https://doi.org/10.1111/j.1151-2916.2003.tb03318.x>
- ⁶⁵ R. Murugan, V. Thangadurai, W. Weppner, Fast lithium ion conduction in garnet-type Li₇La₃Zr₂O₁₂, *Angew. Chem. Int. Ed.* 46 (41) (2007) 7778–7781, <https://doi.org/10.1002/anie.200701144>
- ⁶⁶ L. Xu, et al., “Garnet solid electrolyte for advanced all-solid-state Li batteries, *Adv. Energy Mater.* (May 2020) 2000648, <https://doi.org/10.1002/aenm.202000648>
- ⁶⁷ V. Thangadurai, W. Weppner, Recent progress in solid oxide and lithium ion conducting electrolytes research, *Ionics* 12 (1) (May 2006) 81–92, <https://doi.org/10.1007/s11581-006-0013-7>
- ⁶⁸ T. Takahashi, H. I.-E. Conversion, and undefined, Ionic Conduction in Perovskite-type Oxide Solid Solution and its Application to the Solid Electrolyte Fuel Cell, “Elsevier, 1971
- ⁶⁹ Y. Inaguma, et al., High ionic conductivity in lithium lanthanum titanate, *Solid State Commun.* 86 (10) (Jun. 1993) 689–693, [https://doi.org/10.1016/0038-1098\(93\)90841-A](https://doi.org/10.1016/0038-1098(93)90841-A)
- ⁷⁰ Mara Olivares–Marín, Andrea Sorrentino, Rung–Chuan Lee, Eva Pereiro, Nae–Lih Wu, and Dino Tonti, “Spatial Distributions of Discharged Products of Lithium–Oxygen Batteries Revealed by Synchrotron X-ray Transmission Microscopy”, *Nano Lett.* 2015
- ⁷¹ L. Zhou, A. Assoud, Q. Zhang, X. Wu, L.F. Nazar, New family of argyrodite thioantimonate lithium superionic conductors, *J. Am. Chem. Soc.* 141 (48) (Dec.2019) 19002–19013, <https://doi.org/10.1021/jacs.9b08357>
- ⁷² Y. Wang, et al., Design principles for solid-state lithium superionic conductors, *Nat. Mater.* 14 (10) (Oct. 2015) 1026–1031, <https://doi.org/10.1038/nmat4369>
- ⁷³ P. Knauth, Inorganic solid Li ion conductors: an overview, *Solid State Ionics* 180(14–16) (Jun. 2009) 911–916, <https://doi.org/10.1016/j.ssi.2009.03.022>
- ⁷⁴ J.B. Bates, et al., Fabrication and characterization of amorphous lithium electrolyte thin films and rechargeable thin-film batteries, *J. Power Sources* 43 (1–3) (Mar. 1993) 103–110, [https://doi.org/10.1016/0378-7753\(93\)80106-Y](https://doi.org/10.1016/0378-7753(93)80106-Y)
- ⁷⁵ Chen, J., Yang, Y., Tang, Y., Wang, Y., Li, H., Xiao, X., Wang, S., Darma, M.S.D., Etter, M., Missyul, A., Tayal, A., Knapp, M., Ehrenberg, H., Indris, S. and Hua, W. (2023), Constructing a Thin Disordered Self-Protective Layer on the LiNiO₂ Primary Particles Against Oxygen Release (*Adv. Funct. Mater.* 6/2023). *Adv. Funct. Mater.*, 33: 2370034. <https://doi.org/10.1002/adfm.202370034>

- ⁷⁶ Gorbunov, Mikhail V. et al. "Studies of Li₂Fe_{0.9}Mo_{1.0}SO Antiperovskite Materials for Lithium-Ion Batteries: The Role of Partial Fe²⁺ to M²⁺ Substitution." *Frontiers in Energy Research* (2021) *ACS Appl. Energy Mater.* 2022, 5, 11, 13735–13750 Publication Date: October 19, 2022 <https://doi.org/10.1021/acsaem.2c02402>
- ⁷⁷ Anna Windmüller, Tatiana Renzi, Hans Kungl, Svitlana Taranenka, Emmanuelle Suard, François Fauth, Mathieu Duttine, Chih-Long Tsai, Ruoheng Sun, Yasin Emre Durmus, Hermann Tempel, Peter Jakes, Christian Masquelier, Rüdiger-A. Eichel, Laurence Croguennec, and Helmut Ehrenberg, "Feasibility and Limitations of High-Voltage Lithium-Iron-Manganese Spinels", *Journal of The Electrochemical Society*, 2022 169 070518
- ⁷⁸ Christian Baur, Monica-Elisabeta Lacatușu, Maximilian Fichtner, and Rune E. Johnsen, Insights into Structural Transformations in the Local Structure of Li₂VO₂F Using Operando X-ray Diffraction and Total Scattering: Amorphization and Recrystallization *ACS Applied Materials & Interfaces* 2020 12 (24), 27010–27016 DOI: 10.1021/acsaem.2c02391
- ⁷⁹ Romain Wernert, Long H. B. Nguyen, Emmanuel Petit, Paula Sanz Camacho, Antonella Iadecola, Alessandro Longo, François Fauth, Lorenzo Stievano, Laure Monconduit, Dany Carlier, and Laurence Croguennec, "Controlling the Cathodic Potential of KVPO₄F through Oxygen Substitution", *Chemistry of Materials* 2022 34 (10), 4523–4535 DOI: 10.1021/acs.chemmater.2c00295
- ⁸⁰ Luca Porcarelli, M. Ali Aboudzadeh, Laurent Rubatat, Jijeeesh R. Nair, Alexander S. Shaplov, Claudio Gerbaldi, David Mecerreyes, Single-ion triblock copolymer electrolytes based on poly(ethylene oxide) and methacrylic sulfonamide blocks for lithium metal batteries, *Journal of Power Sources* Volume 364, 1 October 2017, 191–199, DOI: 10.1016/j.jpowsour.2017.08.023
- ⁸¹ Andreas Bergfeldt, Laurent Rubatat, Daniel Brandell, Tim Bowden, Poly(benzyl methacrylate)-poly[(oligo ethylene glycol) methyl ether methacrylate] triblock-copolymers as solid electrolyte for lithium batteries, *Solid State Ionics* Volume 321, August 2018, 55–61, DOI: 10.1016/j.ssi.2018.04.006
- ⁸² Tianze Xu, Chunrun Chen, Tianwei Jin, Shuaifeng Lou, Ruiwen Zhang, Xianghui Xiao, Xiaojing Huang and Yuan Yang, Chemical Heterogeneity in PAN/LLZTO Composite Electrolytes by Synchrotron Imaging, 2021 *J. Electrochem. Soc.* 168 110522
- ⁸³ Marcos Lucero, Shen Qiu, Xhenxing Feng, In situ characterizations of solid–solid interfaces in solid-state batteries using synchrotron X-ray techniques, *Carbon Energy*. 2021;3:762–783. DOI: 10.1002/cey2.131
- ⁸⁴ Lemme, M. C.; Akinwande, D.; ... C. H.-N.; 2022, undefined. 2D Materials for Future Heterogeneous Electronics. *nature.com*.
- ⁸⁵ Moore, G. E. Cramming More Components onto Integrated Circuits, Reprinted from *Electronics*, Volume 38, Number 8, April 19, 1965, Pp. 114 Ff. *IEEE solid-state circuits society newsletter* 2006, 11 (3), 33–35.
- ⁸⁶ https://en.wikipedia.org/wiki/Field-effect_transistor
- ⁸⁷ Graef, M. Positioning More Than Moore Characterization Needs and Methods within the 2011 ITRS. *AIP Conference Proceedings* 2011, 1395 (1), 345–350. <https://doi.org/10.1063/1.3657913>
- ⁸⁸ Arden, W.; Brillouët, M.; Cogez, P.; Graef, M.; Huizing, B.; Mahnkopf, R. More-than-Moore White Paper. Version 2010, 2, 14
- ⁸⁹ Roy, K.; Jung, B.; Peroulis, D.; Raghunathan, A. Integrated Systems in the More-than-Moore Era: Designing Low-Cost Energy-Efficient Systems Using Heterogeneous Components. *IEEE Design & Test* 2013, 33 (3), 56–65
- ⁹⁰ Andrae, A. S. G.; Challenges, T. E.-; 2015, undefined. On Global Electricity Usage of Communication Technology: Trends to 2030. *mdpi.com*
- ⁹¹ Manipatruni, S.; Nikonov, D.; Physics, I. Y.-N.; 2018, undefined. Beyond CMOS Computing with Spin and Polarization. *nature.com* 2018. <https://doi.org/10.1038/s41567-018-0101-4>
- ⁹² Juge, R.; Je, S.-G.; Chaves, D. de S.; Buda-Prejbeanu, L. D.; Peña-García, J.; Nath, J.; Miron, I. M.; Rana, K. G.; Aballe, L.; Foerster, M.; Genuzio, F.; Mentès, T. O.; Locatelli, A.; Maccherozzi, F.; Dhési, S. S.; Belmeguenai, M.; Roussigné, Y.; Auffret, S.; Pizzini, S.; Gaudin, G.; Vogel, J.; Bouille, O. Current-Driven Skyrmion Dynamics and Drive-Dependent Skyrmion Hall Effect in an Ultrathin Film. *Phys. Rev. Appl.* 2019, 12 (4), 044007. <https://doi.org/10.1103/PhysRevApplied.12.044007>
- ⁹³ Huang, M.; Hasan, M. U.; Klyukin, K.; Zhang, D.; Lyu, D.; Gargiani, P.; Valvidares, M.; Sheffels, S.; Churikova, A.; Büttner, F.; Zehner, J.; Caretta, L.; Lee, K. Y.; Chang, J.; Wang, J. P.; Leistner, K.; Yildiz, B.; Beach, G. S. D. Voltage Control of Ferrimagnetic Order and Voltage-Assisted Writing of Ferrimagnetic Spin Textures. *Nature Nanotechnology* 2021, 16 (9), 981–988. <https://doi.org/10.1038/s41565-021-00940-1>
- ⁹⁴ Manipatruni, S.; Nikonov, D. E.; Lin, C. C.; Gosavi, T. A.; Liu, H.; Prasad, B.; Huang, Y. L.; Bonturim, E.; Ramesh, R.; Young, I. A. Scalable Energy-Efficient Magnetolectric Spin-Orbit Logic. *Nature* 2019, 565 (7737), 35–42. <https://doi.org/10.1038/s41586-018-0770-2>
- ⁹⁵ Ramesh, R.; Royal, S. M.-P. of the; 2021, undefined. Electric Field Control of Magnetism. *royalsocietypublishing.org* 2021, 477 (2251). <https://doi.org/10.1098/rspa.2020.0942>.
- ⁹⁶ <https://indico.cells.es/e/ALBAII/workshop-2D-materials>
- ⁹⁷ <https://indico.cells.es/event/373/>
- ⁹⁸ Kent, N.; Reynolds, N.; Raftrey, D.; Campbell, I. T. G.; Virasawmy, S.; Dhuey, S.; Chopdekar, R. V.; Hierro-Rodríguez, A.; Sorrentino, A.; Pereiro, E.; Ferrer, S.; Hellman, F.; Sutcliffe, P.; Fischer, P. Creation and Observation of Hopfions in Magnetic Multilayer Systems. *Nat Commun* 2021, 12 (1), 1562. <https://doi.org/10.1038/s41467-021-21846-5>.
- ⁹⁹ Sanz-Hernández, D.; Hierro-Rodríguez, A.; Donnelly, C.; Pablo-Navarro, J.; Sorrentino, A.; Pereiro, E.; Magén, C.; McVitie, S.; de Teresa, J. M.; Ferrer, S.; Fischer, P.; Fernández-Pacheco, A. Artificial Double-Helix for Geometrical Control of Magnetic Chirality. 2020, 1–19
- ¹⁰⁰ Ukleev, V.; Yamasaki, Y.; Morikawa, D.; Karube, K.; Shibata, K.; Tokunaga, Y.; Okamura, Y.; Amemiya, K.; Valvidares, M.; Nakao, H. Element-Specific Soft x-Ray Spectroscopy, Scattering, and Imaging Studies of the Skyrmion-Hosting Compound Co₈Zn₈Mn₄. *Physical Review B* 2019, 99 (14), 144408
- ¹⁰¹ Wartelle, A.; Trapp, B.; Staño, M.; Thirion, C.; Bochmann, S.; Bachmann, J.; Foerster, M.; Aballe, L.; Mentès, T. O.; Locatelli, A.; Sala, A.; Cagnon, L.; Toussaint, J.-C.; Fruchart, O. Bloch-Point-Mediated Topological Transformations of Magnetic Domain Walls in Cylindrical Nanowires. *Phys. Rev. B* 2019, 99 (2), 024433. <https://doi.org/10.1103/PhysRevB.99.024433>.
- ¹⁰² Bedoya-Pinto, A.; Ji, J. R.; Pandeya, A. K.; Gargiani, P.; Valvidares, M.; Sessi, P.; Taylor, J. M.; Radu, F.; Chang, K.; Parkin, S. S. P.

- Intrinsic 2D-XY Ferromagnetism in a van Der Waals Monolayer. *Science* 2021, 374 (6567), 616–620. <https://doi.org/10.1126/science.abd5146>
- ¹⁰³ Ares, P.; Pakdel, S.; Palacio, I.; Paz, W. S.; Rassekh, M.; Rodríguez-San Miguel, D.; Aballe, L.; Foerster, M.; Ruiz del Árbol, N.; Martín-Gago, J. Á.; Zamora, F.; Gómez-Herrero, J.; Palacios, J. J. Few-Layer Antimonene Electrical Properties. *Applied Materials Today* 2021, 24, 101132. <https://doi.org/10.1016/j.apmt.2021.101132>.
- ¹⁰⁴ Bikaljević, D.; González-Orellana, C.; Peña-Díaz, M.; Steiner, D.; Dreiser, J.; Gargiani, P.; Foerster, M.; Niño, M. Á.; Aballe, L.; Ruiz-Gomez, S.; Friedrich, N.; Hieulle, J.; Jingcheng, L.; Ilyn, M.; Rogero, C.; Pascual, J. I. Noncollinear Magnetic Order in Two-Dimensional NiBr₂ Films Grown on Au(111). *ACS Nano* 2021, 15 (9), 14985–14995. <https://doi.org/10.1021/acsnano.1c05221>.
- ¹⁰⁵ Vidas, L.; Günther, C. M.; Miller, T. A.; Pfau, B.; Perez-Salinas, D.; Martínez, E.; Schneider, M.; Gührs, E.; Gargiani, P.; Valvidares, M.; Marvel, R. E.; Hallman, K. A.; Haglund, R. F.; Eisebitt, S.; Wall, S. Imaging Nanometer Phase Coexistence at Defects during the Insulator-Metal Phase Transformation in VO₂ Thin Films by Resonant Soft X-ray Holography. *Nano Letters* 2018, 18 (6), 3449–3453. <https://doi.org/10.1021/acs.nanolett.8b00458>.
- ¹⁰⁶ Spagnolo, M.; Morris, J.; Piacentini, S.; Antesberger, M.; Massa, F.; Crespi, A.; Ceccarelli, F.; Osellame, R.; Walther, P. Experimental Photonic Quantum Memristor. *Nature Photonics* 2022 16:4 2022, 16 (4), 318–323. <https://doi.org/10.1038/s41566-022-00973-5>
- ¹⁰⁷ Grollier, J.; Querlioz, D.; Camsari, K. Y.; Everschor-Sitte, K.; Fukami, S.; Stiles, M. D. Neuromorphic Spintronics. *Nat Electron* 2020, 3 (7), 360–370. <https://doi.org/10.1038/s41928-019-0360-9>.
- ¹⁰⁸ Stoliar, P.; Tranchant, J.; Corraze, B.; Janod, E.; Besland, M. P.; Tesler, F.; Rozenberg, M.; Cario, L. A Leaky-Integrate-and-Fire Neuron Analog Realized with a Mott Insulator. *Advanced Functional Materials* 2017, 27 (11), 1604740. <https://doi.org/10.1002/adfm.201604740>.
- ¹⁰⁹ Martins, S.; de Rojas, J.; Tan, Z.; Cialone, M.; Lopeandia, A.; Herrero-Martín, J.; Costa-Krämer, J. L.; Menéndez, E.; Sort, J. Dynamic Electric-Field-Induced Magnetic Effects in Cobalt Oxide Thin Films: Towards Magneto-Ionic Synapses. *Nanoscale* 2022, 14 (3), 842–852.
- ¹¹⁰ Domain Wall Automotion in Three-Dimensional Magnetic Helical Interconnectors | *ACS Nano*. <https://pubs.acs.org/doi/10.1021/acsnano.1c10345> (accessed 2023-01-18)
- ¹¹¹ Dawidek, R. W.; Hayward, T. J.; Vidamour, I. T.; Broomhall, T. J.; Venkat, G.; Mamoori, M. A.; Mullen, A.; Kyle, S. J.; Fry, P. W.; Steinke, N.-J.; Cooper, J. F. K.; Maccherozzi, F.; Dhese, S. S.; Aballe, L.; Foerster, M.; Prat, J.; Vasilaki, E.; Ellis, M. O. A.; Allwood, D. A. Dynamically Driven Emergence in a Nanomagnetic System. *Advanced Functional Materials* 2021, 31 (15), 2008389. <https://doi.org/10.1002/adfm.202008389>
- ¹¹² A distributed sextupoles lattice for the ALBA low emittance upgrade. G. Benedetti, M. Carlà, U. Irso, Z. Martí, F. Pérez. [ed.] Jacow. Campinas, Brasil : s.n., 2021. IPAC21
- ¹¹³ SOLEIL Synchrotron, “Conceptual design report, synchrotron SOLEIL upgrade”, SYNCHROTRON SOLEIL, l’orme des merisiers, 91190 saint-aubin. www.grouperouge.vif.fr - GROUPE ROUGE VIF - 26896 - Décembre 2020
- ¹¹⁴ A. Streun, M. Aiba, S. Bettoni, M. Böge, B. Riemann, V. Schlott, “SLS 2.0 Baseline Lattice”, SLS2-SA81-004-17- 2021
- ¹¹⁵ Permanent Magnets LEAPS Internal Collaboration - <https://indico.cells.es/event/623/overview> - PERMALIC 1st Workshop -2021
- ¹¹⁶ Fornek, T. - Advanced Photon Source Upgrade Project, Final Design Report - APSU-2.01-RPT-003, 2019
- ¹¹⁷ <https://www.esrf.fr/Accelerators/Groups/InsertionDevices/Software/Radia>
- ¹¹⁸ <https://www.ansys.com/products/electronics/ansys-maxwel>
- ¹¹⁹ <https://www.3ds.com/products-services/simulia/products/opera/>
- ¹²⁰ E. Al-Dmour, et al., “Diffraction-limited storage-ring vacuum technology”, *Journal of Synchrotron Radiation*, ISSN 1600-5775, Sept. 2014. DOI: 10.1107/S1600577514010480.
- ¹²¹ P. Chiggiato and R. Kersevan, “Synchrotron Radiation-Induced Desorption from a NEG-Coated Vacuum Chamber”, in Proc. 6th European Vacuum Conference (EVC-6), Vacuum 60 (2001): 67-72, Villeurbanne, France, Dec. 1999. DOI:10.1016/S0042-207X(00)00247-5.
- ¹²² R. Kersevan and M. Ady, CERN, “Recent developments of monte-carlo codes Molflow+ and Synrad+”, in Proc. 10th Int. Particle Accelerator Conf. (IPAC2019), Melbourne, Australia, May. 2019. doi:10.18429/JACoW-IPAC2019-TUPMP037.
- ¹²³ Molflow+, <https://molflow.web.cern.ch/>
- ¹²⁴ C. Benvenuti, “Non-evaporable getters: from pumping strips to thin film coatings”, CERN, CH-1211 Geneva 23.
- ¹²⁵ C. Benvenuti, et al., “Vacuum properties of TiZrV non-evaporable getter films”, in Proc. 6th European Vacuum Conference (EVC-6), Vacuum 60 (2001): 67-72, Villeurbanne, France, Dec. 1999. CERN EST/99-007 (SM). DOI:10.1016/S0042-207X(00)00246-3.
- ¹²⁶ M. Grabskia and E. Al-Dmoura, “Commissioning and operation status of the MAX IV 3 GeV storage ring vacuum system”, *Journal of Synchrotron Radiation*, Volume 28, Part 3, Pages 718-731, May 2021, DOI: 10.1107/S1600577521002599.
- ¹²⁷ I. Bellafont, “Proposal of an RF System for ALBA II storage ring”, internal ALBA document 2021-AC-RF-0001, 2021.
- ¹²⁸ N. Carmignani, “Touschek Lifetime Studies and Optimization of the European Synchrotron Radiation Facility”, Università di Pisa, 2014.
- ¹²⁹ B. Nash, F. Ewald, L. Farvacque, J. Jacob, E. Plouviez, J.-l. Revol and K. Scheidt, “Touschek lifetime and momentum acceptance measurements for ESRF”, in Proceedings of IPAC 2011, San Sebastián, 2011.
- ¹³⁰ P. Elleaume, C. Fortgang, C. Penel, E. Tarazona. “Measuring Beam Sizes and Ultra-Small Electron Emittances Using an X-ray Pinhole Camera”. *Journal of Synchrotron Radiation*, 1995.

- ¹³¹ U. Iriso, "Emittance Monitors for Low Emittance Rings", <https://agenda.infn.it/event/20813/>. Low emittance Ring Workshop 2020, Roma (Italy).
- ¹³² <https://www.bergoz.com/dcct>
- ¹³³ <https://www.bergoz.com/ict>
- ¹³⁴ L. Torino and U. Iriso, "Filling pattern measurements at ALBA using TCSPC", Proc. Of IBIC'14, Monterrey (USA).
- ¹³⁵ U. Iriso, M. Alvarez, A. Nosych and A. Molas. "Streak Camera Calibration Using RF Switches", Proc. Of IBIC'16, Barcelona (Spain).
- ¹³⁶ U. Iriso, "Emittance Monitors for Low Emittance Rings", <https://agenda.infn.it/event/20813/>. Low emittance Ring Workshop 2020, Roma (Italy).
- ¹³⁷ L. Torino, "New Beam Loss Detector System for EBS-ESRF", Proc. Of IBIC18, Shanghai (China).
- ¹³⁸ A. Olmos, U. Iriso, J. Moldes, F. Perez, M. Abbott, G. Rehm, I. Uzun. "Integration of the Diamond Transverse Multibunch Feedback system at ALBA", Proc. Of IBIC'15, Melbourne (Australia).
- ¹³⁹ https://indico.cern.ch/event/1096767/contributions/4692953/attachments/2383768/4073382/ESRW22_N-HUBERT.pdf
- ¹⁴⁰ A. Nosych, U. Iriso, J. Ollé. "Electrostatic Finite-Element Code to Study Geometrical Nonlinear Effects in BPMs", Proc. Of IBIC'15, Melbourne (Australia).
- ¹⁴¹ L. Torino, U. Iriso. "Performance of BPM Readout Electronic Based on Pilot-Tone Generator and a Modified Libera Spark", Proc. Of IBIC'21, Pohang (Korea).
- ¹⁴² A. B. Temnykh, "Delta undulator for Cornell energy recovery linac", Physical Review Special Topics - Accelerators and Beams Vol.11, 120702 (2008)
- ¹⁴³ T.Schmidt and M.Calvi, "APPLE X Undulator for the SwissFEL Soft X-ray Beamline Athos", Synchrotron Radiation News, Vol.31, p 35 (2018)
- ¹⁴⁴ J. Bahrtdt, E. Gluskin, "Cryogenic permanent magnet and superconducting undulators", Nuclear Instruments and Methods in Physics Research, Section A, V.907, 149 (2018)
- ¹⁴⁵ J.Citadini et al. "Sirius-Details of the new 3.2T permanent magnet superbend", IEEE Transactions on Applied Superconductivity, Vol.28, 4101104 (2018)
- ¹⁴⁶ Goldberg, K.A.; Wojdyla, A.; Bryant, D. Binary Amplitude Reflection Gratings for X-ray Shearing and Hartmann Wavefront Sensors. Sensors 2021, 21, 536. <https://doi.org/10.3390/s21020536>
- ¹⁴⁷ https://research-and-innovation.ec.europa.eu/strategy/strategy-2020-2024/our-digital-future/open-science_en
- ¹⁴⁸ <https://network.geant.org>
- ¹⁴⁹ <https://www.esrf.fr/Instrumentation/DetectorsAndElectronics/icepap>
- ¹⁵⁰ <https://accelconf.web.cern.ch/icaleps2017/papers/tuaplo4.pdf>
- ¹⁵¹ <https://www.tango-controls.org>
- ¹⁵² <https://www.sardana-controls.org>
- ¹⁵³ <https://www.taurus-scada.org>
- ¹⁵⁴ <http://www.silx.org>
- ¹⁵⁵ <https://mxcube.github.io/mxcube/>
- ¹⁵⁶ <https://icatproject.org>
- ¹⁵⁷ <https://www.umbrellaid.org>
- ¹⁵⁸ <https://www.calipsoplus.eu/joint-research-activities-jra/jra2-daas/>
- ¹⁵⁹ <https://expands.eu>
- ¹⁶⁰ <https://www.panosoc.eu>
- ¹⁶¹ <https://ispyb.github.io/ISPyB/>
- ¹⁶² <https://eosc.eu>
- ¹⁶³ <https://www.csic.es/>
- ¹⁶⁴ <https://www.irbbarcelona.org/es>
- ¹⁶⁵ <https://www.crg.eu/>
- ¹⁶⁶ <https://www.uab.cat/>
- ¹⁶⁷ <https://www.icmab.es/>
- ¹⁶⁸ <https://www.ciencia.gob.es/home/Estrategias-y-Planes/Plan-de-Recuperacion-Transformacion-y-Resiliencia-PRTR/Planes-complementarios-con-CCAA;jsessionid=6F2731C4ECD8DA056A7A96167F66C56A.1>
- ¹⁶⁹ <http://www.ifae.es/eng/>
- ¹⁷⁰ <https://eurecat.org/es/>
- ¹⁷¹ <https://itq.upv-csic.es/>
- ¹⁷² <https://www.parcdelalba.cat/>
- ¹⁷³ <https://cerca.cat/>
- ¹⁷⁴ <https://www.pic.es/>
- ¹⁷⁵ https://ec.europa.eu/clima/eu-action/climate-strategies-targets/2030-climate-energy-framework_en
- ¹⁷⁶ Forecasting the socio-economic impact of the Large Hadron Collider: A cost-benefit analysis to 2025 and beyond – ScienceDirect <https://doi.org/10.1016/j.techfore.2016.03.007>
- ¹⁷⁷ Social benefits and costs of large scale research infrastructures, Volume 112, November 2016, Pages 65-78, <https://doi.org/10.1016/j.techfore.2015.11.024>
- ¹⁷⁸ Ceccagnoli, M., Gambardella, A., Giuri, P., Licht, G., & Mariani, M. (2005). Study on evaluating the knowledge economy-What

are patents actually worth? The value of patents for today's economy and society. European Commission, DG Internal Market, Tender No. MARKT/2004/09/E, Final Report for Lot, 1

¹⁷⁹ Sartori, D., Catalano, G., Genco, M., Pancotti, C., Sirtori, E., Vignetti, S., et al. (2014). Guide to Cost-Benefit Analysis of Investment Projects. Economic Appraisal Tool for Cohesion Policy 2014–2020. Brussels: European Commission.

¹⁸⁰ Economics of Outdoor Recreation by Marion Clawson, Jack L. Knetsch, doi.org/10.4324/9781315064215

¹⁸¹ <https://www.sendeco2.com>

¹⁸² Comisión Nacional del Mercado de la Competencia, <https://www.cnmec.es/>

List of Figures and Tables

Figure 1-1: ALBA and future ALBA II extension.....	8	Figure 3-18: Examples of “More than Moore” systems-on-a-chip (SoC) for mobile devices, connectivity and IoT products.....	38
Figure 2-1: Layout of present ALBA Beamlines around the tunnel of the accelerators.....	16	Figure 3-19: Share of communication technology of global electricity usage 2010-2030.....	39
Figure 2-2: Renovation plans for European synchrotrons including a shutdown period of about two years for the installation and commissioning of the new systems.....	17	Figure 3-20 3-21: Synchrotron radiation imaging for novel spintronic concepts and devices.....	40
Figure 2-3: ALBA II Layout including long beamline paths.....	18	Figure 3-22: Examples of 2D van der Waals materials investigated at ALBA.....	40
Figure 3-1: Multi-length scale approach of ALBA and the expected impact of ALBA II.....	23	Figure 3-23: Nanoscale coherent imaging of magnetic and electronic phase transitions in Quantum Materials.....	41
Figure 3-2: Determination of intracellular location of iridium in human breast cancer MCF7 cells.....	25	Figure 3-24: Artificial neurons for neuromorphic computing.....	42
Figure 3-3: Techniques used for the structural determination of the yeast nuclear pore complex (NPC).....	26	Figure 4-1: Optics functions for a machine quadrant.....	47
Figure 3-4: First time-resolved crystallography experiment at ALBA. Scheme and time scales of the light-driven sodium-pumping KR2 rhodopsin photocycle (left).....	26	Figure 4-2: Arrangement of the magnets in a portion of a cell.....	47
Figure 3-5: Effect of TiO ₂ nature on product yields and methanol.....	28	Figure 4-3: IBS emittance increase in %, as a function of the bunch lengthening factor, computed with the ZAP code.....	48
Figure 3-6: Representative aberration-corrected STEM-HAADF micrographs.....	28	Figure 4-4: Typical cell of ALBA II, equipped with a super-bend magnet to provide hard X-rays for dipole-based beam lines.....	48
Figure 3-7: Mo 3d NAP-XPS analysis at 275 °.....	29	Figure 4-5: Impact on the performance due to the presence of a high field region (super-bend) in one dipole per cell.....	48
Figure 3-8: Graphical illustration of some of the most important intermediate reaction steps to form from CO ₂ and H ₂ Methanol.....	29	Figure 4-6: Dynamical aperture simulated for 500 turns....	49
Figure 3-9: Density functional theory results describing the various possible intermediates and their energetic relationship to each other.....	30	Figure 4-7: Schematic representation of half 6BA cell of ALBA II lattice, illustrating the assumed distances between magnet yokes.....	51
Figure 3-10: TEM images of RuC samples prepared by hydrothermal synthesis with different ratios of Ru/EDTA.....	30	Figure 4-8: Technological choices for the magnets depending on the source of the magnetic flux: electromagnets (EM), pure permanent magnets (PM) or hybrid designs.....	51
Figure 3-11: XPS data sets of four RuC catalysts prepared according various recipes.....	31	Figure 4-9: ALBA II Lattice Layout example.....	52
Figure 3-12: Graphical explanation of all necessary steps to optimize and understand a catalyst using big-data science.....	32	Figure 4-10: Small aperture vacuum chambers effective pumping speed.....	53
Figure 3-13: Schematic of a solid-state battery with a metallic Lithium anode and metallic current collector on top (grey plane).....	34	Figure 4-11: Left: Molflow+ PSD Desorption map and Dynamic pressure map. Right: Dynamic pressure (With NEG).....	53
Figure 3-14: Radar chart presenting the most relevant properties of the polymer, composite, oxide and sulfide families of solid-state electrolytes.....	34	Figure 4-12: ALBA II chamber and cooling pipe.....	53
Figure 3-15: ALBA current imaging capabilities of interfaces and particles.....	35	Figure 4-13: 3rd harmonic cavity installed in the Bessy II ring for the performance tests.....	54
Figure 3-16: In situ synchrotron X-ray techniques used to study the interphase between electrode materials and solid-state electrolytes.....	36	Figure 4-14: Main cavity phasor diagram.....	55
Figure 3-17: road map prospect with branching on emerging conceptual technologies for solving the ICT challenges over the next 15 years, and potential role of 2D materials.....	37	Figure 4-15: Main and harmonic voltage as function of time.....	55
		Figure 4-16: Main cavity phasor diagram.....	55
		Figure 4-17: View of a section of the accelerator with ALBA and ALBA II orbits.....	57
		Figure 4-18: Distribution of the 9 BPMs in a ALBA II cell: 9 BPMs are used for orbit correction (black dots), while a spare BPM (red dot) is left for diagnostics purposes.....	57
		Figure 4-19: ALBA II Layout. The ALBA II lattice and exit lines have been integrated in the present tunnel.....	58

Figure 4-20: Sketch of the pulsed magnets and injection trajectory in the 4 m long injection section.....	59	Figure 6-1: Estimated progression of annual data production at ALBA beamlines.....	79
Figure 4-21: The prototype DDK.....	59	Figure 6-2: Diagram of foreseen IT infrastructures.....	83
Figure 4-22: Simulation of the horizontal position and angle of the injected beam at the septum exit for the first three turns without errors...	60	Figure 6-3: Sketch of future ALBA II data service to users.....	83
Figure 4-23: List of beamlines at ALBA, indicating the corresponding operating energy range and the associated photon source.....	61	Figure 7-1: ALBA II and ASTIP preliminary layout. The four long beamlines paths are sketched for showing all the future possibilities.....	89
Figure 4-24: Left: Comparison of the spectral brilliance for undulator-type ID sources operating in the present.....	62	Figure 7-2: LEAPS scheme, highlighting its members.	90
Figure 4-25: Evolution of horizontal coherent fraction with ALBA upgrade.....	62	Figure 8-1: Sketch of energy efficiency evolution.....	94
Figure 4-26: Spectral brilliance in wiggler approximation from wiggler-type IDs operating in the present.....	62	Figure 9-1: ALBA II Organization Structure.....	97
Figure 4-27: Spectral flux density of a SCU of a period length of 15mm as compared to the present SCW of a period of 30mm.....	63	Figure 9-2: Shows the ALBA staff evolution from 2023 to 2033.....	99
Figure 4-28: Spectral brilliance of dipoles at ALBA and of the proposed dipolar sources at ALBA II. Vertical lines indicate the critical energy for each source.....	63	Figure 9-3: ALBA II Timeline.....	100
Figure 4-29: Field profile for the proposed 3.2T superbend compared with the standard QD magnet for ALBA II.....	63	Figure A1: Distribution of the income NPV.....	108
Figure 5-1: Increase of the angular flux density of the source for a photon energy of 3 keV.....	65	Figure A2: NPV (Income-Investments) evolution 2023-2055.....	109
Figure 5-2: Simulation of the beam spot at the sample position of BLO6-XAIRA considering different scenarios.....	65	TABLE 2-1: MAIN TECHNIQUES OFFERED BY ALBA BEAMLINES.....	15
Figure 5-3: Example of adaptive optics system installed at the XAIRA beamline at ALBA.....	66	TABLE 2-2: ELECTRON MICROSCOPES OFFERED BY JEMCA AND InCAEM.....	15
Figure 5-4: Optical scheme used in the single-grating shearing interferometry and Hartmann wavefront, assuming an expanded converging beam.....	66	TABLE 4-1: ALBA II LATTICE PRELIMINARY MAIN PARAMETERS.....	47
Figure 5-5: Profile of the three long beamlines with experimental stations in the new plots.....	69	TABLE 4-2: REALISTIC ERROR SOURCES USED FOR THE SIMULATIONS.....	49
Figure 5-6: Flux emitted by different undulators within the energy range of ALBA II.....	70	TABLE 4-3: MAGNET TYPES AND QUANTITIES FOR ALBA II STORAGE RING.....	51
Figure 5-7: Source size and divergence for ALBA II ports BLO2 and BLO4.....	70	TABLE 4-4: CHARACTERISTICS OF THE DIFFERENT TYPES OF MAGNETS FOR ALBA II STORAGE RING.....	51
Figure 5-8: Horizontal coherent fraction of the sources of ports BLO2 and BLO4, for ALBA II.....	71	TABLE 4-5: ALBA II MAIN RF PARAMETERS.....	54
Figure 5-9: Source sizes and divergences for an undulator source installed at BLO8.....	71	TABLE 4-6: ALBA II MAIN CAVITY PARAMETERS.....	55
Figure 5-10: Coherent fraction of the flux emitted by an undulator installed at BLO8.....	72	TABLE 4-7: ALBA II 3H CAVITY PARAMETERS.....	55
Figure 5-11: Achievable spot size as a function of the image distance to the sample for low and high photon energies.....	72	TABLE 4-8: LIST OF DIAGNOSTICS COMPONENTS FORESEEN FOR ALBA II.....	56
Figure 5-12: Flux emitted by the bending magnets of ALBA II, assuming acceptance of the full vertical divergence and 1 mrad of horizontal acceptance.....	72	TABLE 4-9: ALBA II BEAMLINES DISTRIBUTION.....	58
Figure 5-13: Vertical divergence of the beam emitted by the bending magnets of ALBA II.....	72	TABLE 4-10: EXPECTED OCCUPANCY OF STRAIGHT SECTIONS FOR ALBA II.....	62
Figure 5-14: Chronogram showing when the different beamlines came into operation at ALBA.....	73	TABLE 5-1: LONG BEAMLINES TECHNICAL PARAMETERS SUMMARY.....	69
		TABLE 9-1: MILESTONE PLAN AND ASSOCIATED RISKS.....	101
		TABLE 9-2: IDENTIFICATION OF GENERAL RISKS....	102
		TABLE 10-1: LIST OF KEY INDICATORS.....	105
		TABLE 10-2: RESULTS OF THE ECONOMIC ANALYSIS.....	105
		TABLE A1: ECONOMIC IMPACT OF ALBA II (€).....	107
		TABLE A2: RESULTS OF THE FINANCIAL ANALYSIS.....	107
		TABLE A3: LIST OF KEY INDICATORS.....	109
		TABLE A4: RESULTS OF THE ECONOMIC ANALYSIS.....	109



Generalitat de Catalunya
**Departament de Recerca
i Universitats**



ALBA Synchrotron - www.albasynchrotron.es
Carrer de la Llum 2-26, 08290 Cerdanyola del Vallès (Barcelona) Spain / Tel. +34 93 592 4300